Nitrile Reduction and Carbon Monoxide Replacement in Tungsten(II) Bis(acetylacetonate) Complexes

Andrew B. Jackson

A dissertation submitted to the faculty of the University of North Carolina at Chapel Hill in partial fulfillment of the requirements for the degree of Doctor of Philosophy in the Department of Chemistry

Chapel Hill
2008

Approved by:

Joseph L. Templeton

Cynthia Schauer

Maurice Brookhart

Jeff Johnson

Wenbin Lin

ABSTRACT

Andrew B. Jackson: Nitrile Reduction and Carbon Monoxide Replacement in Tungsten(II) Bis(acetylacetonate) Complexes
(Under the direction of Joseph L. Templeton)

A substitutionally labile tungsten(II) reagent, $W(CO)_3(acac)_2$ (acac = acetylacetonate) has been synthesized and isolated. Initial reactivity investigations include replacement of one CO ligand with two-electron donors, such as phosphines, or replacement of two equivalents of CO with conventional four-electron donor ligands, such as alkynes and nitriles. Aldehydes, imines, and ketones surprisingly bind to tungsten as four-electron donors relying on lone-pair donation from the heteroatom to satisfy the eighteen electron requirement. Nitrile complexes of the form $W(CO)(acac)_2(\eta^2\text{-N}\equiv\text{CR})$ (R = Ph, Me) undergo alkylation at the nitrogen lone pair with MeOTf and EtOTf (OTf = CF_3SO_3) yielding cationic iminoacyl complexes of the form $[W(CO)(acac)_2(\eta^2\text{-MeN=CR})][OTf]$. Nucleophilic attack occurs at the iminoacyl carbon with hydride ($Na[HB(OMe)_3]$) or methyl (MeMgBr) reagents reducing the iminoacyl to a sidebound imine ligand. The attack generates a new chiral center at the imine carbon with diastereomeric ratios on the order of 2:1. Cationic iminoacyl-carbonyl complexes exhibit facile carbon monoxide replacement with a variety of reagents. The CO ligand in the iminoacyl cations can be replaced thermally with isonitrile and bulky phosphine reagents yielding complexes of the type $[W(L)(acac)_2(\eta^2\text{-MeN=CPh})]^+$ (L = isonitrile or bulky phosphine). Addition of tricyclohexylphosphine (PCy_3) to $[W(CO)(acac)_2(\eta^2\text{-MeN=CPh})]^+$ liberates CO to form $[W(PCy_3)(acac)_2(\eta^2\text{-MeN=CPh})]^+$, a

molecule exhibiting fluxional behavior on the NMR time scale due to rapid and reversible phosphine dissociation. Smaller phosphine reagents, such as trimethylphosphine, attack the iminoacyl carbon to form $[W(CO)(acac)_2(\eta^2\text{-MeN-C}(PMe_3)Ph)]^+$. Under photolytic conditions, alkyne reagents replace CO yielding cationic alkyne-iminoacyl complexes of the type $[W(\eta^2\text{-alkyne})(acac)_2(\eta^2\text{-MeN=CR})]^+$. Nucleophilic attack with $Na[HB(OMe)_3]$ delivers a hydride to the iminoacyl carbon yielding a neutral alkyne-imine complex of the formula $W(\eta^2\text{-alkyne})(acac)_2(\eta^2\text{-MeN=CHPh})$, a molecule that is fluxional on the NMR time scale due to rotation of the alkyne ligand. Addition of MeOTf to the neutral alkyne-imine complex results in a second nitrogen-methyl linkage to yield a cationic alkyne-iminium complex of the form $[W(acac)_2(\eta^2\text{-Me}_2\text{N=CHPh})(\eta^2\text{-MeC}\equiv\text{CMe})]^+$. Formally, the original sidebound nitrile ligand undergoes three ligand based manipulations while being reduced to a sidebound iminium ligand.

ACKNOWLEDGEMENTS

Five years of graduate school may seem like an eternity to some people, but this period of my life has felt like a blink of an eye. It's hard to imagine life without the countless lessons learned, experiences shared, and friendships forged during my tenure at UNC-Chapel Hill. Our department thrives because of hard work from all the faculty, staff, and students. I would like to thank UNC chemistry as a whole for sustaining a strong tradition of excellence.

Working for Joe Templeton has been one of the best experiences of my life. Joe's professionalism, patience, hospitality, sense of humor, and all around class will be missed, but my departure paves the way for other students to experience these attributes. As an educator, Joe readily molds himself to fit the needs of individual students, a necessity while juggling several unique personalities co-existing in one laboratory, as well as numerous undergraduate students. It has been a pleasure to work with such a well-respected man. Thank you so much Joe!

My labmates in the Templeton group have been a source of friendship and made lab time much less dull. Thank you especially to Neil Vogeley, Ned West, Abby O'Connor, Margaret McDonald, Andrew Garrett, Chetna Khosla, and Kristi Engelman for their help with critiquing presentations, proofreading papers, and tolerating my nonsense. Each has helped create a positive working atmosphere. Maurice Brookhart and those in his group have been wonderful friends and colleagues over the years. Special thanks to Marc Walter and Wes Bernskoetter for their assistance in assigning spectroscopic data.

I also thank Dave Harris and Marc ter Horst for maintaining the NMR lab and teaching me several NMR techniques. Working with them as a teaching assistant for nearly three years familiarized me with proper operation of a spectrometer, and also forced me to use my time wisely.

Our crystallographer Peter White solved my crystal structures and was always willing to try diffraction of rather poor looking crystals. Thanks for being so friendly and patient.

My family has been a source of encouragement, comfort, and support throughout my entire educational career, not only graduate school. My father Dennis, my mother Jodi, my brother Matt, my sister Tracy, her husband Bryan, and her son, and my nephew Jackson have been among my biggest fans. Their reinforcement has made all of this easier. I love all of you very much!

Finally, I thank several close friends outside chemistry whose occasional visits kept my spirits high during graduate school. Adam Humes, Brian Gilroy, Paul Alberico, Joe Thompson, Matt "Coach" Johnson, Gregg Gebhardt, and Cody DeWitt helped to preserve a level of spice in my life to balance the inherent nerdiness that comes with being a graduate student.

TABLE OF CONTENTS

LIST OF FIGURES

LIST OF SCHEMES

LIST OF TABLES

LIST OF ABBREVIATIONS AND SYMBOLS

Me	Methyl group, $-CH_3$
IR	infrared
CO	carbonyl
cm^{-1}	wavenumber
π	Greek pi: pi bond
NMR	nuclear magnetic resonance
ppm	parts per million
$\Delta G^{\ddagger}$	Gibbs Free Energy of Activation
°C	degrees Celsius
THF	tetrahydrofuran
^{t}BuLi	tertiary butyl group, $-C(CH_3)_3$
R	alkyl group
OTf	trifluoromethane sulfonate, $[CF_3SO_3]^-$
Hz	hertz
K	equilibrium constant
Ph	phenyl group, C_6H_5-
Ar	aryl group
J	coupling constant
η	Greek eta: hapticity
dippe	bis(diisopropylphosphino)ethane
β	Greek beta: crystallographic angle
ν	Greek nu: IR absorption band frequency
^{n}BuLi	n-butyl group, $-C_4H_9$
BAr'_4	tetrakis(3,5-bis(trifluoromethyl)phenyl)borate
Et	ethyl group, $-CH_2CH_3$
α	Greek alpha: crystallographic angle
E	electrophile
ORTEP	Oak Ridge Thermal Ellipsoid Plot
δ	Greek delta: chemical shift

σ	Greek sigma: sigma bond
Cp	cyclopentadienyl, [C_5H_5]
kcal	kilocalorie
mol	mole
K	Kelvin
q	quartet
d	doublet
t	triplet
s	singlet
γ	Greek gamma: crystallographic angle
m	multiplet
br	broad
Tp′	hydridotris(3,5-dimethylpyrazolyl)borate
Et_2O	diethylether
dr	diastereomeric ratio
COSY	COrrellation SpectroscopY
Å	Angstrom
CH_2Cl_2	dichloromethane

Chapter 1

Characterization and Reactivity of η^2-Nitrile and η^2-Iminoacyl Complexes

Nitrile ligands are ubiquitous in organometallic chemistry, and once bound they offer several sites for probing reactivity pathways[1-3] due to the polarized carbon-nitrogen triple bond and the lone pair of electrons available on nitrogen. While the vast majority of nitrile ligands bind via the lone pair on nitrogen (σ-bound), a handful of complexes boast a nitrile ligand which binds to the metal center via the carbon-nitrogen triple bond (π-bound). In depth reactivity studies of η^2-nitrile complexes are lacking.

Many examples of η^2-nitrile ligands involve Group VI complexes of molybdenum(II) and tungsten(II). These d^4 metal ions require an additional fourteen electrons for valence saturation. Binding seven 2-electron donors creates a crowded, coordination sphere with extended bond lengths often leading to fluxional behavior. To add fourteen electrons in a six-coordinate octahedral framework, one ligand must be capable of donating four electrons. Alkynes readily fulfill these requirements with donation from alkyne $\pi_{||}$ (Figure 1.1, **A**) and $\pi_{\perp}$ (Figure 1.1, **B**) filled orbitals on the ligand into available vacant metal-based orbitals. Further stabilization stems from an alkyne's π-acid capability in which dπ-electrons on the metal center are donated into an anti-bonding $\pi^*_{||}$ orbital (Figure 1.1, **C**) on the alkyne ligand. These bonding interactions are well documented and prevalent for alkyne ligands,[4,5] but only recently have similar interactions been observed with nitriles. The π-acid properties of sidebound alkynes and nitriles are especially important for low-valent metals. Nitriles, like alkynes, can serve as variable electron donors and provide anywhere from two to four electrons depending on the electronic requirements of the metal center. Stabilization of electrons in dπ orbitals renders the metal center less susceptible to oxidation.

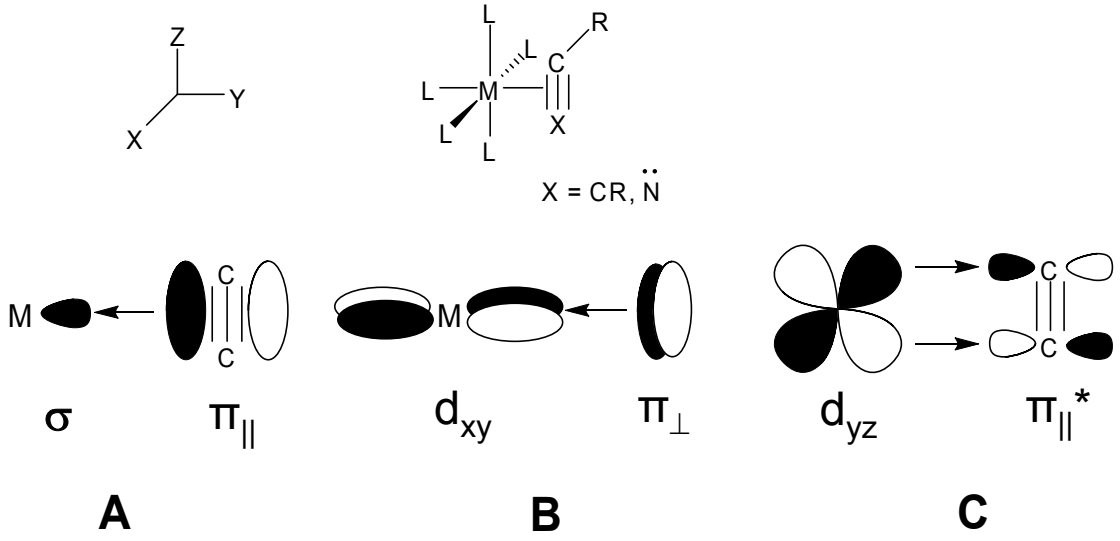

Figure 1.1 Orbital interactions of η^2-alkynes and η^2-nitriles with a metal center.

Characterizing η^2-Nitrile Complexes

Early efforts to characterize proposed side-bound nitrile complexes relied on IR spectroscopy. The difference between an end-on nitrile ligand and a sidebound nitrile ligand can be seen in the stretching frequency of the C≡N multiple bond.[6-8] End-on nitrile coordination is accompanied by a slight increase in the stretching frequency of the C≡N triple bond compared to the free ligand, whereas a significant decrease (~400-500 cm^{-1}) is characteristic of sidebound nitrile ligands. Although IR spectroscopy can be a useful tool for geometric assignments, it is not conclusive. The carbon-nitrogen triple bond can be difficult to detect via IR spectroscopy, and exceptions to these guidelines have been observed. ^{13}C NMR spectroscopy also aides in distinguishing between the two binding modes. The nitrile carbon for end-on coordinated nitriles typically resonates in the 120-150 ppm range, while the analogous peak for a side-on ligand tends to resonate farther downfield, somewhere in the 180-240 ppm range. Again, these characterization methods are at best supplementary to X-

ray structural data. While a handful of sidebound nitrile transition metal complexes were purportedly synthesized in the 1960s and 1970s, the first definitive structural assignment was completed by Wilkinson and co-workers.[9] X-ray analysis of the red prisms of $Cp_2Mo(\eta^2$-N≡CMe), synthesized by reduction of Cp_2MoCl_2 with sodium amalgam in acetonitrile, confirmed coordination of the nitrile ligand to molybdenum through both the carbon and nitrogen atoms. In this complex, acetonitrile donates two electrons to molybdenum. Subsequent examples of complexes with η^2-nitrile ligands coordinated to a variety of metals have since been reported.[10-14]

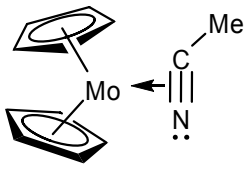

Figure 1.2. $Cp_2Mo(\eta^2$-N≡CMe): the first structurally characterized η^2-nitrile complex.

In 1991, Harman and co-workers reported the first crystal structure of a tungsten(II) η^2-acetonitrile complex, $[WCl(bpy)(PMe_3)_2(\eta^2$-N≡CMe)][$PF_6$].[15] Additionally, the nitrile ligand was assigned as a four-electron donor based on the significant lengthening of the carbon-nitrogen triple bond (1.27 Å), the short tungsten-nitrogen (2.01 Å) and tungsten-carbon (2.00 Å) bond lengths, and the substantial downfield chemical shift of the nitrile carbon in the ^{13}C NMR spectrum (235 ppm). These data imply donation from $\pi_\perp$ on the nitrile ligand. Previous structurally characterized η^2-nitrile complexes contained formal two-electron donor nitrile ligands. Harman's work demonstrated the similarity between alkynes and nitriles as four-electron donor ligands.[16] Additionally Harman also observed rotation of

the η^2-nitrile ligand in solution. Low temperature NMR experiments revealed rotational barrier values similar to those of alkynes ($\Delta G_{rot}^{\ddagger}$ = 8-11 kcal/mol for various nitrile and alkyne complexes surveyed).

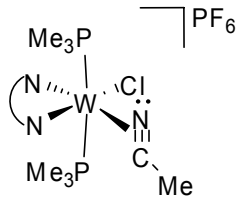

Figure 1.3. Acetonitrile as a side-bound, four-electron donor ligand.

Richmond and co-workers also reported sidebound coordination of nitriles to a low-valent d^4 tungsten center.[17,18] Under refluxing conditions, fluorinated aromatic nitriles displace two equivalents of carbon monoxide from WF(NMe-Paa)$(CO)_3$ to generate WF(NMe-Paa)(CO)(η^2-N≡C-C_6F_5) (see Scheme 1.1 for reaction sequence and depiction of NMe-Paa). Structural and spectroscopic data indicate the presence of a four-electron donor nitrile. The nitrile ligand binds trans to fluoride, and the chelating NMe-Paa ligand adopts a *mer* configuration. For comparison, alkyne analogs were also synthesized, and interestingly, X-ray data shows a *fac* configuration for the chelate in WF(NMe-Paa)(CO)(η^2-PhC≡CH), with the alkyne ligand cis to fluoride. Nitriles are better π-acceptors than alkynes due to the electronegativity of nitrogen, and readily accept π-donation from fluoride when the two ligands are trans. Alkynes are better π-donors and avoid unfavorable filled-filled interactions when cis to fluoride. Although sharing the capacity to use both $\pi_{||}$ and $\pi_{\perp}$ when binding to a metal center, Richmond's system exploits the inherent electronic differences of sidebound nitrile and alkyne ligands.

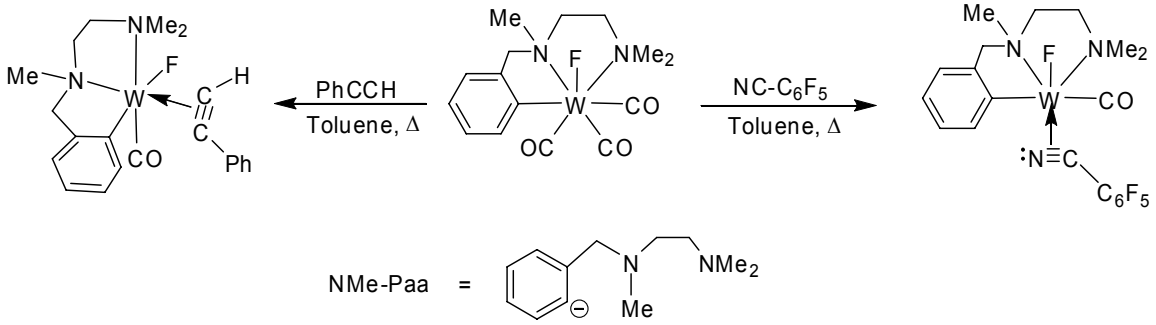

Scheme 1.1. Coordination geometries of η^2-alkyne and η^2-nitrile ligands in Richmond's WF(NMe-Paa)(CO) system.

Table 1.1. Salient structural and spectroscopic data for selected η^2-nitrile complexes.

Complex	M-N (Å)	M-C (Å)	C-N (Å)	^{13}C, N≡*C* (δ)	IR, ν_{CN} (cm^{-1})	*N*[a]
$Cp_2Mo(\eta^2$-N≡C-Me)	2.22	2.12	1.20	170.8	1750	2
$[WCl(bpy)(PMe_3)_2(\eta^2$-N≡C-Me)]$^+$	2.01	2.00	1.27	235	n/a	4
Tp′Nb(CO)(η^2-N≡C-Ph) (η^2-Ph-C≡C-Me)	2.14	2.17	1.21	186.7	1737	3
(dippe)Ni(η^2-N≡C-Ph)	1.90	1.87	1.22	169.2	1745	2
W(NMe-Paa)(CO)(η^2-N≡C-C_6F_5)	2.00	2.01	1.26	224.1	n/a	4
Cp^*Ir(CO)(η^2-N≡C-*p*-ClC_6H_4)	2.19	2.04	1.21	n/a	1781	2
Tp′^{Br}WBr(CO)(η^2-N≡C-Me)	2.07	2.04	1.10	207.5	1688	4
Mo(N[*t*-Bu]Ar)$_3$(η^2-N≡C-NMe_2)	2.03	2.04	1.27	n/a	n/a	3

a: *N* = formal number of electrons donated from nitrile ligand to metal.

A comparison of salient X-ray and available spectroscopic data of structurally characterized η^2-nitrile complexes is found in Table 1.1. In general, bond distances from the metal center to each atom in the η^2-nitrile ligand are nearly equal, especially if the η^2-nitrile is assigned as a four-electron donor. The iridium complex, Cp^*Ir(CO)(η^2-N≡C-*p*-ClC_6H_4),[19,20] reported by Hawthorne, boasts a rather long iridium-nitrogen bond (2.19 Å) attributed to a lack of π-backbonding from the metal center to the nitrile. Nitriles assigned as four-electron donors tend to have slightly longer carbon-nitrogen multiple bonds due to increased interaction with the metal center compared to two-electron donors. Young's complex, Tp′^{Br}WBr(CO)(η^2-N≡C-Me), shows a surprisingly short carbon-nitrogen bond

(1.10 Å), shorter than the corresponding bond in free nitrile, that may reflect heavy atom distortion of the triangular W-C-N parameters. Spectroscopic data, when available, correlate well with electron donation formalisms. Nitrile ligands assigned as four-electron donors contain a highly deshielded nitrile carbon, leading to downfield resonances in the ^{13}C NMR spectrum.

Reactivity of η^2-Nitrile Complexes

An early example from Hawthorne[19-21] depicts the lability of η^2-nitrile ligands. Thermolysis of a five-membered iridacycle extrudes carbon dioxide to yield $Cp^*Ir(CO)(\eta^2$-$N{\equiv}C$-*p*-$ClC_6H_5)$, which is structurally characterized. Photolysis of the isolable η^2-nitrile iridium complex in hydrocarbon (R-H) solvents generates iridium(III) species of the formula, $Cp^*Ir(CO)(R)(H)$. The proposed reaction sequence involves dissociation of the η^2-nitrile ligand to form a reactive "$Cp^*Ir(CO)$" fragment, which readily activates a carbon-hydrogen bond in a solvent molecule to produce the oxidative addition product. Photolytic induced lability of the nitrile ligand proved to facilitate the C-H activation. Displacement of η^2-nitrile ligands has been observed in other systems, usually promoted by addition of a strong ligand.[17,22] It has been postulated that displacement of η^2-nitrile ligands occurs via slippage to an η^1 coordination mode prior to expulsion from the coordination sphere. η^2-Alkynes are far more resistant to such displacement pathways.

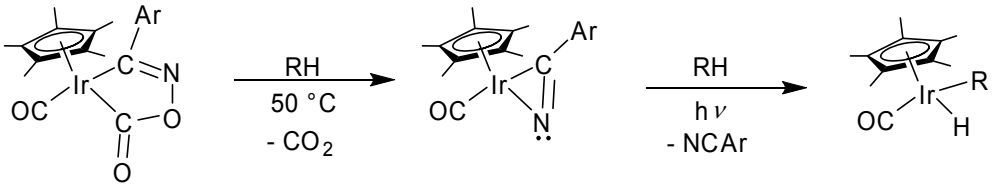

Scheme 1.2. Photolytic induced displacement of η^2-nitrile leading to C-H activation.

Jones and co-workers recently reported sidebound coordination of benzonitrile to a nickel(0) center to form (dippe)Ni(η^2-N≡CPh).[23-25] After long periods in solution, another product identified as (dippe)Ni(CN)(Ph) is observed in equilibrium, reflecting cleavage of the carbon-carbon bond in the benzonitrile ligand to yield the intramolecular oxidative addition product. Both products were isolated and structurally characterized. A pure sample of the oxidative addition product showed conversion back to the η^2-nitrile starting complex, establishing the presence of the equilibrium. This result shows facile cleavage of carbon-carbon bonds in an η^2-nitrile ligand.

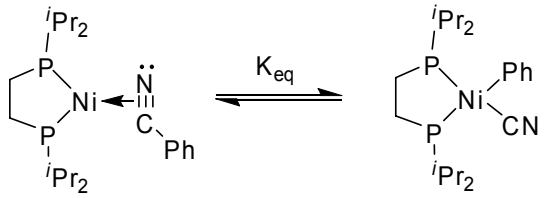

Scheme 1.3. Equilibrium between η^2-nitrile and oxidative addition nickel complexes

π-Bound nitriles can be prone to oxidation at the nitrile carbon. Young's Tp′ tungsten(II) monocarbonyl monohalide fragment readily binds nitriles as sidebound, four-electron donor ligands.[26,27] Addition of pyridine *N*-oxide to Tp′WI(η^2-N≡CMe)(CO) was expected to

produce the oxo derivative, Tp′WOI(CO), but instead an air stable, diamagnetic acetylimido complex of the formula Tp′WI{NC(O)Me}(CO) was generated.[28] The isolated product reflects oxygen atom transfer to the nitrile carbon and a formal oxidation of tungsten(II) to tungsten(IV). Similar oxidation reactions of η^2-nitrile ligands have been observed in other systems.[22,29]

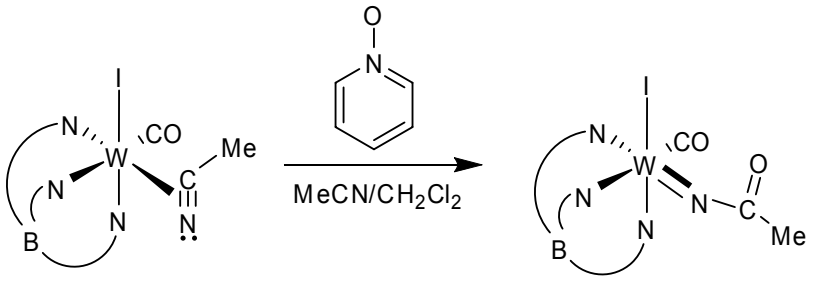

Scheme 1.4. Net oxygen atom addition to η^2-nitrile to form an acetylimido ligand.

η^2-Nitriles as Intermediates and Transition States.

Recently Naota and co-workers observed nitrogen to carbon linkage isomerism of cyanocarbanions in a cyclopentadienyl ruthenium(II) system.[30] Upon reflux in benzene, the *N*-bound zwitterionic complex, in which the nitrile binds through its lone pair, isomerizes to yield the neutral *C*-bound product. Kinetic data and DFT measurements suggest the mechanism involves an η^2-nitrile transition state followed by a "metal-sliding" process to generate the ruthenium-carbon bond. Other systems have also identified possible η^2-nitrile transition states[31,32] or intermediates[33-35].

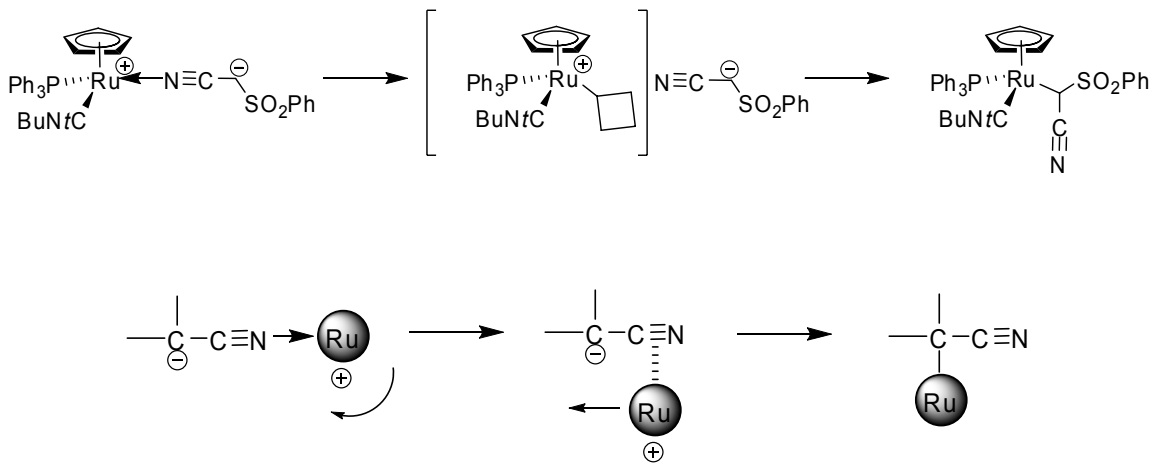

Scheme 1.5. Likely mechanism of linkage isomerism proposed by Naota.

Electrophilic Addition to η^2-Nitriles.

Reactivity studies of η^2-nitriles often focus on the available lone pair on the nitrogen atom. Addition of an electrophilic reagent (E^+) can form a new nitrogen-E^+ bond if the lone pair is sufficiently nucleophilic. A few examples of this reactivity exist among low-valent Group VI metal complexes. Parkin reported alkylation of $Cp^{tBu}{}_2Mo(\eta^2\text{-}N{\equiv}CCH_3)$ with alkyl halides (R-X) to form cationic $[Cp^{tBu}{}_2Mo(\eta^2\text{-}RN{\equiv}CCH_3)][X]$ complexes.[36] Likewise, Harman reported similar reactivity with low-valent $TpW(NO)(PMe_3)(\eta^2\text{-}N{\equiv}CMe)$.[37] The resulting cationic complexes, $[TpW(NO)(PMe_3)(\eta^2\text{-}RN{\equiv}CMe)][X]$, showed a mixture of four isomers as detected by ^1H NMR spectroscopy. These complexes are of particular interest because the chiral tungsten center introduces stereochemistry in the nitrile activation process, and could be used in further stereoselective functionalization reactions at the carbon-nitrogen multiple bond.

These alkylation reactions transform the η^2-nitrile into an iminoacyl ligand. Nitrogen's lone pair, not tied to the metal center in a sidebound nitrile ligand, forms a bond

with an electrophile which barely perturbs the carbon-nitrogen multiple bond. The carbon-nitrogen linkage retains significant multiple bond character, and the iminoacyl carbon remains highly unsaturated based on ^{13}C NMR resonances (see Table 1.2). Sidebound iminoacyl ligands are more prevalent in the literature than η^2-nitrile ligands with several examples forming via insertion reactions of nitriles or isonitriles into metal-carbon or metal-silicon bonds.[38-42]

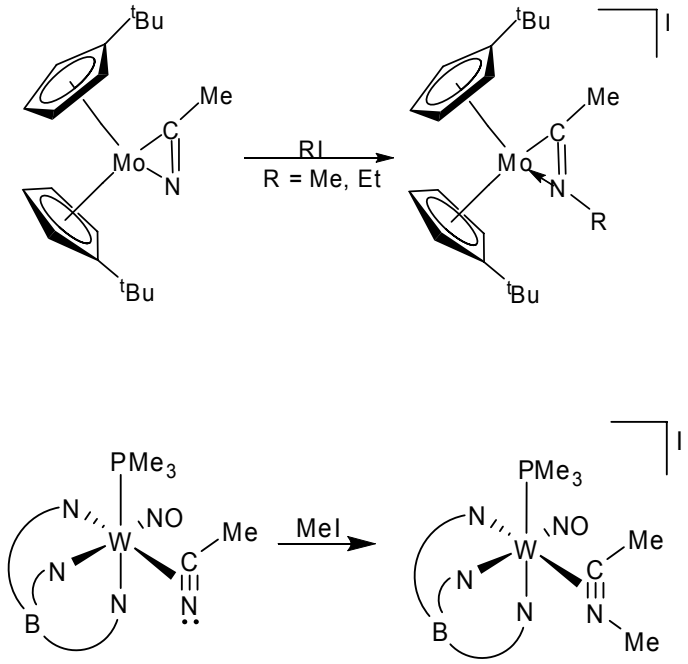

Scheme 1.6. Alkylation reactions of η^2-nitriles with alkyl halides.

Alkylation of a purported tungsten(IV) η^2-nitrile species was reported by our laboratory in 2004.[22] Addition of methyl trifluorosulfonate (MeOTf) to Tp′W(O)(I)(η^2-N≡C-Me) formed two products in a 5:1 ratio as detected by ^1H NMR spectroscopy (Scheme 1.7). The products were assigned as η^2-iminoacyl cations of the form [Tp′W(O)(I)(η^2-MeN≡C-Me)][OTf]

related by orientation geometry of the iminoacyl ligand. Although no X-ray structure was solved for either the η^2-nitrile starting reagent or the η^2-iminoacyl product, spectroscopic data were consistent with their formation. The isomeric distribution suggests hindered rotation of the iminoacyl ligand, since only one product was observed for the nitrile complex. Iminoacyl ligands are capable of rotation along the metal-iminoacyl centroid similar to their nitrile precursors.

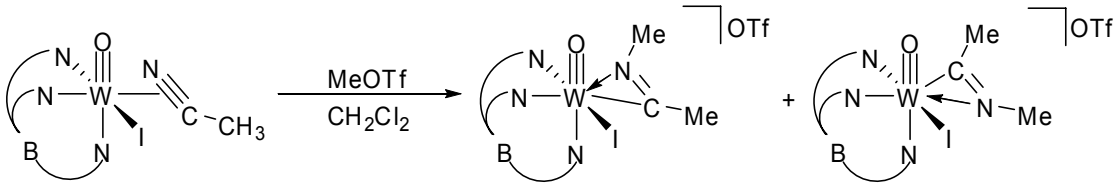

Scheme 1.7. Alkylation of Tp′W(O)(I)(η^2-N≡C-Me) with MeOTf

Jones could also activate the nitrogen lone pair in (dippe)Ni(η^2-N≡CMe) with BPh_3 to yield (dippe)Ni(η^2- Ph_3BN=CMe) with the iminoacyl ligand remaining coordinated to nickel through both the nitrogen and carbon atoms. Here BPh_3 acts as a Lewis acid in coordinating to nitrogen's lone pair. The resultant neutral product shows that a positively charged electrophile is not required for activation of the lone pair. Previously discussed alkylation reactions by Parkin, Harman, and Templeton resulted in cationic iminoacyl complexes.

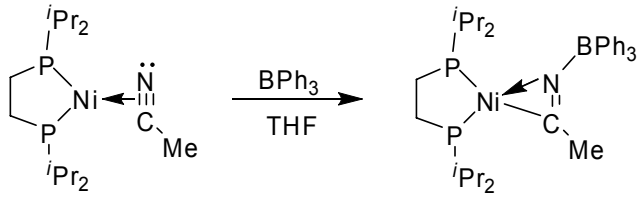

Scheme 1.8. Coordination of BPh_3 to the η^2-nitrile lone pair in (dippe)Ni(η^2-N≡CMe).

An unprecedented type of η^2-nitrile reactivity was observed by Etienne.[44] Addition of HBF_4 to a cold solution of TpNb(CO)(η^2-N≡CPh)(η^2-PhC≡CMe)[45] results in protonation at nitrogen yielding the cationic iminoacyl species, [TpNb(CO)(η^2-HN≡CPh)(η^2-PhC≡CMe)][BF_4], observable at low temperature. Upon warming, this species loses CO to produce the neutral TpNb(F)(=C(Ph)-C(Me)=C(Ph)-NH) complex (Scheme 1.9). This product reflects intramolecular cyclization of the nitrile and alkyne ligands to generate a five-membered metallocycle. Formally, the metal center becomes oxidized from niobium(I) to niobium(III) upon addition of H-F across the niobium-nitrogen bond. Protonation at nitrogen demonstrates the nucleophilicity of the lone pair in an η^2-nitrile ligand, and also facilitates the cyclization.

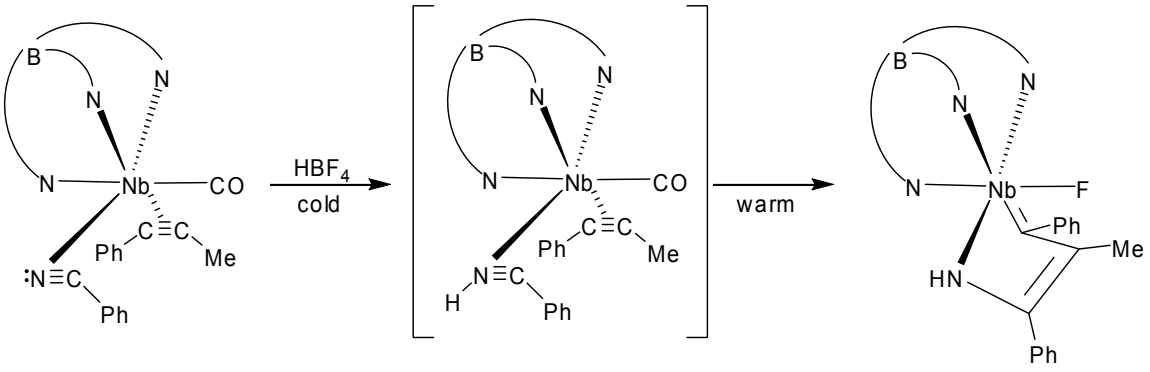

Scheme 1.9. Protonation of η^2-nitrile ligand facilitating intramolecular cyclization.

Traditional Methods of Forming η^2-Iminoacyl Ligands

A common method of synthesizing iminoacyl derivatives involves insertion of free nitrile into a M-Si bond. A recent example from the Tobita group provides structural

evidence for an η^2-iminoacyl ligand stemming from insertion of acetonitrile into a tungsten-silicon bond. This rearrangement is preceded by the reductive elimination of methane from a tungsten(IV) center. The resultant d^4 tungsten ion probably promotes the insertion in order to maximize backbonding interactions from tungsten.

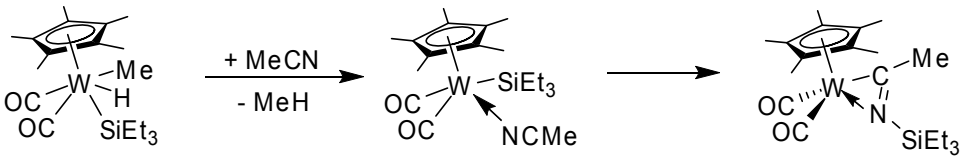

Scheme 1.10. Nitrile insertion into a tungsten-silicon bond.

Mechanistically, iminoacyl ligands can stabilize reactive intermediates.[46] Bergman and Brookhart proposed an η^2-iminoacyl intermediate in their mechanism of carbon-carbon bond cleavage of aryl and alkyl cyanides in a rhodium(III) system based on observations in low temperature NMR experiments.[47,48] Indeed, a crystal structure of the intermediate was solved indicating nitrile inserts into the rhodium-silicon bond to form an η^2-iminoacyl ligand.

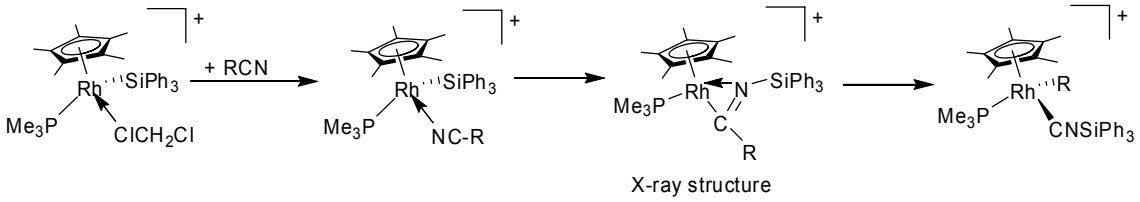

Scheme 1.11. Insertion of nitrile into a rhodium-silicon bond.

Formation of iminoacyl ligands via insertion of isonitrile reagents into M-X bonds[49,50] (X = alkyl, hydrido, silyl, amido, phosphido), particularly in early metal transition metal complexes, is a common organometallic reaction. In particular, Royo and co-workers have demonstrated this type of reactivity with high-valent Cp^*Ta complexes.

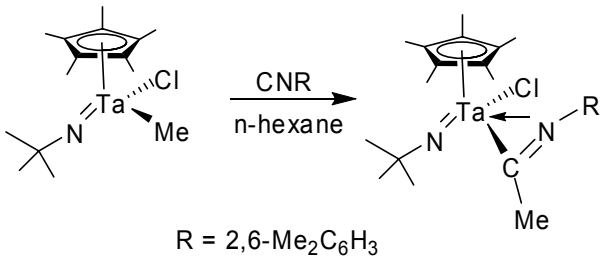

Scheme 1.12. Insertion of isonitrile into a tantalum-carbon bond.

A direct route to iminoacyl containing complexes involves addition of a nitrilium salt to a transition metal center. This approach bypasses traditional nitrile or isonitrile insertion pathways. The first such example from Barefield involved reacting vanadocene with one equivalent of [PhCNMe][BF_4] in THF to yield the cationic iminoacyl complex, [$Cp_2Ta(\eta^2$-MeN=CPh)][BF_4].[51]

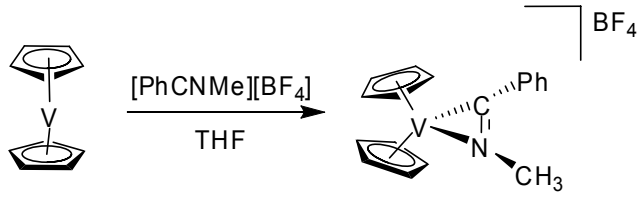

Scheme 1.13. Direct formation of an η^2-iminoacyl ligand via addition of nitrilium salt to vanadocene.

Table 1.2. Salient structural and spectroscopic data for selected η^2-iminoacyl complexes.

Complex	M-N (Å)	M-C (Å)	C-N (Å)	^{13}C, N≡*C* (δ)	IR, ν_{CN} (cm^{-1})
$[Cp^{tBu}{}_2Mo(\eta^2\text{-EtN}\equiv\text{C-CH}_3)]^+$	2.11	2.11	1.18	188.4	1745
$Cp^*TaCl(N\textit{t}Bu)(\eta^2\text{-C[C(Me)=NR]=NR})$[a]	2.16	2.19	1.25	238.2	n/a
$[Cp_2V(\eta^2\text{-MeN}\equiv\text{C-Ph})]^+$	2.05	2.03	1.24	n/a	1745
$Cp^*W(CO)_2(\eta^2\text{- R}_3\text{SiN}\equiv\text{C-Me})$[b]	2.22	2.09	1.27	235.2	1620
$[TpMo(NO)(MeIm)(\eta^2\text{-Bz-N}\equiv\text{C-Me})]^+$	2.13	2.12	1.24	202.6	n/a
$[Cp^*Rh(PMe_3)(\eta^2\text{- Ph}_3\text{Si-N}\equiv\text{C-}p\text{-OMeC}_6\text{H}_4)]^+$	2.13	1.96	1.25	196.8	n/a
$(dippe)Ni(\eta^2\text{- Ph}_3\text{B-N}\equiv\text{C-Me})$	1.90	1.84	1.24	n/a	n/a

[a] R = 2,6-$Me_2C_6H_3$, [b] R = *p*-Tol,

Relevant examples of structurally characterized η^2-iminoacyl complexes are found in Table 2. In general bond distances from the metal to each atom in the iminoacyl ligand are nearly equal. The intermediate isolated by Brookhart and Bergman,[47,48] along with the nitrile insertion product synthesized by Tobita[52] show a marked contrast between the metal-carbon and metal-nitrogen bond lengths. Although no formal explanation was proposed in either case, both complexes contain a bulky triphenylsilyl group on the iminoacyl nitrogen and Cp^* as an ancillary ligand. Steric relief may result in longer metal-nitrogen bonds. Little deviation is observed in the carbon-nitrogen multiple bond comparing η^2-nitrile and η^2-iminoacyl ligands. Iminoacyl carbon chemical shifts remain downfield in the deshielded range.

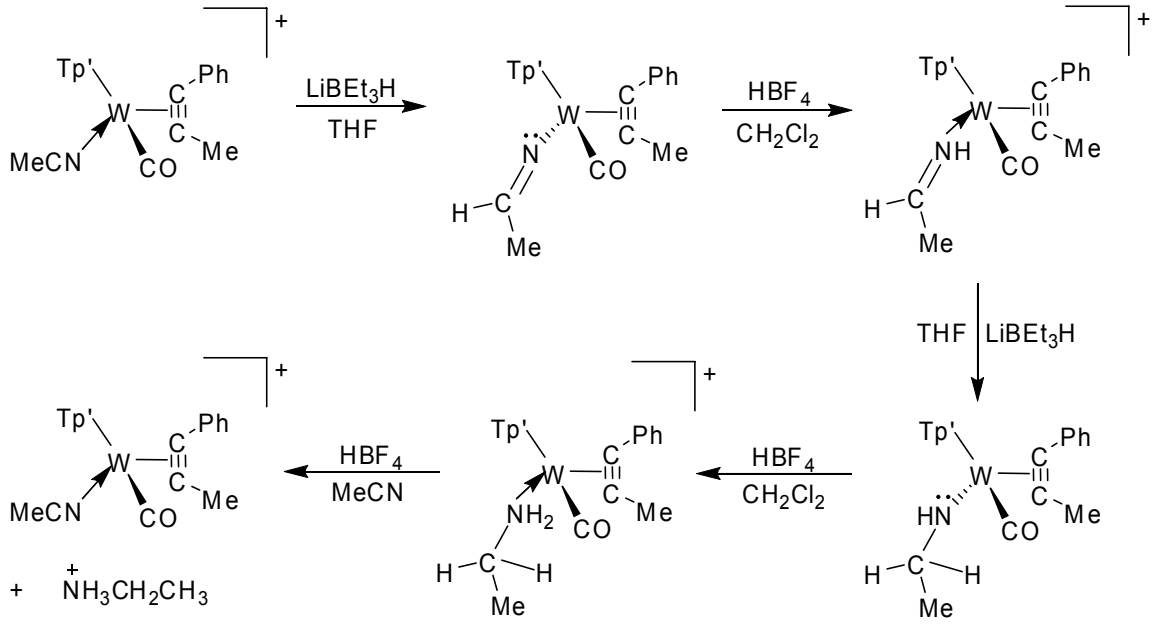

Scheme 1.14. Stepwise reduction of acetonitrile.

Our laboratory demonstrated stereoselective stepwise reduction of σ-bound acetonitrile to an amine aided by the presence of a variable electron donor alkyne in a low-valent tungsten coordination sphere in the late 1980s (Scheme 1.14).[53,54] Starting with $[Tp'W(CO)(\eta^2\text{-PhC}\equiv\text{CMe})(\sigma\text{-N}\equiv\text{CMe})]^+$ sequential additions of hydride and proton reduces the nitrile ligand to an amine. Addition of HBF_4 to the cationic amine complex in acetonitrile liberates the ammonium salt, and allows acetonitrile to coordinate to tungsten to regenerate $[Tp'W(CO)(\eta^2\text{-PhC}\equiv\text{CMe})(\sigma\text{-N}\equiv\text{CMe})]^+$ thus completing the stoichiometric cycle. Although not an example involving η^2-nitrile ligands, this reaction sequence illustrates the reactivity of the carbon-nitrogen multiple bond in the coordination sphere of a transition metal.

An early example of η^2-nitrile reactivity, reported by Thomas, shows the promise of reducing the carbon-nitrogen triple bond.[43] Stirring $Cp_2Mo(\eta^2\text{-N}\equiv\text{CCF}_3)$ in water with

hydrochloric acid generates an oxidized η^1-iminium cationic complex of the formula $[Cp_2MoCl(H_2N{=}CCF_3)][Cl]$. The iminium ligand binds through carbon and the product reflects addition of two protons to the original nitrile nitrogen atom. Presumably, the electron withdrawing ability of the trifluoromethyl substituent renders the nitrile nitrogen nucleophilic enough to bind two hydrogen atoms. Although a harsh reaction, this result highlights the favorable reactivity of η^2-nitriles toward reduction and further functionalization beyond iminoacyl derivatives.

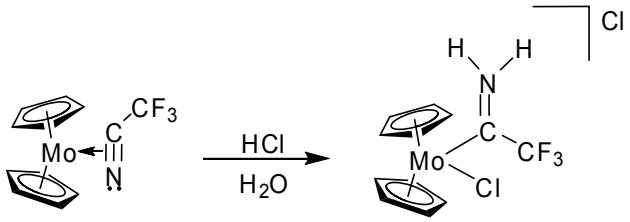

Scheme 1.15. Addition of HCl to η^2-N≡CCF_3 to form an η^1-iminium ligand.

Reported η^2-nitrile chemistry focuses on synthesis and structures of the η^2-nitrile complexes, while reactivity of the coordinated nitrile is underdeveloped. Initial efforts from our laboratory using dialkyldithiocarbamate (dtc) ancillary ligands were highly successful in generating sidebound alkyne ligands, but nitriles did not bind to the $(dtc)_2W(CO)$ fragment. Additionally, the sulfur-bound chelates engaged in undesirable cleavage and oxidation reactions.[55,56] To avoid potential reactivity at the ancillary ligand, we turned our attention to acetylacetonate (acac). The more electronegative oxygen chelates are "harder" ligands than their sulfur-based counterparts, and they are not as susceptible to alternate reactivity at the ligand. Acetylacetonate chelates also boast a larger bite angle (~80-85°) than dithiocarbamate chelates (69-70°) and thus favor octahedral geometries more in the metal coordination sphere.

We have constructed a low-valent tungsten center that promotes sidebound coordination of nitriles; these η^2-nitrile ligands are prone to additional ligand based manipulations. The acac ligands provide a reasonably rigid framework to stabilize the tungsten center and also promote η^2-binding of not only nitriles but several other unsaturated organic molecules starting from the $W(CO)_3(acac)_2$ reagent. We have reduced sidebound nitriles to sidebound iminium ligands aided in part by the presence of a variable electron donor alkyne. A key complex, $[W(CO)(acac)_2(\eta^2\text{-MeN=CPh})]^+$, proved to be a particularly agile reagent and a springboard for many reactions. The following chapters detail the development of tungsten(II) bis(acetylacetonate) chemistry showcased by several X-ray structures and detailed NMR analysis which highlight the synthetic manipulations discussed therein.

References

1. Kukushkin, V. Y.; Pombeiro, A. J. L. *Chem. Rev.* **2002**, *102*, 1771.

2. Kuznetsov, M. L. *Russ. Chem. Rev.* **2002**, *71*, 265.

3. Michelin, R. A.; Mozzon, M.; Bertani, R. *Coord. Chem. Rev.* **1996**, *147*, 299.

4. Morrow, J. R.; Tonker, T. L.; Templeton, J. L. *J. Am. Chem. Soc.* **1985**, *107*, 6956.

5. Templeton, J. L. *Adv. Organomet. Chem.* **1989**, *29*, 1.

6. Farona, M. F.; Bremer, N. J. *J. Am. Chem. Soc.* **1966**, *88*, 3735.

7. Farona, M. F.; Kraus, K. F. *Inorg. Chem.* **1970**, *9*, 1700.

8. Storhoff, B. N.; Lewis, H. C. *Coord. Chem. Rev.* **1977**, *23*, 1.

9. Wright, T. C.; Wilkinson, G.; Motevalli, M.; Hursthouse, M. B. *J. Chem. Soc. Dalton Trans.* **1986**, 2017.

10. Anderson, S. J.; Wells, F. J.; Wilkinson, G.; Hussain, B.; Hursthouse, M. B. *Polyhedron* **1988**, *7*, 2615.

11. Bullock, R. M.; Headford, C. E. L.; Hennessy, K. M.; Kegley, S. E.; Norton, J. R. *J. Am. Chem. Soc.* **1989**, *111*, 3897.

12. Churchill, D.; Shin, J. H.; Hascall, T.; Hahn, J. M.; Bridgewater, B. M.; Parkin, G. *Organometallics* **1999**, *18*, 2403.

13. Tsai, Y.; Stephens, F. H.; Meyer, K.; Mendiratta, A.; Gheorghiu, M. D.; Cummins, C. C. *Organometallics* **2003**, *22*, 2902.

14. Wadepohl, H.; Arnold, U.; Pritzkow, H.; Calhorda, M. J.; Veiros, L. F. *J. Organomet. Chem.* **1999**, *587*, 233.

15. Barrera, J.; Sabat, M.; Harman, W. D. *J. Am. Chem. Soc.* **1991**, *113*, 8178.

16. Barrera, J.; Sabat, M.; Harman, W. D. *Organometallics* **1993**, *12*, 4381.

17. Kiplinger, J. L.; Arif, A. M.; Richmond, T. G. *Organometallics* **1997**, *16*, 246.

18. Kiplinger, J. L.; Arif, A. M.; Richmond, T. G. *J. Chem. Soc. Chem. Commun.* **1996**, 1691.

19. Chetcuti, P. A.; Hawthorne, M. F. *J. Am. Chem. Soc.* **1987**, *109*, 942.

20. Chetcuti, P. A.; Knobler, C. B.; Hawthorne, M. F. *Organometallics* **1986**, *5*, 1913.

21. Chetcuti, P. A.; Knobler, C. B.; Hawthorne, M. F. *Organometallics* **1988**, *7*, 650.

22. Cross, J. L.; Garrett, A. D.; Crane, T. W.; White, P. S.; Templeton, J. L. *Polyhedron* **2004**, *23*, 2831.

23. Garcia, J. J.; Arevalo, A.; Brunkan, N. M.; Jones, W. D. *Organometallics* **2004**, *23*, 3997.

24. Garcia, J. J.; Brunkan, N. M.; Jones, W. D. *J. Am. Chem. Soc.* **2002**, *124*, 9547.

25. Garcia, J. J.; Jones, W. D. *Organometallics* **2000**, *19*, 5544.

26. Thomas, S.; Tiekink, E. R. T.; Young, C. G. *Organometallics* **1996**, *15*, 2428.

27. Thomas, S.; Young, C. G.; Tiekink, E. R. T. *Organometallics* **1998**, *17*, 182.

28. Thomas, S.; Lim, P. J.; Gable, R. W.; Young, C. G. *Inorg. Chem.* **1998**, *37*, 590.

29. Nielson, A. J.; Hunt, P. A.; Rickard, C. E. F.; Schwerdtfeger, P. *J. Chem. Soc. Dalton Trans.* **1997**, 3311.

30. Naota, T.; Tannna, A.; Kamuro, S.; Hieda, M.; Ogata, K.; Murahashi, S.; Takaya, H. *Chem. Eur. J.* **2008**, *14*, 2482.

31. Sakaki, S.; Biswas, B.; Sugimoto, M. *Organometallics* **1998**, *17*, 1278.

32. Nakazawa, H.; Kawasaki, T.; Miyoshi, K.; Suresh, C. H.; Koga, N. *Organometallics* **2004**, *23*, 117.

33. Nakao, Y.; Oda, S.; Hiyama, T. *J. Am. Chem. Soc.* **2004**, *126*, 13904.

34. Hashimoto, H.; Matsuda, A.; Tobita, H. *Organometallics* **2006**, *25*, 472.

35. Tsai, Y.; Johnson, M. J. A.; Mindiola, D. J.; Cummins, C. C. *J. Am. Chem. Soc.* **1999**, *121*, 10426.

36. Shin, J. H.; Savage, W.; Murphy, V. J.; Bonanno, J. B.; Churchill, D. G.; Parkin, G. *J. Chem. Soc. Dalton Trans.* **2001**, 1732.

37. Lis, E. C.; Delafuente, D. A.; Lin, Y. Q.; Mocella, C. J.; Todd, M. A.; Liu, W. J.; Sabat, M.; Myers, W. H.; Harman, W. D. *Organometallics* **2006**, *25*, 5051.

38. Bochmann, M.; Wilson, L. M.; Hursthouse, M. B.; Motevalli, M. *Organometallics* **1988**, *7*, 1148.

39. Campion, B. K.; Falk, J.; Tilley, T. D. *J. Am. Chem. Soc.* **1987**, *109*, 2049.

40. Daff, P. J.; Monge, A.; Palma, P.; Poveda, M. L.; Ruiz, C.; Valerga, P.; Carmona, E. *Organometallics* **1997**, *16*, 2263.

41. Wu, Z.; Diminnie, J. B.; Xue, Z. *Organometallics* **1999**, *18*, 1002.

42. Durfee, L. D.; Rothwell, I. P. *Chem. Rev.* **1988**, *88*, 1059.

43. Thomas, J. L. *J. Am. Chem. Soc.* **1975**, *97*, 5943.

44. Etienne, M.; Carfagna, C.; Lorente, P.; Mathieu, R.; de Montauzon, D. *Organometallics* **1999**, *18*, 3075.

45. Lorente, P.; Carfagna, C.; Etienne, M.; Donnadieu, B. *Organometallics* **1996**, *15*, 1090.

46. Galakhov, M. V.; Gomez, M.; Jimenez, G.; Royo, P.; Pellinghelli, M. A.; Tiripicchio, A. *Organometallics* **1995**, *14*, 1901.

47. Taw, F. L.; Mueller, A. H.; Bergman, R. G.; Brookhart, M. *J. Am. Chem. Soc.* **2003**, *125*, 9808.

48. Taw, F. L.; White, P. S.; Bergman, R. G.; Brookhart, M. *J. Am. Chem. Soc.* **2002**, *124*, 4192.

49. Sanchez-Nieves, J.; Royo, P.; Pellinghelli, M. A.; Tiripicchio, A. *Organometallics* **2000**, *19*, 3161.

50. Chamberlain, L. R.; Rothwell, I. P.; Huffman, J. C. *J. Chem. Soc. Chem. Commun.* **1986**, 1203.

51. Carrier, A. M.; Davidson, J. G.; Barefield, E. K.; Van Derveer, D. G. *Organometallics* **1987**, *6*, 454.

52. Suzuki, E.; Komuro, T.; Okazaki, M.; Tobita, H. *Organometallics* **2007**, *26*, 4379.

53. Feng, S. G.; Templeton, J. L. *J. Am. Chem. Soc.* **1989**, *111*, 6477.

54. Feng, S. G.; Templeton, J. L. *Organometallics* **1992**, *11*, 1295.

55. Brower, D. C.; Tonker, T. L.; Morrow, J. R.; Rivers, D. S.; Templeton, J. L. *Organometallics* **1986**, *5*, 1093.

56. Morrow, J. R.; Tonker, T. L.; Templeton, J. L. *Organometallics* **1985**, *4*, 745.

Chapter 2

Bis(acetylacetonato)tricarbonyltungsten(II): A Convenient Precursor to Chiral Bis(acac) Tungsten(II) Complexes

Introduction

Widespread utilization of acetylacetonato (acac) derivatives as ligands over the past four decades[1-5] and the recent renaissance of NacNac chemistry[6-9] provide a wealth of literature knowledge for launching Group VI d^4 $(acac)_2ML_n$ chemistry. To date few complexes of Group VI metals with two acac ligands have been reported. Monomeric Group VI d^4 complexes containing anionic bidentate S-donor dialkyldithiocarbamate (dtc) ligands have been thoroughly investigated, but examples with two anionic bidentate O-donor ligands bound to Group VI metals are scarce. Higher oxidation states of molybdenum, such as IV[10] and VI,[11] readily bind two equivalents of acetylacetonate. The venerable $Mo(O)_2(acac)_2$ complex has been used as a catalyst for epoxidation of olefins[12] and as a catalyst in dehydrative cyclizations.[13] Dimeric d^4 paddlewheel complexes of tungsten(II) and molybdenum(II) that boast bidentate anionic oxygen chelates, including acac, have multiple bonding between metal centers.[14] Chromium(II) bis(acac)[15] is one of few Group VI d^4 complexes in the literature with two coordinated acac chelates. No low valent monomeric Group VI complex has been available as a convenient source of the metal bis(acac) fragment for developing additional chemistry.

One motivation for using oxygen donor ligands to build a chiral bis(L—$X)_2M$ d^4moiety comparable to $(dtc)_2W(CO)_3$ was to build a more robust fragment to use as an auxiliary. The rich chemistry of $(dtc)_2WL_3$ includes sulfur redox chemistry, evident in unwanted dtc C-S cleavage reactions.[16-23] We chose to investigate acac in order to better control both electronic and steric factors around the metal center and to avoid the undesirable reactivity of the sulfur

donor chelates. Acetylacetonate was an attractive choice because of its ease of preparation and storied history. Previous attempts to coordinate acac to tungsten(II) carbonyl complexes generated a series of mono(acac) complexes;[24-29] only one W(II) bis(acac) complex has been reported.[30] Coordination of two formato ligands to a Group VI d^4 metal has been reported, but attempts to incorporate acetylacetonate into that system yielded only mono(acac) derivatives.[31] We report here coordination of two acetylacetonate ligands to tungsten(II) centers to form d^4 W(II) bis(acac) derivatives.

Results and Discussion

Synthesis of $W(CO)_3(acac)_2$ (1). Stoichiometric amounts of $[NEt_4][W(CO)_5I]$ and elemental iodine were stirred in methylene chloride at room temperature. Oxidation to tungsten(II) resulted in formation of the seven-coordinate anionic species, $[NEt_4][W(CO)_4I_3]$[33] (Scheme 2.1). In a separate flask, two equivalents of 2,4-pentanedione (H-acac) were combined with two equivalents of triethylamine in a small amount of CH_2Cl_2 (~5 mL). This solution was cannula transferred into the solution of $[NEt_4][W(CO)_4I_3]$. Infrared spectroscopy suggested the presence of $W(CO)_3(acac)_2$, **1**, as metal carbonyl stretches appeared at 2026 and 1916 cm^{-1}, with an intensity pattern compatible with a tricarbonyl species (Scheme 2.1). Separation of the neutral bis(acac) tungsten(II) tricarbonyl product from unwanted byproducts was achieved by extraction with hexanes, thus eliminating residual salts and unreacted tetracarbonyltriiodotungsten(II) anion.

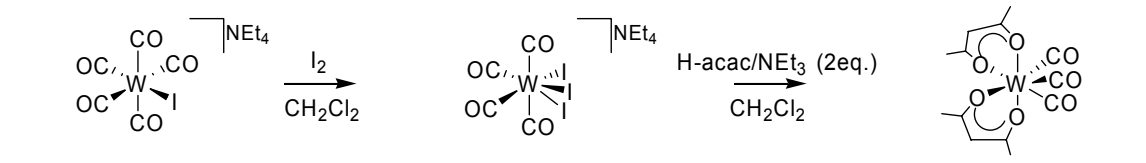

ν_{CO} = 2063, 1922, 1854 cm^{-1} ν_{CO} = 2072, 2001, 1935 cm^{-1} ν_{CO} = 2026, 1916 cm^{-1}

Scheme 2.1. Synthetic route to hepta-coordinate $W(CO)_3(acac)_2$ (**1**).

X-ray Structure of $W(CO)_3(acac)_2$ (1). Crystals for X-ray diffraction studies were generated from a concentrated solution of **1** in hexanes at -30 °C. The red, needle-like crystals were air and solvent sensitive, decomposing after a few hours. The crystal structure confirmed the formulation as a heptacoordinate tungsten(II) complex containing three metal carbonyl ligands, all *cis* relative to one another, and two acetylacetonate ligands, both chelated to the metal (Figure 2.1). Coordination of two bidentate chelates in this fashion generates a chiral metal center. *Cis* orientation of the carbon monoxide ligands maximizes their ability to accept π-electron density from the d^4 tungsten(II) center.

Bite angles adopted by the two acac chelates in **1** are 86.2 and 82.4°. Note that coordination of the two acac chelates to the smaller chromium metal in planar $Cr(acac)_2$ yielded bite angles of approximately 90°.[15] The related Mo(VI) d^0 complex, $Mo(acac)_2(O)_2$, contained acac chelate bite angles of 81 and 84°,[34] respectively, close to the values observed here for the acac ligands.

Tungsten-oxygen bond lengths to the four acac oxygen atoms ranged from 2.08 to 2.12 Å for $W(CO)_3(acac)_2$, comparable to the other Group VI bis(acac) distances. The molybdenum(VI) dioxo complex showed a wider range of metal-oxygen bond lengths (1.97 to 2.21 Å),[34] reflecting the *trans* effect of the oxo ligands. Both C-C and C-O bond lengths within each chelate ring reflected delocalization of π-electron density. Each carbon-carbon and carbon-oxygen bond was shorter than a typical single bond, yet longer than a typical

double bond. The same geometric description of the chelate ring holds true for other structures determined and discussed herein.

The three carbon monoxide ligands exhibited typical tungsten-carbon bond lengths for tungsten carbonyl complexes: 1.96, 1.99, and 2.00 Å.[35] Ligand-metal-ligand bond angles among the three carbon monoxide ligands with a common tungsten central atom in $W(CO)_3(acac)_2$ (67.9, 69.7, and 104.5°) were slightly smaller but surprisingly comparable to the OC-W-CO angles in $W(CO)_3(dtc)_2$ (71.7, 74.4, and 107.8°).[36]

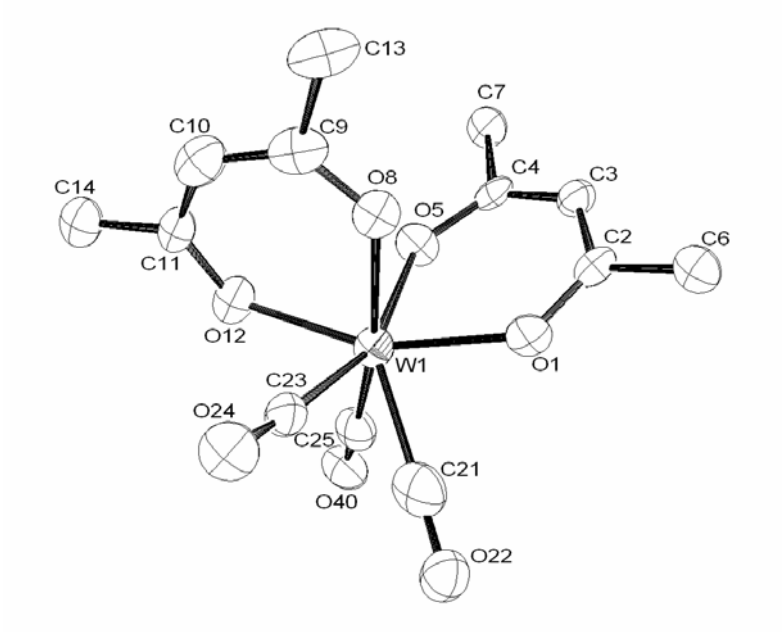

Figure 2.1. ORTEP diagram of $W(CO)_3(acac)_2$ (**1**).

Table 2.1. Selected bond lengths (Å) in $W(CO)_3(acac)_2$ (**1**).

W(1)-C(25)	1.960 (12)
W(1)-C(21)	1.994 (15)
W(1)-C(23)	1.997 (11)
W(1)-O(8)	2.083 (7)
W(1)-O(12)	2.092 (7)
W(1)-O(1)	2.106 (7)
W(1)-O(5)	2.115 (7)

Table 2.2. Selected bond angles (°) in $W(CO)_3(acac)_2$ (**1**).

C(25)-W(1)-C(21)	69.7 (5)
C(25)-W(1)-C(23)	104.5 (4)
C(21)-W(1)-C(23)	67.9 (4)
O(8)-W(1)-O(12)	86.2 (3)
O(1)-W(1)-O(5)	82.4 (3)

NMR Data for $W(CO)_3(acac)_2$ (1). The room temperature ^{1}H NMR spectrum of $W(CO)_3(acac)_2$ showed two singlets in a 6:1 ratio; one for the twelve acac methyl protons (2.08 ppm) and one for the two acac methine protons (5.67 ppm), respectively. As a result of the chiral tungsten(II) center and an absence of any rotation axis, all four acac methyl groups and both acac methine protons are positioned in unique chemical environments in the solid state, so the room temperature ^{1}H NMR spectrum is clearly incompatible with a static structure in solution. The simplicity of the spectrum, combined with the C_1 symmetry of the solid state structure, suggested that a fluxional process equilibrates all four methyl environments and both methine environments on the NMR time scale.

At ambient temperature, the ^{13}C NMR spectrum also reflected fluxionality. A single peak was observed for all four acac methyl carbons (27.4 ppm), one for the two acac methine carbons (102.8 ppm), one for the four acac carbonyl carbons (190.1 ppm), and one for the three metal carbonyl carbons (242.5 ppm). Lowering the acquisition temperature to 153 K resolved these signals into separate resonances. The room temperature carbon monoxide peak was resolved into three distinct resonances (231, 236, and 258 ppm), compatible with the C_1 symmetry of the solid state structure. Resolution of these three metal carbonyl carbon peaks at low temperature confirmed the fluxionality of this seven-coordinate molecule.

Synthesis of $W(CO)_2(L)(acac)_2$ (2). [L = PMe_3 (2a) or PMe_2Ph (2b)]. Addition of one equivalent of the appropriate phosphine to a solution of tricarbonyl complex **1** in methylene chloride led to replacement of one carbonyl ligand by the added phosphine, forming a dicarbonylbis(acac)phosphinetungsten(II) complex (Scheme 2.2). The reaction can be monitored via IR spectroscopy, and it was complete when the tricarbonyl pattern was replaced by the appearance of dicarbonyl absorptions at 1920 and 1810 cm^{-1}. Extraction of neutral complex **2** with ether left behind contaminating byproducts.

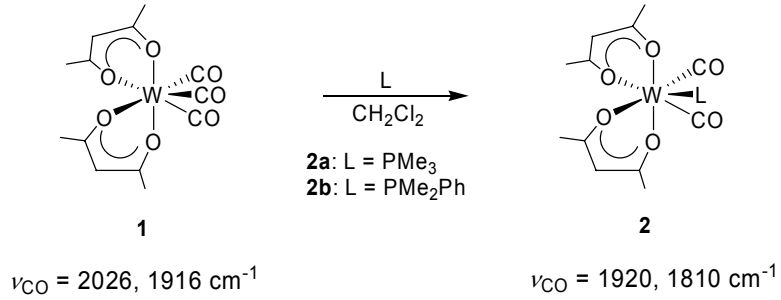

Scheme 2.2. Synthetic route to hepta-coordinate W(II)dicarbonylphosphine complexes.

X-ray Structure of $W(CO)_2(PMe_3)(acac)_2$ (2a). Dark red crystals were grown from a solution of **2a** in methylene chloride layered with hexanes which was cooled to -30°C for ten days. The X-ray structure of **2a** confirmed the identity of this hepta-coordinate tungsten(II) complex containing two acetylacetonate chelates, two carbon monoxide ligands and one trimethylphosphine ligand in the coordination sphere (Figure 2.2). The two carbonyl ligands were *cis* to one another, consistent with maximization of π-backbonding from the two filled dπ orbitals on the d^4 metal center to CO π^* orbitals. The two tungsten-

carbon bond lengths (1.96 and 1.97 Å) were nearly equal, and their values are typical of W-C distances for tungsten-carbonyl complexes.[35]

Bond angles among the two carbon monoxide ligands and the phosphine ligand with tungsten as the vertex can be definitively mapped to comparable angles among the three carbonyl ligands in **1**. Two acute angles and a third obtuse angle, which is ~35° larger, characterize the ML_3 fragment geometries of both **1** and **2a**. The phosphorus atom constitutes one leg of the obtuse angle in the bis(acac) phosphine complexes. This thermodynamically preferred isomer is no doubt easily accessible on the soft seven-coordinate energy surface.

Tungsten-oxygen bond lengths for the two acetylacetonate ligands range from 2.12 to 2.18 Å and are, on average, slightly longer for the dicarbonyl phosphine complex **2a** than for the parent tricarbonyl complex **1**. Increased σ-donation from the phosphine relative to the displaced carbon monoxide provides more electron density to the tungsten(II) center, perhaps lengthening the tungsten-oxygen bonds. More likely replacement of one small carbonyl ligand by a bulky phosphine ligand crowds the coordination sphere and lengthens the tungsten-oxygen bonds.

In accord with the steric hindrance created by trimethylphosphine, the bite angles of the acac chelates in the phosphine complex were, on average, slightly smaller than those in the parent tricarbonyl complex. Loss of carbon monoxide and coordination of a bulkier phosphine ligand perhaps forces the two acac chelates to adopt a smaller bite angle in a crowded seven-coordinate tungsten coordination sphere.

The tungsten-phosphorus bond length in the bis(acac) trimethylphosphine complex, **2a**, was 2.49 Å. This value is slightly shorter than bond lengths reported for other

tungsten(II)-carbonyl-phosphine complexes.[37,38] In **2a**, the chelates adopt a slightly different conformation than in precursor complex **1** in order to accommodate the incoming phosphine ligand.

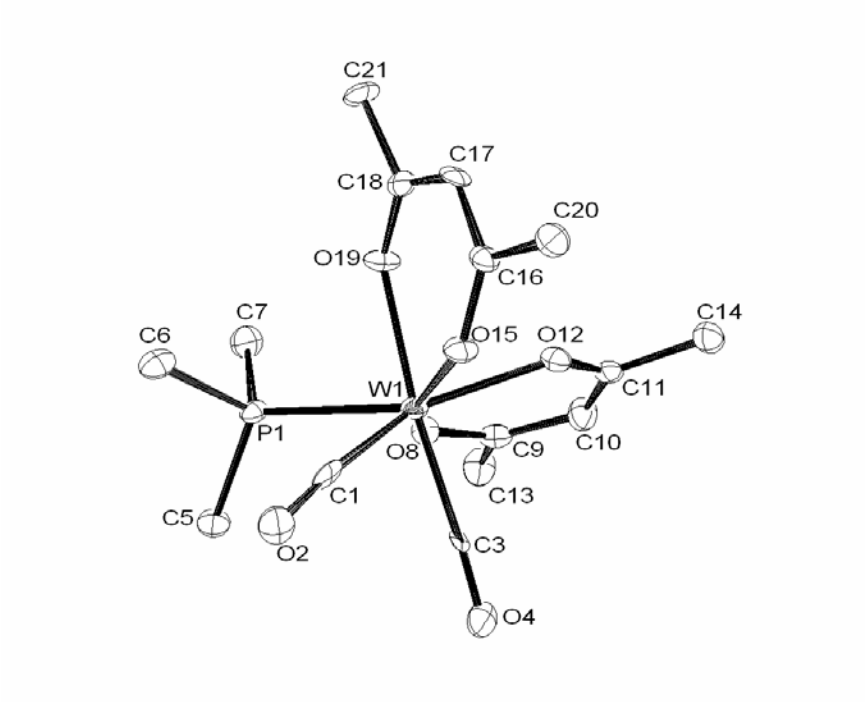

Figure 2.2. ORTEP diagram of $W(CO)_2(PMe_3)(acac)_2$ (**2a**).

Table 2.3. Selected bond lengths (Å) in $W(CO)_2(PMe_3)(acac)_2$ (**2a**).

W(1)-C(3)	1.962 (7)
W(1)-C(1)	1.971 (8)
W(1)-O(12)	2.118 (5)
W(1)-O(15)	2.128 (5)
W(1)-O(8)	2.141 (5)
W(1)-O(19)	2.183 (5)
W(1)-P(1)	2.496 (18)

Table 2.4. Selected bond angles (°) in $W(CO)_2(PMe_3)(acac)_2$ (**2a**).

C(3)-W(1)-C(1)	73.2 (3)
C(1)-W(1)-P(1)	71.4 (2)
C(3)-W(1)-P(1)	107.6 (18)
O(15)-W(1)-O(19)	83.5 (18)
O(12)-W(1)-O(8)	82.6 (18)

NMR Data for $W(CO)_2(L)(acac)_2$. The room temperature ^{1}H NMR spectrum of dimethylphenylphosphine complex **2b** showed a distinct peak for each of the two methine protons (5.76 and 5.40 ppm), indicating two inequivalent acac environments. In the room temperature ^{1}H NMR spectrum, the PMe_2Ph ligand displays a lone doublet (1.77 ppm, $^2J_{P\text{-}H}$ = 10 Hz) in the upfield methyl region. Note that the solid state structure should lead to two doublets as a result of phosphorus coupling to two distinct diastereotopic methyl groups. Only three acac methyl peaks were observed, with one integrating for 6H, and the other two appearing as much broader signals and integrating for 3H each.

A rapid rearrangement on the NMR time scale seemed likely, and indeed, the fluxional process was sufficiently slow at 193 K to allow observation of all four unique acac methyl peaks (2.16, 2.12, 1.96, 1.91 ppm). More informative was the presence of two doublets from the methyl groups of the PMe_2Ph ligand (1.73 and 1.66 ppm, $^2J_{P\text{-}H}$ = 10 Hz). These two methyl groups are diastereotopic at low temperature, so the phosphine ligand is indeed bound to a chiral tungsten center. Evidence of *intramolecular* fluxionality was provided by the $^{31}P\{^1H\}$ NMR spectrum at room temperature in which the lone singlet displayed tungsten satellites (^{183}W (14.28%), I = ½). Tungsten satellites would not be present if the phosphine ligand were rapidly dissociating and exchanging with other metal

centers. These data indicated that an intramolecular rearrangement process is rapidly exchanging both the acac sites and the two carbonyl ligand sites at room temperature, as well as equilibrating the two phosphine methyl groups.

Additional experiments were conducted using variable temperature NMR to probe activation energies for the fluxional process. The activation barrier, $\Delta G^{\ddagger}$, was calculated from the Eyring equation after the Gutowsky-Holm equation was used to calculate k_{ex} at the coalescence temperature.[39] At 210 K in the ^{1}H NMR spectrum, the two phosphine methyl signals coalesced into a broad singlet, prior to emerging into the doublet seen at ambient temperature. The coalescence temperature and chemical shift difference led to a calculated activation energy of 13.0 kcal/mole. The acac methyl groups remained as distinguishable singlets until coalescence occured at 213 K, which combined with the low temperature chemical shift difference to yield an activation energy of 13.2 kcal/mole. Both the phosphine methyl and the acac methyl exchange processes are attributed to a single fluxional process with an activation barrier near 13 kcal mol^{-1}.

The low temperature ^{1}H NMR data for **2b** was consistent with the static C_1 tungsten(II) bis(acac) phosphine structure observed in the solid state for **2a**. At room temperature the coalescence of the two diastereotopic phosphine methyl signals and convergence of only one pair of acac methyl signals suggested the presence of an effective mirror plane (as a result of the intramolecular fluxional process) *containing* one acac metallacycle and *bisecting* the other. One can imagine that the phosphine ligand swings through the mirror plane, thus converting the diastereotopic methyl groups to enantiomers of one another as it passes through the C_S intermediate structure.

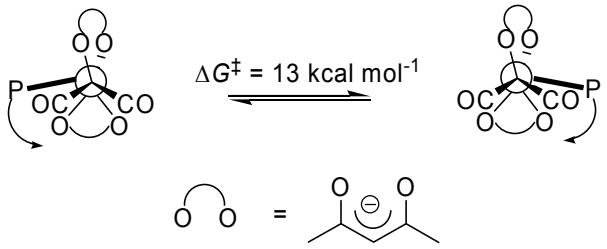

Scheme 2.3. Proposed movement of phosphine ligand (viewed parallel to the averaged mirror plane which is vertical and perpendicular to the paper).

The room temperature ^{13}C NMR spectrum provided further insight into the fluxional behavior displayed by the phosphine complex, **2b**. One key feature was the presence of two acac α-carbon peaks, indicating inequivalent chelate environments even in the fast exchange limit. Three resonances appeared for the acac ketone carbons, consistent with the presence of an effective mirror plane at room temperature. Two of these keto carbons are unique and lie in the mirror plane and the remaining two are equivalent to one another and lie on opposite sides of it. However, rather than observing three acac methyl carbon peaks, the spectrum showed only two. Given the fact that three acac methyl carbons should be observed based on analogy to the ^{1}H NMR spectrum, the data suggested that one purely coincidental chemical shift overlap occurred. A methyl doublet was observed upfield at 13.7 ppm ($^{1}J_{P\text{-}C}$ = 33 Hz) for the PMe_2Ph ligand. The presence of only one doublet demonstrated that the mirror plane also relates the two phosphine methyl carbons to one another. The two metal carbonyl peaks appeared as a broad singlet in the ^{13}C NMR spectrum at room temperature; this signal decoalesced at low temperature. At 193 K the metal carbonyl carbons appeared as widely separated doublets at 245.9 ($^{2}J_{P\text{-}C}$ = 8 Hz) and 277.3 ppm ($^{2}J_{P\text{-}C}$ = 43 Hz). Based on an empirical correlation of $^{2}J_{P\text{-}C}$ coupling constant with angle, the larger coupling constant suggests that carbon lies at a more obtuse angle to the phosphine ligand than the carbon with the smaller coupling constant.[40,41] (Since these complexes are seven-coordinate, not

octahedral, the distinction is not between *cis* and *trans,* but rather between acute and obtuse.) Crystallographic data showed that a larger angle exists between P1 and C3, so presumably this C3 carbon resonates at low field and displays the larger coupling constant.

Synthesis of W(CO)(η^2-$R^1C{\equiv}CR^2$)(acac)$_2$. [R^1 = Ph, R^2 = H (3^a), R^1 = R^2 = CH_3 (3b)]. Addition of one equivalent of alkyne to tricarbonyl complex **1** at ambient temperature displaced two carbon monoxide ligands resulting in η^2-coordination of the incoming alkyne ligand and yielding a monocarbonylmonoalkynebis(acac)tungsten(II) complex (Scheme 2.4). The reaction can be monitored via IR spectroscopy and was complete when the tricarbonyl infrared pattern was replaced by a single CO stretch at 1895 cm^{-1} indicating formation of a neutral monocarbonyl complex. Isolation of **3a** and **3b** was accomplished via column chromatography on silica using methylene chloride to elute a dark orange/brown band.

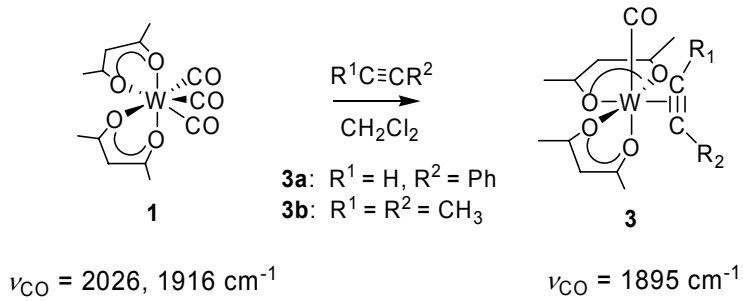

Scheme 2.4. Synthetic route to W(II)mono(carbonyl)mono(alkyne) complexes.

X-ray Structure of W(CO)(η^2-PhC≡CH)(acac)$_2$ (3a). Black crystals of **3a** were obtained via evaporation from a solution of methylene chloride and hexanes following column chromatography. The X-ray crystal structure of **3a** showed a tungsten atom surrounded by two acetylacetonate ligands, one carbon monoxide ligand, and one phenylacetylene ligand bound in an η^2-manner (Figure 2.3). The two chelates exhibited bite

angles of 82.4 and 85.4°, similar to those present in the parent tricarbonyl complex **1**. The average W-O bond distance was 2.10 Å, also comparable to the W-O distances in **1**.

The solid state structure showed that the alkyne and carbonyl ligands are *cis* with respect to each other, and they adopt a parallel configuration in terms of the C≡C triple bond axis and the W-C≡O axis. In the solid state the phenyl ring on the alkyne is oriented *anti* to the carbonyl ligand. This arrangement affords the phenyl ring an opportunity to engage in π-stacking with a pseudo-aromatic acac metallacycle.

The triple bond carbons (C3 and C4) in the alkyne ligand were separated by 1.30 Å, indicating a loss of some triple bond character upon coordination to the tungsten(II) center. This bond length is actually closer to that of a carbon-carbon double bond, and thus compatible with a metallacyclopropene resonance description. Formally, **3a** can be classified as either a six or seven-coordinate molecule, and metal-ligand bond angles reflect this ambiguity. It is easy to map the geometry of **3a** onto a distorted octahedral skeleton with the alkyne ligand occupying a single site. An angle of 161.5° was reported for O11-W1-O22, and 163.5° for O18-W1-C1. These values reflect significant deviation from an ideal octahedral geometry, as the atoms constituting these angles have shifted to accommodate the incoming alkyne ligand.

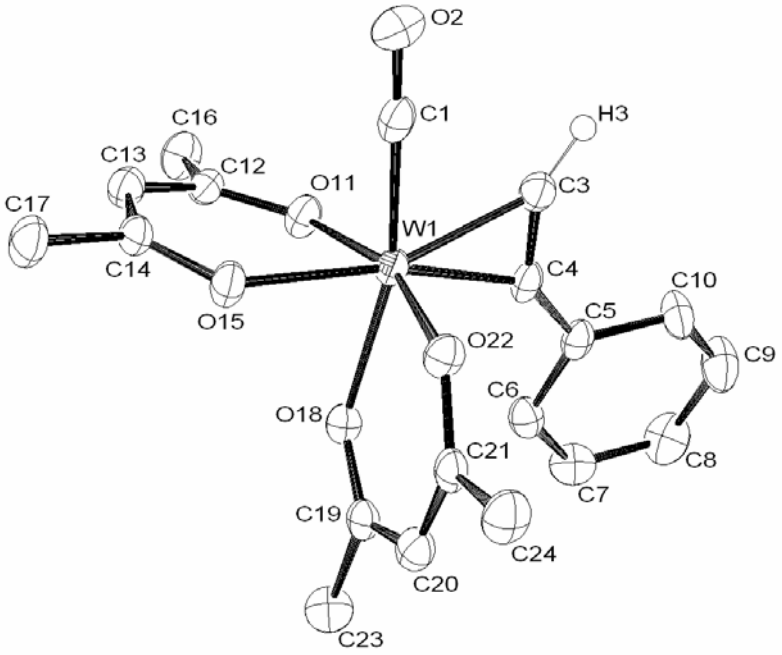

Figure 2.3. ORTEP diagram of W(CO)(η^2-PhC≡CH)(acac)$_2$ (**3a**).

Table 2.5. Selected bond lengths (Å) in W(CO)(η^2-PhC≡CH)(acac)$_2$ (**3a**).

W(1)-C(1)	1.946 (6)
W(1)-C(3)	2.036 (5)
W(1)-C(4)	2.037 (5)
W(1)-O(11)	2.058 (4)
W(1)-O(15)	2.117 (3)
W(1)-O(18)	2.145 (3)
W(1)-O(22)	2.070 (3)
C(3)-C(4)	1.301 (8)

Table 2.6. Selected bond angles (°) in W(CO)(η^2-PhC≡CH)(acac)$_2$ (**3a**).

C(1)-W(1)-C(3)	72.0 (21)
C(1)-W(1)-C(4)	109.2 (21)
C(3)-W(1)-C(4)	37.3 (21)
O(11)-W(1)-O(15)	82.4 (13)
O(18)-W(1)-O(22)	85.4 (13)

NMR Data for W(CO)(η^2-RC≡CR′)(acac)$_2$. The room temperature ^{1}H NMR spectrum of **3a** displayed four unique methyl signals and two unique methine signals, reflecting the inequivalent environments of the two β-diketonate ligands. Resonating at 12.95 ppm, the terminal alkyne proton appeared as a broad singlet at room temperature. Based on the empirical correlation between terminal alkyne proton chemical shifts of the coordinated acetylenic proton and electron donation, the alkyne ligand donates four electrons to the tungsten atom.[42-45] The broadness of the acetylenic proton peak can be attributed to rotation about the formal metal-alkyne centroid interconverting two isomers.[42,43] Observation of both alkyne rotamers was accomplished by low temperature NMR. At 193 K, the broad acetylenic proton signal separated into two sharp singlets; the major isomer (~98%) resonated at 12.98 ppm and the minor isomer (~2%) resonated at 12.49 ppm. Tungsten satellites are evident for the major isomer acetylenic proton peak ($^2J_{\text{W-H}}$ = 5 Hz). The phenyl ring does not reflect the fluxionality of the alkyne ligand in the ^{1}H NMR spectrum: *ortho, meta,* and *para* protons remained sharp and distinguishable at all temperatures. Presumably the chemical shift variations for the aromatic protons are much less than the roughly one-half ppm of the terminal alkyne proton, so exchange with the minor isomer does not noticeably broaden the aromatic peaks. The acetylacetonate ligands and carbon monoxide ligand remained static as the alkyne ligand rotates, and presumably the chemical shift differences between the isomers are small so that no evidence of fluxionality was observed in the proton signals for these ligands by NMR spectroscopy.

At room temperature, the ^{13}C NMR spectrum of **3a** also reflected the helical coordination mode of the two acac ligands. Four distinct signals were present both for the acac methyl carbons and for the acac ketone carbons, as well as two signals for the central

acac α-carbons, compatible with C_1 symmetry for this complex. The metal carbonyl carbon and the carbon atoms of the alkyne ligand were detected only at low temperature. Rotation of the alkyne ligand at room temperature broadened the carbon signals to the point that these ^{13}C peaks were not observable. At 193 K it was possible to assign resonances for the triple bond carbons, as well as for the carbon atoms in the phenyl ring. Chemical shift values for the alkyne carbons in both **3a** (211.7 and 185.6 ppm) and **3b** (209.2 and 188.4 ppm) were shifted downfield nearly 80-100 ppm from two-electron donor alkyne ligands.[42,46,47] These ^{13}C chemical shifts suggest that the alkyne ligand in these tungsten(II) bis(acac) complexes acts as a four electron donor to the metal center, resulting in a formal eighteen-electron complex.

Trapping the tricarbonyl complex **1** with a symmetric alkyne, in this case 2-butyne to yield **3b**, allowed extraction of the rotational barrier for the alkyne ligand. The rotational activation barrier, $\Delta G^{\ddagger}$, was calculated from the Eyring equation after the Gutowsky-Holm equation was used to calculate k_{ex} at the coalescence temperature. Variable temperature NMR indicated a coalescence temperature of 286 K for the rotating 2-butyne ligand, and the barrier to rotation for this symmetric alkyne derivative was found to be 17.8 kcal mol^{-1} (Scheme 2.5).

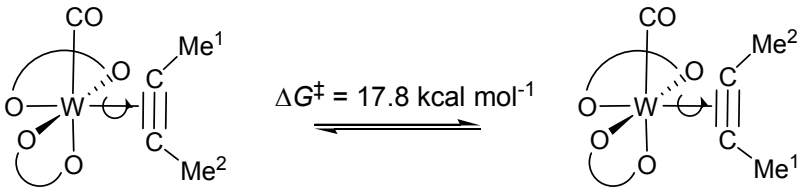

Scheme 2.5. Rotation of the alkyne ligand along the metal-alkyne centroid

The room temperature ^{13}C NMR spectrum of **3b** also reflected helical coordination of the acac ligands. As for the phenylacetylene derivative **3a**, ten distinct peaks were observed

for the ten unique carbons that constitute the two anionic chelates in **3b**. Two broad peaks representing the two methyl carbons on the alkyne ligand were resolved into sharp singlets in the low temperature spectrum. They are accompanied by tungsten satellites ($^2J_{W\text{-}C}$ = 65 Hz), whose presence indicates that the alkyne remains bound to the tungsten center while rotating. Characterization data for **3b** here differs from data reported earlier for this same complex, which was synthesized by a different route. The discrepancy lies in the ^{1}H and ^{13}C NMR data: two methine proton peaks and two acac methyl peaks were reported[30] in contrast to the C_1 symmetry reflected in two methine peaks and four acac methyl groups observed in this work. Additionally the signals reported for the metal carbonyl carbon and the triple bond carbon are assigned differently here. The NMR data presented here for both alkyne derivatives is compatible with the observed solid state conformation of **3a**.

Synthesis of W(η^2-PhC≡CPh)$_2$(acac)$_2$ (4). Refluxing tricarbonyl reagent **1** with excess diphenylacetylene led to replacement of all three carbon monoxide ligands by two alkyne ligands, resulting in tungsten(II) bis(acac) bis(diphenylacetylene), complex **4** (Scheme 2.6). The reaction was complete upon disappearance of the single carbonyl stretching absorption of the monoalkyne monocarbonyl derivative. Isolation of pure bis(alkyne) complex was achieved via column chromatography using toluene to elute a yellow band.

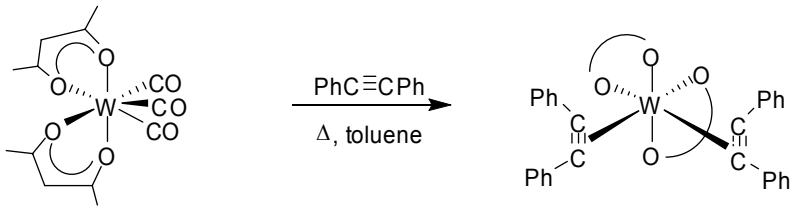

1 **4**

Scheme 2.6. Synthetic route to W(η^2-PhC≡CPh)$_2$(acac)$_2$ (**4**).

X-ray Structure of W(η^2-PhC≡CPh)$_2$(acac)$_2$ (4). Bright yellow crystals of complex **4** were grown by evaporating a solution of **4** in methylene chloride and hexanes. X-ray diffraction studies of **4** verify coordination of two acetylacetonate ligands and two diphenylacetylene ligands, coordinated in a *cis* fashion, to a tungsten center (Figure 2.4). Both alkyne ligands are parallel to one another; the triple bonds are aligned. This mode of coordination has been observed in other group VI bis(alkyne) complexes with two anionic bidentate chelates.[48,49] Tungsten-oxygen bond lengths (2.12 to 2.14 Å) are slightly longer, on average, than those seen in complexes **1** and **3a**, but they are comparable to those of the phosphine adduct, complex **2a**. The bite angles of the oxygen donor chelates are nearly equal in **4** (82.5 and 82.8°), reflecting the C_2 symmetry generated by coordination of two symmetric alkynes. The four phenyl rings of the two alkyne ligands appear to orient themselves in a manner suitable for π-stacking.

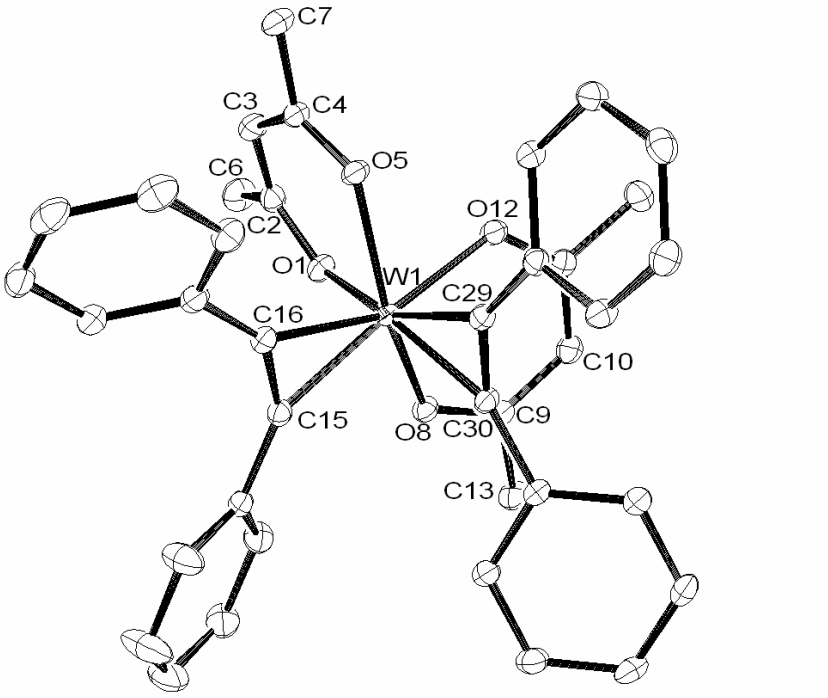

Figure 2.4. ORTEP diagram of W(η^2-PhC≡CPh)$_2$(acac)$_2$ (**4**).

Table 2.7. Selected bond lengths (Å) in W(η^2-PhC≡CPh)$_2$(acac)$_2$ (**4**).

W(1)-C(16)	2.062 (13)
W(1)-C(30)	2.067 (13)
W(1)-C(15)	2.068 (13)
W(1)-C(29)	2.073 (13)
W(1)-O(1)	2.116 (10)
W(1)-O(8)	2.130 (10)
W(1)-O(5)	2.137 (9)
W(1)-O(12)	2.144 (10)
C(15)-C(16)	1.314 (19)
C(29)-C(30)	1.311 (18)

Table 2.8. Selected bond angles (°) in W(η^2-PhC≡CPh)$_2$(acac)$_2$ (**4**).

C(16)-W(1)-C(15)	37.1 (5)
C(30)-W(1)-C(29)	36.9 (5)
O(1)-W(1)-O(5)	82.5 (4)
O(8)-W(1)-O(12)	82.8 (4)

NMR Data for W(η^2-PhC≡CPh)$_2$(acac)$_2$ (4). The room temperature ^{1}H NMR spectrum for **4** showed two acac methyl resonances (2.17 and 1.82 ppm) and one acac methine resonance (5.44 ppm) in addition to indistinguishable multiplets in the aromatic region (7.15-7.85 ppm), consistent with formation of a bis(acac)bis(alkyne) complex. For symmetric alkyne ligands, such as diphenylacetylene, these molecules contain a C_2 axis. The two acac ligands are equivalent to one another because of the C_2 axis, but within each acac ligand one of the methyl proton reporter groups is *cis* to an alkyne ligand, and one is *trans*, thus producing two methyl signals in the ^{1}H NMR.

Room temperature ^{13}C NMR data for **4** confirmed the presence of a two-fold axis generated by the coordination of two coparallel alkynes to the tungsten(II) bis(acac) fragment. The spectrum mimicked the behavior displayed in the ^{1}H NMR spectrum: two resonances were present for the four acac methyl carbons (26.6 and 28.1 ppm), and one resonance appeared for the two acac α-carbons, which was accompanied by tungsten satellites (102.0 ppm, $^3J_{W\text{-}C}$ = 62 Hz). Likewise, only two peaks were present for the four acac ketone carbons (185.4 and 190.4 ppm).

Previous studies have shown that the number of electrons donated by η^2-bound alkyne ligands roughly correlates with the chemical shift of the alkyne carbons.[47] The alkyne carbons of **4** were slightly broadened in the room temperature ^{13}C NMR spectrum, suggesting that the rate of rotation of the alkyne ligands was approaching the NMR time scale. The chemical shifts of these two alkyne carbons appeared at δ = 194.3 and 201.4 ppm (avg. = 197.9 ppm). This averaged ^{13}C chemical shift is farther downfield than comparable values for other complexes containing two alkyne ligands that formally donate three electrons each to the metal center.[47-49] Perhaps this stems from the electronegativity of the oxygen-donor

chelates. Surrounded by four oxygen atoms, the tungsten center is more electron deficient than in the analogous dithiocarbamate complexes, and as a result, the two alkyne ligands provide greater π-electron donation to counteract this effect. Of course formal electron counting is merely a method of bookkeeping, and not sophisticated enough to track the continuum of bonding options available to alkyne ligands.

Table 2.9. Crystal and Data Collection Parameters for $W(CO)_3(acac)_2$ (**1**), $W(CO)_2(PMe_3)(acac)_2$ (**2a**), $W(CO)(\eta^2\text{-PhC}\equiv\text{CH})(acac)_2$ (**3a**), $W(\eta^2\text{-PhC}\equiv\text{CPh})_2(acac)_2$ (**4**).

Complex	**1**	**2a**	**3a**	**4**
EMPIRICAL FORMULA	$C_{13}H_{14}O_7W$	$C_{15}H_{23}O_6PW$	$C_{19}H_{20}O_5W$	$C_{38}H_{34}O_4W$
Formula Weight	466.09	514.15	512.24	738.50
Color	red	dark red	black	bright yellow
Temperature	100 K	100 K	100 K	100 K
Wavelength	0.71703 Å	0.71703 Å	0.71703 Å	0.71703 Å
Crystal System	Monoclinic	Monoclinic	Monoclinic	Triclinic
Space Group	*C*2/*c*	$P2_1/c$	$P2_1/n$	*P*-1
Unit Cell Dimensions	a = 15.261 Å b = 15.416 Å c = 12.883 Å α = 90° β = 94.87° γ = 90°	a = 12.891 Å b = 9.4512 Å c = 15.714 Å α = 90° β = 105.093° γ = 90°	a = 8.439 Å b = 20.224 Å c = 11.192 Å α = 90° β = 106.649° γ = 90°	a = 9.545 Å b = 9.897 Å c = 16.929 Å α = 98.517° β = 91.869° γ = 91.631°
Volume	3020 $Å^3$	1848 $Å^3$	1830 $Å^3$	1580$Å^3$
Z	8	4	4	2
Density (calculated)	2.050 Mg/m^3	1.848 Mg/m^3	1.866 Mg/m^3	1.552 Mg/m^3
Absorption Coefficient	7.68 mm^{-1}	6.36 mm^{-1}	6.35 mm^{-1}	6.70 mm^{-1}
F(000)	1776	1000	998	736
Crystal size	0.30 x 0.05 x 0.05 mm^3	0.25 x 0.20 x 0.10 mm^3	0.20 x 0.20 x 0.10 mm^3	0.35 x 0.20 x 0.15 mm^3
Theta range	1.88 to 24.07°	2.71 to 25.00°	5.00 to 56.00	2.08 to 30.00
Index Ranges	-17<=h<=17 -17<=k<=17 -14<=l<=12	-14<=h<=15 -11<=k<=10 -18<=l<=18	-11<=h<=10 0<=k<=26 0<=l<=14	-13<=h<=13 -13<=k<=13 -23<=l<=23
Reflections Collected	13400	10605	17909	44704
Independent reflections	2347 [R(int) = 0.0694]	3237 [R(int) = 0.0313]	4433 [R(int) = 0.042]	9174 [R(int) = 0.0218]
Data/restraints/parameters	2347/0/195	3237/0/216	4433/0/227	9174/0/392
Goodness-of-fit on F^2	1.083	1.177	1.313	1.031
Final R indices[I>2sigma(I)]	R1 = 0.0379 wR2 = 0.0709	R1 = 0.0338 wR2 = 0.0742	R1 = 0.032 wR2 = 0.039	R1 = 0.0139 wR2 = 0.0341
R indices (all data)	R1 = 0.0689 wR2 = 0.0837	R1 = 0.0420 wR2 = 0.0769	R1 = 0.044 wR2 = 0.141	R1 = 0.0145 wR2 = 0.1343
Largest diff. peak and hole	1.273 and -1.355 e $Å^{-3}$	1.859 and -1.382 e $Å^{-3}$	2.000 and -1.430 e $Å^{-3}$	0.907 and -0.652 e $Å^{-3}$

Summary

Chiral, neutral, monomeric complexes containing the W(II)(acac)$_2$ (acac = acetylacetonate) moiety have been synthesized from a convenient starting material, the pentacarbonyl iodotungsten(0) anion. Oxidation of the tungsten(0) reagent with elemental iodine and subsequent addition of two equivalents of the acac anion resulted in formation of a reactive seven-coordinate eighteen-electron tricarbonyl complex, W(CO)$_3$(acac)$_2$ (**1**). Addition of phosphine nucleophiles (L = PMe_3 (**2a**), PMe_2Ph (**2b**)) to **1** generated seven-coordinate complexes of the type W(CO)$_2$(L)(acac)$_2$. The parent complex, **1**, also reacted readily with alkynes (PhC≡CH (**3a**) and MeC≡CMe (**3b**)) to form complexes of the type W(CO)(η^2-$R^1C{\equiv}CR^2$)(acac)$_2$. Refluxing with excess diphenylacetylene led to coordination of two alkyne ligands and yielded the bis(alkyne) complex, W(PhC≡CPh)$_2$(acac)$_2$ (**4**). X-ray crystallography provided structural assignments for a representative molecule from each class of these complexes, and variable temperature ^{1}H and ^{13}C NMR probed the fluxional processes within this series of bis(acetylacetonate) tungsten d^4 complexes.

Experimental

General Information. Reactions were performed under a dry nitrogen atmosphere using standard Schlenk techniques. Methylene chloride, diethyl ether, hexanes, toluene, and pentane were purified by passage through an activated alumina column under a dry argon atmosphere. Methylene chloride-d_2 was dried over CaH_2 and degassed. All other reagents were purchased from commercial sources and were used without further purification.

NMR spectra were recorded on Bruker DRX400, AMX400, or AMX300 spectrometers. Infrared spectra were recorded on an ASI Applied Systems ReactIR 1000 FT-IR spectrometer. Elemental analysis was performed by Atlantic Microlab, Norcross, GA.

The $[NEt_4][W(CO)_5I]$ reagent was made in accordance with a literature procedure.[32] It was important to purify this reagent prior to use via chromatography on an alumina column with acetone as eluent.

$W(CO)_3(acac)_2$ (1). In a 200 mL Schlenk flask a solution of $[NEt_4][W(CO)_5I]$ (590 mg, 1.0 mmol) was combined with a stoichiometric amount of elemental iodine (265 mg, 1.0 mmol) in CH_2Cl_2 (20 mL). The solution was stirred for 20 min. until formation of the orange $[NEt_4][W(CO)_4I_3]$ species was complete. In a separate flask, a solution of 2,4-pentanedione (H-acac) (0.220 mL, 2.05 mmol) in CH_2Cl_2 (10 mL) was deprotonated by triethylamine (0.285 mL, 2.05 mmol) to yield $[acac]^-$ *in situ*. This solution was combined with the solution containing the tetracarbonyl triiodide complex and then stirred for 2h to yield $W(CO)_3(acac)_2$, whose formation was monitored by *in situ* IR spectroscopy. The solvent volume was reduced *in vacuo* and then hexanes were added. The remainder of the CH_2Cl_2 solvent was removed, and the dark red residual liquid was cannula filtered into another flask and stored at -30°C for crystallization (90 mg, 20%). IR (hexanes): ν_{CO} = 2028, 1924 cm^{-1},

(KBr): 2026, 1908, 1895 cm^{-1}. ^1H NMR (CD_2Cl_2, 298 K, δ): 5.67 (s, 2H, acac C*H*), 2.08 (s, 12H, acac CH_3); $^{13}C\{^1H\}$ NMR (CD_2Cl_2, 298 K δ): 27.4 (acac *C*H_3), 102.8 (acac *C*H), 190.1 (acac *C*O), 242.5 (*C*≡O); $^{13}C\{^1H\}$ NMR ($CDCl_2F$, 153 K, δ): 231.0 (*C*≡O), 235.6 (*C*≡O), 257.8 (*C*≡O). Anal. Calcd for $C_{13}H_{14}O_7W$: C, 33.50; H, 3.03. Found: C, 33.10; H, 3.19%.

$W(CO)_2(PMe_3)(acac)_2$ (2a). Complex **1** was synthesized as described *vide supra*. The volume of CH_2Cl_2 solvent was reduced *in vacuo* and hexane was added to precipitate unreacted starting material. The tricarbonyl precursor, complex **1,** was extracted into the filtrate and the remainder of the CH_2Cl_2 solvent was removed *in vacuo.* In a separate flask, trimethylphosphine (0.040 mL, 0.50 mmol) was added to hexanes (7 mL). The hexane solution of **1** was cannula filtered into the flask with the hexane solution of trimethylphosphine, and the reaction mixture was stirred for 1h. The solvent was removed *in vacuo* to yield a dark red solid. IR (hexanes): ν_{CO} = 1928, 1831 cm^{-1}. ^1H NMR (CD_2Cl_2, 298 K, δ): 5.75, 5.37 (each a s, each 1H, acac C*H*), 2.15 (br s, 6H, acac CH_3), 1.93 (s, 6H, acac CH_3), 1.52 (d, P-CH_3, $^2J_{P\text{-}H}$ = 10 Hz); $^{13}C\{^1H\}$ NMR (CD_2Cl_2, 298 K, δ): 14.6 (d, P*Me*$_3$, $^1J_{C\text{-}P}$ = 33 Hz, $^2J_{W\text{-}C}$ = 69 Hz), 27.3, 27.4 (acac *C*H_3), 101.1, 102.2 (acac *C*H), 188.6, 188.9, 189.7 (acac *C*O); $^{13}C\{^1H\}$ NMR (CD_2Cl_2, 193 K, δ): 246.7 (*C*≡O, $^1J_{W\text{-}C}$ = 166 Hz, $^2J_{C\text{-}P}$ = 8 Hz), 276.6 (*C*≡O, $^1J_{W\text{-}C}$ = 144 Hz, $^2J_{P\text{-}C}$ = 41 Hz); $^{31}P\{^1H\}$ NMR (CD_2Cl_2, 298 K, δ): 11.21 (s, $^1J_{W\text{-}P}$ = 217 Hz). Anal. Calcd for $C_{15}H_{23}O_6PW$: C, 35.45; H, 4.57. Found: C, 34.76; H, 4.57%.

$W(CO)_2(PMe_2Ph)(acac)_2$ (2b). Complex **1** was synthesized as described *vide supra*. The volume of CH_2Cl_2 solvent was reduced *in vacuo* and hexane was added to precipitate unreacted starting material. The tricarbonyl precursor, complex **1,** was extracted into the

filtrate and the remainder of the CH_2Cl_2 solvent was removed *in vacuo*. In a separate flask, dimethylphenylphosphine (0.070 mL, 0.50 mmol) was added to hexanes (7 mL). The hexane solution of **1** was cannula filtered into the flask with the hexane solution of dimethylphenylphosphine, and the reaction mixture was stirred for 1h. The solvent was removed *in vacuo* to yield a dark red solid. (160 mg, 26%). IR (hexanes): ν_{CO} = 1930, 1835 cm^{-1}. ^1H NMR (CD_2Cl_2, 298 K δ): 7.50-7.51 (m, 2H, P-C_6H_5), 7.40-7.43 (m, 3H, P-C_6H_5), 5.76, 5.40 (each a s, each 1H, acac C*H*), 2.16, 2.12 (each a s, each 3H, acac CH_3), 1.94 (s, 6H, acac CH_3), 1.76 (d, 6H, PMe_2Ph, $^2J_{P\text{-}H}$ = 10 Hz); ^1H NMR (CD_2Cl_2, 193 K δ): 1.96, 1.91 (each a s, each 3H, acac CH_3), 1.73, 1.66 (each a d, each 3H, P-CH_3, $^2J_{P\text{-}H}$ = 10 Hz); $^{13}C\{^1H\}$ NMR (CD_2Cl_2, 298 K, δ): 13.7 (d, PMe_2Ph, $^1J_{P\text{-}C}$ = 33 Hz), 27.3, 27.5 (acac CH_3), 101.1, 102.3 (acac *C*H), 128.5 (d, *o*-C_6H_5, $^2J_{P\text{-}C}$ = 9 Hz), 130.3 (*p*-C_6H_5), 131.2 (d, *m*-C_6H_5, $^3J_{P\text{-}C}$ = 8 Hz), 135.6 (d, *ipso*- C_6H_5, $^1J_{P\text{-}C}$ = 49 Hz), 188.6, 188.9, 189.9 (acac *C*O); $^{13}C\{^1H\}$ NMR (CD_2Cl_2, 193 K, δ): 245.9 (d, *C*≡O, $^2J_{P\text{-}C}$ = 8 Hz), 277.3 (d, *C*≡O, $^2J_{P\text{-}C}$ = 43 Hz); $^{31}P\{^1H\}$ NMR (CD_2Cl_2, δ): 18.7 (s, $^1J_{P\text{-}W}$ = 225 Hz).

W(CO)(PhC≡CH)(acac)$_2$ (3a). Complex **1** was synthesized as described *vide supra*. Excess phenylacetylene (~2 eq.) was added to the tricarbonyl complex and the solution was stirred for 2 h. The solvent was removed *in vacuo* and the desired product was extracted with diethyl ether. Purification was accomplished by chromatography on a silica column using CH_2Cl_2 and hexanes to elute a dark orange/brown band. Black crystals were obtained by layering CH_2Cl_2 with hexanes (27%). IR (hexanes): ν_{CO} = 1920 cm^{-1}, (KBr): ν_{CO} = 1903 cm^{-1}. ^1H NMR (CD_2Cl_2, 298 K, δ): 12.96 (br s, 1H, PhC≡C*H*, $^2J_{W\text{-}H}$ = 5 Hz), 7.58-7.60 (m, 2H, C_6H_5 *ortho*), 7.44-7.48 (m, 2H, C_6H_5 *meta*), 7.28-7.32 (m, 1H, C_6H_5 *para*), 5.58, 5.51 (each a s, each 1H, acac C*H*), 2.20, 2.16, 2.14, 1.89 (each a s, each 3H, acac CH_3); ^1H NMR

(CD_2Cl_2, 193 K, δ): 13.00 (s, PhC≡C*H*, major rotamer, 98%), 12.49 (s, PhC≡C*H*, minor rotamer, 2%), $^{13}C\{^1H\}$ NMR (CD_2Cl_2, 298 K, δ): 26.1, 26.6, 26.7, 28.3 (acac *C*H_3), 100.2, 102.1 (acac *C*H), $^{13}C\{^1H\}$ NMR (CD_2Cl_2, 193 K, δ): 128.3 (*C*$_6H_5$-*ortho*), 129.5 (*C*$_6H_5$-*para*), 130.7 (*C*$_6H_5$-*meta*), 133.9 (*C*$_6H_5$-*ipso*) 185.4, 187.8, 188.2, 194.9 (acac *C*O), 185.6 (Ph*C*≡CH), 211.7 (PhC≡*C*H), 240.9 (*C*≡O) Anal. Calcd for $C_{19}H_{20}O_5W$: C, 44.56; H, 3.94; O, 15.62. Found: C, 44.71; H, 3.93; O, 15.51%.

W(CO)(MeC≡CMe)(acac)$_2$ (3b). Complex **1** was synthesized as described *vide supra*. Excess 2-butyne (~2 eq.) was added and the reaction mixture was stirred for 1h. The solvent was removed *in vacuo* and the desired product was extracted with diethyl ether before being further purified on a silica column using CH_2Cl_2 and hexanes to elute a dark orange/brown band. IR (hexanes): ν_{CO} = 1906 cm^{-1}. ^1H NMR (CD_2Cl_2, 298 K, δ): 5.53, 5.49 (each a s, each 1H, acac C*H*), 3.14 (br s, 6H, *H*$_3$C-C≡C-C*H*$_3$), 2.18, 2.16, 2.09, 1.86 (each a s, each 3H, acac C*H*$_3$); ^1H NMR (CD_2Cl_2, 250 K, δ): 3.18, 3.13 (each a s, each 3H, *H*$_3$C-C≡C-C*H*$_3$); $^{13}C\{^1H\}$ NMR (CD_2Cl_2, 298 K, δ): 26.2, 26.7, 26.8, 28.4 (acac *C*H_3), 100.2, 101.7 (acac *C*H), 186.1, 187.6, 188.1, 194.4 (acac *C*O); $^{13}C\{^1H\}$ NMR (CD_2Cl_2, 193 K, δ): 16.2, 20.1 (H$_3$*C*-C≡C-*C*H$_3$, $^2J_{W\text{-}C}$ = 65 Hz), 188.4 (H$_3$C-C≡*C*-CH$_3$), 209.2 (H$_3$C-*C*≡C-CH$_3$, $^1J_{W\text{-}C}$ = 29 Hz), 242.4 (*C*≡O, $^1J_{W\text{-}C}$ = 80 Hz) Anal. Calcd for $C_{15}H_{20}O_5W$: C, 38.81; H, 4.35; O, 17.23. Found: C, 38.51; H, 4.46; O, 16.83%.

W(PhC≡CPh)$_2$(acac)$_2$ (4). Complex **1** was synthesized as described *vide supra*, and then it was extracted with toluene and cannula filtered into a separate flask. Excess diphenylacetylene (~5 eq) was added, and the solution was refluxed until IR spectroscopy indicated an absence of metal carbonyl stretches. The solvent was removed *in vacuo*, and the crude material was chromatographed on alumina using toluene as an eluent, yielding a dark

yellow band. The toluene was removed on a rotary-evaporator and the yellow product was washed with pentane to remove excess alkyne. Bright yellow crystals were grown by slow evaporation of a solution of **4** in CH_2Cl_2/hexanes (150 mg, 20%). IR (KBr): $\nu_{C\equiv C}$ = 1742 cm^{-1}; ^1H NMR (CD_2Cl_2, 298 K, δ): 7.15-7.85 (m, 20H, C_6H_5), 5.44 (s, 2H, acac C*H*), 2.17, 1.82 (each a s, each 6H, acac CH_3); $^{13}C\{^1H\}$ NMR (CD_2Cl_2, 298 K, δ): 26.6 , 28.1 (acac CH_3), 102.0 (acac *C*H, $^3J_{W\text{-}C}$ = 62 Hz), 127.7, 128.0, 128.2, 128.7, 128.8, 129.7, 130.9, 131.9, 141.1 ($H_5C_6C{\equiv}CC_6H_5$), 185.4, 190.4 (acac *C*O), 194.3, 201.4 (Ph*C*≡*C*Ph) Anal. Calcd for $C_{38}H_{34}O_4W$: C, 61.79; H, 4.65; O, 8.66. Found: C, 61.93; H, 4.60; O, 8.61%.

References

1. Yamazaki, S. *Heterogeneous Chem. Rev.* **1995**, *2*, (2), 103.

2. Joshi, K. C.; Pathak, V. N. *Coord. Chem. Rev.* **1977**, *22*, 37.

3. Fortman, J. J.; Sievers, R. E. *Coord. Chem. Rev.* **1971**, *6*, 331.

4. Fackler, J. P. *Prog. Inorg. Chem.* **1966**, *7*, 361.

5. Fay, R. C. *Coord. Chem. Rev.* **1996**, *154*, 99.

6. Lappert, M. F.; Severn, J. R.; Bourget-Merle, L. *Chem. Rev.* **2002**, *102*, 3031.

7. Piers, W. E.; Emslie, D. J. H. *Coord. Chem. Rev.* **2002**, *233*, 131.

8. Eckert, N. A.; Smith, J. M.; Lachicotte, R. J.; Holland, P. L. *Inorg. Chem.* **2004**, *43*, 3306.

9. Fekl, U.; Kaminsky, W.; Goldberg, K. I. *J. Am. Chem. Soc.* **2003**, *125*, 15286.

10. van den Bergen, A.; Murray, K. S.; West, B. O. *Aust. J. Chem* **1972**, *25*, 705.

11. Jones, M. M. *J. Am. Chem. Soc.* **1958**, *81*, 3188.

12. Ahn, J. H.; Kim, J. C.; Ihm, S. K.; Oh, C. G.; Sherrington, D. C. *Ind. Eng. Chem. Res.* **2005**, *44*, 8560.

13. Ishihara, K.; Sakakura, A.; Kondo, R. *Org. Lett.* **2005**, *7*, (10), 1971.

14. Chisholm, M. H.; Folting, K.; Putilina, E. F. *Inorg. Chem.* **1992**, *31*, (1510).

15. Cotton, F. A.; Rice, C. E.; Rice, G. W. *Inorg. Chim. Acta* **1977**, *24*, 231.

16. Herrick, R. S.; Nieter-Burgmayer, S. J.; Templeton, J. L. *J. Am. Chem. Soc.* **1983**, *105*, 2599.

17. Goh, L. Y.; Weng, Z.; Hor, A. T. S.; Leong, W. K. *Organometallics* **2002**, *21*, 4408.

18. Gilletti, P. F.; Femec, D. A.; Keen, F. I.; Brown, T. M. *Inorg. Chem.* **1992**, *31*, 4008.

19. Ricard, L.; Estienne, J.; Weiss, R. *Inorg. Chem.* **1973**, *12*, 2182.

20. Morrow, J. R.; Tonker, T. L.; Templeton, J. L. *Organometallics* **1985**, *4*, 745.

21. Morrow, J. R.; Templeton, J. L.; Bandy, J. A.; Bannister, C.; Prout, C. K. *Inorg. Chem.* **1986**, *25*, 1923.

22. Brower, D. C.; Tonker, T. L.; Morrow, J. R.; Rivers, D. S.; Templeton, J. L. *Organometallics* **1986**, *5*, 1093.

23. Coucouvanis, D. *Prog. Inorg. Chem.* **1979**, *26*, 301.

24. Baker, P. K.; Kendrick, D. A. *Polyhedron* **1991**, *10*, (4/5), 433.

25. Baker, P. K.; Flower, K. R. *J. Organomet. Chem.* **1993**, *447*, 67.

26. Baker, P. K.; Drew, M. G. B.; Evans, D. S.; Johans, A. W.; Meehan, M. M. *J.Chem. Soc., Dalton Trans.* **1999**, 2541.

27. Baker, P. K.; Clark, A. I.; Drew, M. G. B.; Durrant, M. C.; Richards, R. L. *J.Organomet. Chem.* **1997**, *549*, 193.

28. Baker, P. K.; Clark, A. I.; Coles, S. J.; Drew, M. G. B.; Durrant, M. C.; Hursthouse, M. B.; Richards, R. L. *J. Chem. Soc., Dalton Trans.* **1998**, 1281.

29. Armstrong, E. A.; Baker, P. K.; Drew, M. G. B. *Organometallics* **1988**, *7*, 319.

30. Armstrong, E. A.; Baker, P. K. *Inorg. Chim. Acta* **1988**, *143*, 13.

31. Brower, D. C.; Winston, P. B.; Tonker, T. L.; Templeton, J. L. *Inorg. Chem.* **1986**, *25*, 2883.

32. Abel, E. W.; Butler, I. S.; Reid, J. G. *J. Chem. Soc.* **1963**, 2068.

33. Burgmayer, S. J. N.; Templeton, J. L. *Inorg. Chem.* **1985**, *24*, 2224.

34. Krasochka, O. N.; Sokolova, Y. A.; Atovmyan, L. O. *J. Struct. Chem.* **1975**, *16*, (4), 696.

35. Drew, M. G. B.; Rix, C. J. *J. Organomet. Chem.* **1975**, *102*, 467.

36. Templeton, J. L.; Ward, B. C. *Inorg. Chem.* **1980**, *19*, 1753.

37. Drew, M. G. B.; Tomkins, I. B.; Colton, R. *Aust. J. Chem* **1970**, *23*, (2517).

38. Churchill, M. R.; Youngs, W. J. *Inorg. Chem.* **1979**, *18*, 2454.

39. Gutowsky, H. S.; Holm, C. H. *J. Chem. Phys.* **1956**, *25*, 1228.

40. Templeton, J. L.; Ward, B. C. *J. Am. Chem. Soc.* **1981**, *103*, 3743.

41. Day, R. O.; Batschelet, W. H.; Archer, R. D. *Inorg. Chem.* **1980**, *19*, 2113.

42. Ward, B. C.; Templeton, J. L. *J. Am. Chem. Soc.* **1980**, *102*, 1532.

43. Templeton, J. L. *Adv. Organomet. Chem.* **1989**, *29*, 1.

44. McDonald, J. W.; Corbin, J. L.; Newton, W. E. *J. Am. Chem. Soc.* **1975**, *97*, 1970.

45. King, R. B. *Inorg. Chem.* **1968**, *7*, 1044.

46. Thomas, J. L. *Inorg. Chem.* **1978**, *17*, 1507.

47. Templeton, J. L.; Ward, B. C. *J. Am. Chem. Soc.* **1980**, *102*, 3288.

48. Herrick, R. S.; Nieter-Burgmayer, S. J.; Templeton, J. L. *Inorg. Chem.* **1983**, *22*, 3275.

49. Herrick, R. S.; Templeton, J. L. *Organometallics* **1982**, *1*, 842.

Chapter 3

Tungsten(II) Monocarbonyl Bis(acetylacetonate): A Fourteen-Electron Docking Site for η^2 Four-Electron Donor Ligands

Introduction

Organometallic complexes of d^4 tungsten and molybdenum often promote formal four-electron bonding of alkynes,[1-3] and nitriles[4-9] from the triple bond. Molecules containing a carbon-heteroatom double bond such as imines,[10-13] and aldehydes and ketones,[14-18] typically bind to these metals as formal two-electron donors whether bound as η^1 or η^2 ligands. We recently reported the reactivity of $W(CO)_3(acac)_2$, **1**, (acac = acetylacetonate) with four-electron donor alkynes and two-electron donor phosphines.[19] Coordination of alkynes as formal four-electron donor ligands via the C≡C triple bond π-electrons[19] prompted us to explore isoelectronic nitrile reagents as possible four-electron donor ligands to this tungsten(II) center.

Results and Discussion

Indeed, when $W(CO)_3(acac)_2$ **1** is exposed to nitriles, two equivalents of carbon monoxide are released to accommodate coordination of an η^2-nitrile ligand. Monitoring reaction progress via IR spectroscopy revealed the growth of a single CO stretch consistent with the formation of $W(CO)(acac)_2(\eta^2$-N≡CR) [R = Me (**2a**), Ph (**2b**)] (Scheme 3.1).

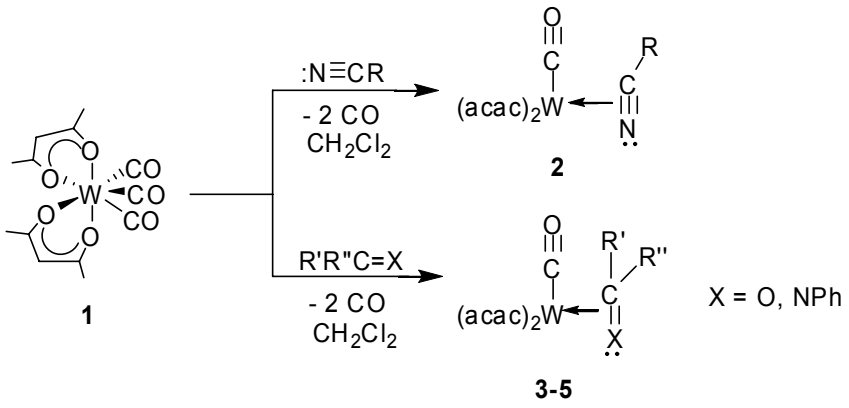

2a. N≡CMe **3**. PhN=CHPh **4a**. O=CHPh **5**. O=C(CH$_3$)$_2$
2b. N≡CPh **4b**. O=CHAr
2c. N≡CAr Ar = 2,6-dichlorophenyl

Scheme 3.1. General method to form W(CO)(acac)$_2$(η^2-L) complexes.

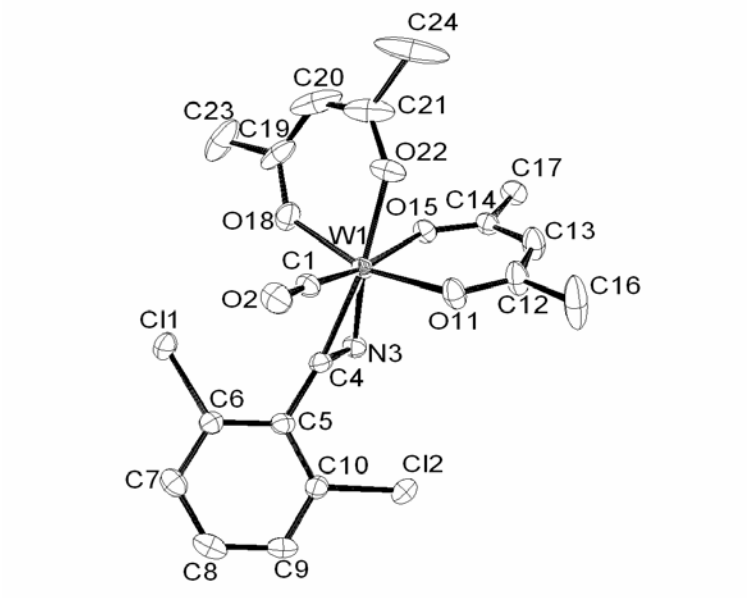

Figure 3.1 ORTEP diagram of W(CO)(acac)$_2$(η^2-2,6 dichlorobenzonitrile) (**2c**).

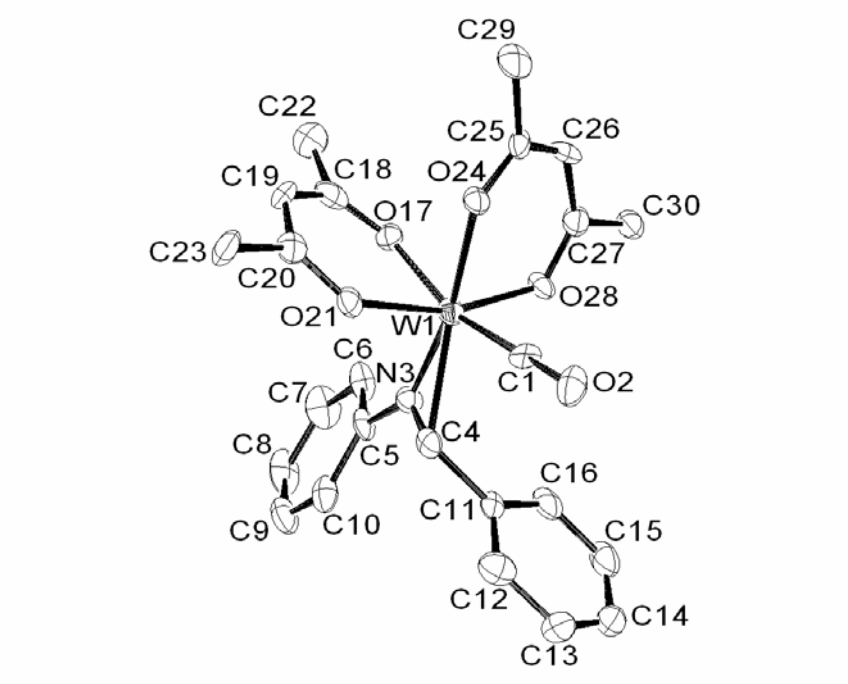

Figure 3.2. ORTEP diagram of W(CO)(acac)$_2$(η^2-PhN=CHPh) **3**.

The ^{1}H NMR spectrum of the acetonitrile adduct, W(CO)(acac)$_2$(η^2-N≡CCH$_3$), **2a**, exhibits two singlets for the acac methine protons and four singlets for the acac methyl groups. The methyl group of the bound acetonitrile resonates downfield at 3.71 ppm, suggestive of a π-bound nitrile ligand. More diagnostic than proton NMR data is the ^{13}C NMR chemical shift for the nitrile carbon at 208.7 ppm, consistent with data reported for other four-electron donor nitriles.[4-9]

The X-ray structure of the 2,6-dichlorobenzonitrile derivative **2c** shows two acac chelates and one carbon monoxide ligand bound to tungsten with a π-bound nitrile ligand occupying the sixth site of a primitive octahedron. The η^2-nitrile ligand is located cis to carbon monoxide, and the C≡N triple bond is approximately parallel to the W-C≡O axis (Figure 3.1). The carbon atom in the nitrile ligand is located *proximal* to carbon monoxide and the nitrogen atom is located *distal* to CO. Bond distances to the nitrile ligand are nearly

equal: W(1)-C(4) = 2.04 Å and W(1)-N(3) = 2.02 Å. The carbon-nitrogen triple bond distance in the coordinated nitrile ligand is 1.27 Å.

Selective coordination of nitrile reagents through the π-system reflects the propensity of the $W(CO)(acac)_2$ fragment to bind a ligand that will provide four electrons to the metal. Could other small molecules containing heteroatom π-bonds serve as formal four-electron donors to the 14-electron $W(CO)(acac)_2$ fragment?

Surprisingly, treatment of **1** with *N*-benzylideneaniline (PhN=CHPh) in CH_2Cl_2 at room temperature generates an η^2-imine complex of the formula $W(CO)(acac)_2(\eta^2$-PhN=CHPh), **3** (Scheme 3.1). Coordination of the imine to tungsten creates a new stereocenter at the imine carbon, with tungsten as a second stereocenter. Formation of two diastereomers in a 2:1 ratio is indicated in the ^{1}H NMR spectrum by an upfield shift in the imine proton to 6.15 (major) and 5.71 (minor) ppm. An even more dramatic upfield shift is observed for the imine carbon which resonates at 57.3 (major) and 54.3 (minor) ppm in the ^{13}C NMR spectrum. Although η^2-imine complexes are well-known,[10-13] simple substitution of two carbon monoxide ligands by an imine reagent at room temperature is unprecedented. Similar results were obtained upon addition of benzaldehyde to tricarbonyl reagent **1**. The ^{1}H NMR spectrum for $W(CO)(acac)_2(\eta^2$-O=CHPh), **4a**, shows two diastereomers in a 5:4 ratio. Coordination to the tungsten(II) center shifts the aldehyde proton upfield to 7.73 (major) and 7.66 (minor) ppm. ^{13}C NMR data shows the coordinated aldehyde carbon shifted upfield to 88.9 (major) and 86.7 (minor) ppm.

To check ketone reactivity, **1** was stirred in neat acetone. As with the imine and aldehyde substrates, IR spectroscopy suggested a tungsten product retaining one CO ligand. Note that $W(CO)(acac)_2[\eta^2$-O=C$(CH_3)_2]$, **5**, lacks a second stereocenter, so only one product

was observed in the ^{1}H NMR spectrum. The diastereotopic methyl groups of coordinated acetone resonate at 2.53 and 2.31 ppm in the ^{1}H NMR spectrum, while the ketone carbon resonates upfield at 97.2 ppm in the ^{13}C NMR spectrum.

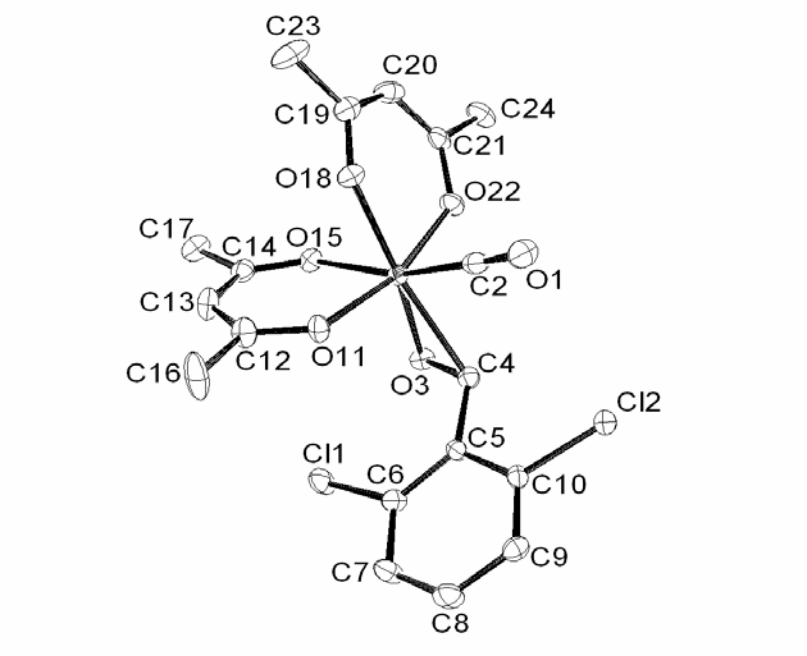

Figure 3.3. ORTEP diagram of W(CO)(acac)$_2$(η^2-2,6 dichlorobenzaldehyde) (**4b**).

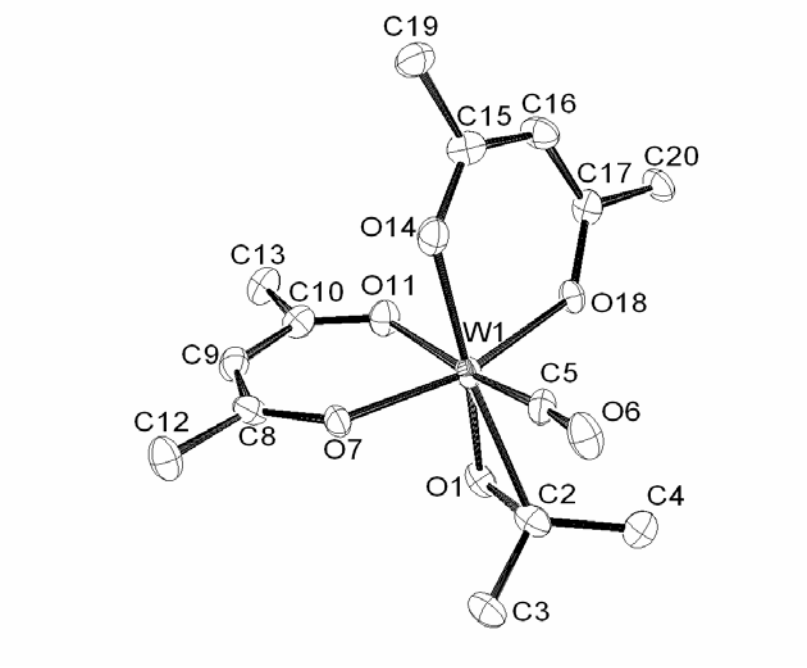

Figure 3.4. ORTEP diagram of $W(CO)(acac)_2(\eta^2$-acetone) (**5**).

X-ray structures of complexes with imine **3** (Figure 3.2), aldehyde **4b**, and ketone **5** (Figures 3.3 and 3.4) ligands show η^2-coordination of the organic substrate with the C=X (X = N, O) unit aligned nearly parallel to the W-C≡O axis. This system exhibits a definitive preference for positioning the carbon atom *proximal* to CO and the heteroatom *distal* to CO. This geometry allows optimal back-donation to both carbon monoxide and the carbon of the C=X entity (A) (Figure 3.5) while simultaneously enabling lone pair donation from the heteroatom into the vacant d_{xy} orbital (B).

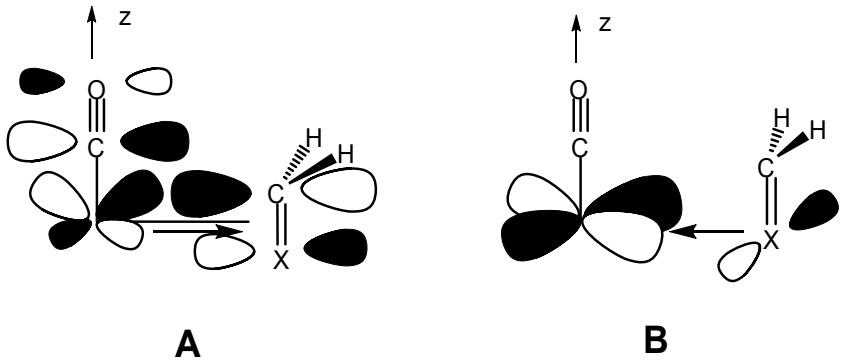

Figure 3.5. Orbital interactions of tungsten and π-bound substrate.

Structural data for complexes **3**, **4b**, and **5** present a skewed bonding arrangement for each η^2-ligand. Bond lengths from tungsten to the carbon and to the heteroatom differ substantially relative to the analogous W-C and W-N bonds in the nitrile complex, **2c** (Table 3.1). The average tungsten-carbon bond length for these three structures is 2.22 Å, and the average tungsten-heteroatom bond length is 1.94 Å, reflecting significant W-X double-bond character. Upon coordination to tungsten, the C=X double bond in each substrate lengthens approximately 0.1 Å, a considerable loss of C=X double-bond character. Structural data do not reflect additional π-electron donation from the acetylacetonate chelates.

Table 3.1. Selected bond lengths (in Å). *a*: X = N (**2c**, **3**), O (**4b**, **5**).

	2c	**3**	**4b**	**5**
W-C	2.038(5)	2.237(7)	2.210(3)	2.211(8)
W-X[a]	2.018(5)	1.934(6)	1.954(4)	1.934(5)
X[a]-C	1.270(7)	1.403(8)	1.377(4)	1.380(10)

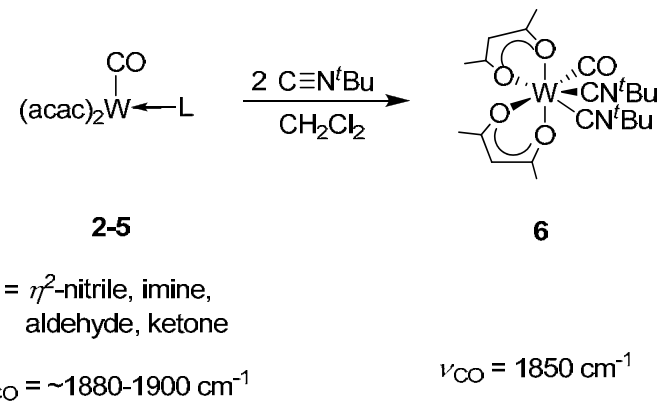

Scheme 3.2 Displacement of η^2-L with *tert*-butyl isonitrile to form **6**.

Displacement of each sidebound ligand occurs with a strong σ-donor. In a representative reaction, two equivalents of *tert*-butyl isocyanide are added to a solution of **2b** in CH_2Cl_2. A color change from amber to red-orange accompanied by a shift in the CO absorption ~40 cm^{-1} to lower energy. These observations reflect displacement of the nitrile ligand by two isocyanide ligands resulting in the seven coordinate $W(CO)(acac)_2(CN^tBu)_2$ complex, **6** (Scheme 3.2). Exposure of **3**, **4a**, and **5** to the same isocyanide reagent also produces **6**. Addition of one molar equivalent of isocyanide leads to 50% conversion to **6**, as seen by ^1H NMR spectroscopy. Complex **6** exhibits fluxional behavior on the NMR time scale, a common feature of seven-coordinate low-valent Group VI complexes. At room temperature, three peaks are observed: one for both acac methine protons (5.50 ppm), one for all four acac methyl groups (2.01 ppm), and one for both *tert*-butyl groups (1.48 ppm). Suitable crystals for X-ray analysis were obtained by placing a concentrated hexanes solution of **6** in a freezer at -30 °C in which dark red blocks formed overnight. The solid state structure shows a tungsten center surrounded by two acac chelates, one carbon monoxide ligand, and two *tert*-butyl isocyanide ligands. The isocyanide ligands are arranged cis with respect to each other. Considerable deviation from linearity in the C3-N4-C5 (163.7°) and

C9-N10-C11 (142.2°) bond angles reflect the need to ease steric crowding in a congested seven-coordinate complex. Formation of **6** strengthens the claim that the $W(CO)(acac)_2$ fragment contains fourteen valence electrons and the sidebound ligand in each precursor complex (**2**-**5**) provides the final four electrons to the metal center.

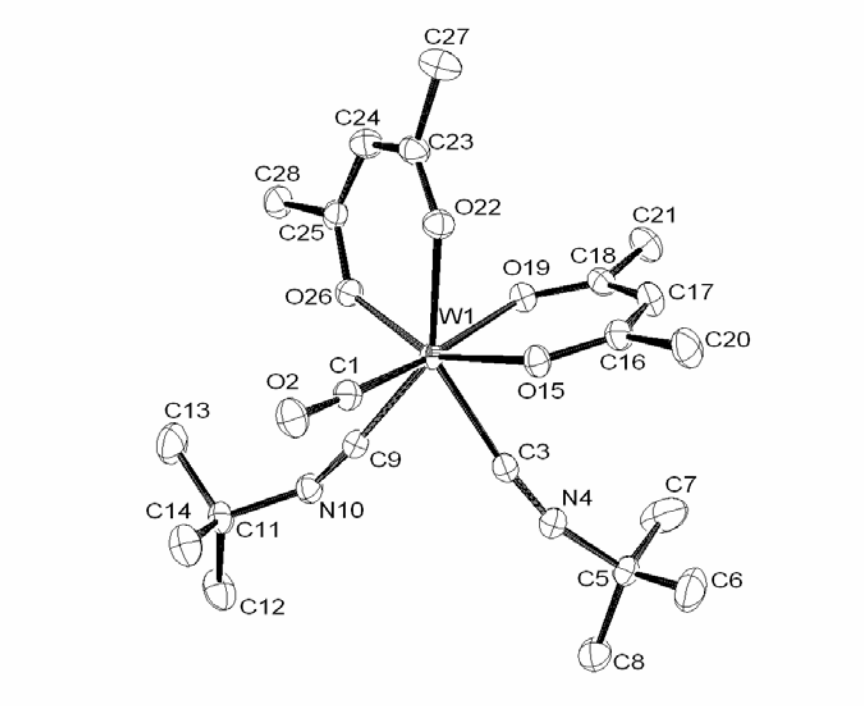

Figure 3.6. ORTEP diagram of $W(CO)(acac)_2(CN^tBu)_2$ (**6**).

To gain additional insight into the structural features arising from the four-electron binding mode of heteroatom π-bonds, DFT calculations[20] were carried out on d^4 $W(acac)_2(CO)(\eta^2\text{-}CH_2O)$ (**7**), together with the hypothetical d^6 model complexes, $[W(acac)_2(CO)(\eta^2\text{-}CH_2O)]^{2-}$ (**8**) and $Os(acac)_2(CO)(\eta^2\text{-}CH_2O)$ (**9**), where the aldehyde is restricted to a two-electron donor role. Metric parameters of the optimized DFT structures are summarized in Table 3.2. As in the structurally characterized aldehyde complex, **4b**, the lowest-energy rotamer of the model formaldehyde complex **7** positions the oxygen atom *distal* to CO, with the *proximal* rotamer lying 11.5 kcal mol^{-1} higher in energy. The

difference in the M-C and M-O distances in **4b** (0.26 Å) is reproduced well in the calculated structure for **7** (0.24 Å). Calculated structures for both of the d^6 complexes show a significantly longer M-O bond, which gives rise to a smaller difference between the M-O and M-C distances (0.06 Å). These calculated structural features are consistent with the absence of lone-pair donation from oxygen in these η^2-aldehyde adducts. Additionally, the lowest energy rotamer of the d^6 complexes aligns the C=O unit perpendicular to CO, allowing backbonding to the η^2-aldehyde from d_{xy} without competition from CO.

Table 3.2 Selected bond lengths (in Å) from DFT studies of $W(acac)_2(CO)(CH_2O)$ (**7**), $W(acac)_2(CO)(CH_2O)^{2-}$ (**8**) and $Os(acac)_2(CO)(CH_2O)$ (**9**)

	7	**8**	**9**
M-C	2.167	2.126	2.150
M-O	1.926	2.057	2.092
O-C	1.372	1.376	1.304

Summary

In summary, we report a tungsten(II) d^4 center that seeks four-electrons from η^2-nitriles, imines, aldehydes, and ketones. Nitrile ligands donate four electrons from the two orthogonal π-orbitals of the triple bond. Imines, aldehydes, and ketones also provide four electrons to the d^4 metal center, but two originate in the C=X π-bond and the other two arise from a lone pair on the heteroatom.

Experimental

W(CO)(acac)$_2$(η^2-N≡CCH$_3$) (2a). In the drybox 1.30 g of **1** was added to a dry 200 mL Schlenk flask. Methylene chloride was added (30 mL) generating a brick red solution. To this was added 1eq. of 2,6-dichlorobenzonitrile, and after 7 hours a color change from brick red to dark brown was observed. The solvent was removed *in vacuo* resulting in a brown solid. Column chromatography on silica using methylene chloride eluted a dark amber band (750 mg, 60%). IR (KBr): ν_{CO} = 1895 cm^{-1}, ν_{CN} = 1675 cm^{-1}. ^{1}H NMR (CD_2Cl_2, 298 K, δ): 5.69, 5.63 (each a s, each 1H, acac C*H*), 3.71 (s, 3H, C-C*H*$_3$), 2.22, 2.22, 2.10, 1.93 (each a s, each 3H, acac C*H*$_3$); ^{13}C{^{1}H} NMR (CD_2Cl_2, 298 K, δ): 22.6 (N≡C*C*H$_3$), 25.8, 26.1, 26.3, 28.5 (acac *C*H$_3$), 99.6, 102.0 (acac *C*H), 184.2, 187.8, 188.6, 196.5 (acac *C*O), 208.8 (N≡*C*CH$_3$), 237.6 (*C*≡O).

W(CO)(acac)$_2$(η^2-N≡CPh) (2b). In the drybox 500 mg of **1** was added to a dry 200 mL Schlenk flask. Methylene chloride was added (15 mL) generating a brick red solution. To this was added 5 eq. of benzonitrile, and after 2 hours a color change from brick red to dark brown was observed. The solvent was removed *in vacuo* resulting in a brown solid. Column chromatography on silica using methylene chloride eluted a dark amber band (305 mg, 56%). IR (KBr): ν_{CO} = 1895 cm^{-1}, ν_{CN} = 1634 cm^{-1}. ^{1}H NMR (CD_2Cl_2, 298 K, δ): 8.13 (d, 2H, *o*-C$_6$*H*$_5$), 7.63 (t, 2H, *m*-C$_6$*H*$_5$), 7.55 (t, 1H, *p*-C$_6$*H*$_5$), 5.64, 5.32 (each a s, each 1H, acac C*H*), 2.27, 2.26, 2.25, 1.94 (each a s, each 3H, acac C*H*$_3$); ^{13}C{^{1}H} NMR (CD_2Cl_2, 298 K, δ): 25.9, 26.2, 26.4, 28.6 (acac *C*H$_3$), 99.9, 102.2 (acac *C*H), 129.3 (*o*-*C*$_6$H$_5$), 131.7 (*p*-*C*$_6$H$_5$), 132.6 (*m*-*C*$_6$H$_5$), 135.4 (*ipso*-*C*$_6$H$_5$), 184.8, 188.1, 188.9, 196.4 (acac *C*O), 211.2 (η^2-*C*≡N), 240.2 (*C*≡O) Anal. Calcd for $WC_{18}H_{19}O_5N$: C, 42.12; H, 3.74; N, 2.73. Found: C, 42.25; H, 3.77; N, 2.75%.

W(CO)(acac)$_2$(η^2-2,6-dichlorobenzonitrile) (2c). In the drybox 100 mg of **1** was added to a dry 100 mL Schlenk flask. Methylene chloride was added (15 mL) generating a brick red solution. To this was added 1eq. of 2,6-dichlorobenzonitrile, and after 7 hours a color change from brick red to dark brown was observed. The solvent was removed *in vacuo* resulting in a brown solid. Column chromatography on silica using methylene chloride eluted a dark orange band (22 mg, 18%). IR (KBr): ν_{CO} = 1912 cm^{-1}, ν_{CN} = 1600 cm^{-1}. ^{1}H NMR (CD_2Cl_2, 298 K, δ): 7.50 (d, 2H, *m*-$C_6H_3Cl_2$), 7.31 (t, 1H, *p*-$C_6H_3Cl_2$), 5.72, 5.64 (each a s, each 1H, acac C*H*), 2.30, 2.29, 2.26, 1.95 (each a s, each 3H, acac CH_3); ^{13}C{^{1}H} NMR (CD_2Cl_2, 298 K, δ): 25.8, 26.1, 26.3, 28.6 (acac *C*H$_3$), 100.4, 102.6 (acac *C*H), 128.6, 131.5 (*o,m*-$C_6H_3Cl_2$), 133.1 (*p*-$C_6H_3Cl_2$), 136.6 (*ipso*-$C_6H_3Cl_2$), 185.1, 188.4, 189.9, 197.1 (acac *C*O), 214.3 (η^2-*C*≡N), 236.3 (*C*≡O).

W(CO)(acac)$_2$(η^2-PhN=CHPh) (3). In the drybox 100 mg of **1** was added to a 100 mL Schlenk flask. Methylene chloride was added (15 mL) and the flask was placed under a nitrogen atmosphere. *N*-Benzylideneaniline (2eq.) was added and after one hour of stirring, the brick red color was replaced by cherry red. The solvent was removed *in vacuo* yielding a sticky red solid. Column chromatography on silica using methylene chloride as eluent yielded a dark red band (66 mg, 52%). IR (KBr): ν_{CO} = 1881 cm^{-1}. ^{1}H NMR (CD_2Cl_2, 298 K, major diastereomer, δ): 6.15 (s, 1H, N=C*H*), 5.78, 5.39 (each a s, each 1H, acac C*H*), 2.75, 2.30, 2.17, 1.97 (each a s, each 3H, acac CH_3). ^{1}H NMR (CD_2Cl_2, 298 K, minor diastereomer, δ): 5.71 (s, 1H, N=C*H*), 5.71, 5.55 (each a s, each 1H, acac C*H*), 2.64, 2.24, 2.07, 1.90 (each a s, each 3H, acac CH_3). ^{13}C{^{1}H} NMR (CD_2Cl_2, 298 K, major diastereomer, δ): 25.7, 26.4, 27.6, 27.8 (acac *C*H$_3$), 57.3 (N=*C*), 98.7, 101.2 (acac *C*H), 185.3, 185.5, 187.2, 193.7 (acac *C*O), 234.5 (*C*≡O). ^{13}C{^{1}H} NMR (CD_2Cl_2, 298 K, minor

diastereomer, δ): 25.5, 26.7, 27.4, 27.8 (acac *C*H_3), 54.3 (N=*C*), 98.6, 101.7 (acac *C*H), 184.9, 186.4, 187.3, 194.4 (acac *C*O), 236.2 (*C*≡O). Anal. Calcd for $WC_{24}H_{25}O_5N$: C, 48.74; H, 4.27; N, 2.37. Found: C, 48.48; H, 4.29; N, 2.33%.

W(CO)(acac)$_2$(η^2-O=CHPh) (4a). In the drybox, 100 mg of **1** was added to a 100 mL Schlenk flask. Methylene chloride was added (15 mL) resulting in a brick red solution. Two equivalents of benzaldehyde were added with stirring, and within 15 minutes the brick red color was replaced by a brighter cherry red. IR spectroscopy indicated the presence of a monocarbonyl product. The solvent was removed *in vacuo* yielding a gooey red solid, which was purified via column chromatography on silica using methylene chloride to elute a dark red band (74 mg, 67%). IR (KBr): ν_{CO} = 1866 cm^{-1} (major diastereomer), 1878 cm^{-1} (minor diastereomer). ^{1}H NMR (CD_2Cl_2, 298 K, major diastereomer, δ): 7.73 (s, 1H, O=C*H*), 5.66, 5.62 (each a s, each 1H, acac C*H*), 2.88, 2.34, 2.32, 2.07 (each a s, each 3H, acac CH_3),. ^{1}H NMR (CD_2Cl_2, 298 K, minor diastereomer, δ): 7.66 (s, 1H, O=C*H*), 5.70, 5.69 (each a s, each 3H, acac C*H*), 2.94, 2.32, 2.11, 2.03 (each a s, each 3H, acac CH_3). ^{13}C{^{1}H} NMR (CD_2Cl_2, 298 K, both diastereomers, δ): 24.9, 25.1, 25.6, 25.8, 26.9, 27.1, 28.0, 28.1 (acac *C*H_3), 86.7, 88.9 (O=*C*HPh), 97.4, 98.0, 101.1, 101.5 (acac *C*H), 125.2, 126.3, 127.3, 127.5 (*o/m*-C_6H_5), 128.3, 128.6 (*p*-C_6H_5), 145.7, 146.3 (*ipso*-C_6H_5), 183.7, 185.4, 185.7, 186.92, 186.94, 187.3, 197.7, 198.4 (acac *C*O), 226.4, 226.5 (*C*≡O). Anal. Calcd for $WC_{18}H_{20}O_6$: C, 41.88; H, 3.91. Found: C, 41.96; H, 3.90%.

W(CO)(acac)$_2$(η^2-2,6-dichlorobenzaldehyde) (4b). In the drybox, 100 mg of **1** was added to a 100 mL Schlenk flask. Methylene chloride was added (15 mL) resulting in a brick red solution. Two equivalents of 2,6-dichlorobenzaldehyde were added with stirring, and within 4 hours the brick red color was replaced by a brighter cherry red. IR spectroscopy

indicated the presence of a monocarbonyl product. The solvent was removed *in vacuo* yielding a gooey red solid, which was purified via column chromatography on silica using methylene chloride to elute a dark red band (66 mg, 53%). IR (KBr): ν_{CO} = 1891 cm^{-1} (major diastereomer), 1877 cm^{-1} (minor diastereomer). ^1H NMR (CD_2Cl_2, 298 K, major diastereomer, δ): 8.03 (s, 1H, O=C*H*), 7.31 (d, 2H, *m*-$C_6H_3Cl_2$), 6.91 (t, 1H, *p*-$C_6H_3Cl_2$), 5.75, 5.62 (each a s, each 1H, acac C*H*), 3.02, 2.45, 2.31, 2.04 (each a s, each 3H, acac CH_3). ^1H NMR (CD_2Cl_2, 298 K, minor diastereomer, δ): 8.26 (s, 1H, O=C*H*), 7.24 (d, 2H, *m*-$C_6H_3Cl_2$), 6.89 (t, 1H, *p*-$C_6H_3Cl_2$),5.69, 5.64 (each a s, each 3H, acac C*H*), 2.95, 2.33, 2.13, 2.08 (each a s, each 3H, acac CH_3). $^{13}C\{^1H\}$ NMR (CD_2Cl_2, 298 K, major diastereomer, δ): 25.0, 25.1, 27.3, 27.9 (acac *C*H_3), 89.0 (O=*C*HAr), 96.6, 101.0 (acac *C*H), 125.2, 126.3, 127.3, 127.5 (*o/m*-C_6H_5), 128.3, 128.6 (*p*-C_6H_5), 145.7, 146.3 (*ipso*-C_6H_5), 184.6, 186.5, 186.9, 196.9 (acac *C*O), 224.2 (*C*≡O). $^{13}C\{^1H\}$ NMR (CD_2Cl_2, 298 K, minor diastereomer, δ): 24.8, 25.8, 26.8, 27.9 (acac *C*H_3), 84.9 (O=*C*HAr), 97.8, 101.3 (acac *C*H), 184.8, 186.6, 187.8, 197.5 (acac *C*O), 227.2 (*C*≡O).

W(CO)(acac)$_2$[η^2-O=C(CH$_3$)$_2$] (5). In the drybox, 100 mg of **1** was added to a 100 mL Schlenk flask. Acetone was added (10 mL) and the solution was stirred, resulting in a color change from brick red to red-violet in 15 min. IR spectroscopy indicated the presence of a monocarbonyl product. The acetone was removed *in vacuo* yielding a gooey red solid, which was purified via column chromatography on silica using methylene chloride to elute a dark red band (77 mg, 76%). IR (hexanes): ν_{CO} = 1883 cm^{-1}. ^1H NMR (CD_2Cl_2, 298 K, δ): 5.60 (s, 2H, acac C*H*), 2.53, 2.31 (each a s, each 3H, O=C(CH_3)$_2$), 2.77, 2.28, 2.22, 2.02 (each a s, each 3H, acac CH_3). $^{13}C\{^1H\}$ NMR (CD_2Cl_2, 298 K, δ): 25.3, 25.7, 27.0, 28.1 (acac *C*H_3), 32.4, 34.6 (O=C(*C*H_3)$_2$), 97.2 (O=*C*), 98.0, 101.1 (acac *C*H), 183.7, 185.7, 187.6, 197.6 (acac

*C*O), 226.9 (*C*≡O). Anal. Calcd for $WC_{14}H_{20}O_6$: C, 35.92; H, 4.31. Found: C, 36.10; H, 4.15%.

W(CO)(acac)$_2$(CN^{t}Bu)$_2$ (6). In a 200 mL Schlenk flask, **2b** (352 mg) was combined with methylene chloride and stirred under an atmosphere of nitrogen. To this solution was added *tert*-butyl isonitrile (2 eq.). A color change from amber to orange/red quickly occurred. *In situ* IR spectroscopy revealed a new CO stretch around 1850 cm^{-1}. The reaction was allowed to stir 30 minutes before the solvent volume was reduced *in vacuo*. Hexanes were added (~80 mL) and the solvent volume was further reduced to remove any additional methylene chloride. The dark red hexanes solution was placed in the freezer at -30°C overnight to induce crystallization of a dark red solid (300 mg, 76%). IR (hexanes): ν_{CO} = 1847 cm^{-1}. ^{1}H NMR (CD_2Cl_2, 298 K, δ): 5.50 (s, 2H, acac C*H*), 2.01 (s, 12H, acac CH_3), 1.48 (s, 18H, ^{t}Bu).

Table 3.3. Crystal data and refinement parameters for **2c**, **3**, and **4a**.

Complex	**2c**	**3**	**4a**
Empirical Formula	$C_{18}H_{17}Cl_2NO_5W$	$C_{20}H_{25}NO_5W$	$C_{18}H_{18}Cl_2O_6W$
Mol wt	582.08	543.26	585.07
Color	Orange	Red	Red
Temperature	100 K	100(2) K	100(2) K
Wavelength	0.71703 Å	0.71703 Å	0.71703 Å
Cryst Syst	Orthorhombic	Monoclinic	Orthorhombic
Space Group	*Pbcn*	$P2_1/n$	$P2_12_12_1$
a, Å	27.7307(11)	8.3192(3)	7.7644(4)
b, Å	9.6208(4)	14.2955(4)	8.5412(4)
c, Å	14.9968(5)	17.0591(6)	29.7831(13)
α, deg	90	90	90
β, deg	90	92.92	90
γ, deg	90	90	90
Vol. Å^3	4001.0(3)	2026.15(12)	1975.13(16)
Z	8	4	4
Density (calculated)	1.933 Mg/m^3	1.781 Mg/m^3	1.968 Mg/m^3
μ, mm^{-1}	6.070	5.73	6.510
F(000)	2240	1064	1128
Crystal size	0.25 x 0.10 x 0.02 mm^3	0.10 x 0.10 x 0.10 mm^3	0.10 x 0.10 x 0.02 mm^3
2θ range	2.24 to 28.00°	1.86 to 30.07°	4.75 to 30.00°
Index Ranges	-35<=h<=36 -12<=k<=12 -19<=l<=19	-11<=h<=11 -20<=k<=20 -24<=l<=23	-10<=h<=10 -12<=k<=12 -41<=l<=41
Reflections Collected	51674	88084	27144
Independent reflections	4834 [R(int) = 0.0331]	88084 [R(int) = 0.0000]	5721 [R(int) = 0.0389]
Data/restraints/parameters	4834/0/248	88084/0/252	5721/0/249
Goodness-of-fit on F^2	1.072	1.004	1.039
Final R indices[I>2sigma(I)]	R1 = 0.0410 wR2 = 0.0944	R1 = 0.0394 wR2 = 0.1014	R1 = 0.0219 wR2 = 0.0423
R indices (all data)	R1 = 0.0468 wR2 = 0.0977	R1 = 0.0530 wR2 = 0.1065	R1 = 0.0250 wR2 = 0.0433
Largest diff. peak and hole	6.671 and -2.567 e Å^{-3}	2.564 and -1.866 e Å^{-3}	0.977 and -0.860 e Å^{-3}

Table 3.4. Crystal data and refinement parameters for **5** and **6**.

Complex	**5**	**6**
Empirical Formula	$C_{14}H_{20}O_6W$	$C_{21}H_{32}N_2O_5W$
Mol wt	468.15	576.34
Color	Red	Red
Temperature	100(2) K	100(2) K
Wavelength	0.71703 Å	0.71703 Å
Cryst Syst	Orthorhombic	Monoclinic
Space Group	$P2_12_12_1$	$P2_1/n$
a, Å	8.9457(1)	8.8722(6)
b, Å	13.5475(2)	15.7242(11)
c, Å	26.6866(4)	17.5395(13)
α, deg	90	90
β, deg	90	103.252(3)
γ, deg	90	90
Vol. Å^3	3234.20(8)	2381.7(3)
Z	8	4
Density (calculated)	1.923 Mg/m^3	1.607
μ, mm^{-1}	7.166	4.881
F(000)	1808	1144
Crystal size	0.25 x 0.15 x 0.10 mm^3	0.30 x 0.20 x 0.05 mm^3
2θ range	1.53 to 30.00°	1.76 to 36.32
Index Ranges	-12<=h<=12 -14<=k<=19 -37<=l<=22	-14<=h<=14 -26<=k<=26 -29<=l<=29
Reflections Collected	23675	123657
Independent reflections	9361 [R(int) = 0.0470]	11534 [R(int) = 0.0346]
Data/restraints /parameters	9361/0/391	11534/0/272
Goodness-of-fit on F^2	1.107	1.101
Final R indices[I>2sigma(I)]	R1 = 0.0437 wR2 = 0.0898	R1 = 0.0189 wR2 = 0.0405
R indices (all data)	R1 = 0.0516 wR2 = 0.0929	R1 = 0.0277 wR2 = 0.0439
Largest diff. peak and hole	1.583 and -2.175 e Å^{-3}	1.731 and -1.468 e Å^{-3}

References

1. Templeton, J. L. *Adv. Organomet. Chem.* **1989**, *29*, 1.

2. Templeton, J. L.; Ward, B. C. *J. Am. Chem. Soc.* **1980**, *102*, 3288.

3. Ward, B. C.; Templeton, J. L. *J. Am. Chem. Soc.* **1980**, *102*, 1532.

4. Barrera, J.; Sabat, M.; Harman, W. D. *J. Am. Chem. Soc.* **1991**, *113*, 8178.

5. Barrera, J.; Sabat, M.; Harman, W. D. *Organometallics* **1993**, *12*, 4381.

6. Kiplinger, J. L.; Arif, A. M.; Richmond, T. G. *Chem. Commun.* **1996**, 1691.

7. Kiplinger, J. L.; Arif, A. M.; Richmond, T. G. *Organometallics* **1997**, *16*, 246.

8. Thomas, S.; Tiekink, E. R. T.; Young, C. G. *Organometallics* **1996**, *15*, 2428.

9. Thomas, S.; Young, C. G.; Tiekink, E. R. T. *Organometallics* **1998**, *17*, 182.

10. Ainscough, E. W.; Brodie, A. M.; Burrell, A. K.; Kennedy, S. M. F. *J. Am. Chem. Soc.* **2001**, *123*, 10391.

11. Galakhov, M. V.; Gomez, M.; Jimenez, G.; Royo, P. *Organometallics* **1995**, *14*, 1901.

12. Coles, N.; Harris, M. C. J.; Whitby, R. J.; Blagg, J. *Organometallics* **1994**, *13*, 190.

13. Okuda, J.; Herberich, G. E.; Raabe, E.; Bernal, I. *J. Organomet. Chem.* **1988**, *353*, 65.

14. Graham, P. M.; Mocella, C. J.; Sabat, M.; Harman, W. D. *Organometallics* **2005**, *24*, 911.

15. Lis, E. C.; Delafuente, D. A.; Lin, Y. Q.; Mocella, C. J.; Todd, M. A.; Liu, W. J.; Sabat, M.; Myers, W. H.; Harman, W. D. *Organometallics* **2006**, *25*, 5051.

16. Schuster, D. M.; White, P. S.; Templeton, J. L. *Organometallics* **2000**, *19*, 1540.

17. Looman, S. D.; Giese, S.; Arif, A. M.; Richmond, T. G. *Polyhedron* **1996**, *15*, 2809.

18. Burkey, D. J.; Debad, J. D.; Legzdins, P. *J. Am. Chem. Soc.* **1997**, *119*, 1139.

19. Jackson, A. B.; White, P. S.; Templeton, J. L. *Inorg. Chem.* **2006**, *45*, 6205.

20. See Appendix R for references and DFT computational details.

Chapter 4

Reduction of π-Bound Nitriles to π-Bound Imines in a Tungsten(II) Bis(Acetylacetonate) Coordination Sphere

Introduction

The majority of organometallic nitrile complexes demonstrate σ-bonding of the nitrile, with the nitrile carbon susceptible to nucleophilic attack.[1,2] Metal-mediated hydrolysis of nitriles to amides and on to carboxylic acids involves initial hydroxide attack at the nitrile carbon.[1-6] Reduction from a nitrile to an amine can be accomplished via alternating nucleophilic attack at carbon and protonation at nitrogen beginning with initial hydride attack at the nitrile carbon.[7]

Less is known about the chemistry of π-bound nitriles. Although rare compared to their σ-bound counterparts, π-bound nitrile complexes have been known for two decades.[8-23] We recently reported the reaction of $W(CO)_3(acac)_2$[24] with nitriles to form complexes of the type $W(CO)(acac)_2(\eta^2\text{-N}\equiv\text{CR})$, where the nitrile acts as a four-electron donor ligand to tungsten.[25]

Coordination of the RC≡N triple bond leaves the nitrile susceptible to alkylation at the nucleophilic nitrogen lone pair, resulting in cationic η^2-iminoacyl complexes.[21-23] A number of neutral π-bound iminoacyl complexes are known,[26-38] but cationic complexes that offer enhanced reactivity toward nucleophiles are rare.[20-23,37-43] Common methods of formation of π-bound iminoacyl complexes include (1) migratory insertion of isocyanide into a metal-alkyl or a metal-hydride bond[38] and (2) addition of alkyl halides to anionic isocyanide complexes.[26-28] Reactivity studies with the cationic π-bound iminoacyl complexes have shown them to be agile reagents susceptible to nucleophilic attack at the iminoacyl carbon to form η^2-imines.[38,44-47] We now report addition of strong alkylating reagents R′OTf (R′ = Me, Et) to π-bound nitrile ligands to form cationic iminoacyl-carbonyl complexes

[W(CO)(acac)$_2$(η^2-R′N=CR)][OTf]. Nucleophilic addition at the iminoacyl carbon of the cationic complex forms η^2-imines of the type W(CO)(acac)$_2$(η^2-R′N=CRR″) (R″ = H, Me). This is the first example of stepwise addition of an electrophile and a nucleophile to an η^2-nitrile.

Results and Discussion

Combining stoichiometric amounts of W(CO)(acac)$_2$(η^2-N≡CPh) (**1a**) and MeOTf in methylene chloride at room temperature generates [W(CO)(acac)$_2$(η^2-MeN=CPh)][OTf] (**2a**) (Scheme 4.1). *In situ* IR spectroscopy indicates the presence of a single carbon monoxide absorbance at 1985 cm^{-1} in the product, an increase of approximately 90 cm^{-1} from the starting material. Alkylation of alkyl or aryl nitriles gives similar results. Addition of either MeOTf or EtOTf to W(CO)(acac)$_2$(η^2-N≡CMe) **1b** generates W(CO)(acac)$_2$(η^2-R′N=CMe)][OTf] [R′ = Me (**2b**), Et (**2c**)].

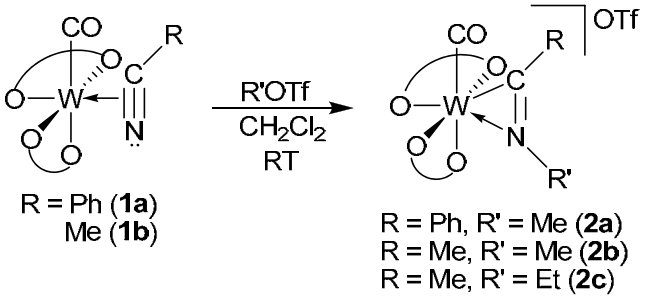

Scheme 4.1. Addition of methyl triflate to η^2-nitrile complexes.

The ^{1}H NMR spectrum of complex **2a** shows a downfield resonance at 4.97 ppm attributed to the newly added methyl group on nitrogen. Complex **2b** displays similar NMR results: the methyl bound to nitrogen resonates at 4.79 ppm, while the methyl group bound to carbon resonates at 4.11 ppm, shifted downfield from 3.71 in the neutral η^2-acetonitrile precursor **1b**. Each methyl peak associated with the iminoacyl ligand in **2b** appears as a sharp singlet at room temperature. As confirmed by an HMQC experiment, the iminoacyl carbon in

2b appears at 233.1 ppm in the ^{13}C NMR spectrum, downfield from 208.7 ppm in the neutral η^2-acetonitrile adduct. The carbonyl carbon shifts upfield to 219.7 ppm from 237.6 ppm in the precursor acetonitrile complex.[25]

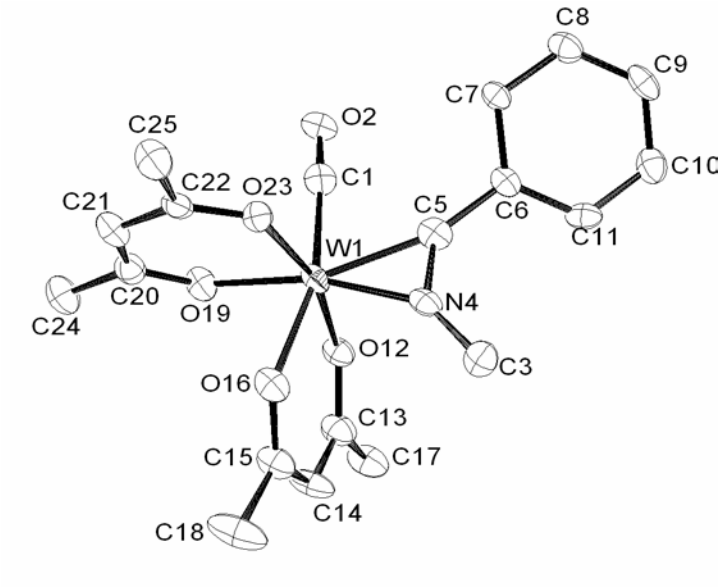

Figure 4.1. ORTEP diagram of [W(CO)(acac)$_2$(η^2-MeN=CPh)][OTf] (**2a**). Thermal ellipsoids are drawn with 50% probability. Hydrogen atoms and triflate counterion omitted for clarity.

The solid state structure of cationic η^2-iminoacyl complex **2a** shows two acetylacetonate chelates and one carbon monoxide ligand bound to tungsten defining five coordination sites of an approximate octahedron. The sixth site is filled with an iminoacyl ligand located *cis* to carbon monoxide with the nitrogen atom positioned *distal* to the carbonyl ligand. The N=C bond of the η^2-iminoacyl ligand is parallel to the W-C≡O axis, reminiscent of the C≡N orientation observed in the nitrile complex.[25] The tungsten-nitrogen bond distance, W1-N4, decreases slightly from 2.018(5) Å in the nitrile complex to 1.977(7) Å, and the bond distance to the iminoacyl carbon, W1-C5, increases slightly from 2.038(5) to 2.069(8) Å. The carbon-nitrogen bond distance (1.283(10) Å) remains virtually unchanged from the value observed for the analogous bond in the nitrile complex (1.270(7) Å).[25] In

summary, formal addition of a cationic methyl group to the lone pair of the η^2-nitrile nitrogen does little to distort the geometry of the robust W-C-N triangle.

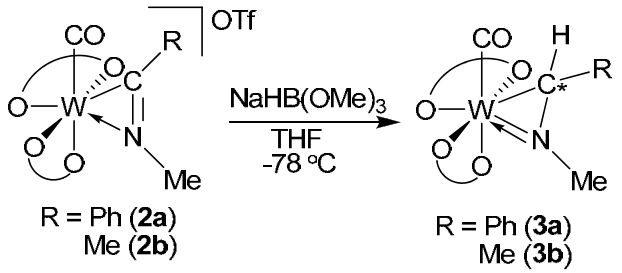

Scheme 4.2. Addition of sodium trimethoxyborohydride to cationic iminoacyl complexes.

Addition of Na[HB(OMe)$_3$] to [W(CO)(acac)$_2$(MeN=CPh)][OTf] **2a** in THF at -78°C reduces the iminoacyl ligand to a coordinated imine in W(CO)(acac)$_2$(η^2-MeN=CHPh) (**3a**) via nucleophilic attack of hydride at the iminoacyl carbon (Scheme 4.2). The room temperature ^{1}H NMR spectrum shows two diastereomers in a 2:1 ratio, reflecting chirality at both tungsten and carbon. The N-methyl on the imine ligand shifts upfield to 3.71 (major) ppm from 4.97 ppm in the cationic complex. Two resonances attributed to the imine C-*H* appear between 5 and 6 ppm, the same region as the acac methines. A COSY experiment shows the imine C-*H* peaks at 5.56 (major) and 5.80 (minor) ppm. The ^{13}C NMR spectrum displays the imine carbon at 60.8 (major) and 57.2 (minor) ppm, an upfield shift of ~170 ppm from the iminoacyl carbon in complex **2a**. This significant change in the ^{13}C chemical shift reflects the sp^3 character of the imine carbon in complex **3a**. IR spectroscopy of **3a** in hexanes also indicates two isomers with carbonyl C≡O absorptions at 1904 and 1889 cm^{-1} (Figure 4.2). Addition of a nucleophilic methyl group to **2a** using MeMgBr as a reagent produces W(CO)(acac)$_2$(η^2-MeN=CMePh) **4** (Scheme 4.3).

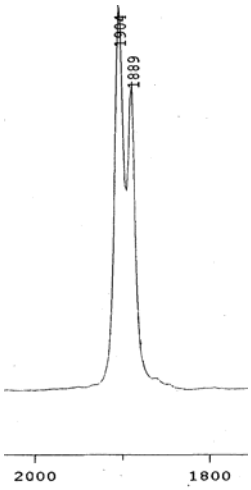

Figure 4.2. Expanded IR spectrum of W(CO)(acac)$_2$(η^2-MeN=CHPh) (**3a**) in hexanes showing the CO absorption frequency of both diastereomers.

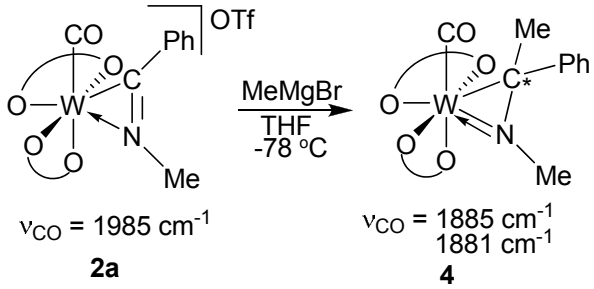

Scheme 4.3. Addition of methylmagnesium bromide to **2a**.

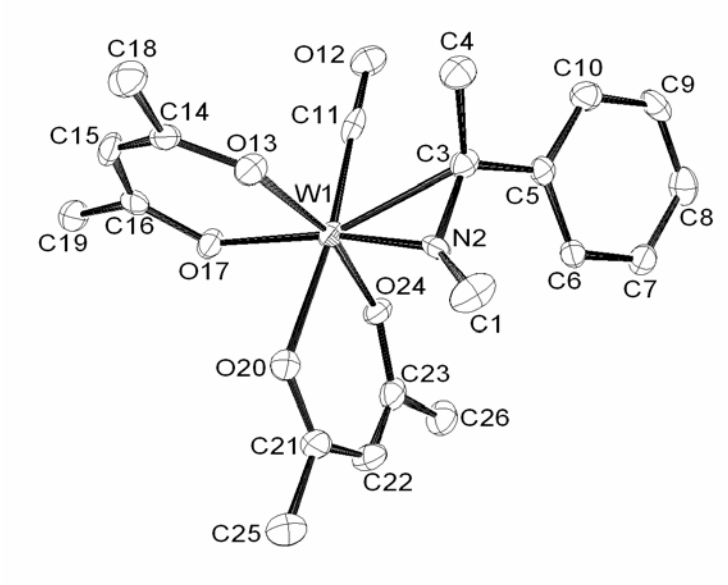

Figure 4.3. ORTEP diagram of W(CO)(acac)$_2$(η^2-MeN=CMePh) (**4**). Thermal ellipsoids are drawn with 50% probability. Hydrogen atoms are omitted for clarity.

The X-ray structure of **4** depicts the same framework around the metal as is observed in the neutral nitrile and cationic iminoacyl carbonyl complexes: two acetylacetonate chelates and one carbon monoxide ligand surround tungsten with an η^2-N=C linkage in the remaining position. The chiral imine ligand is π-bound to the metal center, *cis* to carbon monoxide, with the nitrogen atom *distal* to the metal carbonyl ligand. Both substituents on the imine carbon skew from the plane defined by the W-C-N triangle in accord with an aziridine geometry. The methyl group bound to nitrogen, on the other hand, deviates only slightly from the same plane. Bond distances from the metal to the imine ligand reflect a large change in the geometry of the W-C-N triangle upon addition of a nucleophile at carbon. The tungsten-carbon bond, W1-C3, lengthens considerably from 2.069(8) to 2.274(2) Å, and the W1-N2 bond decreases from 1.977(7) to 1.905(5) Å, suggestive of lone pair donation from the nitrogen to tungsten, effectively resulting in a double bond from nitrogen to the metal. The carbon-nitrogen bond distance in the imine ligand, N2-C3, elongates from 1.283(10) to

1.383(2) Å. indicating a loss of C-N multiple bond character upon nucleophilic attack. These values mirror those of W(CO)(acac)$_2$(η^2-PhN=CHPh), an imine complex derived from direct addition of an *N*-benzylideneaniline to W(CO)$_3$(acac)$_2$.[25] *Note that no rearrangement in W-C-N connectivity occurs in the transformation from nitrile to iminoacyl and on to imine.* Each η^2-C=N ligand remains π-bound to tungsten in the same orientation of the ligating carbon and nitrogen atoms relative to the rest of the unaltered coordination sphere.

Table 4.1. Comparison of salient bond distances, NMR and IR data

Complex	W-N (Å)	W-C (Å)	C-N (Å)	^{13}C, N≡*C* (δ)	IR, ν_{CO} (cm^{-1})
Nitrile[25]	2.018(5)	2.038(5)	1.270(7)	211.2	1895
Iminoacyl (**2a**)	1.977(7)	2.069(8)	1.283(10)	226.2	1976
Imine (**4**)	1.905(5)	2.274(2)	1.383(2)	59.3, 60.6	1881, 1885

Addition of Na[HB(OMe)$_3$] to **2b** appears to proceed like the other addition reactions, but room temperature ^{1}H NMR spectroscopy does not indicate the presence of two diastereomers in solution. In fact, signals due to the added hydrogen and the methyl of the anticipated H-C-Me unit of the imine are absent at room temperature. However, low temperature ^{1}H NMR spectroscopy reveals that hydride addition indeed occurs to produce W(CO)(acac)$_2$(η^2-MeN=CHMe) (**3b**). At 238 K, two diastereomers are resolved and appear in a 1:1 ratio. The added hydrogen atom is bound to the imine carbon and appears as a quartet at either 4.55 or 5.11 ppm due to the presence of two diastereomers. Variable temperature NMR measurements focusing on the two singlets for the methyl group bound to nitrogen in the two diastereomers reveal a coalescence temperature of 263 K. Using the Gutowsky-Holm equation,[48] this temperature corresponds to a free energy barrier for diastereomer interconversion of $\Delta G^{\ddagger}$ = 13.2 kcal/mole. The fluxional process observed at room temperature results from interconversion of the two diastereomers on the NMR time

scale. This dynamic behavior is observed in the CHMe (**3b**) derivative, but not in the CHPh (**3a**) or the CMePh (**4**) derivatives.

For this interconversion process to occur, one of the two stereocenters in the molecule must racemize. One possible mechanism involves interconversion of chirality at the imine carbon (Scheme 4.4, Pathway A). Dissociation of the carbon atom from the tungsten center could form a sixteen-electron intermediate species in which the imine is σ-bound through the nitrogen atom. Once the imine assumes the planar geometry appropriate for an N-bound ligand, the carbon can coordinate to tungsten through either face. Note that the geometry of the η^2-coordinated imine requires rotation of the CHMe fragment relative to the C=N-Me plane of the κ-N-imine upon binding the imine carbon to tungsten.

Pathway A

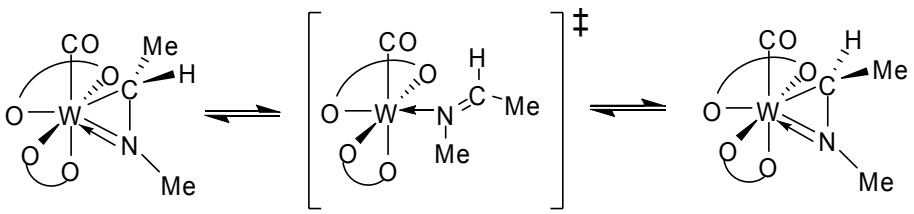

Pathway B

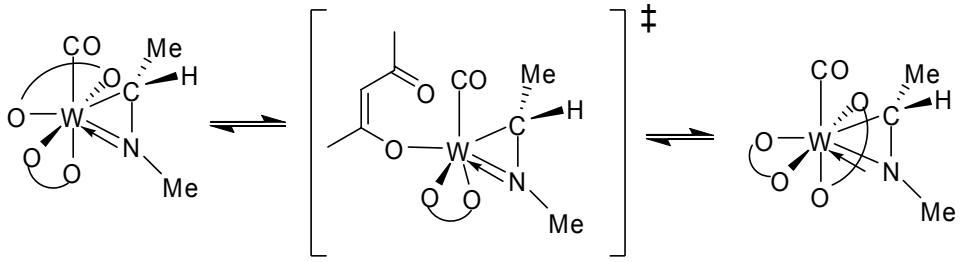

Scheme 4.4. Possible mechanisms for interconversion of diastereomers in **3b**.

A second possibility for isomer interconversion involves inversion of stereochemistry at tungsten via dissociation of an acetylacetonate arm resulting in a sixteen-electron

intermediate species (Scheme 4.4, Pathway B). Re-association of the chelate arm on the opposite side of the metal atom inverts stereochemistry at the tungsten center.

To distinguish between these two possible mechanisms, an imine derivative deprived of a chiral center at the imine carbon was synthesized, and an ethyl substituent on the imine nitrogen was used to probe chirality at the metal using the diastereotopic methylene protons. $W(CO)(acac)_2[\eta^2$-EtN=$CMe_2]$, **5**, was synthesized by alkylation of **1b** using EtOTf, follwed by subsequent nucleophilic attack on the cationic complex with MeMgBr (Scheme 4.5). At room temperature, the ^{1}H NMR spectrum shows one product, with a distinct ABX_3 pattern corresponding to the methylene protons on the nitrogen-ethyl substituent (Figure 4.4). Detection of a chiral environment by the diastereotopic methylene protons at room temperature eliminates facile acetylacetonate dechelation as a mechanism for accessing an intermediate with a mirror plane in this complex and makes it unlikely that acac rearrangement is the dynamic process responsible for diastereomer interconversion in complex **3b**. Dissociation of the imine ligand at carbon to form a κ^1-N imine with a chiral tungsten center becomes the likely mechanism for the dynamic process that interconverts diastereomers in **3b**.

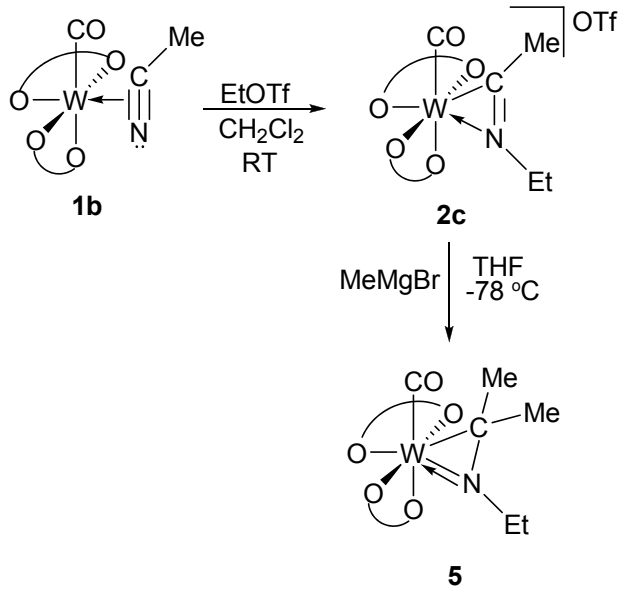

Scheme 4.5. Synthetic route to generate non-chiral imine derivative **5**.

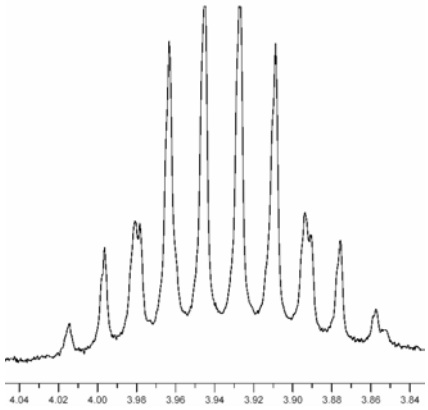

Figure 4.4. Expanded room temperature ^{1}H NMR (CD_2Cl_2) spectrum of W(CO)(acac)$_2$(η^2-EtN=CMeMe), (**5**), showing the ABX_3 splitting pattern attributed to the diastereotopic methylene protons on the imine ligand.

Summary

In summary, the stepwise conversion of π-bound nitriles to π-bound imines has been accomplished. Single crystal X-ray structures have been determined for the cationic iminoacyl complex [W(CO)(acac)$_2$(η^2-MeN=CPh)][OTf], **2a**, and the neutral imine complex

W(CO)(acac)$_2$(η^2-MeN=CMePh), **4**. Complex **3b,** W(CO)(acac)$_2$(η^2-MeN=CHMe), displays fluxionality which interconverts diastereomers via dissociation of the η^2-imine carbon.

Table 4.2. Crystal data and refinement parameters for **2a** and **4**.

Complex	**2a**	**4**
Empirical Formula	$C_{20}H_{22}F_3NO_8SW$	$C_{20}H_{25}NO_5W$
fw	677.29	543.26
Color	Burgundy	Dark red
Temp(K)	100(2)	100(2)
λ (Mo Kα) (Å)	0.71703	0.71703
Cryst Syst	Monoclinic	Monoclinic
Space Group	*C*2/*c*	$P2_1/n$
a (Å)	28.4062(13)	8.3192(3)
B (Å)	7.6114(3)	14.2955(4)
c (Å)	22.3725(10)	17.0591(6)
α (deg)	90	90
B (deg)	98.730(3)	92.92
γ (deg)	90	90
Vol. (Å^3)	4781.1(4)	2026.15(12)
Z	8	4
D_{calc} (Mg/m^3)	1.882	1.781
μ (mm^{-1})	4.99	5.73
F(000)	2638	1064
Cryst size (mm)	0.20 x 0.05 x 0.01	0.10 x 0.10 x 0.10
2θ range (deg)	5.00 to 50.00	1.86 to 30.07
Index Ranges	-33<=h<=33 0<=k<=9 0<=l<=26	-11<=h<=11 -20<=k<=20 -24<=l<=23
Reflections Collected	30525	88084
Independent reflections	4229 [R(int) = 0.0550]	88084 [R(int) = 0.0000]
Data/restraints/parameters	4229/0/308	88084/0/252
Goodness-of-fit on F^2	1.9382	1.004
Final R indices[I>2sigma(I)]	R1 = 0.040 wR2 = 0.042	R1 = 0.0394 wR2 = 0.1014
R indices (all data)	R1 = 0.056 wR2 = 0.044	R1 = 0.0530 wR2 = 0.1065
Largest diff. peak and hole	1.660 and -1.840 e Å^{-3}	2.564 and -1.866 e Å^{-3}

Experimental

General Information. Reactions were performed under a dry nitrogen atmosphere using standard Schlenk techniques. Methylene chloride, hexanes, and pentane were purified by passage through an activated alumina column under a dry argon atmosphere.[49] THF was distilled from a sodium ketal suspension. Methylene chloride-d_2 was dried over CaH_2 and degassed. All other reagents were purchased from commercial sources and were used without further purification.

NMR spectra were recorded on Bruker DRX400, AMX400, or AMX300 spectrometers. Infrared spectra were recorded on an ASI Applied Systems React IR 1000 FT-IR spectrometer. Elemental analysis was performed by Atlantic Mircrolab, Norcross, GA, and Robertson Microlit, Madison, NJ. **1a** and **1b** were made in accordance with a literature procedure.[25]

[W(CO)(acac)$_2$(η^2-MeN=CPh)][OTf] (2a). A 200 mL Schlenk flask was charged with **1a** (1.08 g) and the solid was dissolved in methylene chloride (30 mL) resulting in a dark amber solution. Treatment with 1.5 eq of methyl trifluoromethylsulfonate (MeOTf) caused a color change to burgundy. *In situ* IR spectroscopy revealed a single CO absorbance at ~1985 cm^{-1} after 30 min of stirring. The solvent volume was reduced *in vacuo* and hexanes (50 mL) were added to precipitate the cationic product. Excess solvent was removed via cannula filtration yielding a burgundy powder (1.32 g, 93%). A portion of the isolated burgundy powder **2a** was dissolved in methylene chloride and layered with hexanes in an inert atmosphere at -30°C. Small burgundy needles of **2a** suitable for X-ray analysis formed overnight. IR (KBr): ν_{CO} = 1976 cm^{-1}, ν_{CN} = 1627 cm^{-1}. ^{1}H NMR (CD_2Cl_2, 298 K, δ): 7.88-7.90 (m, 2H, *o*-C_6H_5),

7.80-7.84 (m, 2H, *m*-C_6H_5), 7.69-7.73 (m, 1H, *p*-C_6H_5), 5.95, 5.94 (each a s, each 1H, acac C*H*), 4.97 (s, 3H, N-CH_3), 2.58, 2.38, 2.37, 2.16 (each a s, each 3H, acac CH_3); $^{13}C\{^1H\}$ NMR (CD_2Cl_2, 298 K, δ): 25.4, 26.3, 26.6, 28.4 (acac *C*H_3), 42.3 (N-*C*H_3), 101.6, 104.3 (acac *C*H), 128.0 (*ipso*-C_6H_5), 130.1 (*m*-C_6H_5), 132.1 (*o*-C_6H_5), 136.7 (*p*-C_6H_5), 187.8, 188.9, 193.3, 199.0 (acac *C*O), 220.8 (*C*≡O), 226.2 (N≡*C*). Anal. Calcd for $WC_{20}H_{22}O_8NSF_3$: C, 35.46; H, 3.28; N, 2.07 . Found: C, 35.14; H, 3.14; N, 1.99%.

[W(CO)(acac)$_2$(η^2-MeN=CMe)][OTf] (2b). A 200 mL Schlenk flask was charged with **1b** (0.74 g) and the solid was dissolved in CH_2Cl_2 (20 mL) resulting in a dark amber solution. Treatment with 1 eq of MeOTf caused a color change to olive green. *In situ* IR spectroscopy revealed a single CO absorbance at ~1985 cm^{-1} after 30 min of stirring. The solvent volume was reduced *in vacuo* and hexanes (50 mL) were added to precipitate the cationic product. Excess solvent was removed via cannula filtration yielding an olive green powder (740 mg, 75%). IR (KBr): ν_{CO} = 1968 cm^{-1}, ν_{CN} = 1657 cm^{-1}. ^1H NMR (CD_2Cl_2, 298 K, δ): 5.88, 5.87 (each a s, each 1H, acac C*H*), 4.79 (s, 3H, N-CH_3), 4.11 (s, 3H, N=C-CH_3), 2.53, 2.13 (each a s, each 3H, acac CH_3), 2.32 (s, 6H, acac CH_3); $^{13}C\{^1H\}$ NMR (CD_2Cl_2, 298 K, δ): 20.3 (N≡C-*C*H_3), 25.2, 26.1, 26.4, 28.1 (acac *C*H_3), 41.3 (N-*C*H_3), 101.7, 104.0 (acac *C*H), 187.5, 188.8, 193.3, 198.8 (acac *C*O), 219.7 (*C*≡O), 233.1 (N≡*C*). Anal. Calcd for $WC_{15}H_{20}O_8NSF_3$: C, 29.28; H, 3.28; N, 2.28. Found: C, 29.06; H, 3.01; N, 1.96%.

[W(CO)(acac)$_2$(η^2-EtN=CMe)][OTf] (2c). A Schlenk flask was charged with **1b** (50 mg) and CH_2Cl_2 (20 mL). Ethyl triflate (30 μL) was added at 0 °C and the solution was stirred overnight at room temperature. The green solution was reduced and washed with hexanes to afford a green-brown powder (55 mg, 79%). ^1H NMR (CD_2Cl_2, 298 K, δ): 5.92, 5.87 (each a s, each 1H, acac C*H*), 5.17 (m, 2H, N-CH_2-CH_3), 4.13 (s, 3H, N≡C-CH_3), 2.52, 2.32, 2.30,

2.14 (each a s, each 3H, acac CH_3), 1.46 (t, 3H, N-CH_2-CH_3); $^{13}C\{^1H\}$ NMR (CD_2Cl_2, 298 K, δ): 15.0 (N-CH_2-CH_3), 20.6 (N≡C-CH_3), 25.4, 26.2, 26.4, 28.2 (acac CH_3), 51.8 (N-CH_2-CH_3), 101.6, 104.1 (acac CH), 187.7, 188.9, 193.2, 198.9 (acac CO), 219.5 (C≡O), 232.0 (N≡C).

W(CO)(acac)$_2$(η^2-MeN=CHPh) (3a). Under an inert atmosphere, **2a** (200 mg) was combined with sodium trimethoxyborohydride, Na[HB(OMe)$_3$], (40 mg) in a 200 mL Schlenk flask. The flask was cooled to -78°C and THF (20 mL) was added. A color change from burgundy to cherry red occurred and *in situ* IR spectroscopy revealed a new CO absorbance at 1883 cm^{-1} after 10 min of stirring. The solvent was removed *in vacuo* and the resulting red solid was chromatographed on silica using CH_2Cl_2 to elute a red band (75 mg, 48%). IR (hexanes): ν_{CO} = 1904 cm^{-1} (major diastereomer), ν_{CO} = 1889 cm^{-1} (minor diastereomer). ^{1}H NMR (CD_2Cl_2, 298 K, δ, major diastereomer): 7.24-7.32 (m, 3H, *m* and *p*-C_6H_5), 7.14-7.16 (m, 2H, *o*-C_6H_5), 5.48, 5.72 (each a s, each 1H, acac CH), 5.56 (s, 1H, N-C-H), 3.71 (s, 3H, N-CH_3), 2.57, 2.25, 2.16, 2.03 (each a s, each 3H, acac CH_3). ^{1}H NMR (CD_2Cl_2, 298 K, δ, minor diastereomer): 7.01-7.07 (m, 3H, *m* and *p*-C_6H_5), 6.80-6.83 (m, 2H, *o*-C_6H_5), 5.80 (s, 1H, N-C-H), 5.58, 5.56 (each a s, each 1H, acac CH), 3.83 (s, 3H, N-CH_3), 2.49, 2.13, 2.09, 2.03 (each a s, each 3H, acac CH_3). $^{13}C\{^1H\}$ NMR (CD_2Cl_2, 298 K, δ, major diastereomer): 26.0, 26.3, 27.7, 27.9 (acac CH_3), 43.6 (N-CH_3), 60.8 (N-C), 99.4, 101.0 (acac CH), 127.4 (*m*-C_6H_5), 127.6 (*p*-C_6H_5), 127.9 (*o*-C_6H_5), 148.1 (*ipso*-C_6H_5), 184.3, 186.3, 187.0, 193.8 (acac CO), 233.4 (C≡O). $^{13}C\{^1H\}$ NMR (CD_2Cl_2, 298 K, δ, minor diastereomer): 25.7, 26.9, 27.5, 28.1 (acac CH_3), 43.8 (N-CH_3), 57.2 (N=C), 99.4, 101.5 (acac CH), 126.6 (*m*-C_6H_5), 126.7 (*o*-C_6H_5), 127.0 (*p*-C_6H_5), 147.2 (*ipso*-C_6H_5), 185.5, 185.6,

188.1, 194.7 (acac *C*O), 235.3 (*C*≡O). Anal. Calcd for $WC_{19}H_{23}O_5N$: C, 43.11; H, 4.39; N, 2.65. Found: C, 43.10; H, 4.34; N, 2.66%.

W(CO)(acac)$_2$(η^2-MeN=CHMe) (3b). Under an inert atmosphere, **2b** (30 mg) was placed in a 100 mL Schlenk flask. The flask was cooled to -78°C and THF (15 mL) was added. In a separate flask a solution containing Na[HB(OMe)$_3$] (7 mg) and THF (5 mL) was prepared and cannula transferred to the flask containing **2b** resulting in a color change from green to red. After 30 min of stirring, the solvent volume was reduced *in vacuo* and hexanes (20 mL) were added to precipitate residual salts. The red supernatant was cannula filtered to a separate flask and the remaining solvent was removed *in vacuo* yielding a red-brown solid (17 mg, 75%). ^{1}H NMR (CD_2Cl_2, 240 K, δ, 1:1 diastereomers): 5.64, 5.46, 5.43 (each a s, 2:1:1, acac C*H*), 5.11, 4.55 (each a q, 1H, N-C-*H*, $^2J_{H\text{-}H}$ = 4.9Hz), 3.64, 3.57 (each a s, 3H, N-CH_3), 2.46, 2.45, 2.20, 2.06, 2.05, 2.00, 1.98 (each a s, 3:3:6:3:3:3:3, acac CH_3), 2.23, 1.96 (each a d, each 3H, N=C-CH_3, $^2J_{H\text{-}H}$ = 4.9 Hz); ^{13}C{^{1}H} NMR (CD_2Cl_2, 240 K, δ, 1:1 diastereomers): 19.4-28.1 (acac *C*H$_3$, N=C-*C*H$_3$), 41.2, 43.2 (N-*C*H$_3$), 56.4, 56.7 (N=*C*), 99.4, 99.5, 100.8, 100.9 (acac *C*H), 183.7, 184.1, 184.8, 185.4, 186.0, 186.1, 193.7, 194.1 (acac *C*O), 231.3, 231.9 (*C*≡O).

W(CO)(acac)$_2$(η^2-MeN=CMePh) (4). Under an inert atmosphere, **2a** (50 mg) was placed in a 100 mL Schlenk flask. The flask was cooled to -78°C and THF (10 mL) was added. A solution of methylmagnesiumbromide, MeMgBr, (30 µL, 3M in Et_2O) was added to the flask. After 10 min of stirring, *in situ* IR spectroscopy indicated the presence of one CO absorbance at 1866 cm^{-1}. The solvent was removed *in vacuo* and the resulting red solid was dissolved in a minimal amount of CH_2Cl_2. Hexanes were added to precipitate the residual magnesium salt and the red liquid was cannula filtered to another flask, where the solvent

was removed *in vacuo* to yield a red solid. Column chromatography on silica using methylene chloride eluted a red band (24 mg, 60%). Complex **4** was dissolved in hexanes and placed in a freezer at -30°C. Dark red crystals suitable for X-ray analysis formed after a few days. IR (hexanes): ν_{CO} = 1881, 1885 cm^{-1}; ^1H NMR (CD_2Cl_2, 298 K, δ, both diastereomers): 7.23-7.30 (m, 4H, *m*-C_6H_5), 7.13-7.15 (m, 2H, *o*-C_6H_5), 6.98-7.03 (m, 2H, *p*-C_6H_5), 6.75-6.77 (m, 2H, *o*-C_6H_5), 5.61, 5.55, 5.54, 5.52 (each a s, each 1H, acac C*H*), 3.85, 3.79 (each a s, each 3H, N-CH_3), 2.46, 2.43, 2.26, 2.17, 2.14, 2.10, 2.09, 2.06 (each a s, each 3H, acac CH_3), 2.45, 1.96 (each a s, each 3H, N=C-CH_3). $^{13}C\{^1H\}$ NMR (CD_2Cl_2, 298 K, δ, both diastereomers): 23.2, 24.6 (N=C-*C*H_3), 25.7, 26.0, 26.3, 26.8, 27.5, 27.6, 28.0, 28.1 (acac *C*H_3), 40.0, 40.7 (N-*C*H_3), 59.3, 60.6 (N=*C*), 99.4, 99.6, 101.1, 101.5 (acac *C*H), 126.2, 126.4 (*p*-*C*$_6H_5$), 126.3, 127.1, 127.2, 127.3 (*o/m*-*C*$_6H_5$), 149.7, 150.6 (*ipso*-*C*$_6H_5$), 185.2, 185.7, 185.7, 186.3, 186.4, 187.7, 193.9, 194.3 (acac *C*O), 234.6, 236.5 (*C*≡O). Anal. Calcd for $C_{20}H_{25}O_5NW$: C, 44.21; H, 4.65; N, 2.58. Found: C, 44.03 H, 4.49; N, 2.02%.

W(CO)(acac)$_2$(η^2-EtN=CMe$_2$) (5). A 200 mL Schlenk flask was charged with **2c** (50 mg) and THF (25 mL). The resulting green solution was cooled to -78 °C. A solution of methylmagnesiumbromide (40 μL, 3M in Et_2O) was added to the flask yielding a red-brown solution. Solvent was removed *in vacuo* after 1 h and the product was extracted with hexanes. Removal of solvent gave a red-brown powder (30 mg, 69%). ^1H NMR (CD_2Cl_2, 298 K, δ): 5.58, 5.46 (each a s, each 1H, acac C*H*), 3.94 (m, 2H, N-CH_2-CH_3), 2.40, 2.15, 2.07, 1.99 (each a s, each 3H, acac CH_3), 2.20, 2.03 (each a s, each 3H, N-C(CH_3)-CH_3); $^{13}C\{^1H\}$ NMR (CD_2Cl_2, 298 K, δ): 16.4 (N-CH_2-*C*H_3), 26.1, 26.4, 27.3, 28.0 (acac *C*H_3), 30.0, 31.9 (N-C(*C*H_3)-*C*H_3), 49.6 (N-*C*H_2-CH_3), 59.8 (N=*C*), 99.5, 101.0 (acac *C*H), 185.6, 185.7, 186.2, 194.0 (acac *C*O), 233.6 (*C*≡O).

References

(1) Kukushkin, V. Y.; Pombeiro, A. J. L. *Chem. Rev.* **2002**, *102*, 1771.

(2) Michelin, R. A.; Mozzon, M.; Bertani, R. *Coord. Chem. Rev.* **1996**, *147*, 299.

(3) Parkins, A. W. *Platinum Met. Rev.* **1996**, *40*, 169.

(4) daRocha, Z. N.; Chiericato, G.; Tfouni, E. In *Electron Transfer Reactions*, 1997; Vol. 253.

(5) Murahashi, S. I.; Takaya, H. *Acc. Chem. Res.* **2000**, *33*, 225.

(6) Kukushkin, V. Y.; Pombeiro, A. J. L. *Inorg. Chim. Acta* **2005**, *358*, 1.

(7) Feng, S. G.; Templeton, J. L. *J. Am. Chem. Soc.* **1989**, *111*, 6477.

(8) Wright, T. C.; Wilkinson, G.; Motevalli, M.; Hursthouse, M. B. *J. Chem. Soc., Dalton Trans.* **1986**, 2017.

(9) Chetcuti, P. A.; Knobler, C. B.; Hawthorne, M. F. *Organometallics* **1988**, *7*, 650.

(10) Barrera, J.; Sabat, M.; Harman, W. D. *J. Am. Chem. Soc.* **1991**, *113*, 8178.

(11) Barrera, J.; Sabat, M.; Harman, W. D. *Organometallics* **1993**, *12*, 4381.

(12) Lorente, P.; Carfagna, C.; Etienne, M.; Donnadieu, B. *Organometallics* **1996**, *15*, 1090.

(13) Kiplinger, J. L.; Arif, A. M.; Richmond, T. G. *Chem. Commun.* **1996**, 1691.

(14) Thomas, S.; Tiekink, E. R. T.; Young, C. G. *Organometallics* **1996**, *15*, 2428.

(15) Kiplinger, J. L.; Arif, A. M.; Richmond, T. G. *Organometallics* **1997**, *16*, 246.

(16) Thomas, S.; Young, C. G.; Tiekink, E. R. T. *Organometallics* **1998**, *17*, 182.

(17) Garcia, J. J.; Jones, W. D. *Organometallics* **2000**, *19*, 5544.

(18) Garcia, J. J.; Brunkan, N. M.; Jones, W. D. *J. Am. Chem. Soc.* **2002**, *124*, 9547.

(19) Garcia, J. J.; Arevalo, A.; Brunkan, N. M.; Jones, W. D. *Organometallics* **2004**, *23*, 3997.

(20) Etienne, M.; Carfagna, C.; Lorente, P.; Mathieu, R.; de Montauzon, D. *Organometallics* **1999**, *18*, 3075.

(21) Shin, J. H.; Savage, W.; Murphy, V. J.; Bonanno, J. B.; Churchill, D. G.; Parkin, G. *J. Chem. Soc., Dalton Trans.* **2001**, 1732.

(22) Cross, J. L.; Garrett, A. D.; Crane, T. W.; White, P. S.; Templeton, J. L. *Polyhedron* **2004**, *23*, 2831.

(23) Lis, E. C.; Delafuente, D. A.; Lin, Y. Q.; Mocella, C. J.; Todd, M. A.; Liu, W. J.; Sabat, M.; Myers, W. H.; Harman, W. D. *Organometallics* **2006**, *25*, 5051.

(24) Jackson, A. B.; White, P. S.; Templeton, J. L. *Inorg. Chem.* **2006**, *45*, 6205.

(25) Jackson, A. B.; Schauer, C. K.; White, P. S.; Templeton, J. L. *J. Am. Chem. Soc.* **2007**, *129*, 10628.

(26) Adams, R. D.; Chodosh, D. F. *J. Am. Chem. Soc.* **1977**, *99*, 6544.

(27) Adams, R. D.; Chodosh, D. F. *Inorg. Chem.* **1978**, *17*, 41.

(28) Gamble, A. S.; Birdwhistell, K. R.; Templeton, J. L. *J. Am. Chem. Soc.* **1990**, *112*, 1818.

(29) McMullen, A. K.; Rothwell, I. P.; Huffman, J. C. *J. Am. Chem. Soc.* **1985**, *107*, 1072.

(30) Chamberlain, L. R.; Durfee, L. D.; Fanwick, P. E.; Kobriger, L.; Latesky, S. L.; McMullen, A. K.; Rothwell, I. P.; Folting, K.; Huffman, J. C.; Streib, W. E.; Wang, R. *J. Am. Chem. Soc.* **1987**, *109*, 390.

(31) Lubben, T. V.; Plossl, K.; Norton, J. R.; Miller, M. M.; Anderson, O. P. *Organometallics* **1992**, *11*, 122.

(32) Zambrano, C. H.; Fanwick, P. E.; Rothwell, I. P. *Organometallics* **1994**, *13*, 1174.

(33) Daff, P. J.; Monge, A.; Palma, P.; Poveda, M. L.; Ruiz, C.; Valerga, P.; Carmona, E. *Organometallics* **1997**, *16*, 2263.

(34) Scott, M. J.; Lippard, S. J. *Organometallics* **1997**, *16*, 5857.

(35) Sanchez-Nieves, J.; Royo, P.; Pellinghelli, M. A.; Tiripicchio, A. *Organometallics* **2000**, *19*, 3161.

(36) Sanchez-Nieves, J.; Royo, P.; Mosquera, M. E. G. *Eur. J. Inorg. Chem.* **2006**, 127.

(37) Guram, A. S.; Jordan, R. F. *J. Org. Chem.* **1993**, *58*, 5595.

(38) Durfee, L. D.; Rothwell, I. P. *Chem. Rev.* **1988**, *88*, 1059.

(39) Yoshida, T.; Hirotsu, K.; Higuchi, T.; Otsuka, S. *Chem. Lett.* **1982**, 1017.

(40) Carrier, A. M.; Davidson, J. G.; Barefield, E. K.; Vanderveer, D. G. *Organometallics* **1987**, *6*, 454.

(41) Antinolo, A.; Fajardo, M.; Gil-Sanz, R.; Lopez-Mardomingo, C.; Martin-Villa, P.; Otero, A.; Kubicki, M. M.; Mugnier, Y.; El Krami, S.; Mourad, Y. *Organometallics* **1993**, *12*, 381.

(42) Temme, B.; Erker, G. *J. Organomet. Chem.* **1995**, *488*, 177.

(43) Cook, K. S.; Piers, W. E.; Patrick, B. O.; McDonald, R. *Can. J. Chem.* **2003**, *81*, 1137.

(44) Galakhov, M. V.; Gomez, M.; Jimenez, G.; Royo, P.; Pellinghelli, M. A.; Tiripicchio, A. *Organometallics* **1995**, *14*, 1901.

(45) Durfee, L. D.; Fanwick, P. E.; Rothwell, I. P.; Folting, K.; Huffman, J. C. *J. Am. Chem. Soc.* **1987**, *109*, 4720.

(46) Chiu, K. W.; Jones, R. A.; Wilkinson, G.; Galas, A. M. R.; Hursthouse, M. B. *J. Chem. Soc., Dalton Trans.* **1981**, 2088.

(47) Scott, M. J.; Lippard, S. J. *Organometallics* **1997**, *16*, 5857.

(48) Gutowsky, H. S.; Holm, C. H. *J. Chem. Phys.* **1956**, *25*, 1228.

(49) Pangborn, A. B.; Giardello, M. A.; Grubbs, R. H.; Rosen, R. K.; Timmers, F. J. *Organometallics* **1996**, *15*, 1518.

Chapter 5

Reduction of an η^2-Iminoacyl Ligand to η^2-Iminium Enabled by Adjacent Carbon Monoxide Ligand Replacement with a Variable Electron Donor in a Cationic Tungsten(II) Bis(acetylacetonate) Complex.

Introduction

Unsaturated organic molecules exhibit altered reactivity patterns once they are in the coordination sphere of a transition metal.[1-11] Specifically, nitriles readily undergo reduction when σ-bound to a metal center.[9-14] However, less reactivity is know of π-bound nitrile ligands.[5-8] Low valent Group 6 metals often stabilize dπ electrons at the metal center via backbonding to these fragments. We have constructed a bis(acetylacetonate) tungsten(II) d^4 fragment that preferentially binds nitriles through the C≡N π-system.[15]

We have previously reported reduction of π-bound nitrile complexes of the type W(CO)(η^2-nitrile)$(acac)_2$ to neutral imine-carbonyl complexes of the general formula W(CO) (η^2-imine)$(acac)_2$ via stepwise addition of electrophiles and nucleophiles.[8] Attempts to convert the π-bound imine to an iminium and ultimately to an amine have been unproductive with carbon monoxide as the adjacent ligand in the coordination sphere. Presumably this reflects the need for a four-electron donor ligand to stabilize the six-coordinate d^4 tungsten center.[16] The η^2-imine ligand provides four electrons to tungsten in W(CO)$(acac)_2$(η^2-imine) complexes.[8,15] Addition of a second electrophile to the nitrogen of the sidebound ligand would remove two electrons from the metal, so electrophilic addition at nitrogen is incompatible with the simple constraints imposed by electron counting in this system.

Iminium cations[17] ($R_2N{=}CR_2^+$) are postulated as intermediates in several fundamental organic reactions including Knoevenagel condensations,[18,19] decarboxylation of β-ketoacids,[20,21] and Diels-Alder type cyclizations.[22-24] Iminium ligands in transition metal complexes have resulted from direct reactions of iminium salts with metal reagents,[25,26] from rearrangements involving group transfer to imine ligands,[27,28] from β-hydride elimination of amines,[29,30] and from nitriles using strong reductants or other harsh conditions.[31-33]

We now report conversion of an η^2-imine to an η^2-iminium ligand; this reaction is enabled by replacement of the ancillary two-electron donor CO ligand in [W(CO)(η^2-RN=CR)(acac)$_2$]$^+$ with a variable electron donor alkyne. Substitution of CO by an alkyne in the cationic iminoacyl-CO tungsten(II) reagent relieves the η^2-N=C ligand of its responsibility to function as the sole four-electron donor to tungsten. The nitrogen lone pair, datively tied to tungsten when CO is the ancillary ligand in the coordination sphere, becomes sufficiently nucleophilic to react with potent electrophiles once an alkyne replaces CO. Results presented here are complementary to reactions observed in a related low-valent Tp′ [Tp' = hydridotris(3,5-dimethylpyrazolyl)borate] tungsten(II) system in which coordinated η^1-acetonitrile undergoes sequential reduction to an amine.[34,35]

Results and Discussion

Thermal Substitution of CO with RNC or PR_3 Ligands.

Addition of *tert*-butylisonitrile to a cold solution of η^2-iminoacyl complex [W(CO)(η^2-MeN=CPh)(acac)$_2$]$^+$ **1a** liberates the carbon monoxide ligand and leads to [W(CN^{t}Bu)(η^2-MeN=CPh)(acac)$_2$]$^+$ (**2a**) (Scheme 5.1). No CO absorbance is observed via *in situ* IR spectroscopy after 20 min of stirring at 0 °C; this is a surprisingly facile substitution reaction. For complex **2a**, the N-methyl resonance shifts far downfield to 5.67 ppm from the 4.97 ppm value of the iminoacyl-carbonyl precursor. The iminoacyl carbon resonates downfield at 239.7 ppm ^{13}C NMR spectrostrum, similar to the chemical shift in the parent iminoacyl-carbonyl cation (226.2 ppm). Low temperature ^{13}C NMR spectroscopy (240 K) reveals the metal-bound isonitrile carbon at 146.1 ppm, indicative of σ-bound isonitrile.

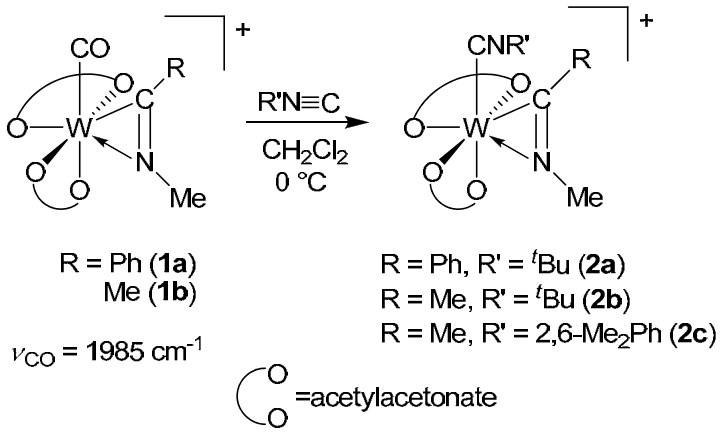

Scheme 5.1. Facile thermal replacement of CO with isonitrile.

The solid state structure of **2c[BAr′$_4$]** (BAr′$_4$ = tetrakis[(3,5-trifluoromethyl)phenyl]borate) reflects simple substitution of the carbon monoxide ligand by 2,6-dimethylphenylisonitrile (Figure 5.1). The nitrogen atom of the iminoacyl ligand is *distal* with respect to the cis isonitrile ligand, thus adopting the same orientation as the parent CO complex. The W-C-N triangular geometry is barely perturbed by replacement of CO with 2,6-dimethylphenylisonitrile. The minor bond length changes observed are presumably due to the greater π-acidity of the CO ligand in **1a** relative to the isonitrile ligand in **2c**.

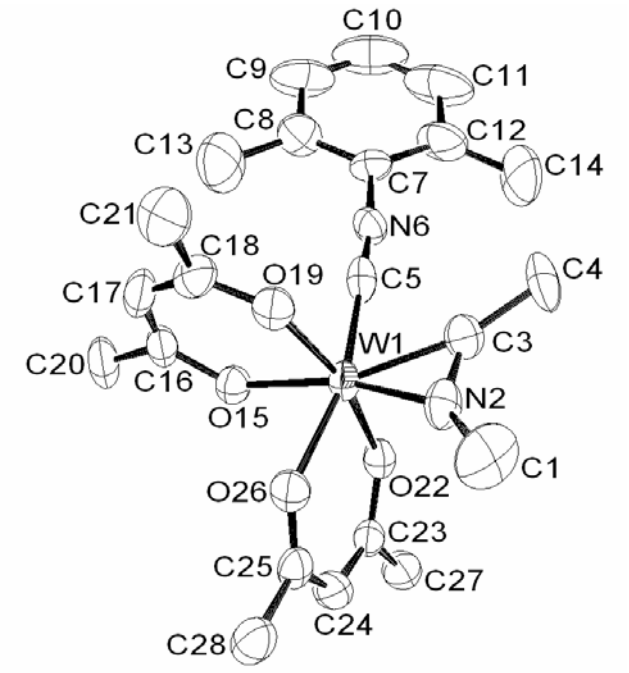

Figure 5.1. ORTEP diagram of **2c[BAr′$_4$]**. Thermal ellipsoids are drawn with 50% probability. Hydrogen atoms, the BAr′$_4$ counterion, and 0.5 Et_2O are omitted for clarity.

Addition of triphenylphosphine to iminoacyl cation **1a** also leads to carbon monoxide replacement. The product is a highly air and moisture sensitive deep purple complex, $[W(PPh_3)(\eta^2\text{-MeN=CPh})(acac)_2]^+$ (**3a**) (Scheme 5.2). Salient spectroscopic data include a peak far downfield at 6.74 ppm in the ^{1}H NMR spectrum attributed to the nitrogen-bound methyl group; the identity of this signal was confirmed via HMBC spectroscopy. The iminoacyl carbon resonates at 241.1 ppm in the ^{13}C NMR spectrum, and no phosphorus coupling is evident. The ^{31}P NMR spectrum displays a single resonance at -5.25 ppm with tungsten satellites [$^1J_{P\text{-}W}$ = 349 Hz, ^{183}W (14.28%), I = ½]. These data are consistent with simple replacement of CO by PPh_3, although the intense purple color and 6.74 ppm methyl chemical shift location are surprising.

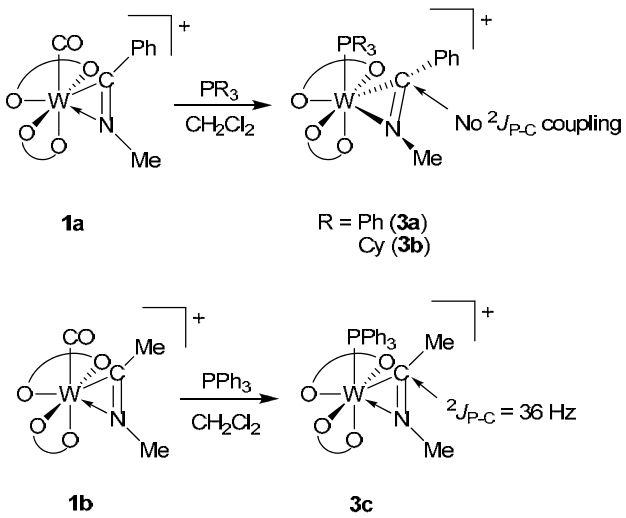

Scheme 5.2. Thermal replacement of CO with bulky phosphine reagents.

Tricyclohexylphosphine (PCy_3) also replaces the CO ligand in **1a**, and $[W(PCy_3)(\eta^2\text{-}MeN{=}CPh)(acac)_2]^+$ (**3b**) forms (Scheme 5.2). However, room temperature NMR spectroscopy shows broad resonances in ^1H, ^{13}C, and ^{31}P spectra. A broad peak attributed to the nitrogen-bound methyl group resonates at 8.44 ppm in the room temperature ^1H spectrum, a significant downfield shift from the analogous resonance in **1a**. Additionally, acetylacetonate methyl signals at 4.14 and 3.58 ppm exhibit similar line broadening and unusual downfield chemical shifts. The room temperature ^{13}C NMR spectrum also shows a broad peak for the nitrogen-bound methyl (43.9 ppm) and two of the acetylacetonate keto-carbons (196.2 and 202.3 ppm). Room temperature ^{31}P NMR spectroscopy reveals a broad peak at -23.2 ppm devoid of tungsten satellites. Variable temperature spectra indicate a temperature dependence for the chemical shift of the nitrogen-bound methyl group. Over a temperature range of 130 degrees with CD_2Cl_2 as solvent, the methyl resonance varies from 6.94 ppm (185 K) to 8.94 ppm (315 K), broadening as the temperature increases. At 200 K, the iminoacyl carbon resonance appears at 247.1 ppm, and as in the analogous complex **3a**,

shows no coupling to phosphorus. At 160 K using $CDCl_2F$ as a solvent the PCy_3 phosphorus resonance appears as a sharper singlet at 18.0 ppm ($^1J_{P\text{-}W}$ = 351 Hz).

Figure 5.2. Room temperature ^{1}H NMR spectrum of $[W(PPh_3)(\eta^2\text{-MeN=CPh})(acac)_2]^+$).

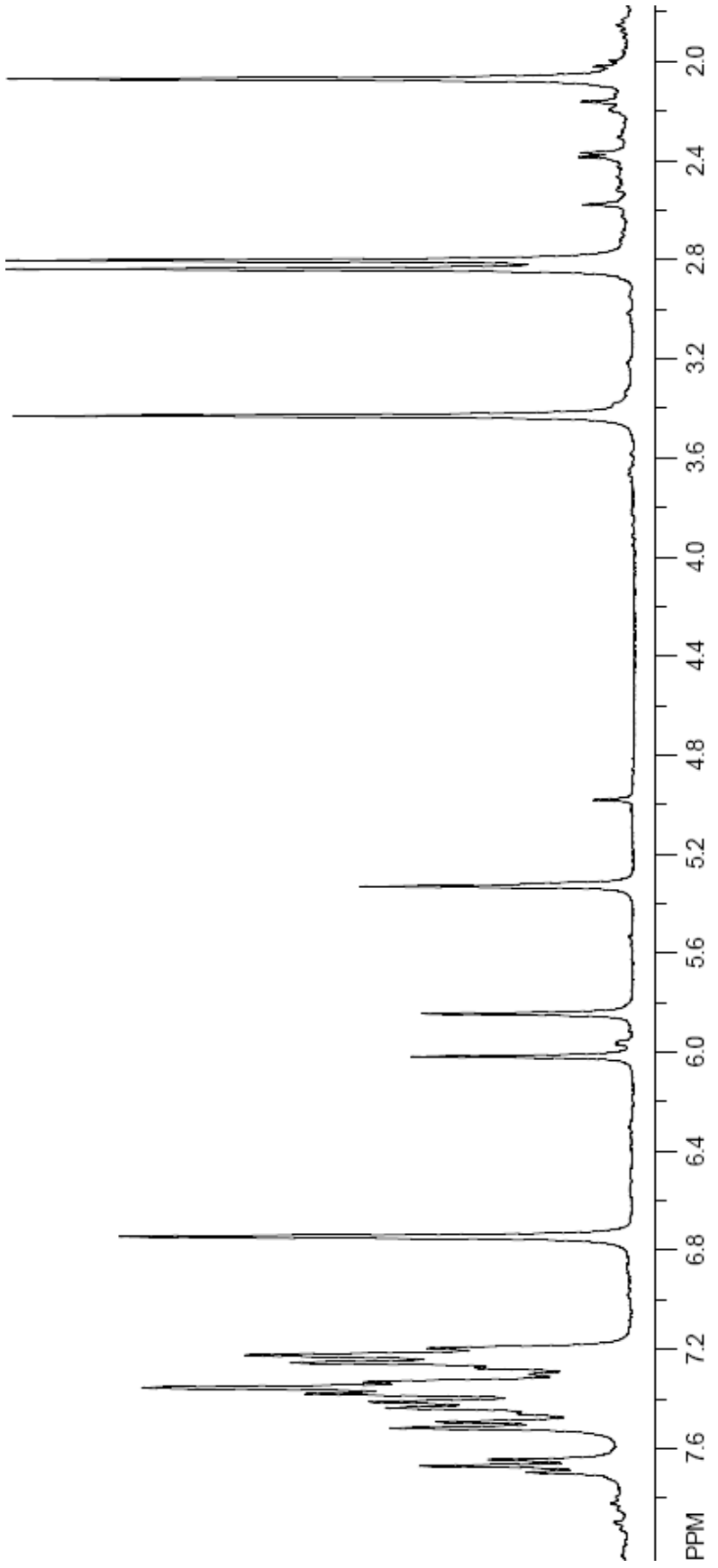
PPM
7.6
7.2
6.8
6.4
6.0
5.6
5.2
4.8
4.4
4.0
3.6
3.2
2.8
2.4
2.0

Figure 5.3. Room temperature ^{1}H NMR spectrum of $[W(PCy_3)(\eta^2\text{-MeN=CPh})(acac)_2]^+$.

PPM
8.4
8.0
7.6
7.2
6.8
6.4
6.0
5.6
5.2
4.8
4.4
4.0
3.6
3.2
2.8
2.4
2.0
1.6
1.2
0.8

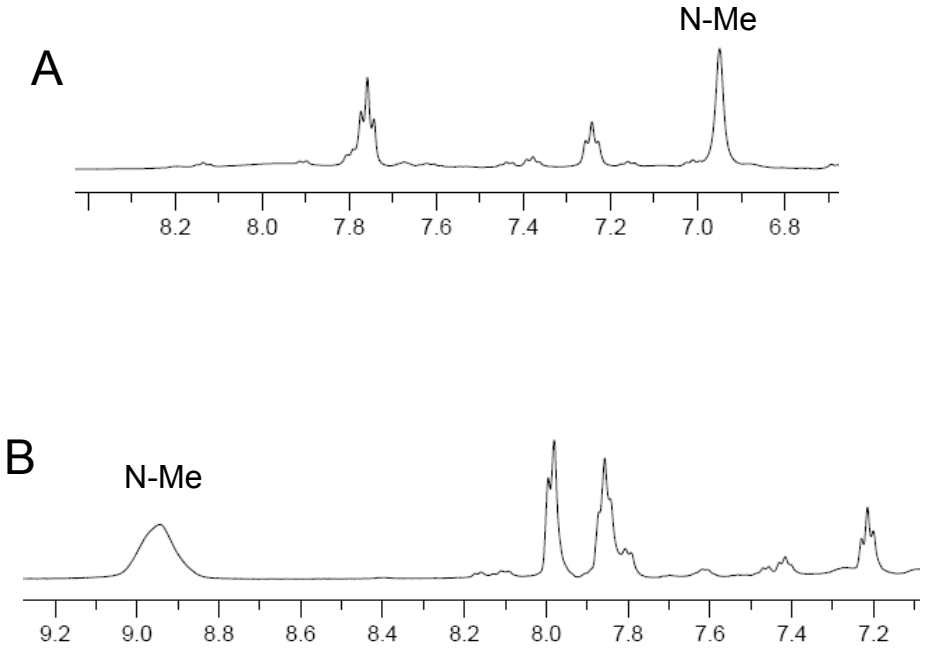

Figure 5.4. Expanded, variable temperature ^{1}H NMR spectra of **3b[OTf]** at 185 K (**A**) and 315 K (**B**).

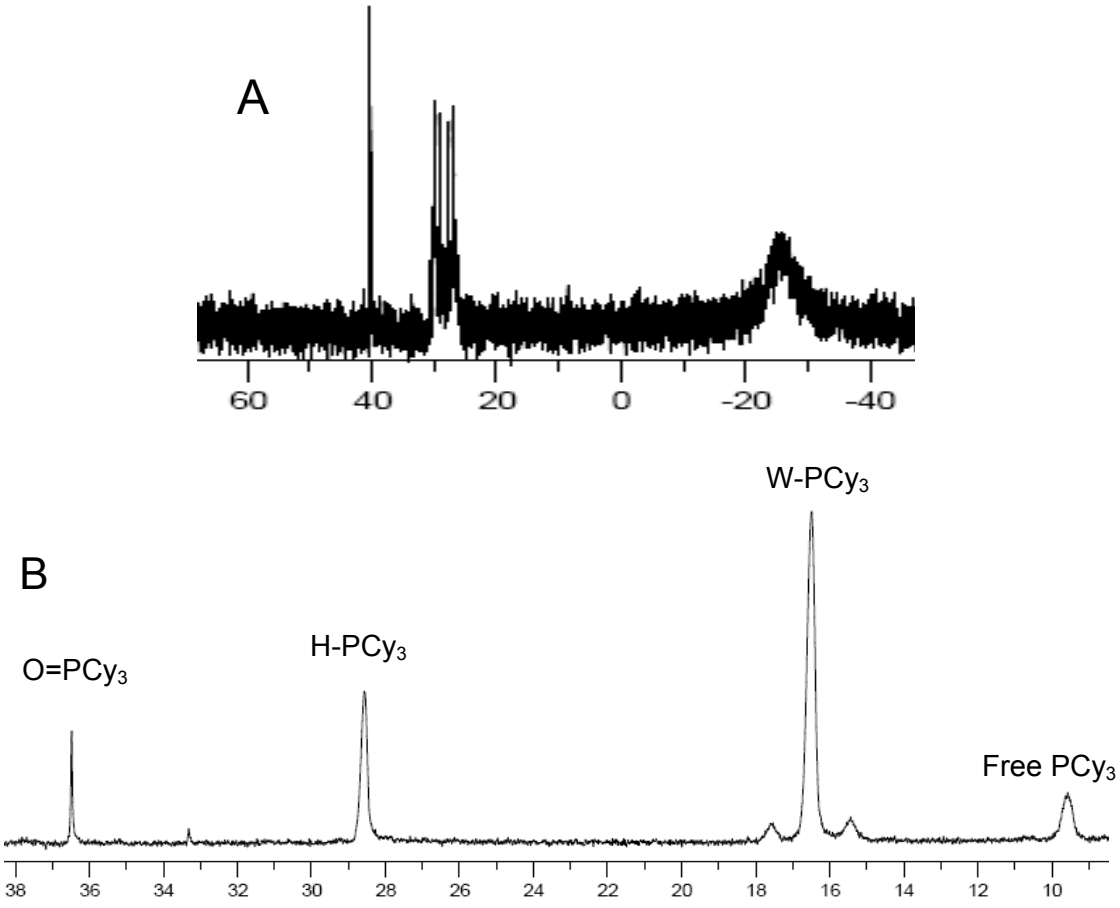

Figure 5.5. Expanded variable temperature ^{31}P NMR spectra of **3b[OTf]** at 298 K (**A**) and 160 K (**B**).

Addition of PPh_3 to **1b** produces $[W(PPh_3)(\eta^2\text{-MeN=CMe})(acac)_2]^+$, **3c**, over the course of several hours. This reaction proceeds considerably slower than the analogous one using **1a**. The N-methyl group in **3c** resonates at 5.80 ppm in the ^1H NMR spectrum, and the iminoacyl carbon appears as a doublet at 235.2 ppm ($^2J_{P\text{-}C}$ = 36 Hz) in the ^{13}C NMR spectrum. Note that addition of PCy_3 does not replace CO in **1b**; only decomposition was observed.

The solid state structure of $[W(PCy_3)(\eta^2\text{-MeN=CPh})(acac)_2][BAr_4']$, **3b[BAr′$_4$]**, confirms replacement of CO with the bulky phosphine reagent (Figure 5.6). Most notable is a change in the W-N-C triangle orientation as the N2-C3 bond of the iminoacyl ligand is orthogonal to the new W1-P1 bond (Scheme 5.3). Presumably, the increased steric demand of PCy_3 in the coordination sphere forces the iminoacyl ligand to rotate 90° from the geometry observed for CO complex **1a**. The aromatic phenyl ring lies in the plane defined by the W1-N2-C3 triangle, perhaps reflecting π-delocalization. Bond distances from tungsten to the C and N atoms in the iminoacyl ligand decrease relative to the same bonds in **1a**. Considerable shortening is observed for W1-C3 (1.990(4) Å), down from 2.069(8) Å in the CO-precursor. The carbon nitrogen bond, N2-C3, lengthens 0.041 Å to 1.324(5) Å. This lengthening suggests the iminoacyl ligand receives more backbonding from tungsten after replacing the strong π-acid CO ligand with a poorer π-acid phosphine ligand. A partially solved structure of PPh_3 adduct **3c** clearly shows that the N=C bond remains parallel to the W-P bond suggesting that without a π-acid adjacent to the iminoacyl ligand the rotational energy profile is relatively shallow (Scheme 5.3). Disorder in one of the auxiliary acetylacetonate chelates prevents refinement.

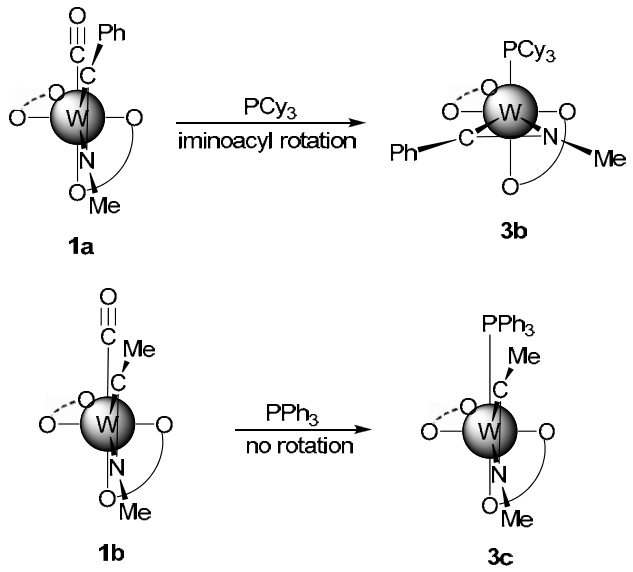

Scheme 5.3. Behavior of the iminoacyl ligand adjacent to bulky phosphine ligands.

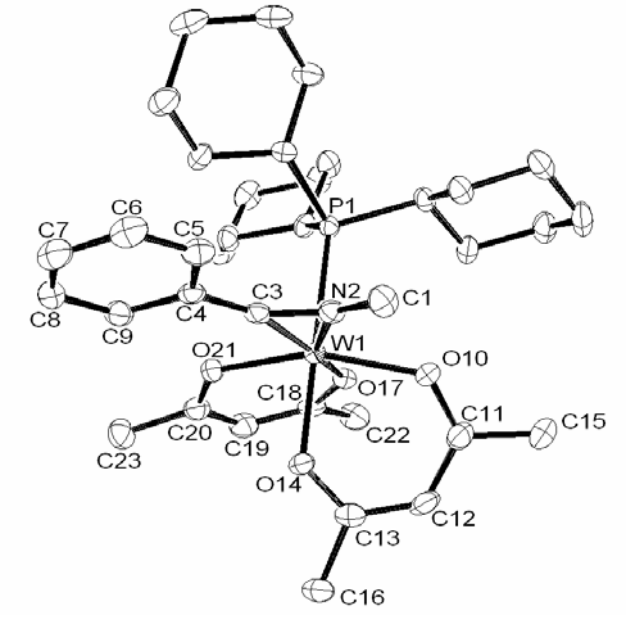

Figure 5.6. ORTEP diagram of **3b[BAr′$_4$]**. Thermal ellipsoids are drawn with 50% probability. Hydrogen atoms, the BAr′$_4$ counterion, and a molecule of Et_2O are omitted for clarity.

Spectroscopic data indicate rapid, reversible phosphine dissociation as one process responsible for the observed fluxionality in $[W(PCy_3)(\eta^2\text{-MeN=CPh})(acac)_2]^+$. Selective broadening is evident for this molecule with a pseudo-octahedral framework. Phosphine

dissociation could allow the acetylacetonate chelate (AB) near the nitrogen-bound methyl to swing up toward the vacant coordination site, altering the geometry of the intermediate to a pseudo-trigonal bipyramid with a mirror plane relating the two ends of the AB acetylacetonate that moved while leaving the other acetylacetonate (CD) in the same NMR environment. Re-coordination of PCy_3 could force the chelate either back to its original position or swing acetylacetonate AB to move end B into the position trans to PCy_3 in the octahedron, producing the enantiomer of the original complex (Scheme 5.4). This mechanism explains the broad NMR resonances observed for only one acetylacetonate chelate and the phosphine, while proton signals for the phenyl ring and the other acetylacetonate chelate remain sharp.

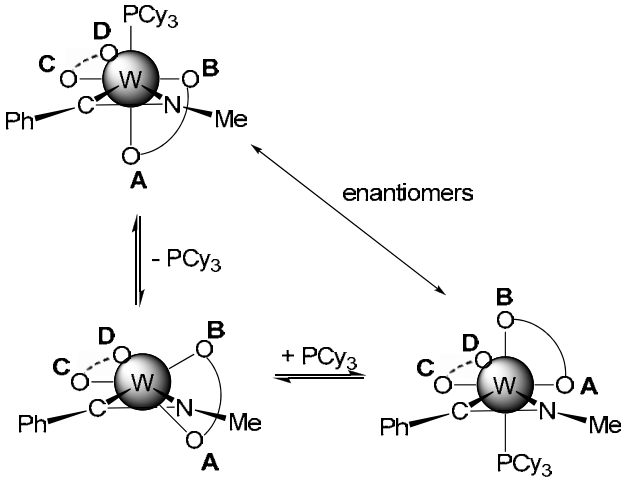

Scheme 5.4. Proposed mechanism of reversible tricyclohexylphosphine dissociation.

The outcome of phosphine addition to **1a** reflects a dependence on the size of the phosphine reagent.[36-39] Unlike PPh_3 or PCy_3, addition of trimethylphosphine (PMe_3) to **1a** leads to a product that reflects nucleophilic attack at the iminoacyl carbon to form $[W(CO)(\eta^2\text{-MeN=C(PMe}_3)\text{Ph})\ (acac)_2]^+$ complex **4** (Scheme 5.5). This result mirrors reactivity observed when $Na[HB(OMe)_3]$ or MeMgBr attacks the cation and reduces the

iminoacyl ligand to an imine.[8] After PMe_3 addition, IR spectroscopy shows a single CO absorbance at 1904 cm^{-1}, a decrease of ~80 cm^{-1} from the starting material. Addition of PMe_3 to the iminoacyl carbon indirectly pushes a significant amount of electron density to the metal center. ^1H NMR spectroscopy shows two diastereomers in an approximate ratio of 2:1. ^{13}C NMR spectroscopy further supports the imine-like nature of the sidebound ligand: a doublet assigned to the "imine" carbon for the major diastereomer resonates at 50.9 ppm ($^1J_{P\text{-}C}$ = 84 Hz). A doublet centered at 241.1 ppm with phosphorus coupling ($^3J_{P\text{-}C}$ = 8 Hz) is assigned to the CO carbon. Similar results were obtained using PMe_2Ph as a reagent. A size dependence could explain attack at the iminoacyl carbon by PMe_3, while the larger PPh_3 and PCy_3 ligands replace CO in the coordination sphere of tungsten.

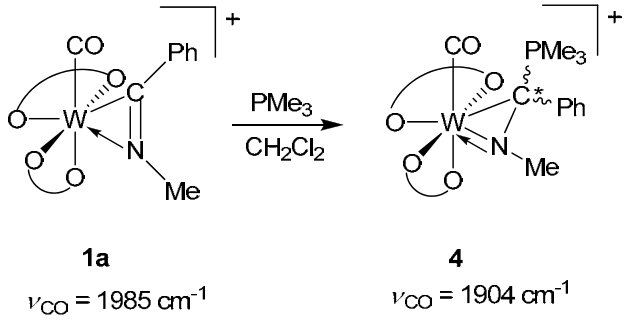

Scheme 5.5. Nucleophilic attack at the iminoacyl carbon with PMe_3.

Photolytic Replacement of CO with Alkyne.

Due to the propensity of tungsten(II) to bind a four-electron donor ligand in a six-coordinate environment,[8,15,40] we investigated replacement of CO with alkyne ligands. Unlike linearly ligating π-acid carbon monoxide ligands, alkynes are excellent single-faced π-acids, and additionally alkynes can serve as variable electrons donor ligands through their $\pi_\perp$ electrons.[16] This π-donor feature has the ability to alter the behavior of the adjacent η^2-iminoacyl ligand.

Refluxing phenylacetylene and **1a** in THF produces a small amount of [W(η^2-PhC≡CH)(η^2-MeN=CPh)(acac)$_2$]$^+$, **5a**. On the other hand, photolysis in methylene chloride produces the alkyne-iminoacyl cation in good yields (65-75%) (Scheme 5.6).

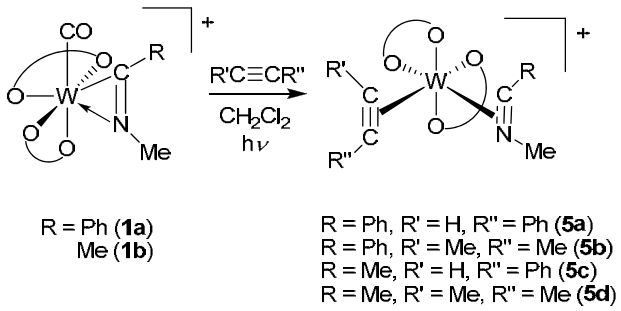

Scheme 5.6. Photolytic replacement of CO with alkyne reagents.

Note that for an unsymmetrical alkyne, four NMR distinguishable isomers are possible (Figure 5.7).

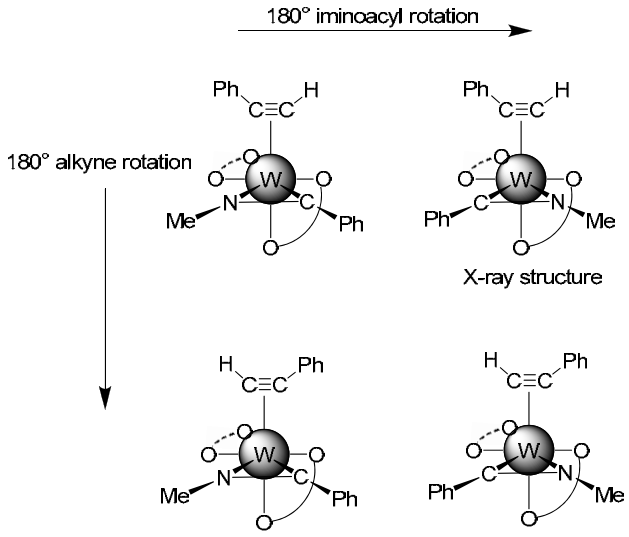

Figure 5.7. The four possible isomers of asymmetric alkyne derivative **5a**.

All four alkyne-iminoacyl derivatives, including the two symmetric 2-butyne complexes **3b** and **3d**, yield two isomers as observed by NMR spectroscopy. The isomer distribution appears to be compatible with a single alkyne orientation relative to the two acetylacetonate

chelates combined with two iminoacyl orientations. The room temperature ^{1}H NMR spectrum of the phenylacetylene adduct, **5a,** shows two isomers in a 3:1 ratio. The terminal alkyne proton on the phenylacetylene ligand for the major isomer resonates downfield at 13.45 ppm in the region typical of four-electron donor alkynes. Both the alkyne and iminoacyl ligands appear to be static on the NMR time scale. At room temperature the ^{13}C NMR spectrum of **5a** shows the iminoacyl carbon resonance at 217.0 ppm. The alkyne carbons of the major isomer resonate at 208.2 (Ph*C*≡CH) and 204.6 ppm (PhC≡*C*H).

The solid state structure of the cationic alkyne-iminoacyl complex **5a[BAr′$_4$]** shows the iminoacyl ligand is rotated 90° relative to reagent **1a[OTf]**, with the C-N linkage roughly parallel to the trans O-W-O axis, and the N-methyl group oriented over the plane of the adjacent acetylacetonate chelate (Figure 5.8). The alkyne and iminoacyl ligands are (i) π-bound to the metal, (ii) *cis* to each other, and (iii) parallel to one another. The N-methyl group is oriented *proximal* to the terminal alkyne proton on the phenylacetylene ligand, and the two phenyl rings are *proximal* to each other. In spite of the π-donor capability of the alkyne ligand, the two bonds from tungsten to the iminoacyl differ only slightly from those in the precursor carbonyl-iminoacyl cation. The W1-C3 bond is 2.052(9) Å, and the W1-N2 bond is 1.990(8) Å.

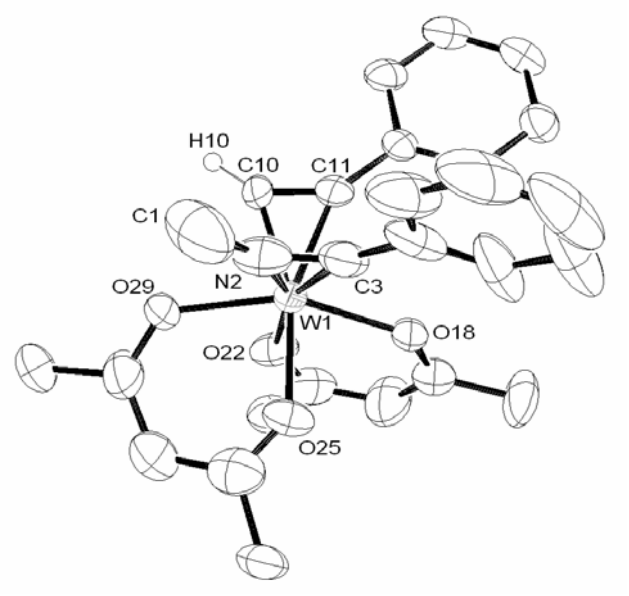

Figure 5.8. ORTEP diagram of **5a[BAr′$_4$]**. Thermal ellipsoids are drawn with 50% probability. Non-essential hydrogen atoms and the BAr′$_4$ counterion are omitted for clarity.

Displacement of Triphenylphosphine.

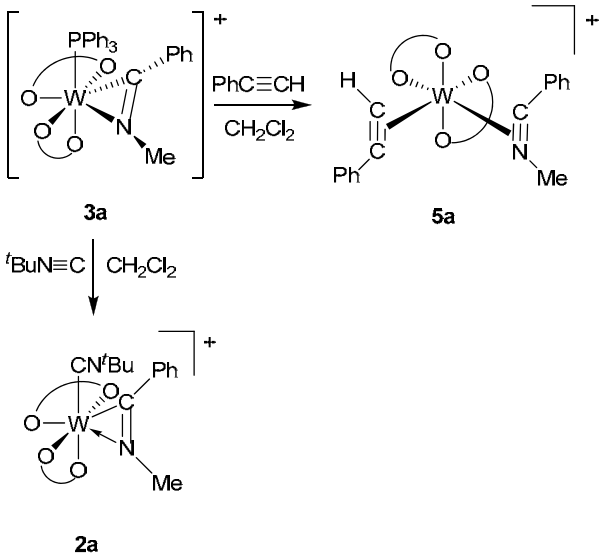

Scheme 5.7. Displacement of triphenylphosphine with either isonitrile or alkyne reagents.

The triphenylphosphine ligand in **3a** can be easily displaced by either isonitrile or alkyne reagents (Scheme 5.7). Following generation of **3a** *in situ*, addition of *tert*-butylisonitrile or phenylacetylene quickly forms either **2a** or **5a**, respectively, as confirmed by ^{1}H NMR

spectroscopy. This stepwise substitution methodology provides an attractive, two-step thermal route to complexes **5a-d** as an alternative to photolytic preparation.

Orbital Interactions and Electron Counting.

Cationic iminoacyl bis(acac) complexes **1a** and **1b** can be mapped to the same MO model as analogous neutral bis(acac) η^2-alkyne or η^2-nitrile complexes in terms of electron donation from the iminoacyl ligand and the oxidation state of the tungsten center (Figure 5.9). If the neutral $(acac)_2W(L)$ (L = CO, CNR) fragment is counted as a low valent d^4 fourteen-electron moiety, four electrons must be supplied from the cationic iminoacyl ligand, equivalent to a nitrilium, to optimally utilize the available electrons and orbitals. Carbon monoxide or isonitrile, situated along the z-axis, will stabilize the dπ orbitals with z-character, and thus dictate the location of the four metal-based electrons. Binding the cationic iminoacyl fragment along the x-axis further stabilizes d_{xz} via backbonding, and also pushes the empty d_{xy} orbital up in energy as the antibonding component reflecting donation from the filled $\pi_\perp$ orbital on the $PhC{\equiv}NMe^+$ ligand. This bonding description treats the cationic four-electron donor ligand like an alkyne. The transparency of mapping $RC{\equiv}NR^+$ onto RC≡CR leads us to favor this description for building a simple MO picture, but it is worthwhile to note that the final result can be constructed using $RC{=}NR^-$ and a d^2 W(IV) formalism with the anionic η^2-iminoacyl providing a total of *6* electrons to the metal.

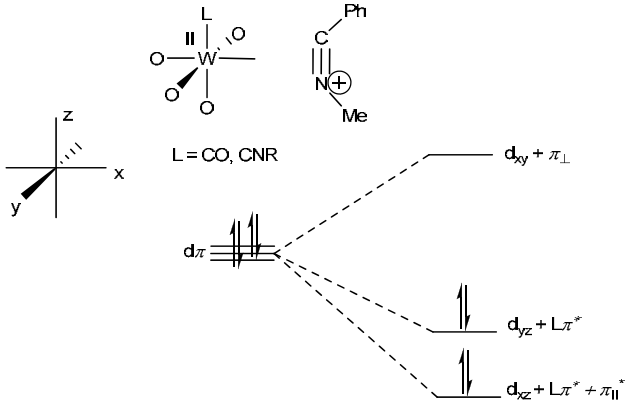

Figure 5.9. Orbital diagram for **1a** and **2**.

A different orbital diagram emerges for phosphine complex **3a** (Figure 5.10). No significant stabilization of the four dπ electrons is expected from the phosphine. With no dominant electronic preference for binding the η^2-NC ligand either parallel or orthogonal to the W-P bond, the steric interactions between the bulky phosphine ligand and the phenyl ring favor the observed orthogonal orientation of the iminoacyl ligand. The intense color and rapid decomposition upon exposure to air are compatible with a high lying HOMO orbital that lacks stabilization by a π-acid ligand.

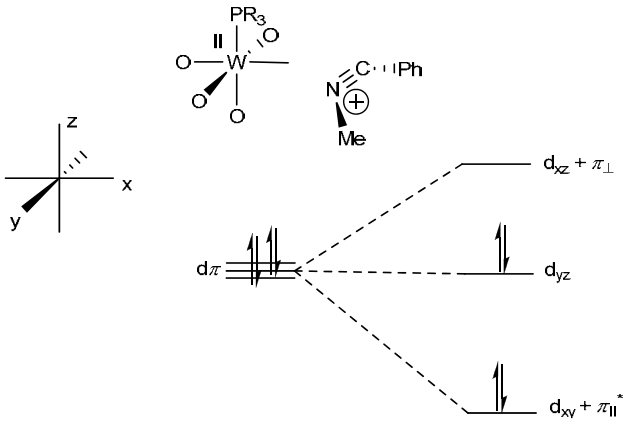

Figure 5.10. Orbital diagram for **3a**

In contrast, complexes **5a-d** feature a variable electron donor alkyne that also serves as a single faced π-acid capable of stabilizing the filled d_{yz} orbital while the iminoacyl ligand

stabilizes the filled d_{xy} orbital (Figure 5.11). Both of these π-bound ligands compete to donate electrons from their respective $\pi_{\perp}$ orbitals into the empty d_{xz} orbital, and the result is a three-center four-electron interaction. This outcome tracks orbital diagrams describing M(II)bis(alkyne) (M = Mo, W) complexes,[41,42] but the symmetry of two equivalent alkyne donors is broken.[43] Spectroscopic and structural data imply that the alkyne ligand contributes more electron density into d_{xz} than the iminoacyl ligand in accord with electronegativity expectations. In the end a total of six electrons must be donated from the two η^2-ligands, but combinations ranging from 2+4 through 3+3 to 4+2 are conceivable in the absence of symmetry constraints.

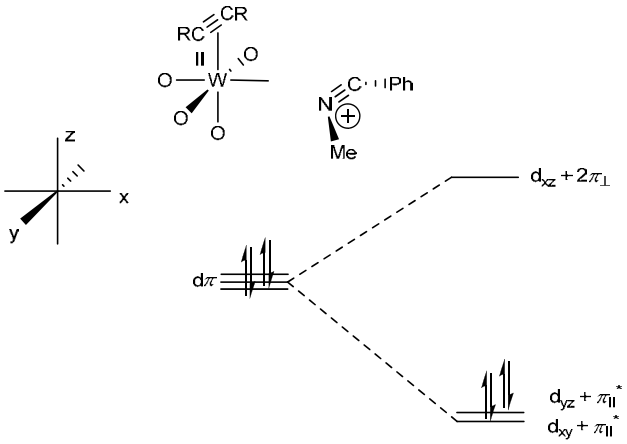

Figure 5.11. Orbital diagram for **5**

Reduction of the Iminoacyl Ligand.

Addition of Na[$HB(OMe)_3$] to [W(η^2-MeC≡CMe)(η^2-MeN=CPh)$(acac)_2]^+$, **5b**, in THF results in hydride addition to form W(η^2-MeC≡CMe) (η^2-MeN=CHPh)$(acac)_2$, **6**, (Scheme 5.8). The molecule is fluxional at room temperature in solution, and NMR peak assignments were based on low temperature spectra. At 200 K, rearrangement processes are sufficiently slow to reveal the presence of four isomers (two diastereomers for both imine orientations) resulting from hydride addition at the iminoacyl carbon. The added hydride of the major

isomer resonates at 2.40 ppm in **6** well upfield from the hydride resonance of the comparable carbonyl-imine complex which resonates at 5.56 ppm.[8]

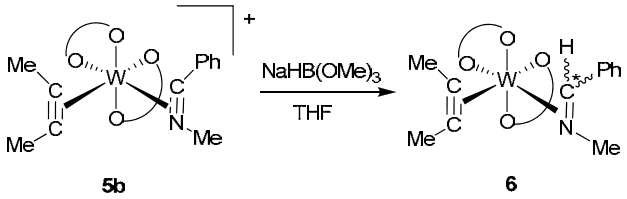

Scheme 5.8. Addition of $Na[HB(OMe)_3]$ to produce the alkyne-imine complex **6**.

One fluxional process that has no bearing on the isomer distribution is rotation of the 2-butyne ligand. Coalescence for 2-butyne rotation occurs at 247 K, corresponding to a free energy value of 14.3 kcal/mol.[44] At 200 K the imine carbon in the major isomer resonates at 73.6 ppm in the ^{13}C NMR spectrum reflecting hybridization to a pseudo-tetrahedral sp^3 carbon resulting from hydride addition. The two alkyne carbons in the major isomer resonate at 204.7 and 208.7 ppm.

X-ray data for **6** reveals the phenyl ring on the iminoacyl ligand lying over the adjacent acetylacetonate chelate. This contrasts with structures for **3b** and **5a** in which the N-methyl group lies near the chelate in the two cis positions. Significant lengthening of both the tungsten-carbon bond [W1-C7 = 2.220(3) Å, (+0.168 Å)] and the nitrogen-carbon bond [N6-C7 = 1.395(4) Å, (+0.134 Å)] results from hydride addition, consistent with reduction of carbon to an sp^3 hybridized center upon hydride attack.

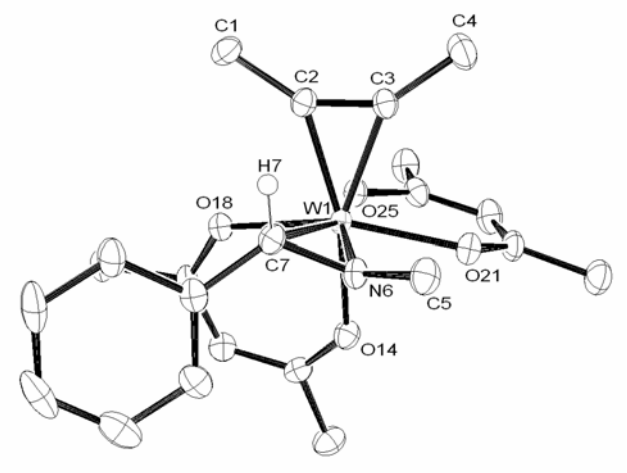

Figure 5.12. ORTEP diagram of **6**. Thermal ellipsoids are drawn with 50% probability. Non-essential hydrogen atoms are omitted for clarity.

Formation of a Coordinated Iminium.

Alkylation of complex **6** with MeOTf yields four isomers of [W(η^2-MeC≡CMe)(η^2-Me_2N=CHPh)$(acac)_2$][OTf], **7[OTf]** (Scheme 5.9). The proton attached on the iminium carbon resonates at 3.99 ppm (major), a downfield shift from the value observed for **6** (2.40 ppm). The diastereotopic nitrogen-bound methyl groups appear as singlets at 2.97 and 2.68 ppm, and the terminal methyl groups on the 2-butyne ligand coincide at 2.82 ppm, probably due to rapid alkyne rotation. The ^{13}C NMR spectrum clearly supports the role of the alkyne ligand as the lone four-electron donor in **7**; the two alkyne carbons resonate at 240 ppm. This chemical shift reflects the role of the η^2-iminium fragment as a simple two-electron donor. The iminium carbon shifts appears at 91 ppm. Overall, the original benzonitrile ligand[15] undergoes three additions (electrophile, nucleophile, electrophile) and is formally reduced to a coordinated iminium fragment.

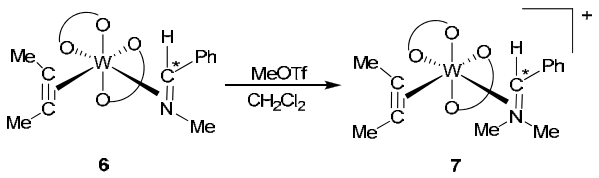

Scheme 5.9. Alkylation with MeOTf to form the alkyne-iminium complex **7[OTf]**.

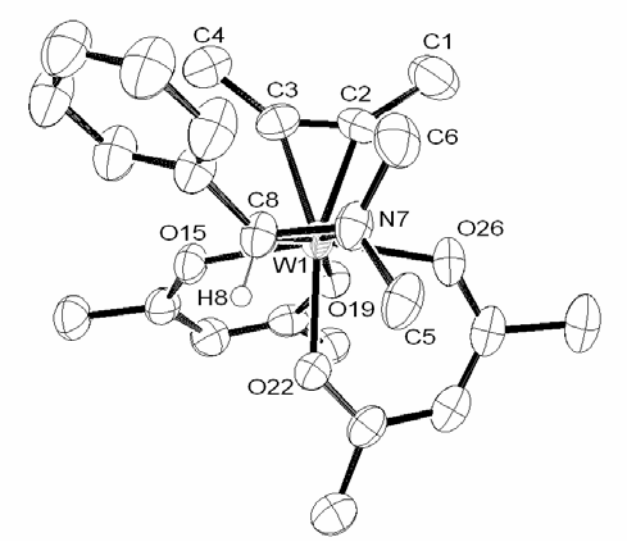

Figure 5.13. ORTEP diagram of **7[BAr′$_4$]**. Thermal ellipsoids are drawn with 50% probability. Non-essential hydrogen atoms and the BAr′$_4$ counterion are omitted for clarity.

The solid state structure shows the added methyl group is bound to the η^2-iminium nitrogen and both N7 and C8 of the iminium ligand assume a tetrahedral geometry (Figure 5.13). The W1-N7 linkage lengthens substantially to 2.190(4) Å, reflecting a loss of double bond character present in the neutral precursor molecule (1.952(3) Å).

Phosphine Addition to Cationic Iminoacyl-Alkyne Complexes.

Addition of PMe_3 to **5b[BAr′$_4$]** produces the cationic imine complex [W(η^2-MeC≡CMe)(η^2-MeN=C(PMe_3)Ph)(acac)$_2$][BAr′$_4$], **8[BAr′$_4$]**, (Scheme 5.10). Two isomers are present in a ratio of ~ 20:1. Room temperature ^{1}H NMR data reveal hindered rotation of the alkyne as evidenced by distinctive broad signals for each methyl group on 2-butyne (2.78 and 1.42 ppm). Additionally, the *ortho* and *meta* phenyl protons are broad indicating

hindered rotation of the phenyl ring. Low temperature NMR studies show sharpening and shifting of alkyne and phenyl resonances, eventually slowing rotation of the phenyl ring to reveal five distinct resonances at 203 K. ^{13}C NMR data indicate decreased electron donation from the alkyne in **8[BAr′$_4$]** with resonances at 182.7 and 182.8 ppm compared to the alkyne in **5b** which has ^{13}C signals at 208 ppm. The former iminoacyl carbon shifts upfield to 52.8 ppm from 217.5 ppm in **5b**. In spite of the direct P-C connection, no phosphorus coupling can be distinguished in this broad C-13 resonance. The solid state structure shows retention of the basic connectivity of **5a** and bond lengths are almost identical to imine product **6** (Figure 11). The high diastereoselectivity (20:1) contrasts with the poor stereoselectivity observed in the analogous reaction to form complex **4** from the CO complex **1a** (d.r. ~ 2:1) discussed above.

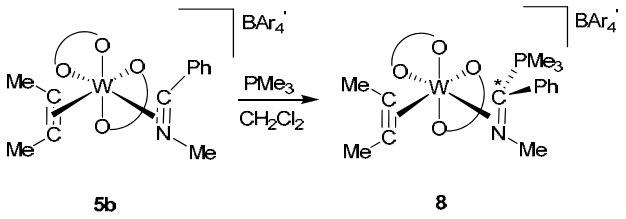

Scheme 5.10. Nucleophilic attack by PMe_3 at iminoacyl carbon in **5b**.

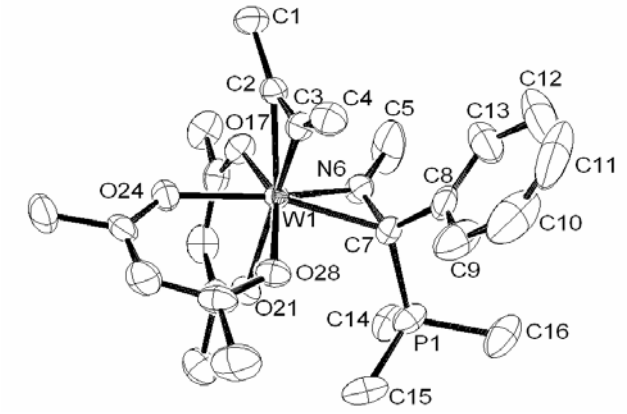

Figure 5.14. ORTEP diagram of **8[BAr′$_4$]**. Thermal ellipsoids are drawn with 50% probability. Hydrogen atoms and the BAr′$_4$ counterion are omitted for clarity.

With a terminal alkyne adjacent to the iminoacyl in **5a[BAr′$_4$]**, addition of PMe_3 generates an η^2-vinyl species, [W(η^2-MeN=CPh)(η^2-PhC=C(H)PMe_3)$(acac)_2$][BAr′$_4$], **9[BAr′$_4$]**, via attack at the terminal alkyne carbon of the coordinated phenylacetylene (Scheme 5.11). ^{1}H NMR spectroscopy confirms the presence of four isomers in a 10:4:3:2 ratio, and no acetylene proton is present at low field. The former acetylenic proton resonates at 3.04 ppm ($^2J_{P\text{-}H}$ = 27 Hz) in the major isomer. The ^{13}C NMR spectrum shows a resonance at 31.6 ppm ($^1J_{P\text{-}C}$ = 85 Hz) corresponding to the four-coordinate η^2-vinyl carbon as confirmed with HMQC spectroscopy. The other vinyl carbon resonates at 241 ppm, indicating alkylidene character. These resonances are typical of η^2-vinyl ligands, also known as metallocyclopropenes. Examples of η^2-vinyls generated by nucleophilic attack on a terminal η^2-alkyne ligand have been known for some time.[45,46]

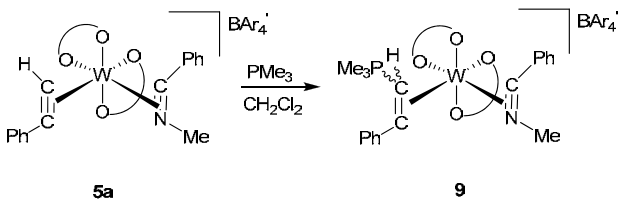

Scheme 5.11. Nucleophilic attack by PMe_3 at the terminal carbon of η^2-PhC≡CH.

Table 5.1. Crystal and Data Collection Parameters for [W(CN-$C_6H_3Me_2$)(η^2-MeN=CMe)(acac)$_2$][BAr′$_4$] (**2c[BAr′$_4$]**); [W(PCy_3)(η^2-MeN=CPh)(acac)$_2$][BAr′$_4$] (**3b[BAr′$_4$]**); [W(η^2-PhC≡CH)(η^2-MeN=CPh)(acac)$_2$][BAr′$_4$] (**5a[BAr′$_4$]**).

Complex	**2c[BAr′$_4$]**	**3b[BAr′$_4$]**	**5a[BAr′$_4$]**
empirical formula	$C_{54}H_{41}BF_{24}N_2O_4W$ ·½ Et_2O	$C_{68}H_{67}BF_{24}NO_4PW$·$Et_2O$	$C_{58}H_{40}BF_{24}NO_4W$
fw	1469.61	1717.98	1465.57
color	Red/brown	Purple	Yellow
T (K)	100(2)	100(2)	100(2)
λ (Å)	0.71703	0.71703	0.71703
cryst syst	Triclinic	Triclinic	Triclinic
space group	*P*-1	*P*-1	*P*-1
a (Å)	13.0368(4)	12.5105(2)	12.9884(4)
B (Å)	13.0932(3)	16.0383(3)	14.3778(5)
c (Å)	20.0413(6)	19.8966(4)	17.9290(6)
α (deg)	76.898(2)	70.525(1)	111.900(2)
β (deg)	80.350(2)	86.315(1)	99.667(2)
γ (deg)	78.311(2)	84.339(1)	99.845(2)
Vol. (Å^3)	3236.10(16)	3740.65(12)	2960.84(17)
Z	2	2	2
ρ_{calcd} (mg/m^3)	1.508	1.525	1.644
μ, mm^{-1}	1.90	1.674	2.073
F(000)	1454	1732	1444
Crystal size (mm^3)	0.20 x 0.20 x 0.05	0.25 x 0.20 x 0.15	0.15 x 0.15 x 0.10
2θ range (deg)	1.05 to 25.00	1.09 to 26.51	1.64 to 25.00
Index Ranges	-15≤h≤15 -11≤k≤14 -23≤l≤19	-15≤h≤15 -20≤k≤20 -22≤l≤24	-15≤h≤15 -17≤k≤17 -21≤l≤21
Reflections Collected	24028	51721	43710
Independent reflections	11344	15443	10391
Data/restraints/parameters	11344/0/798	15443/138/1007	10391/0/808
Goodness-of-fit on F^2	1.018	1.024	1.074
R1, wR2[I>2σ(I)]	0.0663, 0.1725	0.0357, 0.0822	0.0611, 0.1361
R1, wR2 (all data)	0.1088, 0.2064	0.0458, 0.0878	0.0789, 0.1450

Table 5.2. Crystal and Data Collection Parameters for W(η^2-MeC≡CMe)(η^2-MeN=CHPh)(acac)$_2$ (**6**); [W(η^2-MeC≡CMe)(η^2-Me$_2$N=CHPh)(acac)$_2$][BAr′$_4$] (**7[BAr′$_4$]**); [W(η^2-MeC≡CMe)(η^2-MeN=C(PMe$_3$)Ph) (acac)$_2$][BAr′$_4$] (**8[BAr′$_4$]**).

Complex	**6**	**7[BAr′$_4$]**	**8[BAr′$_4$]**
empirical formula	$C_{22}H_{29}NO_4W$	$C_{55}H_{44}BF_{24}NO_4W$	$C_{57}H_{49}BF_{24}NO_4PW$
fw	555.31	1433.57	1493.60
color	Orange	Orange	Yellow
T (K)	100(2) K	100(2) K	100(2) K
λ (Å)	0.71703 Å	1.54178	0.71073
cryst syst	Triclinic	Triclinic	Monoclinic
space group	P-1	P-1	$P2_{1/}c$
a (Å)	8.4166(11)	12.4372(3)	12.7556(3)
B (Å)	10.2419(13)	12.7720(3)	19.0951(5)
c (Å)	13.3165(19)	18.6366(5)	24.7718(6)
α (deg)	99.903(6)	87.162(1)	90
β (deg)	97.032(7)	80.333(1)	96.020(1)
γ (deg)	92.263(6)	79.078(1)	90
Vol. (Å^3)	1120.1(3)	2865.01(12)	6000.4(3)
Z	2	2	4
ρ_{calcd} (mg/m^3)	1.646	1.662	1.653
μ, mm^{-1}	5.182	4.863	2.072
F(000)	548	1416	2960
Crystal size (mm^3)	0.25 x 0.20 x 0.10	0.30 x 0.15 x 0.10	0.43 x 0.37 x 0.16
2θ range (deg)	1.57 to 30.00	2.41 to 67.00	1.60 to 24.96
Index Ranges	-11≤h≤11 -14≤k≤14 -18≤l≤18	-14≤h≤14 -15≤k≤15 -22≤l≤22	-15≤h≤15 -22≤k≤22 -29≤l≤29
Reflections Collected	41685	50256	110435
Independent reflections	6522	9953	10560
Data/restraints/parameters	6522/0/260	9953/18/811	10560/168/896
Goodness-of-fit on F^2	1.110	1.108	1.079
R1, wR2[I>2σ(I)]	0.0274, 0.0765	0.0518, 0.1408	0.318, 0.0750
R1, wR2 (all data)	0.0288, 0.073	0.00521, 0.1411	0.0374, 0.0778

Table 5.3. Salient crystallographic and spectroscopic data.

Complex	W-N (Å)	W-C (Å)	C-N (Å)	^{13}C, N≡*C* (δ)	^{13}C, *C*≡*C* (δ)	IR, ν_{CO} (cm^{-1})
CO-Nitrile[15]	2.018(5)	2.038(5)	1.270(7)	211.2	n/a	1895
1a[OTf][8]	1.977(7)	2.069(8)	1.283(10)	226.2	n/a	1976
CO-Imine[8]	1.905(5)	2.274(2)	1.383(2)	59.3, 60.6	n/a	1881, 1885
2c[BAr′$_4$]	1.963(9)	2.027(11)	1.323(14)	239.8	n/a	n/a
3b[BAr′$_4$]	1.957(3)	1.990(4)	1.324(5)	247.1	n/a	n/a
4[OTf]	n/a	n/a	n/a	50.9, 48.4	n/a	1904
5a[BAr′$_4$]	1.990(8)	2.052(9)	1.264(12)	217.0	204.6, 208.2	n/a
6	1.952(3)	2.220(3)	1.395(4)	76.2	204.7, 208.7	n/a
7[BAr′$_4$]	2.190(4)	2.168(5)	1.444(7)	91.4	240.1	n/a
8[BAr′$_4$]	1.925(3)	2.211(4)	1.395(5)	52.7	182.7, 182.8	n/a

Summary

The carbon monoxide ligand in the iminoacyl-carbonyl cationic complexes (**1a** or **1b**) is easily displaced thermally with either isonitrile or bulky phosphine reagents, or photolytically with alkyne reagents to form [W(L)(η^2-MeN=CR)(acac)$_2$]$^+$ [L = ^{t}BuNC, 2,6-Me$_2$PhNC, PPh$_3$, PCy$_3$, PhC≡CH, MeC≡CMe] complexes. Trimethylphosphine attacks the iminoacyl carbon in these cationic complexes to form [W(L)(η^2-MeN-C(PMe$_3$)Ph)(acac)$_2$]$^+$ (L = CO, 2-butyne) complexes. Replacement of the π-acid CO ligand with four-electron donor alkynes allows further reduction of the iminoacyl ligand to a sidebound iminium ligand via hydride addition and subsequent methylation. An X-ray structure was obtained for a representative molecule from each category.

Experimental

General Information. All air-and moisture-sensitive materials were handled using Schlenk or glovebox techniques under a dry nitrogen or argon atmosphere, respectively. All glassware was oven-dried before use. Methylene chloride, diethyl ether, hexanes, and pentane were purified by passage through an activated alumina column under a dry argon atmosphere.[47] THF was distilled from a sodium ketal suspension. Methylene chloride-d_2 was dried over CaH_2 and degassed. Complexes **1a[OTf]** and **1b[OTf]**[8] and $NaBAr'_4$[48] were made in accordance with literature procedures. All other reagents were purchased from commercial sources and used without further purification. NMR data are given for one salt (OTf or BAr'_4); chemical shift differences between the two salts are negligible.

NMR spectra were recorded on Bruker DRX400, AMX400, or AMX300 spectrometers. Phosphorus chemical shifts were referenced to H_3PO_4 as an external standard. Infrared spectra were recorded on an ASI Applied Systems React IR 1000 FT-IR spectrometer. Elemental analysis was preformed by Atlantic Mircrolab, Norcross, GA, and Robertson Microlit, Madison, NJ. Mass spectra (MS) and high resolution mass spectra (HRMS) were acquired with a Bruker BioTOF II reflectron time-of-flight (reTOF) mass spectrometer equipped with an Apollo electrospray ionization (ESI) source (Billerica, MA). Mass spectral data are reported for most abundant tungsten isotope.

Representative $[BAr'_4]^-$ NMR Data. ^1H and ^{13}C NMR data for the $[BAr'_4]^-$ counterion are reported separately for simplicity. ^1H NMR (CD_2Cl_2, 193 K, δ): 7.77 (br, 8H, *o*-Ar'), 7.60 (br, 4H, *p*-Ar'). $^{13}C\{^1H\}$ NMR (CD_2Cl_2, 193 K, δ): 162.2 (1:1:1:1 pattern, $^1J_{B\text{-}C}$ = 50 Hz, C_{ipso}), 135.3 (C_{ortho}), 129.4 (qq, $^2J_{C\text{-}F}$ = 30 Hz, $^4J_{C\text{-}F}$ = 5 Hz, C_{meta}), 125.1 (q, $^1J_{C\text{-}F}$ = 270 Hz, CF_3), 117.9 (C_{para}).

[W(CO)(η^2-MeN=CPh)(acac)$_2$][BAr′$_4$] (1a[BAr′$_4$]). 1a[OTf] (0.305 g, 0.450mmol) was dissolved in methylene chloride and NaBAr′$_4$ (0.398 g, 0.449 mmol) was added under a backflow of N_2. The solution was stirred for 2 h and cannula filtered away from the residual sodium salts. The red-brown solid was triterated with methylene chloride and hexanes to yield a brown powder (0.450 g, 0.323 mmol, 72%).

[W(CO)(η^2-MeN=CMe)(acac)$_2$][BAr′$_4$] (1b[BAr′$_4$]). 1b[OTf] (0.22 g, 0.36 mmol) was dissolved in methylene chloride and NaBAr′$_4$ (0.35 g, 0.39 mmol) was added under a backflow of N_2. The solution was stirred for 1 h and cannula filtered away from the residual sodium salts. The brown solid was triterated with methylene chloride and hexanes to yield a brown powder (0.350 g, 0.27 mmol, 76%).

[W(CN^{t}Bu)(η^2-MeN=CPh)(acac)$_2$][OTf] (2a[OTf]). A 100-mL Schlenk flask was charged with **1a[OTf]** (85 mg, 0.13 mmol) which was dissolved in methylene chloride (10 mL) at 0 °C resulting in a burgundy solution. Addition of *tert*-butylisonitrile (20 μL, 0.17 mmol) caused a color change from burgundy to deep purple within 5 min. IR spectroscopy indicated no metal-carbonyl absorbances. Hexanes were added to precipitate a dark purple powder (35 mg, 0.048 mmol, 38%). ^{1}H NMR (CD_2Cl_2, 298 K, δ): 7.77-7.81 (m, 2H, *m*-C_6H_5), 7.62-7.65 (m, 2H, *o*-C_6H_5), 7.38-7.42 (m, 1H, *p*-C_6H_5), 5.81, 5.90 (each a s, each 1H, acac C*H*), 5.67 (s, 3H, N-CH_3), 2.88, 2.59, 2.34, 2.15 (each a s, each 3H, acac CH_3), 1.46 (s, 9H, -(CH_3)$_3$). ^{13}C{^{1}H} NMR (CD_2Cl_2, 298 K, δ): 25.0, 25.1, 26.4, 28.0 (acac *C*H$_3$), 32.0 (-(*C*H$_3$)$_3$), 40.0 (N-*C*H$_3$), 59.4 (CN-*C*-(CH$_3$)$_3$), 98.7, 102.9 (acac *C*H), 128.0 (*p*-*C*$_6$H$_5$), 128.6, 133.3 (*o/m*-*C*$_6$H$_5$), 135.7 (*ipso*-*C*$_6$H$_5$), 146.5 (*C*N^{t}Bu), 189.5, 190.0, 191.6, 200.0 (acac *C*O), 234.4 (N=*C*). MS (ESI) *m/z* Calc.: 583.2 (M$^+$), 500.1 (M$^+$- ^{t}BuNC). Found: 583.2, 500.1.

[W(CN^{t}Bu)(η^2-MeN=CMe)(acac)$_2$][BAr′$_4$] (2b[BAr′$_4$]). 1b[BAr′$_4$] (51 mg, 0.038 mmol) was dissolved in methylene chloride (10 mL) in a 100-mL Schlenk flask resulting in an olive green solution. Addition of *tert*-butylisonitrile (10 μL, 0.084 mmol) at 0 °C caused a color change to red after 30 min of stirring. Hexanes (25 mL) were added to precipitate a red solid (45 mg, 0.033 mmol, 85%). ^{1}H NMR (CD_2Cl_2, 298 K, δ): 5.82, 5.73 (each a s, each 1H, acac C*H*), 5.38 (s, 3H, N-CH_3), 4.63 (s, 3H, N=C-CH_3), 2.86, 2.55, 2.25, 2.10 (each a s, each 3H, acac CH_3), 1.50 (s, 9H, C-(CH_3)$_3$). ^{13}C{^{1}H} NMR (CD_2Cl_2, 298 K, δ): 18.6 (N=C-*C*H$_3$), 24.7, 24.9, 26.3, 27.8 (acac *C*H$_3$), 32.8 (C-(*C*H$_3$)$_3$), 38.3 (N-*C*H$_3$), 59.4 (*C*-(CH$_3$)$_3$), 98.7, 102.3 (acac *C*H), 189.7, 190.2, 191.9, 200.3 (acac *C*O), 240.2 (N=*C*). ^{13}C{^{1}H} NMR (CD_2Cl_2, 240 K, δ): 146.2 (*C*N^{t}Bu). HRMS (ESI) *m/z* Calc.: 521.163 (M$^+$), 438.089 (M$^+$-^{t}BuNC). Found: 521.148, 438.071.

[W(2,6-dimethylphenylisonitrile)(η^2-MeN=CMe)(acac)$_2$][BAr′$_4$] (2c[BAr′$_4$]). A 100-mL Schlenk flask was charged with **1b[BAr′$_4$]** (55 mg, 0.041 mmol) which was dissolved in methylene chloride (10 mL) resulting in an olive green solution. Addition of 2,6-dimethylphenylisonitrile (6 mg, 0.046 mmol) at 0 °C caused a color change to red after 30 min of stirring. Addition of hexanes (25 mL) led to precipitation of a red solid (47 mg, 0.033 mmol, 79%). The product was dissolved in a small amount of diethyl ether and layered with hexanes in an inert atmosphere at -30 °C. After three days red-brown needles formed, and these were suitable for X-ray analysis. ^{1}H NMR (CD_2Cl_2, 298 K, δ): 7.26 (d, 2H, *m*-C$_6$*H*$_3$Me$_2$), 7.05 (t, 1H, *p*-C$_6$*H*$_3$Me$_2$), 5.82, 5.78 (each a s, each 1H, acac C*H*), 5.26 (s, 3H, N-CH_3), 4.61 (s, 3H, N=C-CH_3), 2.83, 2.51, 2.28, 2.13 (each a s, each 3H, acac CH_3), 2.51 (s, 6H, C$_6$H$_3$(CH_3)$_2$). ^{13}C{^{1}H} NMR (CD_2Cl_2, 298 K, δ): 18.7 (C$_6$H$_3$(*C*H$_3$)$_2$), 19.4 (N=C-*C*H$_3$), 24.9, 25.1, 26.4, 27.9 (acac *C*H$_3$), 38.7 (N-*C*H$_3$), 98.7, 103.0 (acac *C*H), 128.1, 130.3, 137.2

($C_6H_3Me_2$), 189.4, 190.0, 191.4, 200.0 (acac *C*O), 239.8 (N=*C*). HRMS (ESI) *m/z* Calc.: 569.164(M^+), 438.090 (M^+- ArNC). Found: 569.166, 438.093.

[W(PPh$_3$)(η^2-MeN=CPh)(acac)$_2$][OTf] (3a[OTf]). 1a[OTf] (61 mg, 0.090 mmol) was dissolved in methylene chloride (10 mL) in a 100-mL Schlenk flask resulting in a burgundy solution. Addition of triphenylphosphine (24 mg, 0.092 mmol) caused a color change to deep red-purple within 20 min IR spectroscopy indicated no metal-carbonyl absorbances. Hexanes were added to precipitate a dark purple solid (79 mg, 0.087 mmol, 96%). ^{1}H NMR (CD_2Cl_2, 298 K, δ): 6.74 (s, 3H, N-*C*H$_3$), 6.02, 5.85 (each a s, each 1H, acac C*H*), 3.43, 2.84, 2.80, 2.07 (each a s, each 3H, acac C*H*$_3$). ^{13}C{^{1}H} NMR (CD_2Cl_2, 298 K, δ): 25.4, 26.2, 27.8, 36.4 (acac *C*H$_3$), 36.4 (N-*C*H$_3$), 98.9, 104.2 (acac *C*H), 189.0, 192.3, 196.5, 199.3 (acac *C*O), 241.1 (N=*C*). ^{31}P{^{1}H} NMR (CD_2Cl_2, 298 K, δ): -5.25 (s, *P*Ph$_3$, $^1J_{P\text{-}W}$ = 349 Hz).

[W(PCy$_3$)(η^2-MeN=CPh)(acac)$_2$][OTf] (3b[OTf]). A 100-mL Schlenk flask was charged with **1a[OTf]** (56 mg, 0.083 mmol) which was dissolved in methylene chloride (15 mL) resulting in a burgundy solution. Addition of tricyclohexylphosphine (27 mg, 0.096 mmol) caused a color change to deep purple within 20 min. IR spectroscopy indicated no metal-carbonyl absorbances. Hexanes were added to precipitate at dark purple solid (75 mg, 0.081, 98%). ^{1}H NMR (CD_2Cl_2, 298 K, δ): 8.44 (br, s, 3H, N-C*H*$_3$), 7.98 (d, 2H, *o*-C$_6$*H*$_5$), 7.84 (t, 2H, *m*-C$_6$*H*$_5$), 7.23 (t, 1H, *p*-C$_6$*H*$_5$), 6.40, 5.97 (each a s, each 1H, acac C*H*), 4.11, 3.54, 2.83, 2.11 (each a s, each 3H, acac C*H*$_3$). ^{13}C{^{1}H} NMR (CD_2Cl_2, 298 K, δ): 43.9 (br, N-*C*H$_3$), 98.2, 105.0 (acac *C*H), 127.6 (*m*-*C*$_6$H$_5$), 134.1 (*o*-*C*$_6$H$_5$), 136.8 (*p*-*C*$_6$H$_5$) 192.6, 199.3 (acac *C*O), 196.2, 202.3 (br, acac *C*O). ^{13}C{^{1}H} NMR (CD_2Cl_2, 200 K, δ): 247.1 (N=*C*). ^{31}P{^{1}H} NMR (CD_2Cl_2, 298 K, δ): -23.2 (br, *P*Cy$_3$). ^{31}P{^{1}H} NMR ($CDCl_2F$, 160 K, δ): 18.0 (s, *P*Cy$_3$, $^1J_{P\text{-}W}$ = 351 Hz). MS (ESI) *m/z* Calc.: 780.3 (M^+), 500.1 (M^+- PCy$_3$). Found: 780.4, 500.1.

[W(PCy$_3$)(η^2-MeN=CPh)(acac)$_2$][BAr′$_4$] (3b[BAr′$_4$]) was produced from **1a[BAr′$_4$]** in an analogous manner to **3b[OTf]**. The product was dissolved in a 50:50 mixture of diethyl ether and hexanes and placed in an inert atmosphere at -30°C. Purple crystals suitable for X-ray diffraction formed in two weeks.

[W(PPh$_3$)(η^2-MeN=CMe)(acac)$_2$][BAr′$_4$] (3c[BAr′$_4$]). A 100-mL Schlenk flask was charged with **1b[BAr′$_4$]** (50 mg, 0.038 mmol) which was dissolved in methylene chloride (15 mL) resulting in an olive green solution. Addition of triphenylphosphine (20 mg, 0.076 mmol) caused a color change to red-purple within 2 h. The reaction was allowed to stir several hours under nitrogen to ensure completion. IR spectroscopy indicated no metal-carbonyl absorbances. Hexanes were added to precipitate a dark red-purple solid. The supernatant was removed via cannula, and the solid placed under vacuum (32 mg, 0.020 mmol, 54%). ^{1}H NMR (CD_2Cl_2, 298 K, δ): 7.34-7.50 (m, PPh_3), 5.80 (s, 3H, N-CH_3), 5.73, 5.40 (each a s, each 1H, acac C*H*), 4.06 (d, 3H, N=C-CH_3, $^4J_{P\text{-}H}$ = 1 Hz), 3.06, 2.23, 2.22, 2.11, (each a s, each 3H, acac CH_3). ^{13}C{^{1}H} NMR (CD_2Cl_2, 298 K, δ): 17.6 (N=C-*C*H$_3$), 23.9, 24.6, 26.5, 27.6 (acac *C*H$_3$), 36.8 (N-*C*H$_3$), 96.9, 102.4 (acac *C*H), 189.6, 191.1, 193.0, 200.8 (acac *C*O), 235.2 (d, N=*C*, $^2J_{P\text{-}C}$ = 36 Hz). ^{31}P{^{1}H} NMR (CD_2Cl_2, 298 K, δ): 7.46 (s, *P*Ph$_3$, $^1J_{P\text{-}W}$ = 305 Hz).

[W(CO)(η^2-MeN-C(PMe$_3$)Ph)(acac)$_2$][OTf] (4[OTf]). 1a[OTf] (66 mg, 0.097 mmol) was dissolved in methylene chloride (15 mL) in a 100-mL Schlenk flask resulting in burgundy solution. Trimethylphosphine (20 μL, 0.19 mmol) was added causing a color change to red-brown. Reaction progress was monitored via *in situ* IR spectroscopy and was complete once a single CO absorbance appeared at 1904 cm^{-1}. Solvent volume was reduced *in vacuo* and hexanes were added to precipitate a brown solid (62 mg, 0.081 mmol, 84%). IR

(CH_2Cl_2): ν_{CO} = 1904 cm^{-1}; ^1H NMR (CD_2Cl_2, 298 K, δ, major diastereomer): 7.38-7.43 (m, 3H, *m* and *p*-C_6H_5), 7.08-7.10 (d, 2H, *o*-C_6H_5), 5.70, 5.64 (each a s, each 1H, acac C*H*), 4.07 (s, 3H, N-CH_3), 2.39, 2.22, 2.16, 2.12 (each a s, each 3H, acac CH_3), 1.97 (d, 9H, P-(CH_3)$_3$, $^2J_{P\text{-}H}$ = 13 Hz); $^{13}C\{^1H\}$ NMR (CD_2Cl_2, 298 K, δ, major diastereomer): 10.9 (d, P-(*C*H_3)$_3$, $^1J_{P\text{-}C}$ = 52 Hz), 25.3, 25.6, 27.8, 28.1 (acac *C*H_3), 43.7 (N-*C*H_3), 50.9 (d, N-*C*-P, $^1J_{P\text{-}C}$ = 84 Hz), 99.9, 102.7 (acac *C*H), 122.8 (*p*-*C*$_6$H$_5$), 127.1 (d, *o*-*C*$_6$H$_5$, $^3J_{P\text{-}C}$ = 3 Hz), 129.0 (*m*-*C*$_6$H$_5$), 142.0 (d, *ipso*-*C*$_6$H$_5$, $^2J_{P\text{-}C}$ = 30 Hz), 186.9, 187.2, 194.7, 196.2 (acac *C*O), 241.1 (d, *C*≡O, $^3J_{P\text{-}C}$ = 8 Hz); $^{31}P\{^1H\}$NMR (CD_2Cl_2, 298 K, δ, major diastereomer): 49.1 (s, *P*Me$_3$).

W(η^2-PhC≡CH)(η^2-MeN=CPh)(acac)$_2$][BAr$_4$'] (5a[BAr′$_4$]). In the drybox 125 mg of **1a[BAr′$_4$]** (0.090 mmol) was placed in a Schlenk tube. Methylene chloride was added (50 mL) followed by phenylacetylene was added (50 μL, 0.45 mmol). The vessel was placed in a photolysis hood for 3 h, resulting in a color change from burgundy to light yellow. The solvent was removed *in vacuo* yielding a yellow/brown solid. Column chromatography on silica using methylene chloride eluted a dark yellow band (92 mg, 0.063 mmol, 70%). Yellow crystals suitable for X-ray diffraction formed in after few days via evaporation of a 50:50 mixture of methylene chloride and hexanes. IR (KBr): $\nu_{C\equiv C}$ = 1735 cm^{-1}. ^1H NMR (CD_2Cl_2, 298 K, δ, major isomer): 13.45 (s, 1H, PhC≡C*H*), 5.90, 5.88 (each a s, each 1H, acac C*H*), 3.80 (s, 3H, N-CH_3), 2.62, 2.60, 1.92, 1.86 (each a s, each 3H, acac CH_3). ^1H NMR (CD_2Cl_2, 298 K, minor isomer): 13.47 (s, 1H, PhC≡C*H*), 5.88, 5.63 (each a s, each 1H, acac C*H*), 4.21 (s, 3H, N-CH_3), 2.67, 2.48, 1.90, 1.80 (each a s, each 3H, acac CH_3). $^{13}C\{^1H\}$ NMR (CD_2Cl_2, 298 K, δ, major isomer): 25.2, 26.7, 28.3, 28.4 (acac *C*H_3), 38.7 (N-*C*H_3), 104.6, 105.1 (acac *C*H), 184.6, 189.0, 191.7, 195.1 (acac *C*O), 204.6 (PhC≡*C*H), 208.2 (Ph*C*≡CH), 217.0 (N=*C*). $^{13}C\{^1H\}$ NMR (CD_2Cl_2, 298 K, δ, minor isomer): 25.8, 26.4, 28.5,

28.9 (acac *C*H_3), 37.2 (N-*C*H_3), 104.3, 104.8 (acac *C*H), 186.5, 188.1, 192.2, 196.2 (acac *C*O), 206.4 (Ph*C*≡CH), 214.1 (PhC≡*C*H), 221.5 (N=*C*). Anal. Calcd for $WC_{58}H_{40}O_4F_{24}NB$: C, 47.54; H, 2.75; N, 0.96. Found: C, 47.52; H, 2.44; N, 1.06%.

[W(η^2-MeC≡CMe)(η^2-MeN=CPh)(acac)$_2$][BAr$_4$'] (5b[BAr′$_4$]). In the drybox 270 mg of **1a[OTf]** (0.399 mmol) was placed in a Schlenk tube. Methylene chloride was added (60 mL) follwed by 2-butyne (100 μL, 1.27 mmol). The tube was placed in a photolysis hood for 3 h, resulting in a color change from burgundy to light yellow. Counterion exchange occurred by adding Na[BAr$_4$'] (350 mg, 0.0395 mmol) and stirring for 2 h. Column chromatography on silica using methylene chloride eluted a yellow band (367 mg, 0.259 mmol, 65%). ^{1}H NMR (CD_2Cl_2, 298 K, δ, major isomer): 5.83, 5.82 (each a s, each 1H, acac C*H*), 3.72 (s, 3H, N-CH_3), 3.19 (s, 6H, H_3C-C≡C-CH_3), 2.64, 2.55, 1.89, 1.81 (each a s, each 3H, acac CH_3). ^{1}H NMR (CD_2Cl_2, 298 K, δ, minor isomer): 5.86, 5.55 (each a s, each 1H, acac C*H*), 4.05 (s, 3H, N-CH_3), 3.17 (s, 6H, H_3C-C≡C-CH_3), 2.69, 2.46, 1.88, 1.75 (each a s, each 3H, acac CH_3). ^{13}C{^{1}H} NMR (CD_2Cl_2, 298 K, δ, major isomer): 18.4 (H_3C-C≡C-*C*H_3), 25.3, 26.8, 28.2, 28.5 (acac *C*H_3), 37.8 (N-*C*H_3), 104.1, 104.5 (acac *C*H), 185.2, 189.6, 191.6, 194.6 (acac *C*O), 211.0 (Me*C*≡*C*Me), 217.5 (N=*C*). Anal. Calcd for $WC_{54}H_{40}O_4NBF_{24}$: C, 45.75; H, 2.85; N, 0.99. Found: C, 45.96; H, 2.91; N, 0.89%.

[W(η^2-PhC≡CH)(η^2-MeN=CMe)(acac)$_2$][BAr$_4$'] (5c[BAr′$_4$]). In the drybox 50 mg of **1b[BAr′$_4$]** (0.038 mmol) was placed in a Schlenk tube. Methylene chloride was added (40 mL) followed by phenylacetylene (15 μL, 0.14 mmol). The vessel was placed in a photolysis hood for 3 h, resulting in a color change from olive green to light yellow. The solvent was removed *in vacuo* yielding a yellow/brown solid. Column chromatography on silica using methylene chloride eluted a dark yellow band (38 mg, 0.027 mmol, 72%). ^{1}H NMR (CD_2Cl_2,

298 K, δ, major isomer): 13.25 (s, 1H, PhC≡C*H*), 5.84 (s, 2H, acac C*H*), 3.45 (s, 3H, N-CH_3), 3.15 (s, 3H, N=C-CH_3), 2.58, 2.55, 1.87, 1.86 (each a s, each 3H, acac CH_3). ^{1}H NMR (CD_2Cl_2, 298 K, minor isomer): 13.36 (s, 1H, PhC≡C*H*), 5.90, 5.73 (each a s, each 1H, acac C*H*), 3.76 (s, 3H, N-CH_3), 2.94 (s, 3H, N=C-CH_3), 2.61, 2.51, 1.87, 1.86 (each a s, each 3H, acac CH_3). ^{13}C{^{1}H} NMR (CD_2Cl_2, 298 K, δ, major isomer): 16.7 (N=C-*C*H_3), 25.0, 26.6, 28.3, 28.9 (acac *C*H_3), 37.6 (N-*C*H_3), 104.3, 105.1 (acac *C*H), 183.8, 188.8, 192.0, 195.6 (acac *C*O), 204.5 (PhC≡*C*H), 209.9 (Ph*C*≡CH), 229.0 (N=*C*). Anal. Calcd for $WC_{53}H_{38}O_4F_{24}NB$: C, 45.36; H, 2.73; N, 1.00. Found: C, 45.43; H, 2.67; N, 1.01%.

[W(η^2-MeC≡CMe)(η^2-MeN=CMe)(acac)$_2$][BAr$_4$'] (5d[BAr′$_4$]). In the drybox 50 mg of **1b[BAr′$_4$]** (0.038 mmol) was placed in a Schlenk tube. Methylene chloride was added (40 mL) followed by 2-butyne (0.10 mL, 1.28 mmol). The vessel was placed in a photolysis hood for 3 h, resulting in a color change from olive green to light yellow. The solvent was removed *in vacuo* yielding a yellow/brown solid. Column chromatography on silica using methylene chloride eluted a dark yellow band (38 mg, 0.028 mmol, 75%). IR (KBr): $\nu_{C\equiv C}$ = 1764 cm^{-1}. ^{1}H NMR (CD_2Cl_2, 298 K, δ, major isomer): 5.79, 5.75 (each a s, each 1H, acac C*H*), 3.34 (s, 3H, N-CH_3), 3.12 (s, 6H, H_3C-C≡C-CH_3), 3.01 (s, 3H, N=C-CH_3), 2.56, 2.49, 1.84, 1.81 (each a s, each 3H, acac CH_3). ^{1}H NMR (CD_2Cl_2, 298 K, minor isomer): 5.82, 5.63 (each a s, each 1H, acac C*H*), 3.64 (s, 3H, N-CH_3), 3.08 (s, 6H, H_3C-C≡C-CH_3), 2.78 (s, 3H, N=C-CH_3), 2.63, 2.45, 1.84, 1.79 (each a s, each 3H, acac CH_3). ^{13}C{^{1}H} NMR (CD_2Cl_2, 298 K, δ): 15.7 (N=C-*C*H_3), 18.0 (H_3*C*-C≡C-*C*H_3), 25.1, 26.8, 28.4, 28.7 (acac *C*H_3), 36.7 (N-*C*H_3), 103.7, 104.3 (acac *C*H), 183.9, 189.2, 191.5, 195.2 (acac *C*O), 210.9 (Me*C*≡*C*Me), 230.1 (N=*C*). Anal. Calcd for $WC_{49}H_{38}O_4F_{24}NB$: C, 43.42; H, 2.83; N, 1.03. Found: C, 43.40; H, 2.73; N, 1.06%.

W(η^2-MeC≡CMe)(η^2-MeN=CHPh)(acac)$_2$ (6). 5b[OTf] was generated *in situ* from **1a[OTf]** (210 mg, 0.310 mmol) according to the above procedure. The solvent was removed and the solid was washed with hexanes (40 mL). The brown powder was dissolved in THF (10 mL) resulting in a brown solution. In a separate flask, Na[HB(OMe)$_3$] (50 mg, 0.39 mmol) was dissolved in THF (7 mL). This solution was cannula transferred to the flask containing **5b[OTf]** resulting in a color change from brown to dark orange. The solvent volume was reduced *in vacuo* after 15 min of stirring and hexanes (40 mL) were added to precipitate residual salts. The supernatant was cannula filtered to a separate flask and the remaining solvent was removed *in vacuo* yielding an orange solid. Purification occurred via column chromatography on silica using a mixture of CH_2Cl_2 and diethyl ether (90:10) to elute an orange band (119 mg, 0.214 mmol, 69%). Orange crystals suitable for X-ray analysis formed after a few days in a concentrated pentane solution at -30 °C. ^{1}H NMR (CD_2Cl_2, 200 K, δ, major isomer): 5.50, 4.69 (each a s, each 1H, acac C*H*), 3.43 (s, 3H, N-CH_3), 3.08, 2.62 (each a s, each 3s, H_3C-C≡C-CH_3), 2.45, 1.90, 1.68, 1.59 (each a s, each 3H, acac CH_3), 2.40 (s, 1H, N=C-*H*). ^{13}C{^{1}H} NMR (CD_2Cl_2, 200 K, δ, major isomer): 15.3, 17.9 (H_3C-C≡C-CH_3), 26.2, 26.3, 27.9, 28.4 (acac CH_3), 45.8 (N-CH_3), 73.6 (N=*C*), 98.8, 101.3 (acac *C*H), 147.0 (*ipso*-C_6H_5), 184.7, 186.5, 188.1, 191.0 (acac *C*O), 204.7, 208.7 (Me*C*≡*C*Me). Anal. Calcd for $WC_{22}H_{29}O_4N$: C, 47.58; H, 5.27; N, 2.52. Found: C, 47.74; H, 5.10; N, 2.50%.

[W(η^2-MeC≡CMe)(η^2-Me$_2$N=CHPh)(acac)$_2$][BAr$_4$'] (7[BAr′$_4$]). In a Schlenk flask **6** (338 mg, 0.609 mmol) was combined with methylene chloride (15 mL) resulting in an orange solution. Methyl trifluoromethylsulfonate (MeOTf) was added (50 μL, 0.44 mmol) and the reaction mixture was allowed to stir for two hours. The solvent volume was reduced *in vacuo* and hexanes (40 mL) were added to aid in precipitating an orange solid. The supernatant was

removed via cannula filtration. For counter-ion exchange, the product was dissolved in methylene chloride (15 mL) and combined with Na[BAr′$_4$] (540 mg, 0.609 mmol). The reaction mixture was allowed to stir for 4 hours, at which point the orange liquid was cannula filtered away from residual salt to a separate flask and the solvent was removed *in vacuo*. Purification of the orange solid was achieved via column chromatography on silica using methylene chloride to elute an orange band (542 mg, 0.378 mmol, 62%). Orange needles suitable for X-ray analysis were obtained via evaporation of a solution of 50:50 methylene chloride and hexanes. ^{1}H NMR (CD_2Cl_2, 298 K, δ, major isomer): 7.45 (t, 2H, *m*-C_6H_5), 7.32 (d, 2H, *o*-C_6H_5), 7.17 (s, 1H, *p*-C_6H_5), 5.98, 5.73 (each a s, each 1H, acac C*H*), 3.99 (s, 1H, N=C-*H*), 2.97, 2.64 (each a s, each 3H, N-CH_3), 2.82 (s, 6H, CH_3-C≡C-CH_3), 2.50, 2.49, 2.01, 1.83 (each a s, each 3H, acac CH_3). ^{13}C{^{1}H} NMR (CD_2Cl_2, 298 K, δ, major isomer): 19.8 (*C*H$_3$-C≡C-*C*H$_3$), 25.1, 26.8, 28.4, 28.6 (acac *C*H$_3$), 51.4, 53.1 (N-*C*H$_3$), 91.4 (N=*C*), 103.7, 105.5 (acac *C*H), 184.2, 188.8, 194.5, 194.9 (acac *C*O), 240.1 (Me*C*≡*C*Me). Anal. Calcd for $WC_{55}H_{44}O_4NBF_{24}$: C, 46.08; H, 3.10; N, 0.98. Found: C, 46.32; H, 3.39; N, 0.83%.

[W(η^2-MeC≡CMe)(η^2-MeNC(PMe$_3$)Ph)(acac)$_2$][BAr$_4$'] (8[BAr′$_4$]). A Schlenk flask was charged with **5b[BAr′$_4$]** (52 mg, 0.037 mmol) and CH_2Cl_2 (15 mL) resulting in a yellow solution. Addition of PMe_3 (10 μL, 0.097 mmol) produced no visible color change over the course of stirring for 20 min Hexanes (20 mL) were added to precipitate a pale yellow powder (32 mg, 0.021 mmol, 59%). Yellow crystals suitable for X-ray analysis were obtained by layering pentane over a methylene chloride solution of the product in an inert atmosphere and storing at -30 °C for several days. ^{1}H NMR (CD_2Cl_2, 298 K, δ, major diastereomer): 7.36 (br s, 3H, *o/m*-C_6H_5), 7.08 (t, 1H, *p*-C_6H_5), 6.30 (br s, 1H, *o*-C_6H_5), 5.75, 5.48 (each a s, each 1H, acac C*H*), 3.66 (s, 3H, N-CH_3), 2.78, 1.42 (each a s, each 6H, CH_3-

C≡C-CH_3), 2.43, 2.34, 1.86. 1.76 (each a s, each 3H, acac CH_3), 1.71 (d, 9H, P-(CH_3)$_3$, $^2J_{P\text{-}H}$ = 13 Hz); ^{1}H NMR (CD_2Cl_2, 203 K, δ, major diastereomer): 7.27, 6.17 (each a d, each 1 H, *o*-C_6H_5, $^2J_{H\text{-}H}$ = 6Hz), 7.38, 7.13 (each a t, each 1H, *m*-C_6H_5, $^2J_{H\text{-}H}$ = 6Hz), 6.98 (t, 1H, *p*-C_6H_5, $^2J_{H\text{-}H}$ = 6Hz), 2.69, 1.16 (each a s, each 6H, CH_3-C≡C-CH_3). ^{13}C{^{1}H} NMR (CD_2Cl_2, 203 K, δ, major diastereomer): 11.6 (d, P-(*C*H_3)$_3$, $^1J_{P\text{-}C}$ = 51 Hz), 13.0, 15.8 (*C*H_3-C≡C-*C*H_3), 25.9, 26.4, 27.4, 28.2 (acac *C*H_3), 42.9 (N-*C*H_3), 52.8 (N-*C*-PMe_3), 101.6, 102.7 (acac *C*H), 123.1, 125.4, 128.0, 141.7 (*C*$_6$H$_5$), 182.7, 182.8 (Me*C*≡*C*Me), 184.2, 185.5, 188.0, 191.6 (acac *C*O). ^{31}P NMR (CD_2Cl_2, 203 K, δ, major diastereomer): 35.1 (*P*Me_3). Anal Calcd for $WC_{57}H_{49}BF_{24}NO_4P$: C, 45.84; H, 3.31; N, 0.94. Found: C, 45.82; H, 3.28; N, 0.83%.

[W(η^2-PhC=C(H)PMe_3)(η^2-MeN=CPh)(acac)$_2$][BAr$_4$'] (9[BAr′$_4$]). A Schlenk flask was charged with **5a[BAr′$_4$]** (48 mg, 0.033 mmol) and CH_2Cl_2 (15 mL) resulting in a yellow solution. Addition of PMe_3 (10 μL, 0.097 mmol) produced no visible color change over the course of stirring for 20 min. Hexanes (20 mL) were added and the solvent was removed to produce a yellow powder (35 mg, 0.023 mmol, 69%). ^{1}H NMR (CD_2Cl_2, 298 K, δ, major isomer): 5.81, 5.57 (each a s, each 1H, acac C*H*), 3.83 (s, 3H, N-CH_3), 3.04 (d, 1H, C=C-*H*, $^2J_{P\text{-}H}$ = 27 Hz), 2.25, 2.24, 1.94, 1.82 (each a s, each 3H, acac CH_3), 1.70 (d, 9H, P-(CH_3)$_3$, $^2J_{P\text{-}H}$ = 13 Hz); ^{13}C{^{1}H} NMR (CD_2Cl_2, 298 K, δ, major isomer): 13.0 (d, P-(*C*H_3)$_3$, $^1J_{P\text{-}C}$ = 55 Hz), 26.3, 27.5, 27.7, 28.1 (acac *C*H_3), 31.6, (d, C=*C*(H)PMe_3, $^1J_{P\text{-}C}$ = 85 Hz), 35.3 (N-*C*H_3), 102.2, 102.4 (acac *C*H), 185.4, 187.0, 190.5, 190.9 (acac *C*O), 218.2 (N=*C*), 240.9 (*C*=C(H)PMe_3); ^{31}P NMR (CD_2Cl_2, 298 K, δ, major isomer): 34.8 (*P*Me_3, $^2J_{P\text{-}W}$ = 34 Hz).

References

(1) Patai, S. *Patai's Guide to the Chemistry of Functional Groups*; Wiley: Chichester, 1989.

(2) *Comprehensive Organic Functional Group Transformations*; Katritzky, A. R.; Meth-Cohn, O.; Rees, C. W., Eds.; Pergamon: Oxford, 1995; Vol. 1-7.

(3) Durfee, L. D.; Rothwell, I. P. *Chem. Rev.* **1988**, *88*, 1059.

(4) Kuznetsov, M. L. *Russ. Chem. Rev.* **2002**, *71*, 265.

(5) Shin, J. H.; Savage, W.; Murphy, V. J.; Bonanno, J. B.; Churchill, D. G.; Parkin, G. *J. Chem. Soc., Dalton Trans.* **2001**, 1732.

(6) Cross, J. L.; Garrett, A. D.; Crane, T. W.; White, P. S.; Templeton, J. L. *Polyhedron* **2004**, *23*, 2831.

(7) Lis, E. C.; Delafuente, D. A.; Lin, Y.; Mocella, C. J.; Todd, M. A.; Liu, W.; Sabat, M.; Myers, W. H.; Harman, W. D. *Organometallics* **2006**, *25*, 5051.

(8) Jackson, A. B.; Khosla, C.; Gaskins, H. E.; White, P. S.; Templeton, J. L. *Organometallics* **2008**, *27*, 1322.

(9) Tsai, Y.-C.; Stephens, F. H.; Meyer, K.; Mendiratta, A.; Gheorghiu, M. D.; Cummins, C. C. *Organometallics* **2003**, *22*, 2902.

(10) Kukushkin, V. Y.; Pombeiro, A. J. L. *Chem. Rev.* **2002**, *102*, 1771.

(11) Kukushkin, V. Y.; Pombeiro, A. J. L. *Inorg. Chim. Acta* **2005**, *358*, 1.

(12) Michelin, R. A.; Mozzon, M.; Bertani, R. *Coord. Chem. Rev.* **1996**, *147*, 299.

(13) Kuznetsov, M. L.; Nazarov, A. A.; Pombeiro, A. J. L. *J. Phys. Chem. A* **2005**, *109*, 8187.

(14) Chin, C. S.; Chong, D.; Lee, B.; Jeong, H.; Won, G.; Do, Y.; Park, Y. J. *Organometallics* **2000**, *19*, 638.

(15) Jackson, A. B.; Schauer, C. K.; White, P. S.; Templeton, J. L. *J. Am. Chem. Soc.* **2007**, *129*, 10628.

(16) Templeton, J. L. *Adv. Organomet. Chem.* **1989**, *29*, 1.

(17) Erkkila, A.; Majander, I.; Pihko, P. M. *Chem. Rev.* **2007**, *107*, 5416.

(18) Blanchard, K. C.; Klein, D. L.; MacDonald, J. *J. Am. Chem. Soc.* **1931**, *53*, 2809.

(19) Crowell, T. I.; Peck, D. W. *J. Am. Chem. Soc.* **1953**, *75*, 1075.

(20) Pedersen, K. J. *J. Phys. Chem.* **1934**, *38*, 559.

(21) Pedersen, K. J. *J. Am. Chem. Soc.* **1938**, *60*, 595.

(22) Baum, J. S.; Viehe, H. G. *J. Org. Chem.* **1976**, *41*, 183.

(23) Jung, M. E.; Vaccaro, W. D.; Buszek, K. R. *Tetrahedron Lett.* **1989**, *30*, 1893.

(24) Griesbeck, A. G. *J. Org. Chem.* **1989**, *54*, 4981.

(25) Sepelak, D. J.; Pierpont, C. G.; Barefield, E. K.; Budz, J. T.; Poffenberger, C. A. *J. Am. Chem. Soc.* **1976**, *98*, 6178.

(26) Wilson, R. B.; Laine, R. M. *J. Am. Chem. Soc.* **1985**, *107*, 361.

(27) Matsumoto, M.; Nakatsu, K.; Tani, K.; Nakamura, A.; Otsuka, S. *J. Am. Chem. Soc.* **1974**, *96*, 6777.

(28) Most, K.; Mösch-Zanetti, N. C.; Vidović, D.; Magull, J. *Organometallics* **2003**, *22*, 5485.

(29) Barrera, J.; Orth, S. D.; Harman, W. D. *J. Am. Chem. Soc.* **1992**, *114*, 7316.

(30) Orth, S. D.; Barrera, J.; Rowe, S. M.; Helberg, L. E.; Harman, W. D. *Inorg. Chim. Acta* **1998**, *270*, 337.

(31) Thomas, J. L. *J. Am. Chem. Soc.* **1975**, *97*, 5943.

(32) Brunner, H.; Wachter, J.; Schmidbauer, J. *Organometallics* **1986**, *5*, 2212.

(33) Hasegawa, T.; Kwan, K. S.; Taube, H. *Inorg. Chem.* **1992**, *31*, 1598.

(34) Feng, S. G.; Templeton, J. L. *J. Am. Chem. Soc.* **1989**, *111*, 6477.

(35) Feng, S. G.; Templeton, J. L. *Organometallics* **1992**, *11*, 1295.

(36) Pearson, J.; Cooke, J.; Takats, J.; Jordan, R. B. *J. Am. Chem. Soc.* **1998**, *120*, 1434.

(37) Hamilton, D. H.; Shapley, J. R. *Organometallics* **2000**, *19*, 761.

(38) Reid, S. M.; Mague, J. T.; Fink, M. J. *J. Am. Chem. Soc.* **2001**, *123*, 4081.

(39) Dennett, J. N. L.; Ferguson, M. J.; McDonald, R.; Takats, J. *Can. J. Chem.* **2005**, *83*, 862.

(40) Jackson, A. B.; White, P. S.; Templeton, J. L. *Inorg. Chem.* **2006**, *45*, 6205.

(41) Herrick, R. S.; Templeton, J. L. *Organometallics* **1982**, *1*, 842.

(42) Herrick, R. S.; Burgmayer, S. J. N.; Templeton, J. L. *Inorg. Chem.* **1983**, *22*, 3275.

(43) Etienne, M.; Carfagna, C.; Lorente, P.; Mathieu, R.; de Montauzon, D. *Organometallics* **1999**, *18*, 3075.

(44) Gutowsky, H. S.; Holm, C. H. *J. Chem. Phys.* **1956**, *25*, 1228.

(45) Morrow, J. R.; Tonker, T. L.; Templeton, J. L. *J. Am. Chem. Soc.* **1985**, *107*, 6956.

(46) Frohnapfel, D. S.; Templeton, J. L. *Coord. Chem. Rev.* **2000**, *206*, 199.

(47) Pangborn, A. B.; Giardello, M. A.; Grubbs, R. H.; Rosen, R. K.; Timmers, F. J. *Organometallics* **1996**, *15*, 1518.

(48) Yakelis, N. A.; Bergman, R. G. *Organometallics* **2005**, *24*, 3579.

Appendix A

Bond lengths [Å] and angles [°] for $W(CO)_3(acac)_2$ (Chapter 2, **1**).

W(1)-C(25)	1.960(12)
W(1)-C(21)	1.994(15)
W(1)-C(23)	1.997(11)
W(1)-O(8)	2.083(7)
W(1)-O(12)	2.092(7)
W(1)-O(1)	2.106(7)
W(1)-O(5)	2.115(7)
O(5)-C(4)	1.286(11)
C(3)-C(4)	1.370(14)
C(3)-C(2)	1.395(14)
O(1)-C(2)	1.296(11)
C(4)-C(7)	1.504(13)
C(6)-C(2)	1.473(14)
O(8)-C(9)	1.295(13)
C(10)-C(9)	1.381(16)
C(10)-C(11)	1.381(15)
C(11)-O(12)	1.291(11)
C(11)-C(14)	1.482(14)
C(9)-C(13)	1.517(15)
C(21)-O(22)	1.169(14)
O(24)-C(23)	1.153(12)
O(40)-C(25)	1.175(12)

(25)-W(1)-C(21)	69.7(5)
C(25)-W(1)-C(23)	104.5(4)
C(21)-W(1)-C(23)	67.9(4)
C(25)-W(1)-O(8)	160.6(4)
C(21)-W(1)-O(8)	129.7(4)
C(23)-W(1)-O(8)	86.6(4)
C(25)-W(1)-O(12)	80.1(4)
C(21)-W(1)-O(12)	127.8(4)
C(23)-W(1)-O(12)	80.4(4)
O(8)-W(1)-O(12)	86.2(3)
C(25)-W(1)-O(1)	113.0(4)
C(21)-W(1)-O(1)	74.2(4)
C(23)-W(1)-O(1)	111.3(4)
O(8)-W(1)-O(1)	76.3(3)
O(12)-W(1)-O(1)	157.9(3)
C(25)-W(1)-O(5)	83.6(4)
C(21)-W(1)-O(5)	133.0(4)
C(23)-W(1)-O(5)	158.7(4)
O(8)-W(1)-O(5)	80.8(3)
O(12)-W(1)-O(5)	81.6(3)
O(1)-W(1)-O(5)	82.4(3)
C(4)-O(5)-W(1)	130.8(6)
C(4)-C(3)-C(2)	125.8(10)
C(2)-O(1)-W(1)	130.4(6)
O(5)-C(4)-C(3)	124.4(9)
O(5)-C(4)-C(7)	114.1(9)
C(3)-C(4)-C(7)	121.5(10)
O(1)-C(2)-C(3)	123.8(9)
O(1)-C(2)-C(6)	114.9(9)
C(3)-C(2)-C(6)	121.3(10)
C(9)-O(8)-W(1)	127.5(7)
C(9)-C(10)-C(11)	126.2(11)
O(12)-C(11)-C(10)	125.0(10)
O(12)-C(11)-C(14)	114.5(10)
C(10)-C(11)-C(14)	120.5(10)
C(11)-O(12)-W(1)	127.8(7)
O(8)-C(9)-C(10)	125.5(11)
O(8)-C(9)-C(13)	114.0(11)
C(10)-C(9)-C(13)	120.5(11)
O(22)-C(21)-W(1)	178.8(11)
O(24)-C(23)-W(1)	176.1(9)
O(40)-C(25)-W(1)	174.3(10)

Appendix B

Bond lengths [Å] and angles [°] for $W(CO)_2(PMe_3)(acac)_2$ (Chapter 2, **2a**).

W(1)-C(3)	1.962(7)	O(15)-W(1)-O(19)	83.47(18)
W(1)-C(1)	1.971(8)	O(8)-W(1)-O(19)	88.41(19)
W(1)-O(12)	2.118(5)	C(3)-W(1)-P(1)	107.57(18)
W(1)-O(15)	2.128(5)	C(1)-W(1)-P(1)	71.4(2)
W(1)-O(8)	2.141(5)	O(12)-W(1)-P(1)	146.76(14)
W(1)-O(19)	2.183(5)	O(15)-W(1)-P(1)	127.35(13)
W(1)-P(1)	2.4959(18)	O(8)-W(1)-P(1)	72.30(13)
P(1)-C(6)	1.808(7)	O(19)-W(1)-P(1)	75.56(14)
P(1)-C(5)	1.814(7)	C(6)-P(1)-C(5)	105.3(4)
P(1)-C(7)	1.815(7)	C(6)-P(1)-C(7)	102.4(4)
C(1)-O(2)	1.165(9)	C(5)-P(1)-C(7)	104.2(4)
C(3)-O(4)	1.144(8)	C(6)-P(1)-W(1)	114.8(2)
O(8)-C(9)	1.287(9)	C(5)-P(1)-W(1)	115.7(2)
C(9)-C(10)	1.392(11)	C(7)-P(1)-W(1)	113.1(2)
C(9)-C(13)	1.505(10)	O(2)-C(1)-W(1)	174.0(6)
C(10)-C(11)	1.391(11)	O(4)-C(3)-W(1)	176.3(6)
C(11)-O(12)	1.274(9)	C(9)-O(8)-W(1)	127.7(5)
C(11)-C(14)	1.521(10)	O(8)-C(9)-C(10)	126.1(7)
O(15)-C(16)	1.263(8)	O(8)-C(9)-C(13)	114.5(6)
C(16)-C(17)	1.387(10)	C(10)-C(9)-C(13)	119.3(7)
C(16)-C(20)	1.516(10)	C(11)-C(10)-C(9)	124.4(7)
C(17)-C(18)	1.393(10)	O(12)-C(11)-C(10)	124.7(6)
C(18)-O(19)	1.284(9)	O(12)-C(11)-C(14)	115.4(6)
C(18)-C(21)	1.515(10)	C(10)-C(11)-C(14)	119.9(7)
		C(11)-O(12)-W(1)	130.6(4)
C(3)-W(1)-C(1)	73.2(3)	C(16)-O(15)-W(1)	127.9(5)
C(3)-W(1)-O(12)	90.8(2)	O(15)-C(16)-C(17)	126.6(7)
C(1)-W(1)-O(12)	141.6(2)	O(15)-C(16)-C(20)	114.9(6)
C(3)-W(1)-O(15)	101.0(2)	C(17)-C(16)-C(20)	118.5(6)
C(1)-W(1)-O(15)	76.0(2)	C(16)-C(17)-C(18)	125.2(6)
O(12)-W(1)-O(15)	73.14(18)	O(19)-C(18)-C(17)	125.6(7)
C(3)-W(1)-O(8)	84.1(2)	O(19)-C(18)-C(21)	114.6(7)
C(1)-W(1)-O(8)	128.2(2)	C(17)-C(18)-C(21)	119.7(7)
O(12)-W(1)-O(8)	82.64(18)	C(18)-O(19)-W(1)	127.7(5)
O(15)-W(1)-O(8)	155.25(18)		
C(3)-W(1)-O(19)	170.5(2)		
C(1)-W(1)-O(19)	116.2(2)		
O(12)-W(1)-O(19)	82.40(19)		

Appendix C

Bond lengths [Å] and angles [°] for W(CO)(acac)$_2$(η^2-PhC≡CH) (Chapter 2, **3a**).

W(1)-C(1)	1.946(6)
W(1)-C(3)	2.036(5)
W(1)-C(4)	2.037(5)
W(1)-O(11)	2.058(4)
W(1)-O(15)	2.117(3)
W(1)-O(18)	2.145(3)
W(1)-O(22)	2.070(3)
C(1)-O(2)	1.163(7)
C(3)-C(4)	1.301(8)
C(4)-C(5)	1.461(8)
C(5)-C(6)	1.400(7)
C(5)-C(10)	1.394(7)
C(6)-C(7)	1.380(8)
C(7)-C(8)	1.384(9)
C(8)-C(9)	1.389(9)
C(9)-C(10)	1.380(9)
O(11)-C(12)	1.286(6)
C(12)-C(13)	1.389(7)
C(12)-C(16)	1.486(7)
C(13)-C(14)	1.381(7)
C(14)-O(15)	1.281(6)
C(14)-C(17)	1.499(7)
O(18)-C(19)	1.259(6)
C(19)-C(20)	1.403(8)
C(19)-C(23)	1.510(8)
C(20)-C(21)	1.384(8)
C(21)-O(22)	1.293(6)
C(21)-C(24)	1.511(7)

C(1)-W(1)-C(3)	72.00(21)
C(1)-W(1)-C(4)	109.16(21)
C(1)-W(1)-O(11)	96.55(18)
C(1)-W(1)-O(15)	84.53(18)
C(1)-W(1)-O(18)	163.48(18)
C(1)-W(1)-O(22)	91.53(18)
C(3)-W(1)-C(4)	37.26(21)
C(3)-W(1)-O(11)	99.06(17)
C(3)-W(1)-O(15)	156.52(18)
C(3)-W(1)-O(18)	124.51(17)
C(3)-W(1)-O(22)	99.28(17)
C(4)-W(1)-O(11)	92.13(16)
C(4)-W(1)-O(15)	165.83(18)
C(4)-W(1)-O(18)	87.36(18)
C(4)-W(1)-O(22)	100.94(16)
O(11)-W(1)-O(15)	82.42(13)
O(11)-W(1)-O(18)	82.13(14)
O(11)-W(1)-O(22)	161.47(14)
O(15)-W(1)-O(18)	78.96(14)
O(15)-W(1)-O(22)	81.79(14)
O(18)-W(1)-O(22)	85.39(13)
W(1)-C(1)-O(2)	177.8(4)
W(1)-C(3)-C(4)	71.4(3)
W(1)-C(4)-C(3)	71.3(3)
W(1)-C(4)-C(5)	147.7(4)
C(3)-C(4)-C(5)	140.8(5)
C(4)-C(5)-C(6)	121.3(5)
C(4)-C(5)-C(10)	120.6(5)
C(6)-C(5)-C(10)	118.0(5)
C(5)-C(6)-C(7)	120.7(5)
C(6)-C(7)-C(8)	120.1(5)
C(7)-C(8)-C(9)	120.2(5)
C(8)-C(9)-C(10)	119.3(5)
C(5)-C(10)-C(9)	121.6(5)
W(1)-O(11)-C(12)	132.3(3)
O(11)-C(12)-C(13)	122.8(5)
O(11)-C(12)-C(16)	115.9(4)
C(13)-C(12)-C(16)	121.3(5)
C(12)-C(13)-C(14)	125.6(5)
C(13)-C(14)-O(15)	124.0(5)
C(13)-C(14)-C(17)	119.7(5)
O(15)-C(14)-C(17)	116.1(5)
W(1)-O(15)-C(14)	128.8(3)
W(1)-O(18)-C(19)	128.3(3)
O(18)-C(19)-C(20)	124.9(5)
O(18)-C(19)-C(23)	116.6(5)
C(20)-C(19)-C(23)	118.5(5)
C(19)-C(20)-C(21)	125.7(5)
C(20)-C(21)-O(22)	126.5(5)
C(20)-C(21)-C(24)	119.5(5)
O(22)-C(21)-C(24)	114.0(5)
W(1)-O(22)-C(21)	128.2(3)

Appendix D

Bond lengths [Å] and angles [°] for $W(acac)_2(\eta^2\text{-PhC}\equiv\text{CPh})_2$ (Chapter 2, **4**)

W(1)-C(16)	2.0622(13)	C(33)-C(34)	1.393(2)
W(1)-C(30)	2.0665(13)	C(34)-C(35)	1.393(2)
W(1)-C(15)	2.0680(13)	C(35)-C(36)	1.3917(19)
W(1)-C(29)	2.0728(13)	C(37)-C(38)	1.4032(19)
W(1)-O(1)	2.1162(10)	C(37)-C(42)	1.4052(18)
W(1)-O(8)	2.1303(10)	C(38)-C(39)	1.391(2)
W(1)-O(5)	2.1369(9)	C(39)-C(40)	1.393(2)
W(1)-O(12)	2.1445(10)	C(40)-C(41)	1.390(2)
O(1)-C(2)	1.2819(17)	C(41)-C(42)	1.393(2)
C(2)-C(3)	1.390(2)		
C(2)-C(6)	1.508(2)	C(16)-W(1)-C(30)	101.02(5)
C(3)-C(4)	1.405(2)	C(16)-W(1)-C(15)	37.11(5)
C(4)-O(5)	1.2700(16)	C(30)-W(1)-C(15)	91.80(5)
C(4)-C(7)	1.5053(19)	C(16)-W(1)-C(29)	94.73(5)
O(8)-C(9)	1.2719(16)	C(30)-W(1)-C(29)	36.92(5)
C(9)-C(10)	1.4044(19)	C(15)-W(1)-C(29)	108.65(5)
C(9)-C(13)	1.5030(19)	C(16)-W(1)-O(1)	97.07(5)
C(10)-C(11)	1.390(2)	C(30)-W(1)-O(1)	152.77(5)
C(11)-O(12)	1.2830(16)	C(15)-W(1)-O(1)	90.45(5)
C(11)-C(14)	1.5103(19)	C(29)-W(1)-O(1)	159.90(5)
C(15)-C(16)	1.3144(19)	C(16)-W(1)-O(8)	119.76(5)
C(15)-C(23)	1.4593(18)	C(30)-W(1)-O(8)	78.17(5)
C(16)-C(17)	1.4598(19)	C(15)-W(1)-O(8)	82.74(5)
C(17)-C(18)	1.401(2)	C(29)-W(1)-O(8)	112.50(4)
C(17)-C(22)	1.4032(19)	O(1)-W(1)-O(8)	75.21(4)
C(18)-C(19)	1.396(2)	C(16)-W(1)-O(5)	78.93(5)
C(19)-C(20)	1.391(2)	C(30)-W(1)-O(5)	120.85(5)
C(20)-C(21)	1.389(2)	C(15)-W(1)-O(5)	114.24(5)
C(21)-C(22)	1.393(2)	C(29)-W(1)-O(5)	83.93(4)
C(23)-C(24)	1.397(2)	O(1)-W(1)-O(5)	82.45(4)
C(23)-C(28)	1.395(2)	O(8)-W(1)-O(5)	152.15(4)
C(24)-C(25)	1.393(2)	C(16)-W(1)-O(12)	155.64(5)
C(25)-C(26)	1.382(3)	C(30)-W(1)-O(12)	92.13(4)
C(26)-C(27)	1.383(3)	C(15)-W(1)-O(12)	163.91(5)
C(27)-C(28)	1.393(2)	C(29)-W(1)-O(12)	83.49(4)
C(29)-C(30)	1.3106(18)	O(1)-W(1)-O(12)	79.04(4)
C(29)-C(37)	1.4633(18)	O(8)-W(1)-O(12)	82.81(4)
C(30)-C(31)	1.4566(17)	O(5)-W(1)-O(12)	76.72(4)
C(31)-C(36)	1.4007(19)	C(2)-O(1)-W(1)	130.71(9)
C(31)-C(32)	1.4016(18)	O(1)-C(2)-C(3)	124.99(13)
C(32)-C(33)	1.3909(19)	O(1)-C(2)-C(6)	114.77(13)

C(3)-C(2)-C(6)	120.23(13)	C(28)-C(23)-C(15)	119.92(13)
C(2)-C(3)-C(4)	124.02(13)	C(23)-C(24)-C(25)	120.49(14)
O(5)-C(4)-C(3)	125.60(13)	C(26)-C(25)-C(24)	120.17(15)
O(5)-C(4)-C(7)	114.90(13)	C(27)-C(26)-C(25)	119.86(15)
C(3)-C(4)-C(7)	119.45(12)	C(26)-C(27)-C(28)	120.35(16)
C(4)-O(5)-W(1)	129.26(9)	C(27)-C(28)-C(23)	120.35(16)
C(9)-O(8)-W(1)	127.08(9)	C(30)-C(29)-C(37)	139.63(13)
O(8)-C(9)-C(10)	125.81(13)	C(30)-C(29)-W(1)	71.28(8)
O(8)-C(9)-C(13)	115.64(12)	C(37)-C(29)-W(1)	148.25(10)
C(10)-C(9)-C(13)	118.54(12)	C(29)-C(30)-C(31)	145.43(13)
C(11)-C(10)-C(9)	124.70(13)	C(29)-C(30)-W(1)	71.80(8)
O(12)-C(11)-C(10)	124.94(13)	C(31)-C(30)-W(1)	142.50(10)
O(12)-C(11)-C(14)	115.59(12)	C(36)-C(31)-C(32)	118.75(12)
C(10)-C(11)-C(14)	119.47(13)	C(36)-C(31)-C(30)	121.01(12)
C(11)-O(12)-W(1)	126.69(9)	C(32)-C(31)-C(30)	120.24(12)
C(16)-C(15)-C(23)	141.44(13)	C(33)-C(32)-C(31)	120.62(13)
C(16)-C(15)-W(1)	71.20(8)	C(32)-C(33)-C(34)	120.21(13)
C(23)-C(15)-W(1)	147.32(10)	C(35)-C(34)-C(33)	119.59(13)
C(15)-C(16)-C(17)	143.63(13)	C(36)-C(35)-C(34)	120.32(13)
C(15)-C(16)-W(1)	71.68(8)	C(35)-C(36)-C(31)	120.48(13)
C(17)-C(16)-W(1)	144.66(10)	C(38)-C(37)-C(42)	118.75(12)
C(18)-C(17)-C(22)	118.88(13)	C(38)-C(37)-C(29)	120.07(12)
C(18)-C(17)-C(16)	120.24(12)	C(42)-C(37)-C(29)	121.08(12)
C(22)-C(17)-C(16)	120.88(13)	C(39)-C(38)-C(37)	120.64(13)
C(19)-C(18)-C(17)	120.49(14)	C(38)-C(39)-C(40)	119.95(13)
C(20)-C(19)-C(18)	120.02(15)	C(41)-C(40)-C(39)	120.15(13)
C(21)-C(20)-C(19)	119.99(14)	C(40)-C(41)-C(42)	120.08(13)
C(20)-C(21)-C(22)	120.29(14)	C(41)-C(42)-C(37)	120.39(13)
C(21)-C(22)-C(17)	120.32(14)		
C(24)-C(23)-C(28)	118.77(13)		
C(24)-C(23)-C(15)	121.31(13)		

Appendix E

Bond lengths [Å] and angles [°] for W(CO)(acac)$_2$(η^2-2,6-dichlorobenzonitrile) (Chapter 3, **2c**).

W(1)-C(1)	1.961(5)	N(3)-W(1)-O(22)	160.66(17)
W(1)-N(3)	2.018(5)	C(4)-W(1)-O(22)	162.66(19)
W(1)-C(4)	2.038(5)	O(11)-W(1)-O(22)	81.91(19)
W(1)-O(11)	2.038(4)	O(18)-W(1)-O(22)	82.52(19)
W(1)-O(18)	2.048(4)	C(1)-W(1)-O(15)	167.56(19)
W(1)-O(22)	2.070(4)	N(3)-W(1)-O(15)	82.19(16)
W(1)-O(15)	2.166(4)	C(4)-W(1)-O(15)	118.65(19)
Cl(1)-C(6)	1.741(5)	O(11)-W(1)-O(15)	85.97(15)
Cl(2)-C(10)	1.744(6)	O(18)-W(1)-O(15)	84.27(15)
C(1)-O(2)	1.169(7)	O(22)-W(1)-O(15)	78.66(15)
N(3)-C(4)	1.270(7)	O(2)-C(1)-W(1)	176.7(5)
C(4)-C(5)	1.479(7)	C(4)-N(3)-W(1)	72.6(3)
C(5)-C(10)	1.394(7)	N(3)-C(4)-C(5)	136.9(5)
C(5)-C(6)	1.399(8)	N(3)-C(4)-W(1)	70.9(3)
C(6)-C(7)	1.396(7)	C(5)-C(4)-W(1)	151.8(4)
C(7)-C(8)	1.383(9)	C(10)-C(5)-C(6)	117.0(5)
C(8)-C(9)	1.383(9)	C(10)-C(5)-C(4)	120.4(5)
C(9)-C(10)	1.388(8)	C(6)-C(5)-C(4)	122.6(5)
O(11)-C(12)	1.296(7)	C(7)-C(6)-C(5)	122.1(5)
C(12)-C(13)	1.383(8)	C(7)-C(6)-Cl(1)	118.4(4)
C(12)-C(16)	1.515(9)	C(5)-C(6)-Cl(1)	119.4(4)
C(13)-C(14)	1.413(8)	C(8)-C(7)-C(6)	119.0(5)
C(14)-O(15)	1.267(7)	C(9)-C(8)-C(7)	120.3(5)
C(14)-C(17)	1.506(7)	C(8)-C(9)-C(10)	120.0(5)
O(18)-C(19)	1.277(7)	C(9)-C(10)-C(5)	121.6(5)
C(19)-C(20)	1.396(12)	C(9)-C(10)-Cl(2)	119.3(4)
C(19)-C(23)	1.499(11)	C(5)-C(10)-Cl(2)	119.1(4)
C(20)-C(21)	1.389(13)	C(12)-O(11)-W(1)	128.8(4)
C(21)-O(22)	1.287(8)	O(11)-C(12)-C(13)	126.8(6)
C(21)-C(24)	1.506(11)	O(11)-C(12)-C(16)	112.7(5)
		C(13)-C(12)-C(16)	120.5(5)
C(1)-W(1)-N(3)	110.2(2)	C(12)-C(13)-C(14)	125.4(5)
C(1)-W(1)-C(4)	73.7(2)	O(15)-C(14)-C(13)	124.8(5)
N(3)-W(1)-C(4)	36.48(19)	O(15)-C(14)-C(17)	116.7(5)
C(1)-W(1)-O(11)	90.8(2)	C(13)-C(14)-C(17)	118.5(5)
N(3)-W(1)-O(11)	99.46(19)	C(14)-O(15)-W(1)	127.3(3)
C(4)-W(1)-O(11)	99.55(19)	C(19)-O(18)-W(1)	133.0(5)
C(1)-W(1)-O(18)	95.8(2)	O(18)-C(19)-C(20)	123.0(7)
N(3)-W(1)-O(18)	93.00(19)	O(18)-C(19)-C(23)	115.8(8)
C(4)-W(1)-O(18)	97.37(19)	C(20)-C(19)-C(23)	121.1(7)
O(11)-W(1)-O(18)	162.98(18)	C(21)-C(20)-C(19)	124.5(6)
C(1)-W(1)-O(22)	89.0(2)	O(22)-C(21)-C(20)	123.7(7)

O(22)-C(21)-C(24)	114.0(8)
C(20)-C(21)-C(24)	122.4(7)
C(21)-O(22)-W(1)	131.2(5)

Appendix F

Bond lengths [Å] and angles [°] for W(CO)(acac)$_2$(η^2-PhN=CHPh) (Chapter 3, **3**).

W(1)-C(1)	1.927(7)	C(1)-W(1)-O(21)	95.3(2)
W(1)-N(3)	1.934(6)	N(3)-W(1)-O(21)	94.2(2)
W(1)-O(28)	2.034(4)	O(28)-W(1)-O(21)	163.12(18)
W(1)-O(24)	2.055(5)	O(24)-W(1)-O(21)	80.62(17)
W(1)-O(21)	2.071(4)	C(1)-W(1)-O(17)	164.5(2)
W(1)-O(17)	2.129(4)	N(3)-W(1)-O(17)	89.0(2)
W(1)-C(4)	2.237(7)	O(28)-W(1)-O(17)	82.45(17)
C(1)-O(2)	1.165(7)	O(24)-W(1)-O(17)	79.98(17)
N(3)-C(5)	1.395(8)	O(21)-W(1)-O(17)	86.95(17)
N(3)-C(4)	1.403(8)	C(1)-W(1)-C(4)	70.4(3)
C(4)-C(11)	1.485(9)	N(3)-W(1)-C(4)	38.4(2)
C(5)-C(6)	1.391(9)	O(28)-W(1)-C(4)	113.4(2)
C(5)-C(10)	1.401(10)	O(24)-W(1)-C(4)	149.5(2)
C(6)-C(7)	1.380(10)	O(21)-W(1)-C(4)	83.4(2)
C(7)-C(8)	1.390(11)	O(17)-W(1)-C(4)	125.0(2)
C(8)-C(9)	1.387(11)	O(2)-C(1)-W(1)	178.7(6)
C(9)-C(10)	1.374(10)	C(5)-N(3)-C(4)	127.2(6)
C(11)-C(12)	1.381(9)	C(5)-N(3)-W(1)	147.9(5)
C(11)-C(16)	1.400(9)	C(4)-N(3)-W(1)	82.6(4)
C(12)-C(13)	1.378(10)	N(3)-C(4)-C(11)	119.5(6)
C(13)-C(14)	1.358(11)	N(3)-C(4)-W(1)	59.0(3)
C(14)-C(15)	1.391(11)	C(11)-C(4)-W(1)	125.0(5)
C(15)-C(16)	1.364(10)	C(6)-C(5)-N(3)	119.3(7)
O(17)-C(18)	1.250(8)	C(6)-C(5)-C(10)	120.1(7)
C(18)-C(19)	1.419(10)	N(3)-C(5)-C(10)	120.4(6)
C(18)-C(22)	1.495(10)	C(7)-C(6)-C(5)	118.6(8)
C(19)-C(20)	1.378(9)	C(6)-C(7)-C(8)	121.8(8)
C(20)-O(21)	1.293(8)	C(9)-C(8)-C(7)	118.8(8)
C(20)-C(23)	1.498(9)	C(10)-C(9)-C(8)	120.6(8)
O(24)-C(25)	1.277(8)	C(9)-C(10)-C(5)	120.0(7)
C(25)-C(26)	1.377(9)	C(12)-C(11)-C(16)	118.2(7)
C(25)-C(29)	1.510(9)	C(12)-C(11)-C(4)	119.8(6)
C(26)-C(27)	1.386(9)	C(16)-C(11)-C(4)	122.0(6)
C(27)-O(28)	1.290(8)	C(13)-C(12)-C(11)	121.3(7)
C(27)-C(30)	1.493(9)	C(14)-C(13)-C(12)	119.1(8)
		C(13)-C(14)-C(15)	121.4(8)
C(1)-W(1)-N(3)	106.0(3)	C(16)-C(15)-C(14)	119.0(8)
C(1)-W(1)-O(28)	91.6(2)	C(15)-C(16)-C(11)	120.9(7)
N(3)-W(1)-O(28)	98.7(2)	C(18)-O(17)-W(1)	126.1(5)
C(1)-W(1)-O(24)	85.3(2)	O(17)-C(18)-C(19)	125.5(6)
N(3)-W(1)-O(24)	168.1(2)	O(17)-C(18)-C(22)	116.3(7)
O(28)-W(1)-O(24)	84.61(18)	C(19)-C(18)-C(22)	118.3(7)

C(20)-C(19)-C(18)	126.2(7)
O(21)-C(20)-C(19)	126.2(7)
O(21)-C(20)-C(23)	114.1(6)
C(19)-C(20)-C(23)	119.7(7)
C(20)-O(21)-W(1)	126.3(4)
C(25)-O(24)-W(1)	129.2(4)
O(24)-C(25)-C(26)	124.9(7)
O(24)-C(25)-C(29)	114.9(6)
C(26)-C(25)-C(29)	120.2(7)
C(25)-C(26)-C(27)	124.9(7)
O(28)-C(27)-C(26)	123.6(6)
O(28)-C(27)-C(30)	115.2(6)
C(26)-C(27)-C(30)	121.2(7)
C(27)-O(28)-W(1)	130.3(4)

Appendix G

Bond lengths [Å] and angles [°] for W(CO)(acac)$_2$(η^2-2,6-dichlorobenzaldehyde) (Chapter 3, **4b**).

W(1)-O(3)	1.945(2)	O(3)-W(1)-O(15)	83.45(9)
W(1)-C(2)	1.954(4)	C(2)-W(1)-O(15)	165.80(11)
W(1)-O(22)	2.031(2)	O(22)-W(1)-O(15)	83.07(9)
W(1)-O(18)	2.036(2)	O(18)-W(1)-O(15)	80.29(9)
W(1)-O(11)	2.044(2)	O(11)-W(1)-O(15)	87.50(9)
W(1)-O(15)	2.145(2)	O(3)-W(1)-C(4)	38.04(10)
W(1)-C(4)	2.210(3)	C(2)-W(1)-C(4)	73.62(13)
Cl(1)-C(6)	1.743(3)	O(22)-W(1)-C(4)	103.70(11)
Cl(2)-C(10)	1.749(3)	O(18)-W(1)-C(4)	158.52(11)
O(1)-C(2)	1.164(4)	O(11)-W(1)-C(4)	90.93(11)
O(3)-C(4)	1.377(4)	O(15)-W(1)-C(4)	120.55(10)
C(4)-C(5)	1.475(4)	O(1)-C(2)-W(1)	177.3(3)
C(5)-C(6)	1.406(4)	C(4)-O(3)-W(1)	81.48(16)
C(5)-C(10)	1.422(4)	O(3)-C(4)-C(5)	120.4(3)
C(6)-C(7)	1.389(5)	O(3)-C(4)-W(1)	60.48(14)
C(7)-C(8)	1.389(5)	C(5)-C(4)-W(1)	125.8(2)
C(8)-C(9)	1.377(5)	C(6)-C(5)-C(10)	114.0(3)
C(9)-C(10)	1.386(4)	C(6)-C(5)-C(4)	128.2(3)
O(11)-C(12)	1.302(4)	C(10)-C(5)-C(4)	117.8(3)
C(12)-C(13)	1.377(5)	C(7)-C(6)-C(5)	122.8(3)
C(12)-C(16)	1.500(5)	C(7)-C(6)-Cl(1)	115.7(2)
C(13)-C(14)	1.414(5)	C(5)-C(6)-Cl(1)	121.4(2)
C(14)-O(15)	1.262(4)	C(6)-C(7)-C(8)	120.1(3)
C(14)-C(17)	1.495(5)	C(9)-C(8)-C(7)	120.2(3)
O(18)-C(19)	1.304(4)	C(8)-C(9)-C(10)	118.7(3)
C(19)-C(20)	1.375(5)	C(9)-C(10)-C(5)	124.2(3)
C(19)-C(23)	1.502(5)	C(9)-C(10)-Cl(2)	115.8(2)
C(20)-C(21)	1.397(5)	C(5)-C(10)-Cl(2)	120.0(2)
C(21)-O(22)	1.274(4)	C(12)-O(11)-W(1)	126.7(2)
C(21)-C(24)	1.500(5)	O(11)-C(12)-C(13)	127.1(3)
		O(11)-C(12)-C(16)	113.5(3)
O(3)-W(1)-C(2)	110.36(12)	C(13)-C(12)-C(16)	119.4(3)
O(3)-W(1)-O(22)	92.26(9)	C(12)-C(13)-C(14)	126.5(3)
C(2)-W(1)-O(22)	92.81(12)	O(15)-C(14)-C(13)	124.5(3)
O(3)-W(1)-O(18)	163.44(10)	O(15)-C(14)-C(17)	117.4(3)
C(2)-W(1)-O(18)	85.72(11)	C(13)-C(14)-C(17)	118.1(3)
O(22)-W(1)-O(18)	82.71(10)	C(14)-O(15)-W(1)	126.7(2)
O(3)-W(1)-O(11)	98.02(9)	C(19)-O(18)-W(1)	131.0(2)
C(2)-W(1)-O(11)	93.58(11)	O(18)-C(19)-C(20)	122.9(3)
O(22)-W(1)-O(11)	165.18(10)	O(18)-C(19)-C(23)	113.1(3)
O(18)-W(1)-O(11)	84.45(10)	C(20)-C(19)-C(23)	124.0(3)

C(19)-C(20)-C(21)	125.1(3)
O(22)-C(21)-C(20)	122.0(3)
O(22)-C(21)-C(24)	116.3(3)
C(20)-C(21)-C(24)	121.6(3)
C(21)-O(22)-W(1)	132.7(2)

Appendix H

Bond lengths [Å] and angles [°] for W(CO)(acac)$_2$(η^2-acetone) (Chapter 3, **5**).

W(1)-C(5)	1.922(8)	O(7)-W(1)-O(11)	87.4(2)
W(1)-O(1)	1.934(5)	C(5)-W(1)-C(2)	68.2(3)
W(1)-O(18)	2.018(5)	O(1)-W(1)-C(2)	38.2(3)
W(1)-O(14)	2.039(6)	O(18)-W(1)-C(2)	99.2(3)
W(1)-O(7)	2.063(5)	O(14)-W(1)-C(2)	157.3(3)
W(1)-O(11)	2.161(6)	O(7)-W(1)-C(2)	94.6(3)
W(1)-C(2)	2.211(8)	O(11)-W(1)-C(2)	121.0(3)
O(1)-C(2)	1.380(10)	C(2)-O(1)-W(1)	81.9(4)
C(2)-C(3)	1.514(11)	O(1)-C(2)-C(3)	116.6(7)
C(2)-C(4)	1.515(11)	O(1)-C(2)-C(4)	115.8(7)
C(5)-O(6)	1.164(10)	C(3)-C(2)-C(4)	114.7(7)
O(7)-C(8)	1.312(9)	O(1)-C(2)-W(1)	60.0(4)
C(8)-C(9)	1.376(11)	C(3)-C(2)-W(1)	119.5(6)
C(8)-C(12)	1.503(11)	C(4)-C(2)-W(1)	119.1(6)
C(9)-C(10)	1.416(11)	O(6)-C(5)-W(1)	174.7(8)
C(10)-O(11)	1.253(10)	C(8)-O(7)-W(1)	127.0(5)
C(10)-C(13)	1.495(11)	O(7)-C(8)-C(9)	125.6(8)
O(14)-C(15)	1.294(9)	O(7)-C(8)-C(12)	112.3(7)
C(15)-C(16)	1.385(11)	C(9)-C(8)-C(12)	122.0(7)
C(15)-C(19)	1.500(11)	C(8)-C(9)-C(10)	128.8(8)
C(16)-C(17)	1.391(11)	O(11)-C(10)-C(9)	123.5(8)
C(17)-O(18)	1.284(10)	O(11)-C(10)-C(13)	118.2(7)
C(17)-C(20)	1.515(11)	C(9)-C(10)-C(13)	118.3(8)
		C(10)-O(11)-W(1)	127.7(5)
C(5)-W(1)-O(1)	106.4(3)	C(15)-O(14)-W(1)	131.7(5)
C(5)-W(1)-O(18)	97.1(3)	O(14)-C(15)-C(16)	124.1(7)
O(1)-W(1)-O(18)	94.1(2)	O(14)-C(15)-C(19)	114.2(7)
C(5)-W(1)-O(14)	89.1(3)	C(16)-C(15)-C(19)	121.7(7)
O(1)-W(1)-O(14)	164.5(2)	C(15)-C(16)-C(17)	123.6(8)
O(18)-W(1)-O(14)	83.3(2)	O(18)-C(17)-C(16)	123.4(7)
C(5)-W(1)-O(7)	89.9(3)	O(18)-C(17)-C(20)	115.8(7)
O(1)-W(1)-O(7)	95.6(2)	C(16)-C(17)-C(20)	120.8(7)
O(18)-W(1)-O(7)	166.0(2)	C(17)-O(18)-W(1)	132.9(5)
O(14)-W(1)-O(7)	84.7(2)		
C(5)-W(1)-O(11)	170.6(3)		
O(1)-W(1)-O(11)	82.9(2)		
O(18)-W(1)-O(11)	83.8(2)		
O(14)-W(1)-O(11)	81.7(2)		

Appendix I

Bond lengths [Å] and angles [°] for $W(CO)(acac)_2(CN^tBu)_2$ (Chapter 3, **6**).

W(1)-C(1)	1.9432(16)	C(3)-W(1)-O(15)	72.46(5)
W(1)-C(9)	2.0487(15)	O(26)-W(1)-O(15)	153.73(4)
W(1)-C(3)	2.0866(16)	O(22)-W(1)-O(15)	74.61(4)
W(1)-O(26)	2.1298(11)	C(1)-W(1)-O(19)	170.36(5)
W(1)-O(22)	2.1304(11)	C(9)-W(1)-O(19)	113.15(5)
W(1)-O(15)	2.1371(10)	C(3)-W(1)-O(19)	83.32(5)
W(1)-O(19)	2.1632(11)	O(26)-W(1)-O(19)	79.48(4)
C(1)-O(2)	1.1786(19)	O(22)-W(1)-O(19)	78.94(4)
C(3)-N(4)	1.166(2)	O(15)-W(1)-O(19)	87.39(4)
N(4)-C(5)	1.463(2)	O(2)-C(1)-W(1)	178.14(14)
C(5)-C(7)	1.518(3)	N(4)-C(3)-W(1)	172.99(13)
C(5)-C(8)	1.526(2)	C(3)-N(4)-C(5)	163.74(16)
C(5)-C(6)	1.534(3)	N(4)-C(5)-C(7)	106.80(15)
C(9)-N(10)	1.1904(19)	N(4)-C(5)-C(8)	109.31(13)
N(10)-C(11)	1.478(2)	C(7)-C(5)-C(8)	111.75(18)
C(11)-C(12)	1.525(2)	N(4)-C(5)-C(6)	107.23(14)
C(11)-C(13)	1.530(3)	C(7)-C(5)-C(6)	112.14(19)
C(11)-C(14)	1.530(2)	C(8)-C(5)-C(6)	109.44(16)
O(15)-C(16)	1.2890(18)	N(10)-C(9)-W(1)	175.28(13)
C(16)-C(17)	1.399(2)	C(9)-N(10)-C(11)	142.18(15)
C(16)-C(20)	1.515(2)	N(10)-C(11)-C(12)	108.60(13)
C(17)-C(18)	1.418(2)	N(10)-C(11)-C(13)	106.21(14)
C(18)-O(19)	1.2746(18)	C(12)-C(11)-C(13)	110.77(16)
C(18)-C(21)	1.509(2)	N(10)-C(11)-C(14)	109.08(13)
O(22)-C(23)	1.283(2)	C(12)-C(11)-C(14)	111.31(15)
C(23)-C(24)	1.395(2)	C(13)-C(11)-C(14)	110.70(16)
C(23)-C(27)	1.511(2)	C(16)-O(15)-W(1)	125.42(10)
C(24)-C(25)	1.402(2)	O(15)-C(16)-C(17)	127.56(14)
C(25)-O(26)	1.2732(19)	O(15)-C(16)-C(20)	113.48(14)
C(25)-C(28)	1.509(2)	C(17)-C(16)-C(20)	118.96(14)
		C(16)-C(17)-C(18)	127.46(14)
C(1)-W(1)-C(9)	75.97(6)	O(19)-C(18)-C(17)	124.95(14)
C(1)-W(1)-C(3)	103.15(6)	O(19)-C(18)-C(21)	116.12(14)
C(9)-W(1)-C(3)	71.63(6)	C(17)-C(18)-C(21)	118.93(14)
C(1)-W(1)-O(26)	101.54(5)	C(18)-O(19)-W(1)	127.14(10)
C(9)-W(1)-O(26)	70.63(5)	C(23)-O(22)-W(1)	132.01(10)
C(3)-W(1)-O(26)	127.54(5)	O(22)-C(23)-C(24)	125.22(14)
C(1)-W(1)-O(22)	91.73(5)	O(22)-C(23)-C(27)	115.26(15)
C(9)-W(1)-O(22)	145.28(5)	C(24)-C(23)-C(27)	119.47(15)
C(3)-W(1)-O(22)	143.08(5)	C(23)-C(24)-C(25)	122.65(15)
O(26)-W(1)-O(22)	80.56(4)	O(26)-C(25)-C(24)	125.45(14)
C(1)-W(1)-O(15)	87.80(5)	O(26)-C(25)-C(28)	114.42(14)
C(9)-W(1)-O(15)	135.64(5)	C(24)-C(25)-C(28)	120.04(15)

C(25)-O(26)-W(1)	132.23(10)

Appendix J

Bond lengths [Å] and angles [°] for [W(CO)(acac)$_2$(η^2-MeN=CPh)][OTf] (Chapter 4, **2a**).

		C(1)-W(1)-O(12)	94.3(3)
W(1)-C(1)	1.994(9)	C(1)-W(1)-O(16)	163.3(3)
W(1)-N(4)	1.977(7)	C(1)-W(1)-O(19)	82.4(3)
W(1)-C(5)	2.069(8)	C(1)-W(1)-O(23)	92.7(3)
W(1)-O(12)	2.038(5)	N(4)-W(1)-C(5)	36.9(3)
W(1)-O(16)	2.101(5)	N(4)-W(1)-O(12)	92.64(22)
W(1)-O(19)	2.039(5)	N(4)-W(1)-O(16)	85.08(23)
W(1)-O(23)	2.020(5)	N(4)-W(1)-O(19)	165.84(24)
C(1)-O(2)	1.148(11)	N(4)-W(1)-O(23)	98.69(22)
C(3)-N(4)	1.452(10)	C(5)-W(1)-O(12)	96.39(25)
N(4)-C(5)	1.283(10)	C(5)-W(1)-O(16)	121.8(3)
C(5)-C(6)	1.444(11)	C(5)-W(1)-O(19)	156.6(3)
C(6)-C(7)	1.404(10)	C(5)-W(1)-O(23)	99.86(24)
C(6)-C(11)	1.385(11)	O(12)-W(1)-O(16)	88.19(20)
C(7)-C(8)	1.378(10)	O(12)-W(1)-O(19)	82.38(20)
C(8)-C(9)	1.392(11)	O(12)-W(1)-O(23)	163.53(20)
C(9)-C(10)	1.357(12)	O(16)-W(1)-O(19)	81.54(21)
C(10)-C(11)	1.392(11)	O(16)-W(1)-O(23)	80.95(20)
O(12)-C(13)	1.316(10)	O(19)-W(1)-O(23)	83.79(20)
C(13)-C(14)	1.383(12)	W(1)-C(1)-O(2)	176.8(7)
C(13)-C(17)	1.486(12)	C(21)-C(22)-O(23)	123.0(7)
C(14)-C(15)	1.413(12)	C(21)-C(22)-C(25)	120.6(7)
C(15)-O(16)	1.297(10)	O(23)-C(22)-C(25)	116.4(7)
C(15)-C(18)	1.498(12)	W(1)-O(23)-C(22)	132.6(5)
O(19)-C(20)	1.275(10)	W(1)-N(4)-C(3)	148.7(5)
C(20)-C(21)	1.388(12)	W(1)-N(4)-C(5)	75.4(5)
C(20)-C(24)	1.494(12)	C(3)-N(4)-C(5)	135.9(7)
C(21)-C(22)	1.410(11)	W(1)-C(5)-N(4)	67.7(4)
C(22)-O(23)	1.272(9)	W(1)-C(5)-C(6)	160.2(6)
C(22)-C(25)	1.496(11)	N(4)-C(5)-C(6)	132.1(7)
S(1)-C(26)	1.817(10)	C(5)-C(6)-C(7)	119.9(7)
S(1)-O(30)	1.440(6)	C(5)-C(6)-C(11)	120.3(7)
S(1)-O(31)	1.439(7)	C(7)-C(6)-C(11)	119.6(7)
S(1)-O(32)	1.411(6)	C(6)-C(7)-C(8)	118.9(7)
C(26)-F(27)	1.295(11)	C(26)-S(1)-O(30)	103.6(4)
C(26)-F(28)	1.353(12)	C(26)-S(1)-O(31)	103.0(4)
C(26)-F(29)	1.287(12)	C(7)-C(8)-C(9)	121.1(7)
F(27)-F(28)	2.099(10)	O(30)-S(1)-O(31)	112.7(4)
F(27)-F(29)	2.138(10)	O(30)-S(1)-O(32)	115.2(4)
F(28)-F(29)	2.109(11)	C(8)-C(9)-C(10)	119.6(7)
		S(1)-C(26)-F(27)	112.3(7)
C(1)-W(1)-N(4)	111.2(3)	S(1)-C(26)-F(28)	108.8(7)
C(1)-W(1)-C(5)	74.4(3)	C(9)-C(10)-C(11)	120.6(7)

F(27)-C(26)-F(28)	104.8(8)	S(1)-C(26)-F(29)	112.5(6)
F(27)-C(26)-F(29)	111.8(9)	F(28)-C(26)-F(29)	106.0(9)
C(6)-C(11)-C(10)	120.0(7)	F(28)-F(27)-F(29)	59.7(4)
C(26)-F(27)-F(28)	38.5(5)	C(26)-F(28)-F(27)	36.6(5)
C(26)-F(27)-F(29)	34.0(5)	C(26)-F(28)-F(29)	35.9(5)
W(1)-O(12)-C(13)	125.9(5)	F(27)-F(28)-F(29)	61.1(4)
O(12)-C(13)-C(14)	127.5(8)	C(26)-F(29)-F(27)	34.2(5)
O(12)-C(13)-C(17)	113.6(7)		
C(14)-C(13)-C(17)	118.9(8)		
C(13)-C(14)-C(15)	125.5(8)		
C(26)-F(29)-F(28)	38.1(5)		
F(27)-F(29)-F(28)	59.2(3)		
C(14)-C(15)-O(16)	124.1(7)		
C(14)-C(15)-C(18)	120.5(7)		
O(16)-C(15)-C(18)	115.4(7)		
W(1)-O(16)-C(15)	127.6(5)		
W(1)-O(19)-C(20)	131.4(5)		
O(19)-C(20)-C(21)	124.0(7)		
O(19)-C(20)-C(24)	115.5(7)		
C(21)-C(20)-C(24)	120.4(7)		
C(20)-C(21)-C(22)	123.8(7)		
C(26)-S(1)-O(32)	105.7(4)		
O(31)-S(1)-O(32)	114.8(5)		

Appendix K

Bond lengths [Å] and angles [°] for W(CO)(acac)$_2$(η^2-MeN=CMePh) (Chapter 4, **4**).

W(1)-N(2)	1.9050(15)	O(13)-W(1)-O(20)	85.47(5)
W(1)-C(11)	1.922(2)	O(17)-W(1)-O(20)	82.54(5)
W(1)-O(13)	2.0621(13)	O(24)-W(1)-O(20)	85.69(5)
W(1)-O(17)	2.0636(13)	N(2)-W(1)-C(3)	37.36(6)
W(1)-O(24)	2.0821(12)	C(11)-W(1)-C(3)	66.74(7)
W(1)-O(20)	2.1659(13)	O(13)-W(1)-C(3)	92.93(6)
W(1)-C(3)	2.274(2)	O(17)-W(1)-C(3)	155.53(6)
C(1)-N(2)	1.460(2)	O(24)-W(1)-C(3)	100.56(6)
N(2)-C(3)	1.383(2)	O(20)-W(1)-C(3)	121.31(6)
C(3)-C(5)	1.500(3)	C(3)-N(2)-C(1)	126.41(16)
C(3)-C(4)	1.515(2)	C(3)-N(2)-W(1)	85.94(11)
C(5)-C(10)	1.389(3)	C(1)-N(2)-W(1)	143.59(14)
C(5)-C(6)	1.388(2)	N(2)-C(3)-C(5)	115.68(16)
C(6)-C(7)	1.377(3)	N(2)-C(3)-C(4)	118.22(17)
C(7)-C(8)	1.383(3)	C(5)-C(3)-C(4)	116.48(17)
C(8)-C(9)	1.366(3)	N(2)-C(3)-W(1)	56.70(9)
C(9)-C(10)	1.399(3)	C(5)-C(3)-W(1)	119.41(13)
C(11)-O(12)	1.183(2)	C(4)-C(3)-W(1)	117.02(13)
O(13)-C(14)	1.276(2)	C(10)-C(5)-C(6)	118.00(19)
C(14)-C(15)	1.389(3)	C(10)-C(5)-C(3)	121.79(17)
C(14)-C(18)	1.486(2)	C(6)-C(5)-C(3)	120.16(18)
C(15)-C(16)	1.387(3)	C(7)-C(6)-C(5)	121.22(19)
C(16)-O(17)	1.298(2)	C(6)-C(7)-C(8)	120.13(19)
C(16)-C(19)	1.500(3)	C(9)-C(8)-C(7)	119.9(2)
O(20)-C(21)	1.274(2)	C(8)-C(9)-C(10)	119.98(19)
C(21)-C(22)	1.390(3)	C(5)-C(10)-C(9)	120.71(19)
C(21)-C(25)	1.506(3)	O(12)-C(11)-W(1)	177.80(17)
C(22)-C(23)	1.381(3)	C(14)-O(13)-W(1)	132.32(12)
C(23)-O(24)	1.293(2)	O(13)-C(14)-C(15)	123.27(18)
C(23)-C(26)	1.498(3)	O(13)-C(14)-C(18)	115.41(18)
		C(15)-C(14)-C(18)	121.30(18)
N(2)-W(1)-C(11)	104.10(7)	C(16)-C(15)-C(14)	124.68(18)
N(2)-W(1)-O(13)	91.16(6)	O(17)-C(16)-C(15)	123.99(18)
C(11)-W(1)-O(13)	93.34(7)	O(17)-C(16)-C(19)	114.37(18)
N(2)-W(1)-O(17)	165.66(6)	C(15)-C(16)-C(19)	121.61(18)
C(11)-W(1)-O(17)	89.35(7)	C(16)-O(17)-W(1)	130.34(12)
O(13)-W(1)-O(17)	82.98(5)	C(21)-O(20)-W(1)	125.70(14)
N(2)-W(1)-O(24)	98.23(6)	O(20)-C(21)-C(22)	125.2(2)
C(11)-W(1)-O(24)	93.95(7)	O(20)-C(21)-C(25)	115.5(2)
O(13)-W(1)-O(24)	166.34(5)	C(22)-C(21)-C(25)	119.33(19)
O(17)-W(1)-O(24)	85.57(5)	C(23)-C(22)-C(21)	126.47(19)
N(2)-W(1)-O(20)	83.96(6)	O(24)-C(23)-C(22)	126.8(2)
C(11)-W(1)-O(20)	171.88(6)	O(24)-C(23)-C(26)	112.36(19)

C(22)-C(23)-C(26)	120.80(19)
C(23)-O(24)-W(1)	126.19(13)

Appendix L

Bond lengths [Å] and angles [°] for [W(2,6-dimethylphenylisonitrile)(acac)$_2$(η^2-MeN=CMe)][BAr$_4$′] (Chapter 5, **2c**).

W(1)-N(2)	1.963(9)	C(34)-C(35)	1.382(15)
W(1)-O(19)	2.019(7)	C(35)-C(36)	1.380(14)
W(1)-O(22)	2.020(7)	C(35)-C(38)	1.490(14)
W(1)-C(3)	2.027(11)	C(37)-F(31)	1.319(14)
W(1)-O(15)	2.051(7)	C(37)-F(33)	1.334(13)
W(1)-C(5)	2.064(12)	C(37)-F(32)	1.356(14)
W(1)-O(26)	2.111(7)	C(38)-F(35)	1.324(12)
C(1)-N(2)	1.484(15)	C(38)-F(36)	1.330(12)
N(2)-C(3)	1.323(14)	C(38)-F(34)	1.335(12)
C(3)-C(4)	1.485(14)	C(41)-C(42)	1.384(14)
C(5)-N(6)	1.166(13)	C(41)-C(46)	1.409(14)
N(6)-C(7)	1.407(13)	C(42)-C(43)	1.410(13)
C(7)-C(12)	1.368(16)	C(43)-C(44)	1.376(15)
C(7)-C(8)	1.383(16)	C(43)-C(47)	1.505(15)
C(8)-C(9)	1.382(17)	C(44)-C(45)	1.398(14)
C(8)-C(13)	1.516(19)	C(45)-C(46)	1.401(13)
C(9)-C(10)	1.35(2)	C(45)-C(48)	1.488(15)
C(10)-C(11)	1.37(3)	C(47)-F(43)	1.317(14)
C(11)-C(12)	1.39(2)	C(47)-F(41)	1.322(16)
C(12)-C(14)	1.52(2)	C(47)-F(42)	1.327(16)
O(15)-C(16)	1.298(12)	C(48)-F(44)	1.285(14)
C(16)-C(17)	1.356(17)	C(48)-F(46)	1.318(13)
C(16)-C(20)	1.488(16)	C(48)-F(45)	1.362(14)
C(17)-C(18)	1.424(18)	C(51)-C(52)	1.390(13)
C(18)-O(19)	1.279(13)	C(51)-C(56)	1.401(14)
C(18)-C(21)	1.520(16)	C(52)-C(53)	1.395(14)
O(22)-C(23)	1.304(11)	C(53)-C(54)	1.362(15)
C(23)-C(24)	1.370(14)	C(53)-C(57)	1.514(16)
C(23)-C(27)	1.497(14)	C(54)-C(55)	1.391(16)
C(24)-C(25)	1.410(15)	C(55)-C(56)	1.407(14)
C(25)-O(26)	1.252(12)	C(55)-C(58)	1.486(17)
C(25)-C(28)	1.506(14)	C(57)-F(52)	1.304(14)
B(30)-C(31)	1.627(14)	C(57)-F(51)	1.341(14)
B(30)-C(51)	1.632(14)	C(57)-F(53)	1.343(14)
B(30)-C(41)	1.639(14)	C(58)-F(55)	1.283(15)
B(30)-C(61)	1.639(14)	C(58)-F(56)	1.311(16)
C(31)-C(32)	1.400(13)	C(58)-F(54)	1.319(17)
C(31)-C(36)	1.409(14)	C(61)-C(66)	1.396(13)
C(32)-C(33)	1.401(13)	C(61)-C(62)	1.403(13)
C(33)-C(34)	1.405(14)	C(62)-C(63)	1.360(13)
C(33)-C(37)	1.476(15)	C(63)-C(64)	1.396(15)
		C(63)-C(67)	1.498(15)

C(64)-C(65)	1.371(14)
C(65)-C(66)	1.365(13)
C(65)-C(68)	1.511(14)
C(67)-F(63)	1.320(12)
C(67)-F(61)	1.335(13)
C(67)-F(62)	1.361(15)
C(68)-F(66)	1.314(12)
C(68)-F(65)	1.320(12)
C(68)-F(64)	1.356(12)
O(71)-C(72)	1.337(17)
O(71)-C(72)#1	1.337(17)
C(72)-C(73)	1.455(18)

N(2)-W(1)-O(19)	95.5(3)
N(2)-W(1)-O(22)	97.5(3)
O(19)-W(1)-O(22)	164.2(3)
N(2)-W(1)-C(3)	38.7(4)
O(19)-W(1)-C(3)	98.1(4)
O(22)-W(1)-C(3)	97.6(4)
N(2)-W(1)-O(15)	164.4(3)
O(19)-W(1)-O(15)	83.2(3)
O(22)-W(1)-O(15)	81.9(3)
C(3)-W(1)-O(15)	156.9(4)
N(2)-W(1)-C(5)	114.4(4)
O(19)-W(1)-C(5)	91.1(3)
O(22)-W(1)-C(5)	91.7(3)
C(3)-W(1)-C(5)	75.7(4)
O(15)-W(1)-C(5)	81.2(3)
N(2)-W(1)-O(26)	81.9(3)
O(19)-W(1)-O(26)	86.0(3)
O(22)-W(1)-O(26)	87.0(3)
C(3)-W(1)-O(26)	120.6(4)
O(15)-W(1)-O(26)	82.5(3)
C(5)-W(1)-O(26)	163.7(3)
C(3)-N(2)-C(1)	135.9(10)
C(3)-N(2)-W(1)	73.3(6)
C(1)-N(2)-W(1)	150.8(9)
N(2)-C(3)-C(4)	131.9(11)
N(2)-C(3)-W(1)	68.1(6)
C(4)-C(3)-W(1)	160.0(9)
N(6)-C(5)-W(1)	178.9(9)
C(5)-N(6)-C(7)	173.2(10)
C(12)-C(7)-C(8)	122.9(11)
C(12)-C(7)-N(6)	118.4(11)
C(8)-C(7)-N(6)	118.7(10)
C(9)-C(8)-C(7)	118.5(13)
C(9)-C(8)-C(13)	121.6(14)
C(7)-C(8)-C(13)	119.8(11)
C(10)-C(9)-C(8)	119.9(16)
C(9)-C(10)-C(11)	120.8(14)
C(10)-C(11)-C(12)	121.4(16)
C(7)-C(12)-C(11)	116.5(16)
C(7)-C(12)-C(14)	120.7(12)
C(11)-C(12)-C(14)	122.8(14)
C(16)-O(15)-W(1)	131.6(7)
O(15)-C(16)-C(17)	124.7(11)
O(15)-C(16)-C(20)	114.8(11)
C(17)-C(16)-C(20)	120.5(11)
C(16)-C(17)-C(18)	123.0(10)
O(19)-C(18)-C(17)	123.6(11)
O(19)-C(18)-C(21)	114.7(12)
C(17)-C(18)-C(21)	121.6(11)
C(18)-O(19)-W(1)	133.2(8)
C(23)-O(22)-W(1)	128.6(6)
O(22)-C(23)-C(24)	124.7(10)
O(22)-C(23)-C(27)	113.9(8)
C(24)-C(23)-C(27)	121.3(9)
C(23)-C(24)-C(25)	127.5(10)
O(26)-C(25)-C(24)	123.5(9)
O(26)-C(25)-C(28)	117.9(10)
C(24)-C(25)-C(28)	118.7(10)
C(25)-O(26)-W(1)	128.4(7)
C(31)-B(30)-C(51)	111.6(8)
C(31)-B(30)-C(41)	111.1(8)
C(51)-B(30)-C(41)	103.6(7)
C(31)-B(30)-C(61)	106.0(7)
C(51)-B(30)-C(61)	110.3(7)
C(41)-B(30)-C(61)	114.4(8)
C(32)-C(31)-C(36)	114.9(9)
C(32)-C(31)-B(30)	123.6(8)
C(36)-C(31)-B(30)	121.2(9)
C(31)-C(32)-C(33)	122.8(9)
C(32)-C(33)-C(34)	119.6(9)
C(32)-C(33)-C(37)	119.3(9)
C(34)-C(33)-C(37)	121.0(10)
C(35)-C(34)-C(33)	118.9(9)
C(36)-C(35)-C(34)	120.1(10)
C(36)-C(35)-C(38)	120.5(10)
C(34)-C(35)-C(38)	119.4(10)
C(35)-C(36)-C(31)	123.6(10)
F(31)-C(37)-F(33)	107.0(10)
F(31)-C(37)-F(32)	105.2(11)
F(33)-C(37)-F(32)	104.2(9)
F(31)-C(37)-C(33)	111.8(10)
F(33)-C(37)-C(33)	115.0(10)

F(32)-C(37)-C(33)	112.8(10)
F(35)-C(38)-F(36)	106.2(8)
F(35)-C(38)-F(34)	106.6(8)
F(36)-C(38)-F(34)	105.3(9)
F(35)-C(38)-C(35)	113.1(9)
F(36)-C(38)-C(35)	112.1(8)
F(34)-C(38)-C(35)	112.8(8)
C(42)-C(41)-C(46)	115.6(9)
C(42)-C(41)-B(30)	123.5(9)
C(46)-C(41)-B(30)	120.6(8)
C(41)-C(42)-C(43)	123.3(10)
C(44)-C(43)-C(42)	120.1(10)
C(44)-C(43)-C(47)	119.0(10)
C(42)-C(43)-C(47)	120.9(10)
C(43)-C(44)-C(45)	118.4(9)
C(44)-C(45)-C(46)	120.6(10)
C(44)-C(45)-C(48)	118.0(9)
C(46)-C(45)-C(48)	121.1(9)
C(45)-C(46)-C(41)	121.9(9)
F(43)-C(47)-F(41)	105.4(12)
F(43)-C(47)-F(42)	105.8(11)
F(41)-C(47)-F(42)	104.7(12)
F(43)-C(47)-C(43)	114.3(11)
F(41)-C(47)-C(43)	113.4(10)
F(42)-C(47)-C(43)	112.5(11)
F(44)-C(48)-F(46)	108.8(10)
F(44)-C(48)-F(45)	103.6(10)
F(46)-C(48)-F(45)	105.5(10)
F(44)-C(48)-C(45)	113.9(11)
F(46)-C(48)-C(45)	113.3(9)
F(45)-C(48)-C(45)	111.0(10)
C(52)-C(51)-C(56)	115.4(9)
C(52)-C(51)-B(30)	121.5(8)
C(56)-C(51)-B(30)	123.1(9)
C(51)-C(52)-C(53)	123.4(9)
C(54)-C(53)-C(52)	119.7(10)
C(54)-C(53)-C(57)	121.2(10)
C(52)-C(53)-C(57)	119.2(10)
C(53)-C(54)-C(55)	119.8(10)
C(54)-C(55)-C(56)	119.5(10)
C(54)-C(55)-C(58)	120.5(11)
C(56)-C(55)-C(58)	119.9(11)
C(51)-C(56)-C(55)	122.1(10)
F(52)-C(57)-F(51)	107.7(10)
F(52)-C(57)-F(53)	108.2(11)
F(51)-C(57)-F(53)	105.6(11)
F(52)-C(57)-C(53)	113.3(11)
F(51)-C(57)-C(53)	110.7(10)
F(53)-C(57)-C(53)	111.1(9)
F(55)-C(58)-F(56)	106.5(12)
F(55)-C(58)-F(54)	103.9(13)
F(56)-C(58)-F(54)	102.2(14)
F(55)-C(58)-C(55)	115.4(13)
F(56)-C(58)-C(55)	114.8(11)
F(54)-C(58)-C(55)	112.7(12)
C(66)-C(61)-C(62)	114.0(8)
C(66)-C(61)-B(30)	128.5(8)
C(62)-C(61)-B(30)	117.5(8)
C(63)-C(62)-C(61)	123.8(10)
C(62)-C(63)-C(64)	120.4(9)
C(62)-C(63)-C(67)	119.5(10)
C(64)-C(63)-C(67)	120.1(9)
C(65)-C(64)-C(63)	117.0(9)
C(66)-C(65)-C(64)	122.1(10)
C(66)-C(65)-C(68)	119.7(9)
C(64)-C(65)-C(68)	118.2(9)
C(65)-C(66)-C(61)	122.7(9)
F(63)-C(67)-F(61)	107.4(9)
F(63)-C(67)-F(62)	106.3(10)
F(61)-C(67)-F(62)	104.1(10)
F(63)-C(67)-C(63)	115.4(10)
F(61)-C(67)-C(63)	112.1(9)
F(62)-C(67)-C(63)	110.8(10)
F(66)-C(68)-F(65)	107.3(9)
F(66)-C(68)-F(64)	106.1(9)
F(65)-C(68)-F(64)	105.3(8)
F(66)-C(68)-C(65)	113.0(8)
F(65)-C(68)-C(65)	113.5(9)
F(64)-C(68)-C(65)	111.1(9)
C(72)-O(71)-C(72)#1	180.000(5)
O(71)-C(72)-C(73)	124(2)

Symmetry transformations used to generate equivalent atoms: #1 -x,-y+2,-z+1

Appendix M

Bond lengths [Å] and angles [°] for $[W(PCy_3)(acac)_2(\eta^2\text{-MeN=CPh})][BAr_4']$ (Chapter 5, **3b**).

W(1)-N(2)	1.957(3)	C(37)-C(38)	1.537(5)
W(1)-C(3)	1.990(4)	C(38)-C(39)	1.520(6)
W(1)-O(17)	2.043(2)	C(39)-C(40)	1.522(6)
W(1)-O(14)	2.046(3)	C(40)-C(41)	1.526(5)
W(1)-O(21)	2.086(2)	B(50)-C(71)	1.636(5)
W(1)-O(10)	2.107(2)	B(50)-C(61)	1.643(5)
W(1)-P(1)	2.5707(9)	B(50)-C(81)	1.644(5)
P(1)-C(30)	1.855(3)	B(50)-C(51)	1.646(5)
P(1)-C(24)	1.856(3)	C(51)-C(52)	1.399(5)
P(1)-C(36)	1.859(4)	C(51)-C(56)	1.402(5)
C(1)-N(2)	1.453(5)	C(52)-C(53)	1.390(5)
N(2)-C(3)	1.324(5)	C(53)-C(54)	1.382(5)
C(3)-C(4)	1.445(5)	C(53)-C(57)	1.497(5)
C(4)-C(5)	1.403(5)	C(54)-C(55)	1.393(5)
C(4)-C(9)	1.404(5)	C(55)-C(56)	1.387(5)
C(5)-C(6)	1.391(6)	C(55)-C(58)	1.500(5)
C(6)-C(7)	1.376(6)	C(57)-F(52)	1.306(5)
C(7)-C(8)	1.379(6)	C(57)-F(53)	1.319(5)
C(8)-C(9)	1.389(5)	C(57)-F(51)	1.354(5)
O(10)-C(11)	1.280(5)	C(58)-F(57)	1.254(7)
C(11)-C(12)	1.402(6)	C(58)-F(56)	1.307(7)
C(11)-C(15)	1.496(6)	C(58)-F(59)	1.307(7)
C(12)-C(13)	1.377(6)	C(58)-F(55)	1.340(7)
C(13)-O(14)	1.300(4)	C(58)-F(58)	1.350(7)
C(13)-C(16)	1.500(6)	C(58)-F(54)	1.377(7)
O(17)-C(18)	1.300(4)	C(61)-C(66)	1.394(5)
C(18)-C(19)	1.371(5)	C(61)-C(62)	1.407(5)
C(18)-C(22)	1.500(5)	C(62)-C(63)	1.391(5)
C(19)-C(20)	1.404(5)	C(63)-C(64)	1.389(5)
C(20)-O(21)	1.275(5)	C(63)-C(67)	1.498(5)
C(20)-C(23)	1.510(5)	C(64)-C(65)	1.373(6)
C(24)-C(25)	1.538(5)	C(65)-C(66)	1.398(5)
C(24)-C(29)	1.541(5)	C(65)-C(68)	1.490(6)
C(25)-C(26)	1.528(5)	C(67)-F(63)	1.335(4)
C(26)-C(27)	1.520(6)	C(67)-F(61)	1.344(5)
C(27)-C(28)	1.521(6)	C(67)-F(62)	1.345(5)
C(28)-C(29)	1.534(5)	C(68)-F(64)	1.265(9)
C(30)-C(35)	1.539(5)	C(68)-F(68)	1.278(9)
C(30)-C(31)	1.542(5)	C(68)-F(69)	1.307(9)
C(31)-C(32)	1.531(5)	C(68)-F(65)	1.330(9)
C(32)-C(33)	1.522(6)	C(68)-F(66)	1.401(9)
C(33)-C(34)	1.522(5)	C(68)-F(67)	1.417(10)
C(34)-C(35)	1.532(5)	C(71)-C(76)	1.399(5)
C(36)-C(37)	1.537(5)	C(71)-C(72)	1.405(5)
C(36)-C(41)	1.539(5)	C(72)-C(73)	1.394(5)

C(73)-C(74)	1.391(5)
C(73)-C(77)	1.491(5)
C(74)-C(75)	1.388(5)
C(75)-C(76)	1.386(5)
C(75)-C(78)	1.497(5)
C(77)-F(72)	1.329(5)
C(77)-F(73)	1.339(5)
C(77)-F(71)	1.347(5)
C(78)-F(74)	1.322(5)
C(78)-F(75)	1.324(5)
C(78)-F(76)	1.348(5)
C(81)-C(86)	1.390(5)
C(81)-C(82)	1.403(5)
C(82)-C(83)	1.391(5)
C(83)-C(84)	1.387(5)
C(83)-C(87)	1.501(5)
C(84)-C(85)	1.384(5)
C(85)-C(86)	1.393(5)
C(85)-C(88)	1.496(5)
C(87)-F(82)	1.291(6)
C(87)-F(81)	1.325(5)
C(87)-F(83)	1.330(5)
C(88)-F(85)	1.330(4)
C(88)-F(84)	1.337(4)
C(88)-F(86)	1.339(5)
F(54)-F(59)	1.280(8)
F(54)-F(57)	1.292(9)
F(55)-F(57)	0.917(8)
F(55)-F(58)	1.526(9)
F(56)-F(58)	1.034(8)
F(56)-F(59)	1.275(9)
F(64)-F(69)	0.803(11)
F(64)-F(67)	1.485(12)
F(65)-F(67)	1.114(10)
F(65)-F(68)	1.135(11)
F(66)-F(68)	1.083(11)
F(66)-F(69)	1.717(11)
C(91)-C(92)	1.481(8)
C(92)-O(93)	1.420(6)
O(93)-C(94)	1.414(5)
C(94)-C(95)	1.498(7)

N(2)-W(1)-C(3)	39.18(13)
N(2)-W(1)-O(17)	153.91(11)
C(3)-W(1)-O(17)	163.28(12)
N(2)-W(1)-O(14)	106.66(11)
C(3)-W(1)-O(14)	102.02(12)
O(17)-W(1)-O(14)	83.90(10)
N(2)-W(1)-O(21)	122.84(11)
C(3)-W(1)-O(21)	83.71(12)
O(17)-W(1)-O(21)	82.37(10)
O(14)-W(1)-O(21)	77.32(10)
N(2)-W(1)-O(10)	78.14(11)
C(3)-W(1)-O(10)	116.71(12)
O(17)-W(1)-O(10)	79.11(10)
O(14)-W(1)-O(10)	85.16(10)
O(21)-W(1)-O(10)	155.71(10)
N(2)-W(1)-P(1)	89.31(9)
C(3)-W(1)-P(1)	91.43(10)
O(17)-W(1)-P(1)	80.81(7)
O(14)-W(1)-P(1)	163.94(7)
O(21)-W(1)-P(1)	95.72(7)
O(10)-W(1)-P(1)	96.69(7)
C(30)-P(1)-C(24)	102.29(16)
C(30)-P(1)-C(36)	111.14(16)
C(24)-P(1)-C(36)	103.85(17)
C(30)-P(1)-W(1)	113.16(13)
C(24)-P(1)-W(1)	111.33(12)
C(36)-P(1)-W(1)	114.05(12)
C(3)-N(2)-C(1)	136.5(3)
C(3)-N(2)-W(1)	71.8(2)
C(1)-N(2)-W(1)	149.5(3)
N(2)-C(3)-C(4)	131.4(3)
N(2)-C(3)-W(1)	69.1(2)
C(4)-C(3)-W(1)	159.3(3)
C(5)-C(4)-C(9)	119.3(3)
C(5)-C(4)-C(3)	121.7(3)
C(9)-C(4)-C(3)	119.0(3)
C(6)-C(5)-C(4)	119.8(4)
C(7)-C(6)-C(5)	120.2(4)
C(6)-C(7)-C(8)	120.8(4)
C(7)-C(8)-C(9)	120.1(4)
C(8)-C(9)-C(4)	119.9(4)
C(11)-O(10)-W(1)	127.0(3)
O(10)-C(11)-C(12)	125.0(4)
O(10)-C(11)-C(15)	115.7(4)
C(12)-C(11)-C(15)	119.3(4)
C(13)-C(12)-C(11)	125.2(4)
O(14)-C(13)-C(12)	124.7(4)
O(14)-C(13)-C(16)	113.9(3)
C(12)-C(13)-C(16)	121.5(4)
C(13)-O(14)-W(1)	128.4(2)
C(18)-O(17)-W(1)	132.6(2)
O(17)-C(18)-C(19)	123.1(3)
O(17)-C(18)-C(22)	114.2(3)
C(19)-C(18)-C(22)	122.7(4)
C(18)-C(19)-C(20)	123.7(4)
O(21)-C(20)-C(19)	124.7(4)
O(21)-C(20)-C(23)	115.7(3)

C(19)-C(20)-C(23)	119.5(4)	F(57)-C(58)-F(56)	127.8(5)
C(20)-O(21)-W(1)	128.2(2)	F(57)-C(58)-F(59)	110.9(5)
C(25)-C(24)-C(29)	110.8(3)	F(56)-C(58)-F(59)	58.4(4)
C(25)-C(24)-P(1)	112.2(3)	F(57)-C(58)-F(55)	41.3(4)
C(29)-C(24)-P(1)	111.6(2)	F(56)-C(58)-F(55)	106.0(5)
C(26)-C(25)-C(24)	111.5(3)	F(59)-C(58)-F(55)	134.6(4)
C(27)-C(26)-C(25)	112.2(3)	F(57)-C(58)-F(58)	107.5(6)
C(26)-C(27)-C(28)	110.5(3)	F(56)-C(58)-F(58)	45.8(4)
C(27)-C(28)-C(29)	110.7(3)	F(59)-C(58)-F(58)	103.6(5)
C(28)-C(29)-C(24)	110.6(3)	F(55)-C(58)-F(58)	69.1(5)
C(35)-C(30)-C(31)	108.7(3)	F(57)-C(58)-F(54)	58.6(5)
C(35)-C(30)-P(1)	116.8(3)	F(56)-C(58)-F(54)	107.8(5)
C(31)-C(30)-P(1)	115.5(2)	F(59)-C(58)-F(54)	56.9(4)
C(32)-C(31)-C(30)	109.9(3)	F(55)-C(58)-F(54)	97.5(5)
C(33)-C(32)-C(31)	111.2(3)	F(58)-C(58)-F(54)	137.9(4)
C(32)-C(33)-C(34)	111.1(3)	F(57)-C(58)-C(55)	114.1(4)
C(33)-C(34)-C(35)	111.2(3)	F(56)-C(58)-C(55)	117.3(4)
C(34)-C(35)-C(30)	110.0(3)	F(59)-C(58)-C(55)	110.5(4)
C(37)-C(36)-C(41)	109.6(3)	F(55)-C(58)-C(55)	114.1(4)
C(37)-C(36)-P(1)	113.2(3)	F(58)-C(58)-C(55)	109.7(4)
C(41)-C(36)-P(1)	117.2(3)	F(54)-C(58)-C(55)	112.1(4)
C(38)-C(37)-C(36)	109.7(3)	C(66)-C(61)-C(62)	115.5(3)
C(39)-C(38)-C(37)	111.0(3)	C(66)-C(61)-B(50)	123.8(3)
C(38)-C(39)-C(40)	111.1(3)	C(62)-C(61)-B(50)	120.6(3)
C(39)-C(40)-C(41)	112.8(4)	C(63)-C(62)-C(61)	122.2(3)
C(40)-C(41)-C(36)	110.0(3)	C(64)-C(63)-C(62)	120.8(3)
C(71)-B(50)-C(61)	112.9(3)	C(64)-C(63)-C(67)	120.9(3)
C(71)-B(50)-C(81)	110.5(3)	C(62)-C(63)-C(67)	118.3(3)
C(61)-B(50)-C(81)	105.5(3)	C(65)-C(64)-C(63)	118.0(3)
C(71)-B(50)-C(51)	104.5(3)	C(64)-C(65)-C(66)	121.2(4)
C(61)-B(50)-C(51)	111.9(3)	C(64)-C(65)-C(68)	119.1(4)
C(81)-B(50)-C(51)	111.7(3)	C(66)-C(65)-C(68)	119.7(4)
C(52)-C(51)-C(56)	115.8(3)	C(61)-C(66)-C(65)	122.2(4)
C(52)-C(51)-B(50)	123.6(3)	F(63)-C(67)-F(61)	106.7(3)
C(56)-C(51)-B(50)	120.4(3)	F(63)-C(67)-F(62)	105.9(3)
C(53)-C(52)-C(51)	122.1(3)	F(61)-C(67)-F(62)	105.9(3)
C(54)-C(53)-C(52)	121.1(3)	F(63)-C(67)-C(63)	113.1(3)
C(54)-C(53)-C(57)	120.4(3)	F(61)-C(67)-C(63)	112.7(3)
C(52)-C(53)-C(57)	118.4(3)	F(62)-C(67)-C(63)	111.9(3)
C(53)-C(54)-C(55)	118.0(3)	F(64)-C(68)-F(68)	125.2(6)
C(56)-C(55)-C(54)	120.7(3)	F(64)-C(68)-F(69)	36.4(5)
C(56)-C(55)-C(58)	119.6(3)	F(68)-C(68)-F(69)	113.1(7)
C(54)-C(55)-C(58)	119.7(3)	F(64)-C(68)-F(65)	106.0(7)
C(55)-C(56)-C(51)	122.3(3)	F(68)-C(68)-F(65)	51.5(6)
F(52)-C(57)-F(53)	109.5(4)	F(69)-C(68)-F(65)	128.9(6)
F(52)-C(57)-F(51)	105.1(4)	F(64)-C(68)-F(66)	110.6(7)
F(53)-C(57)-F(51)	103.2(4)	F(68)-C(68)-F(66)	47.4(5)
F(52)-C(57)-C(53)	113.7(4)	F(69)-C(68)-F(66)	78.6(6)
F(53)-C(57)-C(53)	113.7(3)	F(65)-C(68)-F(66)	98.3(6)
F(51)-C(57)-C(53)	110.9(3)	F(64)-C(68)-F(67)	67.0(6)

F(68)-C(68)-F(67)	96.9(7)	F(82)-C(87)-C(83)	113.0(4)
F(69)-C(68)-F(67)	102.0(6)	F(81)-C(87)-C(83)	112.1(3)
F(65)-C(68)-F(67)	47.7(5)	F(83)-C(87)-C(83)	112.5(4)
F(66)-C(68)-F(67)	137.2(6)	F(85)-C(88)-F(84)	106.2(3)
F(64)-C(68)-C(65)	116.9(6)	F(85)-C(88)-F(86)	106.2(3)
F(68)-C(68)-C(65)	117.9(5)	F(84)-C(88)-F(86)	105.3(3)
F(69)-C(68)-C(65)	114.9(6)	F(85)-C(88)-C(85)	113.2(3)
F(65)-C(68)-C(65)	114.1(5)	F(84)-C(88)-C(85)	113.1(3)
F(66)-C(68)-C(65)	109.4(5)	F(86)-C(88)-C(85)	112.2(3)
F(67)-C(68)-C(65)	108.8(5)	F(59)-F(54)-F(57)	110.2(6)
C(76)-C(71)-C(72)	115.1(3)	F(59)-F(54)-C(58)	58.8(4)
C(76)-C(71)-B(50)	122.2(3)	F(57)-F(54)-C(58)	55.9(4)
C(72)-C(71)-B(50)	122.6(3)	F(57)-F(55)-C(58)	64.3(6)
C(73)-C(72)-C(71)	122.5(3)	F(57)-F(55)-F(58)	116.4(8)
C(74)-C(73)-C(72)	120.9(3)	C(58)-F(55)-F(58)	55.8(4)
C(74)-C(73)-C(77)	120.1(3)	F(58)-F(56)-F(59)	129.2(7)
C(72)-C(73)-C(77)	119.1(3)	F(58)-F(56)-C(58)	69.3(5)
C(75)-C(74)-C(73)	117.5(3)	F(59)-F(56)-C(58)	60.8(4)
C(76)-C(75)-C(74)	121.2(3)	F(55)-F(57)-C(58)	74.4(6)
C(76)-C(75)-C(78)	119.5(3)	F(55)-F(57)-F(54)	134.6(9)
C(74)-C(75)-C(78)	119.3(4)	C(58)-F(57)-F(54)	65.5(5)
C(75)-C(76)-C(71)	122.7(3)	F(56)-F(58)-C(58)	64.9(5)
F(72)-C(77)-F(73)	107.2(3)	F(56)-F(58)-F(55)	109.8(6)
F(72)-C(77)-F(71)	105.9(3)	C(58)-F(58)-F(55)	55.1(4)
F(73)-C(77)-F(71)	105.0(3)	F(56)-F(59)-F(54)	116.2(6)
F(72)-C(77)-C(73)	113.1(3)	F(56)-F(59)-C(58)	60.8(4)
F(73)-C(77)-C(73)	113.0(3)	F(54)-F(59)-C(58)	64.3(4)
F(71)-C(77)-C(73)	112.0(3)	F(69)-F(64)-C(68)	74.7(10)
F(74)-C(78)-F(75)	107.3(4)	F(69)-F(64)-F(67)	133.3(13)
F(74)-C(78)-F(76)	105.7(4)	C(68)-F(64)-F(67)	61.4(6)
F(75)-C(78)-F(76)	105.4(4)	F(67)-F(65)-F(68)	127.8(10)
F(74)-C(78)-C(75)	113.8(3)	F(67)-F(65)-C(68)	70.2(6)
F(75)-C(78)-C(75)	113.2(4)	F(68)-F(65)-C(68)	61.9(6)
F(76)-C(78)-C(75)	110.8(3)	F(68)-F(66)-C(68)	60.3(6)
C(86)-C(81)-C(82)	115.6(3)	F(68)-F(66)-F(69)	98.3(8)
C(86)-C(81)-B(50)	125.5(3)	C(68)-F(66)-F(69)	48.3(4)
C(82)-C(81)-B(50)	118.8(3)	F(65)-F(67)-C(68)	62.0(6)
C(83)-C(82)-C(81)	122.3(4)	F(65)-F(67)-F(64)	104.8(9)
C(84)-C(83)-C(82)	120.9(3)	C(68)-F(67)-F(64)	51.6(5)
C(84)-C(83)-C(87)	118.8(3)	F(66)-F(68)-F(65)	137.4(10)
C(82)-C(83)-C(87)	120.3(4)	F(66)-F(68)-C(68)	72.2(7)
C(85)-C(84)-C(83)	117.7(3)	F(65)-F(68)-C(68)	66.6(7)
C(84)-C(85)-C(86)	121.0(4)	F(64)-F(69)-C(68)	68.9(10)
C(84)-C(85)-C(88)	119.2(3)	F(64)-F(69)-F(66)	116.2(12)
C(86)-C(85)-C(88)	119.8(3)	C(68)-F(69)-F(66)	53.1(5)
C(81)-C(86)-C(85)	122.4(3)	O(93)-C(92)-C(91)	109.5(4)
F(82)-C(87)-F(81)	110.4(5)	C(94)-O(93)-C(92)	112.9(4)
F(82)-C(87)-F(83)	105.2(4)	O(93)-C(94)-C(95)	110.2(4)
F(81)-C(87)-F(83)	103.0(4)		

Appendix N

Bond lengths [Å] and angles [°] for [W(η^2-PhC≡CH)(acac)$_2$(η^2-MeN=CPh)][BAr$_4$′] (Chapter 5, **5a**).

W(1)-N(2)	1.990(8)	C(41)-C(46)	1.402(9)
W(1)-C(10)	2.008(8)	C(42)-C(43)	1.392(10)
W(1)-O(22)	2.041(6)	C(43)-C(44)	1.373(12)
W(1)-C(3)	2.052(9)	C(43)-C(47)	1.487(12)
W(1)-O(25)	2.064(5)	C(44)-C(45)	1.381(11)
W(1)-C(11)	2.082(8)	C(45)-C(46)	1.384(10)
W(1)-O(18)	2.101(5)	C(45)-C(48)	1.503(11)
W(1)-O(29)	2.110(5)	C(47)-F(41)	1.313(11)
C(1)-N(2)	1.379(13)	C(47)-F(42)	1.313(12)
N(2)-C(3)	1.264(12)	C(47)-F(43)	1.360(13)
C(3)-C(4)	1.461(12)	C(48)-F(44)	1.314(9)
C(4)-C(5)	1.389(16)	C(48)-F(46)	1.326(11)
C(4)-C(9)	1.399(15)	C(48)-F(45)	1.330(10)
C(5)-C(6)	1.377(14)	C(51)-C(56)	1.401(9)
C(6)-C(7)	1.38(2)	C(51)-C(52)	1.405(9)
C(7)-C(8)	1.40(2)	C(52)-C(53)	1.385(10)
C(8)-C(9)	1.392(16)	C(53)-C(54)	1.396(10)
C(10)-C(11)	1.282(10)	C(53)-C(57)	1.483(10)
C(11)-C(12)	1.427(10)	C(54)-C(55)	1.401(10)
C(12)-C(13)	1.398(10)	C(55)-C(56)	1.377(10)
C(12)-C(17)	1.411(10)	C(55)-C(58)	1.499(10)
C(13)-C(14)	1.368(10)	C(57)-F(51)	1.242(10)
C(14)-C(15)	1.376(11)	C(57)-F(53)	1.272(10)
C(15)-C(16)	1.376(12)	C(57)-F(52)	1.306(10)
C(16)-C(17)	1.381(11)	C(58)-F(55)	1.322(9)
O(18)-C(19)	1.326(13)	C(58)-F(56)	1.334(9)
C(19)-C(20)	1.420(15)	C(58)-F(54)	1.335(9)
C(19)-C(23)	1.519(13)	C(61)-C(66)	1.391(9)
C(20)-C(21)	1.390(14)	C(61)-C(62)	1.406(9)
C(21)-O(22)	1.252(11)	C(62)-C(63)	1.392(10)
C(21)-C(24)	1.449(13)	C(63)-C(64)	1.378(10)
O(25)-C(26)	1.212(11)	C(63)-C(67)	1.509(11)
C(26)-C(27)	1.420(15)	C(64)-C(65)	1.392(10)
C(26)-C(30)	1.522(13)	C(65)-C(66)	1.395(9)
C(27)-C(28)	1.446(15)	C(65)-C(68)	1.492(9)
C(28)-O(29)	1.225(11)	C(67)-F(63)	1.286(11)
C(28)-C(31)	1.503(13)	C(67)-F(61)	1.328(11)
B(40)-C(61)	1.633(10)	C(67)-F(62)	1.333(12)
B(40)-C(51)	1.633(10)	C(68)-F(64)	1.313(9)
B(40)-C(71)	1.639(10)	C(68)-F(65)	1.321(9)
B(40)-C(41)	1.655(10)	C(68)-F(66)	1.323(9)
C(41)-C(42)	1.397(9)	C(71)-C(76)	1.395(9)

C(71)-C(72)	1.399(10)
C(72)-C(73)	1.392(10)
C(73)-C(74)	1.370(11)
C(73)-C(77)	1.483(12)
C(74)-C(75)	1.372(11)
C(75)-C(76)	1.404(10)
C(75)-C(78)	1.475(11)
C(77)-F(72)	1.313(14)
C(77)-F(73)	1.319(13)
C(77)-F(71)	1.323(19)
C(78)-F(74)	1.312(10)
C(78)-F(76)	1.314(11)
C(78)-F(75)	1.342(12)

N(2)-W(1)-C(10)	91.5(3)
N(2)-W(1)-O(22)	158.3(3)
C(10)-W(1)-O(22)	90.1(3)
N(2)-W(1)-C(3)	36.4(3)
C(10)-W(1)-C(3)	101.7(3)
O(22)-W(1)-C(3)	162.1(3)
N(2)-W(1)-O(25)	90.0(3)
C(10)-W(1)-O(25)	162.6(3)
O(22)-W(1)-O(25)	82.2(2)
C(3)-W(1)-O(25)	89.8(3)
N(2)-W(1)-C(11)	99.1(3)
C(10)-W(1)-C(11)	36.5(3)
O(22)-W(1)-C(11)	95.1(3)
C(3)-W(1)-C(11)	86.8(3)
O(25)-W(1)-C(11)	159.5(3)
N(2)-W(1)-O(18)	117.5(3)
C(10)-W(1)-O(18)	116.5(3)
O(22)-W(1)-O(18)	80.8(2)
C(3)-W(1)-O(18)	81.9(3)
O(25)-W(1)-O(18)	77.8(2)
C(11)-W(1)-O(18)	81.7(3)
N(2)-W(1)-O(29)	81.2(3)
C(10)-W(1)-O(29)	79.5(2)
O(22)-W(1)-O(29)	77.9(2)
C(3)-W(1)-O(29)	117.3(3)
O(25)-W(1)-O(29)	83.5(2)
C(11)-W(1)-O(29)	115.9(2)
O(18)-W(1)-O(29)	153.3(2)
C(3)-N(2)-C(1)	135.7(10)
C(3)-N(2)-W(1)	74.5(6)
C(1)-N(2)-W(1)	149.9(9)
N(2)-C(3)-C(4)	134.5(10)
N(2)-C(3)-W(1)	69.1(5)
C(4)-C(3)-W(1)	156.3(9)
C(5)-C(4)-C(9)	120.1(10)
C(5)-C(4)-C(3)	118.4(10)
C(9)-C(4)-C(3)	121.4(11)
C(6)-C(5)-C(4)	120.9(14)
C(5)-C(6)-C(7)	118.3(15)
C(6)-C(7)-C(8)	122.9(12)
C(9)-C(8)-C(7)	117.7(14)
C(8)-C(9)-C(4)	120.0(14)
C(11)-C(10)-W(1)	74.9(5)
C(10)-C(11)-C(12)	142.1(8)
C(10)-C(11)-W(1)	68.6(5)
C(12)-C(11)-W(1)	149.2(6)
C(13)-C(12)-C(17)	117.5(7)
C(13)-C(12)-C(11)	122.8(7)
C(17)-C(12)-C(11)	119.7(7)
C(14)-C(13)-C(12)	121.7(7)
C(13)-C(14)-C(15)	120.1(8)
C(14)-C(15)-C(16)	119.8(8)
C(15)-C(16)-C(17)	120.9(8)
C(16)-C(17)-C(12)	120.0(8)
C(19)-O(18)-W(1)	128.9(6)
O(18)-C(19)-C(20)	126.7(9)
O(18)-C(19)-C(23)	109.5(10)
C(20)-C(19)-C(23)	123.7(10)
C(21)-C(20)-C(19)	122.7(10)
O(22)-C(21)-C(20)	120.2(10)
O(22)-C(21)-C(24)	120.1(9)
C(20)-C(21)-C(24)	119.7(10)
C(21)-O(22)-W(1)	140.6(7)
C(26)-O(25)-W(1)	132.8(7)
O(25)-C(26)-C(27)	123.1(10)
O(25)-C(26)-C(30)	117.7(10)
C(27)-C(26)-C(30)	119.1(10)
C(26)-C(27)-C(28)	123.6(9)
O(29)-C(28)-C(27)	125.2(9)
O(29)-C(28)-C(31)	117.0(10)
C(27)-C(28)-C(31)	117.8(9)
C(28)-O(29)-W(1)	128.0(6)
C(61)-B(40)-C(51)	111.7(5)
C(61)-B(40)-C(71)	105.3(6)
C(51)-B(40)-C(71)	112.2(5)
C(61)-B(40)-C(41)	112.9(5)
C(51)-B(40)-C(41)	103.4(5)
C(71)-B(40)-C(41)	111.6(5)
C(42)-C(41)-C(46)	115.3(6)
C(42)-C(41)-B(40)	122.8(6)

C(46)-C(41)-B(40)	121.4(6)	C(66)-C(61)-B(40)	124.8(6)
C(43)-C(42)-C(41)	122.4(7)	C(62)-C(61)-B(40)	119.3(6)
C(44)-C(43)-C(42)	120.7(7)	C(63)-C(62)-C(61)	121.9(6)
C(44)-C(43)-C(47)	120.2(8)	C(64)-C(63)-C(62)	121.4(6)
C(42)-C(43)-C(47)	119.1(9)	C(64)-C(63)-C(67)	119.9(7)
C(43)-C(44)-C(45)	118.4(7)	C(62)-C(63)-C(67)	118.7(7)
C(44)-C(45)-C(46)	120.8(7)	C(63)-C(64)-C(65)	117.9(6)
C(44)-C(45)-C(48)	119.5(7)	C(64)-C(65)-C(66)	120.5(6)
C(46)-C(45)-C(48)	119.6(7)	C(64)-C(65)-C(68)	119.8(6)
C(45)-C(46)-C(41)	122.4(7)	C(66)-C(65)-C(68)	119.7(6)
F(41)-C(47)-F(42)	108.8(10)	C(61)-C(66)-C(65)	122.6(6)
F(41)-C(47)-F(43)	103.9(7)	F(63)-C(67)-F(61)	107.6(9)
F(42)-C(47)-F(43)	105.3(8)	F(63)-C(67)-F(62)	106.7(9)
F(41)-C(47)-C(43)	113.9(7)	F(61)-C(67)-F(62)	104.8(8)
F(42)-C(47)-C(43)	111.9(7)	F(63)-C(67)-C(63)	114.4(8)
F(43)-C(47)-C(43)	112.3(10)	F(61)-C(67)-C(63)	112.2(7)
F(44)-C(48)-F(46)	106.7(8)	F(62)-C(67)-C(63)	110.6(9)
F(44)-C(48)-F(45)	104.2(7)	F(64)-C(68)-F(65)	106.1(7)
F(46)-C(48)-F(45)	107.9(8)	F(64)-C(68)-F(66)	106.7(7)
F(44)-C(48)-C(45)	112.9(8)	F(65)-C(68)-F(66)	104.4(6)
F(46)-C(48)-C(45)	113.7(7)	F(64)-C(68)-C(65)	113.6(6)
F(45)-C(48)-C(45)	110.8(8)	F(65)-C(68)-C(65)	112.7(6)
C(56)-C(51)-C(52)	114.7(6)	F(66)-C(68)-C(65)	112.6(6)
C(56)-C(51)-B(40)	122.2(6)	C(76)-C(71)-C(72)	115.7(6)
C(52)-C(51)-B(40)	122.8(6)	C(76)-C(71)-B(40)	122.0(6)
C(53)-C(52)-C(51)	123.2(6)	C(72)-C(71)-B(40)	122.1(6)
C(52)-C(53)-C(54)	120.5(6)	C(73)-C(72)-C(71)	121.7(7)
C(52)-C(53)-C(57)	120.3(7)	C(74)-C(73)-C(72)	121.0(7)
C(54)-C(53)-C(57)	119.2(7)	C(74)-C(73)-C(77)	120.3(8)
C(53)-C(54)-C(55)	117.4(6)	C(72)-C(73)-C(77)	118.6(8)
C(56)-C(55)-C(54)	120.9(7)	C(73)-C(74)-C(75)	119.4(7)
C(56)-C(55)-C(58)	121.5(6)	C(74)-C(75)-C(76)	119.5(7)
C(54)-C(55)-C(58)	117.6(6)	C(74)-C(75)-C(78)	120.7(7)
C(55)-C(56)-C(51)	123.2(6)	C(76)-C(75)-C(78)	119.6(7)
F(51)-C(57)-F(53)	108.9(9)	C(71)-C(76)-C(75)	122.7(7)
F(51)-C(57)-F(52)	103.7(9)	F(72)-C(77)-F(73)	110.0(12)
F(53)-C(57)-F(52)	99.9(8)	F(72)-C(77)-F(71)	101.5(12)
F(51)-C(57)-C(53)	115.3(7)	F(73)-C(77)-F(71)	103.2(11)
F(53)-C(57)-C(53)	114.5(7)	F(72)-C(77)-C(73)	114.5(10)
F(52)-C(57)-C(53)	112.9(7)	F(73)-C(77)-C(73)	114.7(10)
F(55)-C(58)-F(56)	106.9(7)	F(71)-C(77)-C(73)	111.7(13)
F(55)-C(58)-F(54)	104.9(6)	F(74)-C(78)-F(76)	107.2(8)
F(56)-C(58)-F(54)	104.7(6)	F(74)-C(78)-F(75)	103.7(8)
F(55)-C(58)-C(55)	113.7(6)	F(76)-C(78)-F(75)	104.9(9)
F(56)-C(58)-C(55)	113.3(6)	F(74)-C(78)-C(75)	114.6(8)
F(54)-C(58)-C(55)	112.6(7)	F(76)-C(78)-C(75)	112.9(7)
C(66)-C(61)-C(62)	115.7(6)	F(75)-C(78)-C(75)	112.7(8)

Appendix O

Bond lengths [Å] and angles [°] for W(η^2-MeC≡CMe)(acac)$_2$(η^2-MeN=CHPh) (**6**, Chapter 5).

W(1)-N(6)	1.952(3)	C(3)-W(1)-O(18)	115.35(11)
W(1)-C(2)	2.041(3)	O(14)-W(1)-O(18)	82.03(9)
W(1)-C(3)	2.063(3)	N(6)-W(1)-O(21)	79.43(10)
W(1)-O(14)	2.117(2)	C(2)-W(1)-O(21)	118.95(11)
W(1)-O(18)	2.126(2)	C(3)-W(1)-O(21)	81.70(11)
W(1)-O(21)	2.135(2)	O(14)-W(1)-O(21)	76.10(9)
W(1)-O(25)	2.159(2)	O(18)-W(1)-O(21)	155.21(9)
W(1)-C(7)	2.220(3)	N(6)-W(1)-O(25)	162.82(11)
C(1)-C(2)	1.495(4)	C(2)-W(1)-O(25)	88.07(11)
C(2)-C(3)	1.312(4)	C(3)-W(1)-O(25)	86.02(11)
C(3)-C(4)	1.488(5)	O(14)-W(1)-O(25)	77.06(9)
C(5)-N(6)	1.452(4)	O(18)-W(1)-O(25)	78.71(8)
N(6)-C(7)	1.395(4)	O(21)-W(1)-O(25)	85.07(9)
C(7)-C(8)	1.476(4)	N(6)-W(1)-C(7)	38.41(11)
C(8)-C(9)	1.394(5)	C(2)-W(1)-C(7)	80.72(12)
C(8)-C(13)	1.406(5)	C(3)-W(1)-C(7)	96.15(12)
C(9)-C(10)	1.395(5)	O(14)-W(1)-C(7)	107.46(11)
C(10)-C(11)	1.382(7)	O(18)-W(1)-C(7)	80.51(10)
C(11)-C(12)	1.405(7)	O(21)-W(1)-C(7)	117.03(10)
C(12)-C(13)	1.392(5)	O(25)-W(1)-C(7)	157.89(11)
O(14)-C(15)	1.281(4)	C(3)-C(2)-C(1)	147.3(3)
C(15)-C(16)	1.389(5)	C(3)-C(2)-W(1)	72.3(2)
C(15)-C(19)	1.512(5)	C(1)-C(2)-W(1)	140.4(2)
C(16)-C(17)	1.411(5)	C(2)-C(3)-C(4)	144.8(3)
C(17)-O(18)	1.275(4)	C(2)-C(3)-W(1)	70.4(2)
C(17)-C(20)	1.510(4)	C(4)-C(3)-W(1)	144.5(3)
O(21)-C(22)	1.275(4)	C(7)-N(6)-C(5)	124.8(3)
C(22)-C(23)	1.407(5)	C(7)-N(6)-W(1)	81.24(17)
C(22)-C(26)	1.513(5)	C(5)-N(6)-W(1)	137.1(2)
C(23)-C(24)	1.397(5)	N(6)-C(7)-C(8)	122.5(3)
C(24)-O(25)	1.279(4)	N(6)-C(7)-W(1)	60.36(15)
C(24)-C(27)	1.513(5)	C(8)-C(7)-W(1)	119.2(2)
		C(9)-C(8)-C(13)	118.3(3)
N(6)-W(1)-C(2)	105.88(12)	C(9)-C(8)-C(7)	123.5(3)
N(6)-W(1)-C(3)	98.94(12)	C(13)-C(8)-C(7)	118.2(3)
C(2)-W(1)-C(3)	37.28(12)	C(8)-C(9)-C(10)	120.6(4)
N(6)-W(1)-O(14)	91.93(10)	C(11)-C(10)-C(9)	121.0(4)
C(2)-W(1)-O(14)	158.16(12)	C(10)-C(11)-C(12)	119.2(4)
C(3)-W(1)-O(14)	153.02(11)	C(13)-C(12)-C(11)	119.9(4)
N(6)-W(1)-O(18)	113.20(10)	C(12)-C(13)-C(8)	121.0(4)
C(2)-W(1)-O(18)	79.39(11)	C(15)-O(14)-W(1)	132.2(2)

O(14)-C(15)-C(16)	125.1(3)
O(14)-C(15)-C(19)	115.2(3)
C(16)-C(15)-C(19)	119.6(3)
C(15)-C(16)-C(17)	123.0(3)
O(18)-C(17)-C(16)	126.2(3)
O(18)-C(17)-C(20)	114.2(3)
C(16)-C(17)-C(20)	119.5(3)
C(17)-O(18)-W(1)	130.9(2)
C(22)-O(21)-W(1)	128.6(2)
O(21)-C(22)-C(23)	126.0(3)
O(21)-C(22)-C(26)	114.4(3)
C(23)-C(22)-C(26)	119.6(3)
C(24)-C(23)-C(22)	126.0(3)
O(25)-C(24)-C(23)	126.0(3)
O(25)-C(24)-C(27)	114.5(3)
C(23)-C(24)-C(27)	119.5(3)
C(24)-O(25)-W(1)	127.9(2)

Appendix P

Bond lengths [Å] and angles [°] for [W(η^2-MeC≡CMe)(acac)$_2$(η^2-Me$_2$N=CHPh)][BAr$_4$′] (Chapter 5, **7**).

W(1)-C(2)	2.015(6)	C(34)-C(35)	1.372(9)
W(1)-O(19)	2.024(3)	C(35)-C(36)	1.400(8)
W(1)-C(3)	2.037(6)	C(35)-C(38)	1.499(8)
W(1)-O(22)	2.107(4)	C(37)-F(33)	1.303(9)
W(1)-O(26)	2.120(4)	C(37)-F(31)	1.315(9)
W(1)-O(15)	2.124(3)	C(37)-F(32)	1.335(10)
W(1)-C(8)	2.168(5)	C(38)-F(36)	1.297(9)
W(1)-N(7)	2.190(4)	C(38)-F(35)	1.323(8)
C(1)-C(2)	1.483(9)	C(38)-F(34)	1.398(9)
C(2)-C(3)	1.311(9)	C(41)-C(46)	1.397(7)
C(3)-C(4)	1.472(9)	C(41)-C(42)	1.402(7)
C(5)-N(7)	1.493(8)	C(42)-C(43)	1.386(8)
C(6)-N(7)	1.476(8)	C(43)-C(44)	1.379(8)
N(7)-C(8)	1.444(7)	C(43)-C(47)	1.497(8)
C(8)-C(9)	1.507(8)	C(44)-C(45)	1.376(8)
C(9)-C(14)	1.365(9)	C(45)-C(46)	1.399(7)
C(9)-C(10)	1.394(9)	C(45)-C481	1.506(8)
C(10)-C(11)	1.379(10)	C(47)-F(42)	1.235(9)
C(11)-C(12)	1.369(10)	C(47)-F(41)	1.312(8)
C(12)-C(13)	1.371(10)	C(47)-F(43)	1.352(9)
C(13)-C(14)	1.383(9)	C(48)-F(45)	1.212(14)
O(15)-C(16)	1.272(6)	C(48)-F(46)	1.295(12)
C(16)-C(17)	1.417(8)	C(48)-F(44)	1.350(12)
C(16)-C(20)	1.493(8)	C(51)-C(52)	1.393(7)
C(17)-C(18)	1.364(8)	C(51)-C(56)	1.407(7)
C(18)-O(19)	1.296(6)	C(52)-C(53)	1.395(7)
C(18)-C(21)	1.484(8)	C(53)-C(54)	1.383(8)
O(22)-C(23)	1.285(7)	C(53)-C(57)	1.508(8)
C(23)-C(24)	1.390(8)	C(54)-C(55)	1.381(8)
C(23)-C(27)	1.493(9)	C(55)-C(56)	1.388(7)
C(24)-C(25)	1.384(9)	C(55)-C(58)	1.496(8)
C(25)-O(26)	1.283(8)	C(57)-F(51)	1.281(9)
C(25)-C(28)	1.501(8)	C(57)-F(53)	1.301(8)
B(30)-C(51)	1.636(6)	C(57)-F(52)	1.340(9)
B(30)-C(61)	1.637(7)	C(58)-F(56)	1.301(8)
B(30)-C(41)	1.639(7)	C(58)-F(54)	1.315(10)
B(30)-C(31)	1.641(7)	C(58)-F(55)	1.317(8)
C(31)-C(32)	1.391(7)	C(61)-C(66)	1.397(7)
C(31)-C(36)	1.396(7)	C(61)-C(62)	1.400(7)
C(32)-C(33)	1.398(8)	C(62)-C(63)	1.389(7)
C(33)-C(34)	1.368(9)	C(63)-C(64)	1.377(8)
C(33)-C(37)	1.513(9)	C(63)-C(67)	1.495(7)

C(64)-C(65)	1.395(8)	C(8)-N(7)-W(1)	69.8(3)
C(65)-C(66)	1.387(8)	C(6)-N(7)-W(1)	115.8(4)
C(65)-C(68)	1.519(8)	C(5)-N(7)-W(1)	119.5(4)
C(67)-F(62)	1.311(8)	N(7)-C(8)-C(9)	120.9(5)
C(67)-F(63)	1.311(7)	N(7)-C(8)-W(1)	71.5(3)
C(67)-F(61)	1.313(7)	C(9)-C(8)-W(1)	132.9(4)
C(68)-F(64)	1.284(9)	C(14)-C(9)-C(10)	118.1(6)
C(68)-F(66)	1.300(10)	C(14)-C(9)-C(8)	120.8(5)
C(68)-F(65)	1.309(12)	C(10)-C(9)-C(8)	120.7(5)
		C(11)-C(10)-C(9)	120.4(6)
C(2)-W(1)-O(19)	93.5(2)	C(12)-C(11)-C(10)	120.9(6)
C(2)-W(1)-C(3)	37.8(3)	C(11)-C(12)-C(13)	118.7(6)
O(19)-W(1)-C(3)	100.73(19)	C(12)-C(13)-C(14)	120.8(6)
C(2)-W(1)-O(22)	162.1(2)	C(9)-C(14)-C(13)	121.0(6)
O(19)-W(1)-O(22)	80.78(14)	C(16)-O(15)-W(1)	130.2(3)
C(3)-W(1)-O(22)	159.9(2)	O(15)-C(16)-C(17)	124.2(5)
C(2)-W(1)-O(26)	79.5(2)	O(15)-C(16)-C(20)	116.1(5)
O(19)-W(1)-O(26)	79.97(15)	C(17)-C(16)-C(20)	119.6(5)
C(3)-W(1)-O(26)	117.2(2)	C(18)-C(17)-C(16)	123.3(5)
O(22)-W(1)-O(26)	82.85(15)	O(19)-C(18)-C(17)	123.7(5)
C(2)-W(1)-O(15)	116.2(2)	O(19)-C(18)-C(21)	114.8(5)
O(19)-W(1)-O(15)	81.29(14)	C(17)-C(18)-C(21)	121.5(5)
C(3)-W(1)-O(15)	80.5(2)	C(18)-O(19)-W(1)	133.6(3)
O(22)-W(1)-O(15)	79.89(14)	C(23)-O(22)-W(1)	128.6(4)
O(26)-W(1)-O(15)	156.28(15)	O(22)-C(23)-C(24)	123.8(6)
C(2)-W(1)-C(8)	107.2(2)	O(22)-C(23)-C(27)	114.7(5)
O(19)-W(1)-C(8)	156.34(19)	C(24)-C(23)-C(27)	121.4(5)
C(3)-W(1)-C(8)	89.5(2)	C(25)-C(24)-C(23)	125.1(6)
O(22)-W(1)-C(8)	82.48(19)	O(26)-C(25)-C(24)	125.3(5)
O(26)-W(1)-C(8)	114.36(18)	O(26)-C(25)-C(28)	114.4(6)
O(15)-W(1)-C(8)	79.40(17)	C(24)-C(25)-C(28)	120.3(6)
C(2)-W(1)-N(7)	91.8(2)	C(25)-O(26)-W(1)	128.6(4)
O(19)-W(1)-N(7)	154.88(17)	C(51)-B(30)-C(61)	113.7(4)
C(3)-W(1)-N(7)	98.5(2)	C(51)-B(30)-C(41)	105.3(4)
O(22)-W(1)-N(7)	86.72(17)	C(61)-B(30)-C(41)	112.7(4)
O(26)-W(1)-N(7)	76.90(16)	C(51)-B(30)-C(31)	110.8(4)
O(15)-W(1)-N(7)	117.95(16)	C(61)-B(30)-C(31)	103.0(4)
C(8)-W(1)-N(7)	38.69(18)	C(41)-B(30)-C(31)	111.6(4)
C(3)-C(2)-C(1)	143.4(7)	C(32)-C(31)-C(36)	115.9(5)
C(3)-C(2)-W(1)	72.0(3)	C(32)-C(31)-B(30)	119.9(4)
C(1)-C(2)-W(1)	144.4(5)	C(36)-C(31)-B(30)	123.8(4)
C(2)-C(3)-C(4)	142.4(6)	C(31)-C(32)-C(33)	122.6(5)
C(2)-C(3)-W(1)	70.2(4)	C(34)-C(33)-C(32)	120.3(5)
C(4)-C(3)-W(1)	147.0(5)	C(34)-C(33)-C(37)	121.1(6)
C(8)-N(7)-C(6)	122.1(5)	C(32)-C(33)-C(37)	118.6(6)
C(8)-N(7)-C(5)	116.4(5)	C(33)-C(34)-C(35)	118.4(5)
C(6)-N(7)-C(5)	108.9(5)	C(34)-C(35)-C(36)	121.6(5)
		C(34)-C(35)-C(38)	118.3(6)

C(36)-C(35)-C(38)	120.1(6)	C(56)-C(55)-C(58)	120.5(5)
C(31)-C(36)-C(35)	121.1(5)	C(55)-C(56)-C(51)	122.0(5)
F(33)-C(37)-F(31)	107.0(7)	F(51)-C(57)-F(53)	107.3(7)
F(33)-C(37)-F(32)	107.1(7)	F(51)-C(57)-F(52)	105.1(6)
F(31)-C(37)-F(32)	105.8(7)	F(53)-C(57)-F(52)	105.9(7)
F(33)-C(37)-C(33)	112.7(7)	F(51)-C(57)-C(53)	113.3(6)
F(31)-C(37)-C(33)	111.8(6)	F(53)-C(57)-C(53)	113.2(6)
F(32)-C(37)-C(33)	112.0(6)	F(52)-C(57)-C(53)	111.5(6)
F(36)-C(38)-F(35)	111.5(7)	F(56)-C(58)-F(54)	106.4(6)
F(36)-C(38)-F(34)	105.9(6)	F(56)-C(58)-F(55)	106.4(7)
F(35)-C(38)-F(34)	102.0(5)	F(54)-C(58)-F(55)	104.3(7)
F(36)-C(38)-C(35)	114.6(5)	F(56)-C(58)-C(55)	114.5(5)
F(35)-C(38)-C(35)	112.2(5)	F(54)-C(58)-C(55)	112.6(7)
F(34)-C(38)-C(35)	109.7(7)	F(55)-C(58)-C(55)	111.9(6)
C(46)-C(41)-C(42)	115.3(4)	C(66)-C(61)-C(62)	115.6(4)
C(46)-C(41)-B(30)	125.6(4)	C(66)-C(61)-B(30)	123.5(4)
C(42)-C(41)-B(30)	119.1(4)	C(62)-C(61)-B(30)	120.2(4)
C(43)-C(42)-C(41)	122.4(5)	C(63)-C(62)-C(61)	122.4(4)
C(44)-C(43)-C(42)	121.0(5)	C(64)-C(63)-C(62)	121.1(5)
C(44)-C(43)-C(47)	119.8(5)	C(64)-C(63)-C(67)	120.0(5)
C(42)-C(43)-C(47)	119.1(5)	C(62)-C(63)-C(67)	118.9(5)
C(45)-C(44)-C(43)	118.3(5)	C(63)-C(64)-C(65)	117.6(5)
C(44)-C(45)-C(46)	120.6(5)	C(66)-C(65)-C(64)	121.1(5)
C(44)-C(45)-C(48)	119.3(5)	C(66)-C(65)-C(68)	118.6(5)
C(46)-C(45)-C(48)	120.1(5)	C(64)-C(65)-C(68)	120.2(5)
C(41)-C(46)-C(45)	122.4(5)	C(65)-C(66)-C(61)	122.2(5)
F(42)-C(47)-F(41)	110.2(8)	F(62)-C(67)-F(63)	104.8(6)
F(42)-C(47)-F(43)	108.0(7)	F(62)-C(67)-F(61)	105.8(6)
F(41)-C(47)-F(43)	98.8(6)	F(63)-C(67)-F(61)	106.7(5)
F(42)-C(47)-C(43)	114.5(6)	F(62)-C(67)-C(63)	112.0(5)
F(41)-C(47)-C(43)	113.1(5)	F(63)-C(67)-C(63)	113.3(5)
F(43)-C(47)-C(43)	111.1(6)	F(61)-C(67)-C(63)	113.5(5)
F(45)-C(48)-F(46)	114.3(15)	F(64)-C(68)-F(66)	108.2(8)
F(45)-C(48)-F(44)	107.1(16)	F(64)-C(68)-F(65)	108.9(8)
F(46)-C(48)-F(44)	97.4(11)	F(66)-C(68)-F(65)	102.0(7)
F(45)-C(48)-C(45)	114.0(9)	F(64)-C(68)-C(65)	113.2(6)
F(46)-C(48)-C(45)	112.3(8)	F(66)-C(68)-C(65)	112.1(6)
F(44)-C(48)-C(45)	110.4(10)	F(65)-C(68)-C(65)	111.8(7)
C(52)-C(51)-C(56)	115.4(4)		
C(52)-C(51)-B(30)	122.2(4)		
C(56)-C(51)-B(30)	122.1(4)		
C(51)-C(52)-C(53)	122.5(5)		
C(54)-C(53)-C(52)	120.9(5)		
C(54)-C(53)-C(57)	119.2(5)		
C(52)-C(53)-C(57)	119.9(5)		
C(55)-C(54)-C(53)	117.8(5)		
C(54)-C(55)-C(56)	121.3(5)		
C(54)-C(55)-C(58)	118.1(5)		

Appendix Q

Bond lengths [Å] and angles [°] for [W(η^2-MeC≡CMe)(acac)$_2$(η^2-MeN=C(PMe$_3$)Ph)][BAr$_4$′] (Chapter 5, **8**).

W(1)-N(6)	1.925(3)	C(43)-C(47)	1.503(6)
W(1)-C(2)	2.060(4)	C(44)-C(45)	1.385(6)
W(1)-C(3)	2.077(4)	C(45)-C(46)	1.393(5)
W(1)-O(24)	2.095(3)	C(45)-C(48)	1.492(6)
W(1)-O(28)	2.113(3)	C(47)-F(41)	1.308(6)
W(1)-O(17)	2.119(3)	C(47)-F(42)	1.310(6)
W(1)-O(21)	2.128(3)	C(47)-F(43)	1.324(5)
W(1)-C(7)	2.211(4)	C(48)-F(44)	1.313(6)
P(1)-C(15)	1.790(5)	C(48)-F(46)	1.331(5)
P(1)-C(14)	1.796(5)	C(48)-F(45)	1.332(5)
P(1)-C(16)	1.803(5)	C(51)-C(52)	1.399(5)
P(1)-C(7)	1.817(4)	C(51)-C(56)	1.403(5)
C(1)-C(2)	1.484(6)	C(52)-C(53)	1.390(5)
C(2)-C(3)	1.279(6)	C(53)-C(54)	1.387(5)
C(3)-C(4)	1.481(6)	C(53)-C(57)	1.502(5)
C(5)-N(6)	1.451(6)	C(54)-C(55)	1.383(5)
N(6)-C(7)	1.395(5)	C(55)-C(56)	1.395(5)
C(7)-C(8)	1.504(6)	C(55)-C(58)	1.502(6)
C(8)-C(9)	1.376(8)	C(57)-F(53)	1.328(5)
C(8)-C(13)	1.381(7)	C(57)-F(52)	1.334(5)
C(9)-C(10)	1.380(8)	C(57)-F(51)	1.352(5)
C(10)-C(11)	1.334(14)	C(58)-F(57)	1.258(8)
C(11)-C(12)	1.401(14)	C(58)-F(54)	1.261(9)
C(12)-C(13)	1.388(10)	C(58)-F(58)	1.274(10)
O(17)-C(18)	1.274(5)	C(58)-F(56)	1.282(7)
C(18)-C(19)	1.392(7)	C(58)-F(55)	1.422(7)
C(18)-C(22)	1.499(7)	C(58)-F(59)	1.429(9)
C(19)-C(20)	1.383(7)	C(61)-C(62)	1.396(5)
C(20)-O(21)	1.290(5)	C(61)-C(66)	1.401(5)
C(20)-C(23)	1.481(7)	C(62)-C(63)	1.394(5)
O(24)-C(25)	1.277(5)	C(63)-C(64)	1.383(6)
C(25)-C(26)	1.370(7)	C(63)-C(67)	1.499(5)
C(25)-C(29)	1.505(6)	C(64)-C(65)	1.384(5)
C(26)-C(27)	1.397(7)	C(65)-C(66)	1.392(5)
C(27)-O(28)	1.276(5)	C(65)-C(68)	1.492(5)
C(27)-C(30)	1.497(6)	C(67)-F(61)	1.326(5)
B(40)-C(71)	1.640(5)	C(67)-F(63)	1.335(5)
B(40)-C(51)	1.642(5)	C(67)-F(62)	1.336(5)
B(40)-C(61)	1.643(5)	C(68)-F(68)	1.300(8)
B(40)-C(41)	1.644(5)	C(68)-F(67)	1.310(9)
C(41)-C(42)	1.399(5)	C(68)-F(69)	1.320(8)
C(41)-C(46)	1.399(5)	C(68)-F(64)	1.324(8)
C(42)-C(43)	1.389(5)	C(68)-F(66)	1.343(8)
C(43)-C(44)	1.385(6)	C(68)-F(65)	1.348(9)

C(71)-C(76)	1.400(5)
C(71)-C(72)	1.403(5)
C(72)-C(73)	1.397(5)
C(73)-C(74)	1.381(5)
C(73)-C(77)	1.496(5)
C(74)-C(75)	1.386(5)
C(75)-C(76)	1.388(5)
C(75)-C(78)	1.491(5)
C(77)-F(71)	1.335(4)
C(77)-F(73)	1.345(4)
C(77)-F(72)	1.347(4)
C(78)-F(77)	1.315(18)
C(78)-F(79)	1.325(16)
C(78)-F(76)	1.325(17)
C(78)-F(78)	1.337(17)
C(78)-F(74)	1.357(15)
C(78)-F(75)	1.358(18)

N(6)-W(1)-C(2)	96.38(15)
N(6)-W(1)-C(3)	101.86(15)
C(2)-W(1)-C(3)	36.02(16)
N(6)-W(1)-O(24)	153.57(13)
C(2)-W(1)-O(24)	85.64(13)
C(3)-W(1)-O(24)	95.22(13)
N(6)-W(1)-O(28)	119.32(13)
C(2)-W(1)-O(28)	113.44(14)
C(3)-W(1)-O(28)	80.25(14)
O(24)-W(1)-O(28)	83.18(11)
N(6)-W(1)-O(17)	77.75(13)
C(2)-W(1)-O(17)	79.44(14)
C(3)-W(1)-O(17)	115.43(14)
O(24)-W(1)-O(17)	76.73(11)
O(28)-W(1)-O(17)	155.32(11)
N(6)-W(1)-O(21)	92.58(13)
C(2)-W(1)-O(21)	159.66(14)
C(3)-W(1)-O(21)	157.17(13)
O(24)-W(1)-O(21)	78.34(10)
O(28)-W(1)-O(21)	77.26(10)
O(17)-W(1)-O(21)	84.69(11)
N(6)-W(1)-C(7)	38.65(14)
C(2)-W(1)-C(7)	107.45(15)
C(3)-W(1)-C(7)	89.54(15)
O(24)-W(1)-C(7)	162.75(13)
O(28)-W(1)-C(7)	81.29(13)
O(17)-W(1)-C(7)	116.05(13)
O(21)-W(1)-C(7)	90.90(13)
C(15)-P(1)-C(14)	108.3(2)
C(15)-P(1)-C(16)	106.5(3)
C(14)-P(1)-C(16)	106.6(2)
C(15)-P(1)-C(7)	115.4(2)
C(14)-P(1)-C(7)	109.1(2)
C(16)-P(1)-C(7)	110.6(2)
C(3)-C(2)-C(1)	147.1(4)
C(3)-C(2)-W(1)	72.7(3)
C(1)-C(2)-W(1)	140.1(3)
C(2)-C(3)-C(4)	143.4(4)
C(2)-C(3)-W(1)	71.3(3)
C(4)-C(3)-W(1)	145.3(3)
C(7)-N(6)-C(5)	133.2(4)
C(7)-N(6)-W(1)	81.8(2)
C(5)-N(6)-W(1)	141.6(3)
N(6)-C(7)-C(8)	123.3(4)
N(6)-C(7)-P(1)	113.8(3)
C(8)-C(7)-P(1)	111.3(3)
N(6)-C(7)-W(1)	59.5(2)
C(8)-C(7)-W(1)	120.7(3)
P(1)-C(7)-W(1)	119.5(2)
C(9)-C(8)-C(13)	118.4(5)
C(9)-C(8)-C(7)	119.4(5)
C(13)-C(8)-C(7)	122.1(5)
C(8)-C(9)-C(10)	121.7(7)
C(11)-C(10)-C(9)	119.9(9)
C(10)-C(11)-C(12)	120.4(7)
C(13)-C(12)-C(11)	119.4(8)
C(8)-C(13)-C(12)	120.1(8)
C(18)-O(17)-W(1)	128.4(3)
O(17)-C(18)-C(19)	126.2(4)
O(17)-C(18)-C(22)	114.0(4)
C(19)-C(18)-C(22)	119.7(4)
C(20)-C(19)-C(18)	126.6(4)
O(21)-C(20)-C(19)	124.1(4)
O(21)-C(20)-C(23)	115.6(4)
C(19)-C(20)-C(23)	120.3(4)
W(2)-O(21)-C(20)	169.4(4)
W(2)-O(21)-W(1)	40.00(15)
C(20)-O(21)-W(1)	129.5(3)
C(25)-O(24)-W(1)	131.3(3)
O(24)-C(25)-C(26)	125.1(4)
O(24)-C(25)-C(29)	114.8(4)
C(26)-C(25)-C(29)	120.0(4)
C(25)-C(26)-C(27)	124.8(4)
O(28)-C(27)-C(26)	125.3(4)
O(28)-C(27)-C(30)	114.6(4)
C(26)-C(27)-C(30)	120.1(4)
C(27)-O(28)-W(1)	130.2(3)
W(2)-O(28)-W(1)	41.98(13)
C(71)-B(40)-C(51)	105.9(3)
C(71)-B(40)-C(61)	114.2(3)
C(51)-B(40)-C(61)	112.8(3)

C(71)-B(40)-C(41)	110.1(3)	F(56)-C(58)-F(55)	100.1(6)
C(51)-B(40)-C(41)	110.7(3)	F(57)-C(58)-F(59)	99.5(7)
C(61)-B(40)-C(41)	103.3(3)	F(54)-C(58)-F(59)	65.9(6)
C(42)-C(41)-C(46)	116.0(3)	F(58)-C(58)-F(59)	98.3(6)
C(42)-C(41)-B(40)	121.4(3)	F(55)-C(58)-F(59)	143.0(5)
C(46)-C(41)-B(40)	122.5(3)	F(57)-C(58)-C(55)	115.6(5)
C(43)-C(42)-C(41)	122.4(4)	F(54)-C(58)-C(55)	116.1(5)
C(44)-C(43)-C(42)	120.4(4)	F(58)-C(58)-C(55)	114.3(6)
C(44)-C(43)-C(47)	119.7(4)	F(56)-C(58)-C(55)	113.8(4)
C(42)-C(43)-C(47)	119.9(4)	F(55)-C(58)-C(55)	108.4(4)
C(45)-C(44)-C(43)	118.5(4)	F(59)-C(58)-C(55)	107.8(4)
C(44)-C(45)-C(46)	120.9(4)	C(62)-C(61)-C(66)	115.7(3)
C(44)-C(45)-C(48)	120.6(4)	C(62)-C(61)-B(40)	123.5(3)
C(46)-C(45)-C(48)	118.5(4)	C(66)-C(61)-B(40)	120.0(3)
C(45)-C(46)-C(41)	121.8(4)	C(63)-C(62)-C(61)	122.0(3)
F(41)-C(47)-F(42)	106.5(4)	C(64)-C(63)-C(62)	121.3(3)
F(41)-C(47)-F(43)	105.9(4)	C(64)-C(63)-C(67)	120.3(3)
F(42)-C(47)-F(43)	105.4(4)	C(62)-C(63)-C(67)	118.4(3)
F(41)-C(47)-C(43)	112.6(4)	C(63)-C(64)-C(65)	117.7(3)
F(42)-C(47)-C(43)	113.4(4)	C(64)-C(65)-C(66)	121.1(3)
F(43)-C(47)-C(43)	112.5(4)	C(64)-C(65)-C(68)	118.9(3)
F(44)-C(48)-F(46)	105.9(4)	C(66)-C(65)-C(68)	120.0(3)
F(44)-C(48)-F(45)	105.4(4)	C(65)-C(66)-C(61)	122.2(3)
F(46)-C(48)-F(45)	106.2(4)	F(61)-C(67)-F(63)	107.7(3)
F(44)-C(48)-C(45)	112.9(4)	F(61)-C(67)-F(62)	105.1(4)
F(46)-C(48)-C(45)	112.6(4)	F(63)-C(67)-F(62)	105.6(3)
F(45)-C(48)-C(45)	113.2(4)	F(61)-C(67)-C(63)	113.3(3)
C(52)-C(51)-C(56)	115.3(3)	F(63)-C(67)-C(63)	112.7(3)
C(52)-C(51)-B(40)	122.4(3)	F(62)-C(67)-C(63)	111.8(3)
C(56)-C(51)-B(40)	122.3(3)	F(68)-C(68)-F(67)	105.8(6)
C(53)-C(52)-C(51)	122.8(3)	F(68)-C(68)-F(69)	106.2(6)
C(54)-C(53)-C(52)	120.6(3)	F(67)-C(68)-F(69)	106.0(6)
C(54)-C(53)-C(57)	121.4(3)	F(68)-C(68)-F(64)	128.7(6)
C(52)-C(53)-C(57)	118.0(3)	F(67)-C(68)-F(66)	129.1(6)
C(55)-C(54)-C(53)	118.1(3)	F(64)-C(68)-F(66)	106.1(6)
C(54)-C(55)-C(56)	120.9(3)	F(64)-C(68)-F(65)	105.2(6)
C(54)-C(55)-C(58)	119.0(4)	F(66)-C(68)-F(65)	103.4(6)
C(56)-C(55)-C(58)	120.1(4)	F(68)-C(68)-C(65)	112.3(5)
C(55)-C(56)-C(51)	122.2(3)	F(67)-C(68)-C(65)	113.5(5)
F(53)-C(57)-F(52)	106.8(3)	F(69)-C(68)-C(65)	112.4(4)
F(53)-C(57)-F(51)	107.3(3)	F(64)-C(68)-C(65)	114.5(5)
F(52)-C(57)-F(51)	104.6(3)	F(66)-C(68)-C(65)	113.9(4)
F(53)-C(57)-C(53)	113.4(3)	F(65)-C(68)-C(65)	112.8(5)
F(52)-C(57)-C(53)	112.8(3)	C(76)-C(71)-C(72)	115.8(3)
F(51)-C(57)-C(53)	111.4(3)	C(76)-C(71)-B(40)	117.7(3)
F(57)-C(58)-F(54)	128.3(6)	C(72)-C(71)-B(40)	126.4(3)
F(57)-C(58)-F(58)	117.7(7)	C(73)-C(72)-C(71)	121.6(3)
F(54)-C(58)-F(56)	112.7(7)	C(74)-C(73)-C(72)	121.1(3)
F(58)-C(58)-F(56)	130.9(6)	C(74)-C(73)-C(77)	117.0(3)
F(54)-C(58)-F(55)	103.9(6)	C(72)-C(73)-C(77)	121.9(3)

C(73)-C(74)-C(75)	118.4(3)	F(74)-C(78)-F(75)	105.0(8)
C(74)-C(75)-C(76)	120.4(3)	F(77)-C(78)-C(75)	114.8(9)
C(74)-C(75)-C(78)	120.2(3)	F(79)-C(78)-C(75)	112.3(8)
C(76)-C(75)-C(78)	119.4(3)	F(76)-C(78)-C(75)	112.6(8)
C(75)-C(76)-C(71)	122.7(3)	F(78)-C(78)-C(75)	112.8(8)
F(71)-C(77)-F(73)	107.2(3)	F(74)-C(78)-C(75)	111.7(7)
F(71)-C(77)-F(72)	106.7(3)	F(75)-C(78)-C(75)	111.0(9)
F(73)-C(77)-F(72)	105.1(3)		
F(71)-C(77)-C(73)	113.3(3)		
F(73)-C(77)-C(73)	111.8(3)		
F(72)-C(77)-C(73)	112.2(3)		
F(77)-C(78)-F(79)	105.7(8)		
F(77)-C(78)-F(76)	120.5(10)		
F(77)-C(78)-F(78)	104.9(9)		
F(79)-C(78)-F(78)	105.5(8)		
F(76)-C(78)-F(74)	106.2(9)		
F(76)-C(78)-F(75)	110.0(10)		

Appendix R

DFT Computational Details and list of references

Computational Details. All density functional theory (DFT) calculations were performed by using the Gaussian 03 package.[1] Geometries of the model aldehyde complexes, $W(acac)_2(CO)(CH_2O)$ (**7**) (O-proximal and O-distal rotamers of aldehyde relative to CO), $[W(acac)_2(CO)(CH_2O)]^{2-}$ (**8**), and $Os(acac)_2(CO)(CH_2O)$ (**9**), were optimized using the hybrid B3LYP exchange-correlation functional[2-4] with a standard double-ζ quality basis set, which for W and Os consists of LANL2DZ with the associated relativistic effective core potential (ECP),[5-7] and the D95V plus polarization basis set for the other atoms.[8] For W and Os, f-polarization functions were added.[8] The addition of polarization functions to the metals resulted in better agreement between the calculated and experimental metal-ligand bond distances. The selected basis set is similar to that employed in a literature study of another third-row transition metal system.[9] Frequency calculations were carried out on all minimum structures, and the resulting frequencies all had positive values. Minima were identified from geometry optimizations started at several different rotamers of the aldehyde complex. No zero point correction was added for the energies presented in the table.

Table R1. Total Electronic Energies of calculated structures, in Hartrees (kcal/mol)

Compound	Energy
$W(acac)_2(CO)(CH_2O)$ (**7**) rotamer with O atom of aldehyde distal to CO	-986.399187
$W(acac)_2(CO)(CH_2O)$ (**7**) rotamer with O atom of aldehyde proximal to CO.	-986.380766
$[W(acac)_2(CO)(OCH_2)]^{2-}$ (**8**)	-986.314798
$Os(acac)_2(CO)(CH_2O)$ (**9**)	-1009.376024

Table R2. Cartesian coordinates (Å) for the optimized structure of $W(acac)_2(CO)(CH_2O)$ (7) in the gas phase; rotamer with O atom of aldehyde distal to CO.

W	-0.01762700	-0.60096600	-0.19233400
C	-0.70981900	-2.07920900	0.87572500
O	-1.10446400	-2.97219000	1.52744500
O	-1.84313600	-0.12339400	-0.86857200
O	0.57002700	1.26875600	-1.07662100
O	-0.53495100	0.63372300	1.36046300
O	1.82685800	-0.62554400	0.72594400
C	1.67494100	1.87871800	-0.92904400
C	2.77399100	0.25600000	0.63866000
C	2.75063700	1.43685800	-0.11202400
C	4.00141500	-0.09300700	1.44720300
H	4.39269400	-1.05829000	1.10481600
H	4.78387300	0.66538400	1.36781800
H	3.71369500	-0.21715700	2.49759300
C	1.81749100	3.17044100	-1.70481900
H	2.74930000	3.69575700	-1.48186800
H	1.77790000	2.94304100	-2.77665600
H	0.96396700	3.81955100	-1.47986800
H	3.63497700	2.06279200	-0.07503300
C	-1.57811700	1.37337000	1.56814900
C	-2.75106400	0.71046000	-0.50828700
C	-2.67362300	1.44285800	0.69761600
H	-3.49818900	2.09684400	0.95571900
C	-3.92526700	0.84630300	-1.44466700
H	-4.65580200	1.56995100	-1.07460700
H	-3.57070800	1.16338800	-2.43244700
H	-4.41318700	-0.12761600	-1.56907100
C	-1.54205600	2.17774700	2.84394400
H	-2.43173200	2.80118000	2.96233700
H	-1.46104900	1.49575600	3.69885600
H	-0.64798300	2.81241000	2.84984000
C	0.52137900	-2.47456300	-1.13738500
O	0.66363500	-1.30969500	-1.84842400
H	-0.26652600	-3.14887100	-1.47956200
H	1.44995000	-2.95173800	-0.80746800

Table R3. Cartesian coordinates (Å) for the optimized structure of $W(acac)_2(CO)(CH_2O)$ (7) in the gas phase; rotamer with O atom of aldehyde proximal to CO.

W	0.00134700	-0.61920200	-0.21841100
C	-0.81762500	-2.03131100	0.93102300
O	-1.29983600	-2.80330600	1.65775600
O	-1.73776200	-0.02236200	-1.02259300
O	0.62143100	1.35168700	-0.88491900
O	-0.55989000	0.63181600	1.34834100
O	1.79485500	-0.66277200	0.75410000
C	1.73624300	1.92937600	-0.70107900
C	2.81037900	0.14118500	0.67276500
C	2.83082400	1.37617700	0.01724300
C	4.03788300	-0.35531300	1.39849300
H	4.30884300	-1.34411100	1.01025400
H	4.88672800	0.32455900	1.29321300
H	3.79986000	-0.48180500	2.46117500
C	1.87031500	3.30842400	-1.31232300
H	2.81305200	3.79297500	-1.04702400
H	1.80224000	3.22501300	-2.40356300
H	1.03119600	3.93026400	-0.98142100
H	3.74101900	1.96178000	0.07947900
C	-1.67868300	1.23824800	1.57320000
C	-2.70966300	0.71573600	-0.62143800
C	-2.73718100	1.31773700	0.65395100
H	-3.61195100	1.89606100	0.92722200
C	-3.84372400	0.88738700	-1.60042700
H	-4.66919600	1.45910900	-1.16936200
H	-3.47949700	1.40403000	-2.49647800
H	-4.20716500	-0.09744700	-1.91602700
C	-1.77508200	1.91518200	2.91894400
H	-2.71031700	2.46761900	3.03873900
H	-1.69845000	1.15853300	3.70901000
H	-0.92627700	2.59791900	3.04198500
C	0.90753700	-1.21476900	-2.02674600
O	0.25887700	-2.20304900	-1.32618000
H	1.99911600	-1.29952300	-2.07472500
H	0.41235200	-0.87852400	-2.94372400

Table R4. Cartesian coordinates (Å) for the optimized structure of $[W(acac)_2(CO)(OCH_2)]^{2-}$ (8) in the gas phase

W	-0.10072800	-0.70497900	-0.10627900
C	-0.73897900	-1.98944200	1.13929700
O	-1.12456300	-2.79791000	1.96566800
O	-2.00449300	-0.12387200	-0.79587000
O	0.67573500	0.91834900	-1.38100100
O	-0.31557400	0.90707100	1.24804500
O	1.82835700	-0.57090800	0.91474500
C	1.78582900	1.52941500	-1.27615600
C	2.76308800	0.25943800	0.67740600
C	2.81314000	1.25070500	-0.33658300
C	3.96421700	0.13772900	1.61913100
H	4.36893900	-0.88231200	1.56355000
H	4.76096400	0.85435300	1.38333800
H	3.63061900	0.29653100	2.65381000
C	1.99542200	2.68079900	-2.26302700
H	2.96452400	3.17867900	-2.13069000
H	1.92495900	2.30208500	-3.29220200
H	1.19178700	3.41939800	-2.13522900
H	3.70446700	1.87397000	-0.37414500
C	-1.28269100	1.74057700	1.39898300
C	-2.75693600	0.84206800	-0.41038700
C	-2.48038200	1.74509300	0.64508500
H	-3.22212700	2.50965600	0.86962200
C	-4.06698100	0.97208900	-1.18240600
H	-4.67013800	1.82070500	-0.83343300
H	-3.85911800	1.09855300	-2.25493900
H	-4.65783700	0.04986300	-1.07789800
C	-1.07828300	2.77220800	2.50239100
H	-1.89665100	3.50337500	2.53745000
H	-1.00963300	2.27517000	3.48262800
H	-0.12839600	3.30462300	2.34673100
C	0.99161700	-1.99939800	-1.39072200
O	-0.32927300	-1.90260400	-1.76240900
H	1.33210900	-2.99473700	-1.04412500
H	1.72354700	-1.53019400	-2.08136000

Table R5. Cartesian coordinates (Å) for the optimized structure of $Os(acac)_2(CO)(CH_2O)$ (9) in the gas phase.

Os	-0.00770200	-0.55776300	-0.08001400
C	-0.62512100	-2.01184700	0.87721400
O	-1.01818800	-2.92637800	1.48563100
O	-1.88299000	-0.20155700	-0.96122100
O	0.62854600	1.10315100	-1.18800800
O	-0.56455400	0.77295800	1.36163000
O	1.75616500	-0.56156800	0.96746700
C	1.78847600	1.63750900	-1.10949600
C	2.74245400	0.23132800	0.74487300
C	2.81258000	1.25805900	-0.21591200
C	3.92616600	-0.01707100	1.65423700
H	4.29775500	-1.03388200	1.48264400
H	4.73499000	0.69806200	1.48681500
H	3.59695800	0.03795900	2.69782300
C	2.03030500	2.77728800	-2.07607800
H	2.99364400	3.26631700	-1.91272300
H	1.99477200	2.38813100	-3.10065500
H	1.22330800	3.51196100	-1.97851500
H	3.73943600	1.81811400	-0.26300700
C	-1.65105900	1.44131000	1.49103800
C	-2.80126000	0.58540600	-0.54004300
C	-2.75429000	1.37677100	0.62401000
H	-3.61525000	1.99356900	0.85259600
C	-4.02820000	0.62854300	-1.42561600
H	-4.80327800	1.28615500	-1.02492200
H	-3.73782200	0.97633200	-2.42364200
H	-4.43023100	-0.38475500	-1.53631800
C	-1.67848200	2.35059600	2.69838500
H	-2.60923700	2.91903600	2.76282500
H	-1.55601200	1.74849800	3.60602300
H	-0.83027700	3.04273900	2.64899600
C	0.06857600	-1.67468900	-1.91554300
O	1.24076300	-1.66194600	-1.34440900
H	-0.13360300	-0.98513800	-2.74543300
H	-0.53858000	-2.58961100	-1.88259700

References

1. Gaussian 03, Revision C.02, Frisch, M. J.; Trucks, G. W.; Schlegel, H. B.; Scuseria, G. E.; Robb, M. A.; Cheeseman, J. R.; Montgomery, Jr., J. A.; Vreven, T.; Kudin, K. N.; Burant, J. C.; Millam, J. M.; Iyengar, S. S.; Tomasi, J.; Barone, V.; Mennucci, B.; Cossi, M.; Scalmani, G.; Rega, N.; Petersson, G. A.; Nakatsuji, H.; Hada, M.; Ehara, M.; Toyota, K.; Fukuda, R.; Hasegawa, J.; Ishida, M.; Nakajima, T.; Honda, Y.; Kitao, O.; Nakai, H.; Klene, M.; Li, X.; Knox, J. E.; Hratchian, H. P.; Cross, J. B.; Bakken, V.; Adamo, C.; Jaramillo, J.; Gomperts, R.; Stratmann, R. E.; Yazyev, O.; Austin, A. J.; Cammi, R.; Pomelli, C.; Ochterski, J. W.; Ayala, P. Y.; Morokuma, K.; Voth, G. A.; Salvador, P.; Dannenberg, J. J.; Zakrzewski, V. G.; Dapprich, S.; Daniels, A. D.; Strain, M. C.; Farkas, O.; Malick, D. K.; Rabuck, A. D.; Raghavachari, K.; Foresman, J. B.; Ortiz, J. V.; Cui, Q.; Baboul, A. G.; Clifford, S.; Cioslowski, J.; Stefanov, B. B.; Liu, G.; Liashenko, A.; Piskorz, P.; Komaromi, I.; Martin, R. L.; Fox, D. J.; Keith, T.; Al-Laham, M. A.; Peng, C. Y.; Nanayakkara, A.; Challacombe, M.; Gill, P. M. W.; Johnson, B.; Chen, W.; Wong, M. W.; Gonzalez, C.; and Pople, J. A.; Gaussian, Inc., Wallingford CT, 2004.

2. A. D. Becke, *J. Chem. Phys.* **1993**, *98*, 5648.

3. Lee, C.; Yang; W. Parr, R. G. *Phys. Rev.* **1988** *B37*, 785.

4. Miehlich, B.; Savin, A.; Stoll, H.; Preuss, H. *Chem. Phys. Lett.* **1989**, *157*, 200.

5. Hay, P. J.; Wadt, W. R. *J. Chem. Phys.* **1985,** *87*, 270.

6. Wadt, W. R.; Hay, P. J. *J. Chem. Phys.* **1985,** *82*, 284.

7. Hay, P. J.; Wadt, W. R. *J. Chem. Phys.* **1985,** *82*, 299.

8. (a) Ehlers, A.W.; Bohme, M; Dapprich, S.; Gobbi, A.; Hollwarth, A.; Jonas, V.; Kohler, K.F.; Stegmann, R.; Veldkamp, A.; Grenking, G. Chem. Phys. Lett. **1993**, *208*, 111; (b) Dunning, T. H., Jr.; Hay, P. J., In *Modern Theoretical Chemistry*, Schaefer, H. F., III Ed. Plenum: New York, 1976; Vol. 3, pp 1.

9. Cui, Q.; Musaev, D. G.; Morokuma, K. *Organomeallics.* **1997,** *16*, 1355.